Troubleshooting, optimization and robustness testing of CeBER process for c-phycocyanin extraction and purification from *Spirulina*

Uzair Kadir

In fulfilment of the requirements for the degree of Master of Science in Chemical Engineering, Bioprocess Engineering

Supervisor: A/Prof Marijke Fagan-Endres
Prof Susan TL Harrison

Department of Chemical Engineering
Faculty of Engineering and the Built Environment
University of Cape Town

2024

University of Cape Town

The copyright of this thesis vests in the author. No quotation from it or information derived from it is to be published without full acknowledgement of the source. The thesis is to be used for private study or non-commercial research purposes only.

Published by the University of Cape Town (UCT) in terms of the non-exclusive license granted to UCT by the author.

University of Cape Town

Plagiarism Declaration

1. I know that plagiarism is wrong. Plagiarism is to use another's work and to pretend that it is ones own.
2. I have used the Harvard system for citation and referencing. Each significant contribution to, and quotation in, this report from the work, or works, of other people has been attributed, and has been cited and referenced.
3. This report is my own unaided work, except for assistance received from the teaching staff.
4. I have not allowed, and will not allow, anyone to copy my work with the intention of passing it off as his or her own work.
5. This thesis/dissertation has been submitted to the Turnitin module and I confirm that my supervisor has seen my report and any concerns revealed by such have been resolved with my supervisor

Signed by candidate

Signature

Abstract

c-Phycocyanin is a natural pigment, found as an intracellular protein in various microalgae. One of the most common sources of c-phycocyanin is *Arthrospira platensis,* more commonly known as *Spirulina*. *Spirulina* is a cyanobacterium, widely renowned for its many health benefits which, experts say, are a direct result of c-phycocyanin (Vernes, et al., 2015).

Previous researchers in CeBER have demonstrated and patented a process to produce cosmetic grade c-phycocyanin (> 1.5 purity ratio) from *Spirulina*. The focus of this study was to optimize operating conditions for the key unit procedures posed previously for the CeBER patented process. The experimental work was performed in two main steps. The first considered the individual unit procedures (cell disruption via bead-milling, c-phycocyanin leaching rom biomass, cell debris removal via centrifugation, c-phycocyanin purification via polyethylene glycol-citrate and polyethylene glycol-maltodextrin aqueous two-phase separation, c-phycocyanin purification via ammonium sulfate precipitation), where the main aim was to optimize the operating conditions of the units and to mitigate redundancies in the pool of unit procedures. The second step involved assessing the performance of the overall process operating at the newly found operating conditions. Robustness of the process was qualified through the use of three different dried *Spirulina* powder samples (sourced from different suppliers) for the experiments.

Bead-milling was demonstrated to narrow out the particle size distributions as expected, however a shift towards smaller cut sizes was only observed for the larger dried powders tested. In subsequent leaching, bead-milling did increase the initial extraction rate of c-phycocyanin from dried *Spirulina* powder. However, it was found that bead-milling may have no effect in the overall leaching time taken to reach an equilibrium concentration of c-phycocyanin in the crude extract. Bead-milling was also shown to have either little to no benefit in the recovery of product containing supernatant over the cell debris removal step. It was found that the c-phycocyanin leaching kinetics from the dried *Spirulina* powders could not be reliably predicting using standard models in literature. The highest R^2 obtained was 0.95 for the fit of a 2nd order kinetic model to a Carbocraft milled sample. Most other samples tested did not yield a good correlation to first or second order leaching kinetics. It was found that to reach an equilibrium concentration across all samples, the minimum leaching time required was 19 hours. The crude extract purity ratios achieved were approximately 0.46, 0.41 and 0.12 in the Brenntag, Carbocraft and Indian *Spirulina* powder samples' crude extracts, respectively.

As predicted, an increase in the g force used for cell debris removal via centrifugation yielded an increase in recovery of the product-containing supernatant. The highest recoveries were achieved at 10 000 g of operation. It was shown that a two-stage cell debris removal with an inter-stage rinsing step improved c-phycocyanin recovery overall.

It was found that both of the ATPS systems investigated by previous CeBER researchers did not perform sufficiently robustly when required to handle a variation in the *Spirulina* source and hence crude extract feed. As such, the ATPS steps was deemed unsuitable for use in a commercialisation process and were removed from the process testing scope. Owing to the removal of the ATPS steps, microfiltration (0.22 μm aperture) was added to the end of the process as an additional c-phycocyanin purification step.

The ammonium sulfate precipitation train was optimized by identifying the ammonium sulfate concentrations that trigger selective c-phycocyanin precipitation and tracking how purity changes over concentration changes too. It was shown that a two-stage ammonium sulfate precipitation will yield a purer c-phycocyanin product than a single stage, producing a product stream with a higher final purity ratio and with less cell debris content. The ammonium sulfate saturation fraction recommended for the first stage is 0.22 where the supernatant is sequestered and treated with additional ammonium sulfate to achieve 0.45 saturation for the second stage. The c-phycocyanin is precipitated out in the second stage.

The full runs of the process at the newly established “best” operating conditions yielded maximum purity ratios of 0.90 ± 0.02, 0.79 ± 0.03, 0.46 ± 0.03 for the Brenntag, Carbocraft and Indian dried *Spirulina* powders respectively. Thus, cosmetic grade c-phycocyanin was not achieved by any of the samples and food grade (> 0.7) only achieved using the Brenntag and Carbocraft samples. The recoveries were 24 ± 8%, 66 ± 8% and 65 ± 14% for the Brenntag, Carbocraft and Indian samples, respectively. It appears that, despite the low recovery obtained in the runs using the Brenntag powder, the amended process is robust enough to extract and purify c-phycocyanin from *Spirulina,* albeit without achieving the overall aim of cosmetic grade. The overall purification factors from the crude extract were approximately 2.6, 2.2 and 4.4 for the Brenntag, Carbocraft and Indian samples, respectively. These purification factors are not far off from those reported in literature for c-phycocyanin purification processes.

It is, therefore, recommended that the process put more emphasis on increasing the purity ratio in the crude extract through means of using fresh *Spirulina* and chitosan/activated-charcoal adsorption techniques (as recommended by Hockey (2020) and Payne (2023)). With these changes it is probable that the amended process will achieve cosmetic grade purity. Further work should also be performed on increasing the recovery, especially over the precipitation stages, without compromising purity.

Acknowledgements

I would like to thank my supervisors, A/Prof Marijke Fagan-Endres and Prof Sue Harrison for this opportunity to work on this fascinating CeBER project at UCT. I have learnt so much about myself (and about algae) whilst on this journey.

Thanks Marijke, for the consistent meetings and the little formatting edits that really saved so much of my time. Thank you for nudging me in the correct directions; letting me figure it all out (mostly) on my own. Thank you, Prof Harrison for setting me on track and for being the first person to tell me that this is going to be a good thesis, I really needed to hear it at the time.

From the lab, thank you to Tich Samkange and Sharon Rademeyer for showing me how to use every new piece of equipment and thank you for keeping me on my toes with respects to housekeeping! Thank you to Melinda Dunnet for being the expert in the lab and making me have faith that my results were not complete nonsense.

To all my post-graduate colleagues, thank you for making my post-graduate time fun and for being great people to work with while on TA shifts.

To my friends, thank you for keeping me sane throughout the years. The tears of laughter are what helped bring me so far. A special vote of thanks to Mamdouh for soldiering with me; from late nights at campus to hours of calls and so-called study breaks.

And to my family; Mommy and Daddy, thank you for all the support you've given me throughout my time at UCT, bringing me meals to campus, and worrying about my health when I'm spending late nights at campus. To my sisters, thank you for referring to me as the nerdy one, it gave me much motivation to live up to it. To my fiancée, Imaan, thank you for believing in me and comforting me when I felt lost, it truly means the world to me. I love you all!

Table of Contents

Abstract i
Acknowledgements iii
Table of Contents iv
List of Figures vi
List of Tables ix
Glossary of Terms xi
Acronyms and Abbreviations xii
1 Introduction 1
1.1 Context 1
1.2 Focus and scope of this project 2
1.2.1 Focus 2
1.2.2 Scope 3
1.3 Structure of dissertation 3
2 Literature Review 5
2.1 c-Phycocyanin 5
2.1.1 Phycobiliproteins 5
2.1.2 Phycobilisomes 5
2.1.3 Properties and uses 5
2.1.4 Sources and production 6
2.2 c-Phycocyanin quality control indicators 7
2.2.1 Purity Ratio 7
2.2.2 Concentration and colour intensity 8
2.2.3 Bacterial contamination 8
2.3 c-Phycocyanin protein extraction and recovery procedures 8
2.3.1 Cell disruption 9
2.3.2 Cell debris removal 10
2.3.3 c-Phycocyanin recovery and purification 10
2.3.4 Drying formulation 11
2.4 Extraction and purification process from Hockey (2020) 12
2.4.1 Key findings 12
2.4.2 Process description 12
2.5 Individual unit processes studied 13
2.5.1 Bead-milling 13
2.5.2 Leaching 14
2.5.3 Cell debris removal via centrifugation 18
2.5.4 Aqueous two-phase separation 21
2.5.5 Ammonium sulfate precipitation 23
2.5.6 Filtration 26
2.6 Robustness and process design 27
2.7 Summary and gaps of literature & previous work 27
2.8 Defining the research project 29
2.8.1 Problem statement 30
2.8.2 Research project objectives 30
2.8.3 Key research questions 30
3 Approach to Project and Methodology 32
3.1 Research methodology 32
3.2 Experimental approach 32
3.3 Experimental methods 32
3.3.1 Materials 32
3.3.2 *Spirulina* powder feed size distribution 33

3.3.3 *Spirulina* cell disruption via bead-milling 34
3.3.4 c-Phycocyanin leaching tests 34
3.3.5 Cell debris removal 35
3.3.6 Aqueous two-phase separation (ATPS) 35
3.3.7 Ammonium sulfate precipitation 37
3.3.8 Microfiltration 39
3.3.9 Full runs of process 40
3.3.10 Analytical methods 42
4 Results and Discussion 45
4.1 *Spirulina* powder size distributions 45
4.2 c-Phycocyanin leaching from Spirulina 49
4.2.1 Leaching profiles 49
4.2.2 Leaching kinetics analysis 53
4.2.3 Leaching discussion 64
4.3 Cell debris removal 66
4.3.1 Cell debris removal results 66
4.3.2 Discussion on cell debris removal 72
4.4 Aqueous two-phase separation 74
4.5 Ammonium sulfate precipitation 78
4.5.1 c-Phycocyanin recovery and purity in the precipitate pellet 78
4.5.2 c-Phycocyanin purity in supernatant 82
4.5.3 Discussion on ammonium sulfate precipitation 84
4.6 Conclusions on individual unit operation testing 85
4.7 Full runs of the process 86
4.7.1 Full run configuration 86
4.7.2 c-Phycocyanin purity and recovery for full runs 87
4.7.3 Key performance indicators of full runs 90
5 Conclusions and Recommendations 93
References 96
Appendix A: Approach to Project and Methodology Appendix 103
A.1 General sample calculations 103
A.1.1 Performance indicators 103
A.2 Aqueous two-phase separation 105
A.2.1 Sample calculation for PEG-citrate ATPS 105
A.2.2 Sample Calculation for PEG-maltodextrin ATPS 106
A.3 Precipitation 107
A.3.1 Ammonium sulfate saturation determination 107
Appendix B: Results and Discussion Appendix 112
B.1 Size distribution 112
B.2 Leaching tests 114
B.2.1 First order leaching kinetic coefficients 114
B.2.2 Second order leaching kinetics 115
B.3 Cell debris removal 116
B.3.1 Terminal settling velocity 116

List of Figures

Figure 1. Block flow diagram of the CeBER patented extraction and purification process to obtain c-phycocyanin from *Spirulina*. The diagram has been simplified to only show key chemical streams, excluding more generic components such as water. 2

Figure 2. Different downstream processing routes available for recovery of microbial metabolites [adapted from Doran (1997)]. 9

Figure 3. Cell disruption operations for intracellular product liberation [adapted from Harrison (2011)]. 10

Figure 4. Proposed CeBER extraction process for c-phycocyanin from *Spirulina* completed at lab-scale, as described in Hockey (2020). 13

Figure 5. Diagram of a cross-section of a centrifuge, with key variables affecting its operation and design 20

Figure 6. Ammonium sulfate saturation concentrations and specific volumes at different temperatures adapted from Wingfield (2001) and Dawson et al. (2002). 24

Figure 7. c-Phycocyanin recovery and purity ratio in the precipitate at different fractional ammonium sulfate saturations adapted from Song, Zhao and Suying (2013) 25

Figure 8. Screenshot of the DinoXcope software interface 33

Figure 9. Diagram of ATPS experimental procedure, with numbers and letters in the figure referring to: (1) Initial c-phycocyanin containing stock solution; (2) PEG 4000/deionized water; (3) Citrate salts/maltodextrin; (4) Top phase; (5) Bottom phase; (a) Benchtop vortex; (b) Centrifuge; (c) Syringe. 36

Figure 10. Diagram describing experimental procedure for a single stage ammonium sulfate precipitation, with numbers and letters in the figure referring to: (1) Ammonium sulfate crystals; (2) Stock solution of *Spirulina* leachate; (3) Precipitate pellet; (4) Supernatant; (a) Benchtop vortex; (b) Benchtop centrifuge. 38

Figure 11. Diagram describing the experimental procedure used for a two-stage ammonium sulfate precipitation, with numbers and letters in the figure referring to: (1) Ammonium sulfate crystals; (2) Stock solution of *Spirulina* leachate; (3) Precipitate pellet after 1st precipitation; (4) Supernatant after 1st precipitation; (5) Precipitate pellet after 2nd precipitation; (6) Supernatant after 2nd precipitation; (a) Benchtop vortex; (b) Benchtop centrifuge. 39

Figure 12. Diagram describing the procedure of using a benchtop vacuum filtration system, with numbers and letters in the figure referring to: (1) Feed solution; (2) Filtrate; (3) Filter retentate cake; (a) centrifuge tube; (b) Filter funnel; (c) Membrane base; (d) Port to vacuum; (e) Vacuum release port; (f) Filter base; (g) Valve for vacuum; (h) Filter membrane. 40

Figure 13. Plot of dilution vs absorbance (OD) at 280, 620 and 650 nm using the FLUOstar Omega spectrophotometer. 43

Figure 14. Cumulative particle size distributions for Brenntag milled and non-milled Spirulina powder samples 47

Figure 15. Cumulative particle size distributions for Carbocraft milled and non-milled Spirulina powder samples 48

Figure 16. Cumulative particle size distribution for the Indian milled and non-milled Spirulina powder samples 48

Figure 17. c-Phycocyanin concentration over leaching time for multiple runs of Carbocraft, Brenntag and Indian milled samples. The numbers (1, 2 and 3) appearing after the *Spirulina* sample name, i.e. Carbocraft, Brenntag and Indian, refer to repeats of the same experiment with sampling performed at different time intervals. Repeats were sampled in triplicate. 50

Figure 18. c-Phycocyanin purity ratio over leaching time for multiple runs of Carbocraft, Brenntag and Indian milled samples. The numbers (1, 2 and 3) appearing after the *Spirulina* sample name, i.e. Carbocraft, Brenntag and Indian, refer to repeats of the same experiment with sampling performed at different time intervals. Repeats were sampled in triplicate. 51

Figure 19. c-Phycocyanin concentration in the leachate over time for Brenntag milled and non-milled runs. Brenntag 1 and 2 refer to repeats of the experiment performed with different time intervals of sampling. Error bars indicate variance from triplicate runs. 52

Figure 20. c-Phycocyanin concentration in the leachate over time for Carbocraft milled and non-milled runs. Carbocraft 1, 2 and 3 refer to repeats of the experiment performed with different time intervals of sampling. Error bars indicate variance from triplicate runs 53
Figure 21. Linearized Carbocraft milled data, for first order leaching kinetics analysis 54
Figure 22. Linearized Carbocraft non-milled data, for first order leaching kinetics analysis 54
Figure 23. Carbocraft non-milled experimental data fitted to the first order kinetic model 55
Figure 24. Carbocraft milled experimental data linearized according to second order kinetics 56
Figure 25. Carbocraft non-milled experimental data linearized according to second order kinetics 56
Figure 26. Carbocraft milled experimental data fitted to the second order kinetic model 57
Figure 27. Carbocraft non-milled experimental data fitted to the second order kinetic model 57
Figure 28. Linearized Brenntag milled data, for first order leaching kinetics analysis 58
Figure 29. Linearized Brenntag non-milled data, for first order leaching kinetics analysis 59
Figure 30. Brenntag milled experimental data fitted to the first order kinetic model between 7.9 and 19 hours 60
Figure 31. Brenntag non-milled experimental data fitted to the first order kinetic model 60
Figure 32. Brenntag milled experimental data linearized according to second order kinetics 61
Figure 33. Brenntag non-milled experimental data linearized according to second order kinetics 62
Figure 34. Brenntag non-milled experimental data fitted onto the second order kinetic model 62
Figure 35. Linearization of milled Indian sample leaching data according to first order leaching kinetics 63
Figure 36. Linearization of milled Indian sample leaching data according to second order leaching kinetics 64
Figure 37. Recovery of the crude liquid leachate following centrifugation over the range of 1000 to 10 000 g force for milled Brenntag, Carbocraft and Indian Spirulina samples after leaching. The error bars indicate variance in the measured recovery for triplicate runs of the samples. 68
Figure 38. Recovery of crude liquid leachate out of centrifuge over the range of 1000 to 10 000 g force for milled and non-milled Carbocraft Spirulina samples after leaching. The error bars indicate variance in the measured recoveries across triplicate runs. 69
Figure 39. Recovery of crude liquid leachate out of centrifuge over the range of 1000 to 10 000 g force for milled and non-milled Brenntag Spirulina samples after leaching. The error bars indicate variance in the measured recoveries across triplicate runs. 70
Figure 40. Purity ratio of the crude liquid leachate recovered out of centrifuge over the range of 1000 to 10 000 g force for Brenntag, Carbocraft and Indian Spirulina samples after leaching. The error bars indicate variance for triplicate runs. 71
Figure 41. Recovery of the milled Carbocraft crude liquid after a first and second centrifugation, i.e. with and without additional cell debris rinsing, at different g forces for the initial cell debris removal centrifugation and 7 000 g for the second centrifugation. The error bars indicate the variance across triplicate runs. 72
Figure 42. Citrate-PEG 4000 ATPS citrate bottom phase volume as a percentage of total volume at different concentrations of crude extract feed for the Brenntag, Carbocraft and Indian *Spirulina* crude extract samples 75
Figure 43. Purification factor in the top PEG phase of the citrate-PEG 4000 ATPS at different crude extract feed concentrations for the Brenntag, Carbocraft and Indian *Spirulina* crude extract samples 76
Figure 44. c-Phycocyanin recovery in the citrate-PEG 4000 ATPS top PEG phase for Brenntag, Carbocraft and Indian *Spirulina* crude extract samples 76
Figure 45. An unexpected three phases forming in the citrate-PEG 4000 ATPS for Carbocraft crude extract at 1× dilution 78
Figure 46. Effect of ammonium sulfate saturation fraction on the recovery of c-phycocyanin in the precipitate pellet for Brenntag, Carbocraft (two leachates tested), Indian and Green Create Nutra *Spirulina* powder crude extracts. Error bars in this figure indicate the variance for triplicate runs of the experiment. 79
Figure 47. Mass of precipitates at lower ammonium sulfate saturations for Carbocraft 1 and Indian samples. Error bars in the figure indicate the variance generated from triplicate runs. 80

Figure 48. Effect of ammonium sulfate saturation fraction on the c-phycocyanin purity ratio of the precipitate pellet of Brenntag, Carbocraft (two leachates tested), Indian and Green Create Nutra *Spirulina* crude extracts. Error bars in the graph indicate the variance for triplicate runs of the experiment. 81
Figure 49. Effect of ammonium sulfate saturation fraction on the c-phycocyanin purity ratio of the precipitate pellet of Brenntag, Carbocraft (two leachates tested), Indian and Green Create Nutra *Spirulina* crude extracts. Error bars in the figure indicate variance for triplicate runs of the experiment. 82
Figure 50. Effect of ammonium sulfate saturation fraction on the c-phycocyanin purity ratio of the precipitation supernatant of Brenntag, Carbocraft (two crude extracts tested), Indian and Green Create Nutra *Spirulina* crude extracts. Error bars in the figure indicate variance for triplicate runs of the experiment. 83
Figure 51. Effect of ammonium sulfate saturation fraction on the c-phycocyanin purification factor of the precipitation supernatant of Brenntag, Carbocraft (two crude extracts tested), Indian and Green Create Nutra Spirulina crude extracts. Error bars in the figure indicate variance for triplicate runs for the experiment. 84
Figure 52. Block flow diagram of the new configuration for the CeBER process for extraction and purification of c-phycocyanin from *Spirulina* 86
Figure 53. c-Phycocyanin purity ratio after each downstream processing step for Brenntag, Carbocraft and Indian *Spirulina* sample feeds. Error bars in the figure indicate variance for triplicate runs of the experiment. 89
Figure 54. c-Phycocyanin recovery across each of the downstream processing steps, as well as the overall process recoveries for Carbocraft, Brenntag and Indian *Spirulina* sample feedstocks. Error bars in the figure indicate variance for triplicate runs of the experiment 90
Figure 55. An example purification method 104
Figure 56. Conductivity of solution as a function of ammonium sulfate added 107
Figure 57. Conductivity in solution as a function of the square root of the ammonium sulfate saturation fraction 109
Figure 58. Calibration of ammonium sulfate saturation fraction to mass of ammonium sulfate in grams added to a 20 mL volume 110
Figure 59. Non-milled Carbocraft Spirulina powder 10× magnification with contrast and saturation adjustment 112
Figure 60. Non-milled Carbocraft Spirulina powder 10× magnification with ImageJ drawing function applied 112
Figure 61. Milled Carbocraft Spirulina powder 10× magnification with contrast and saturation adjustment 112
Figure 62. Milled Carbocraft Spirulina powder 10× magnification with ImageJ drawing function applied 112
Figure 63. Non-milled Brenntag Spirulina powder 10× magnification with contrast and saturation adjustment 113
Figure 64. Non-milled Brenntag Spirulina powder 10× magnification with ImageJ drawing function applied 113
Figure 65. Milled Brenntag Spirulina powder 10× magnification with contrast and saturation adjustment 113
Figure 66. Milled Brenntag Spirulina powder 10× magnification with ImageJ drawing function applied 113
Figure 67. Non-milled Indian Spirulina powder 10× magnification with contrast and saturation adjustment 113
Figure 68. Non-milled Indian Spirulina powder 10× magnification with ImageJ drawing function applied 113
Figure 69. Milled Indian Spirulina powder 10× magnification with contrast and saturation adjustment 114
Figure 70. Milled Indian Spirulina powder 10× magnification with ImageJ drawing function applied 114

List of Tables

Table 1. Summary of c-phycocyanin cell contents of microorganisms typically used for c-phycocyanin production 7
Table 2. Summary of the purity ratios for different quality grade c-phycocyanin 7
Table 3. Comparison of different extraction and purification processes for c-phycocyanin from literature 11
Table 4. Summary of c-phycocyanin (c-PC) purity ratios and yield of c-PC per unit mass of microalgae for different cell liberation techniques and leaching times 15
Table 5. Experimental ranges for operating conditions of a leaching system of c-phycocyanin from *Spirulina,* adapted from Su, et al. (2014) 17
Table 6. Comparison of experimental conditions and outputs of ATPS for c-phycocyanin purification, from literature 22
Table 7. Summary of ammonium sulfate saturation concentrations and specific volumes at different temperatures adapted from Wingfield (2001) and Dawson et al. (2002). 23
Table 8. Critical experimental conditions of ammonium sulfate precipitation and c-phycocyanin purity and recovery outputs on *Spirulina* crude extracts from different studies 26
Table 9. Purity ratio and bacterial contamination of c-phycocyanin product of precipitation adapted from Fagan-Endres, et al. (2019) 26
Table 10. Filter pore size and c-phycocyanin purity and recoveries used by and achieved by different studies, respectively 26
Table 11. Summary of the gaps in the work performed by Hockey (2020) in terms of the parameters calculated in the unit procedures of the recommended process route by Hockey (2020) 28
Table 12. Summary of inputs for "Analyze" tab in ImageJ software 34
Table 13. Summary of inputs for "Distribution" tab in ImageJ software 34
Table 14. Mass fractions of components used for PEG-citrate ATPS procedure, adapted from Hockey (2020) 36
Table 15. Mass fractions for components used for PEG-maltodextrin ATPS procedure, adapted from Hockey (2020) 37
Table 16. Mass fractions for components used for PEG-maltodextrin ATPS procedure for a two-stage ATPS system, adapted from Hockey (2020) 37
Table 17. Filter membranes in order and with pore size used for the micro-filtration procedure 39
Table 18. Summary of the linear ranges for absorbance (OD) at 280, 620 and 650 nm with the coefficient of determination for that range 42
Table 19. Representations of the size distributions for *Spirulina* samples, milled and non-milled. The uncertainty is notated using "±" and was calculated as the standard deviation of triplicate measurements. The STD values indicate the average standard deviation from the mean for the different powder diameter sizes – indicating the width of the particle size distribution. 47
Table 20. Milling stress factors calculated for the bead-milling process 48
Table 21. Summary of the model outputs for leaching performance of the milled and non-milled Carbocraft Spirulina samples. 65
Table 22. Summary of the outputs of the OLS regression analysis performed on the milled *Spirulina* samples liquid recovery data in Figure 37 with linear regression model (Model), coefficient of determination (R^2), probability associated with the F-statistic [Prob(F-statistic)] 68
Table 23. Summary of the regression analysis and t-test statistical significance results performed on the milled and non-milled Carbocraft Spirulina leachate recovery data from Figure 38 70
Table 24. Summary of the regression analysis and t-test statistical significance results performed on the milled and non-milled Brenntag *Spirulin*a leachate recovery data from Figure 39 70
Table 26. Table summarizing key operating conditions for the unit procedures of the newly configured CeBER process 87

Table 27. Key performance indicators for Brenntag, Carbocraft and Indian *Spirulina* feedstocks across the extraction and purification process 91

Glossary of Terms

Biomarker	A natural molecule that can be used to a quantify a biological process
Cut size	Representative size resulting from a purposeful alteration of size
Cyanobacteria	A phylum of gram-negative bacterium that photosynthesize
Homogenization	A preparation of a suspension of cell contents through physical treatment
Hypotonicity	Having a lower relative osmotic pressure than the surrounding fluid
Intracellular	Situated inside a cell
Microalgae	Microscopic algae
Microfiltration	Separation technique using size exclusion to remove micron-sized particles
Photospectroscopy	Electromagnetic spectroscopy dealing with quantifying reflective or transmission of a material as a function of wavelength
Precipitation	Causing a substance to be deposited as a solid from solution
Purification factor	Ratio of purity of a product stream to the feed stream
Robustness	The ability to withstand adverse conditions
Sonication	The act of using sound to agitate particles
Supernatant	Denoting the liquid lying above a solid residue
Supramolecular	Relating to structures comprised of many molecules

Acronyms and Abbreviations

A	Absorbance
ANOVA	Analysis of Variance
ATPS	Aqueous two-phase separation
ave	Average
c-PC	c-Phycocyanin
CeBER	Centre for Bioprocess Engineering Research
CFU	Colony forming units
GRAS	Generally regarded as safe
MW	Molecular weight
OD	Optical density
PBP	Phycobiliprotein
PBS	Phycobilisome
PEG	Polyethylene glycol
pH	Potential of hydrogen
PSD	Particle size distribution
viz.	Namely
wt	Weight

1 Introduction

1.1 Context

c-Phycocyanin is a natural pigment, found as an intracellular protein in various microalgae. One of the most common sources of c-phycocyanin is *Arthrospira platensis,* more commonly known as *Spirulina*. *Spirulina* is a cyanobacterium, widely renowned for its many health benefits which, experts say, are a direct result of c-phycocyanin (Vernes, et al., 2015).

The demand for naturally sourced pigments such as c-phycocyanin is on the rise as a result of many synthetically produced colourants being banned because of their recently-discovered harmful effects on both the consumer and the environment – either through the production process or through disposal of the used product (Dufossé, et al., 2005).

The market for c-phycocyanin has been reported to have a projected compounded annual growth rate of 9.8 % over the period between 2023 and 2030 (Verified Market Research ®, 2024). The market forecast also suggests that the total global revenue for the c-phycocyanin market will reflect a > 2 × increase over this period (Verified Market Research ®, 2024). The selling price of c-phycocyanin depends on the purity of the product. c-Phycocyanin is a high-value pigment, with an estimated price ranging from 10 to 50 US$ per mg for analytical grade and 1 to 5 US$ per gram for use as a food colourants (Ramos *et al.*, 2011).

c-Phycocyanin is used as an alternative to toxic, synthetic dyes (Glazer, 1997). As an example, c-phycocyanin has replaced a synthetic blue dye used in Smarties that which is thought to have contributed towards attention deficit hyperactivity disorder in children (Klein & Buchholz, 2013). The anti-carcinogenic and anti-oxidative properties of c-phycocyanin increase the lucrativeness of the pigment in the cosmetic and food industries (Glazer, 1997).

In light of this present attractive economic climate surrounding c-phycocyanin, the Centre for Bioprocessing Engineering Research (CeBER) at the University of Cape Town has developed and patented a process for the extraction and purification of c-phycocyanin from *Spirulina* (Fagan Endres et al., 2019, patent no. WO2019034955A1). This process has since been modified and optimized, to an extent.

The CeBER patented c-phycocyanin extraction and purification process comprises of four main consecutive procedures as can be seen in Figure 1. Firstly, a cell lysis step is required since the desired c-phycocyanin product is found inside the *Spirulina* cell. No specific unit procedure is specified for this cell lysis step, with options including: high pressure homogenization, sonication and bead-milling. This is followed by an aqueous two-phase separation (ATPS) system. ATPS is a liquid-liquid fractionation technique where both liquids employed are aqueous and where other dissolved substances can move from one liquid phase to the other based on chemical affinity (Asenjo & Andrews, 2011). The patent is centered around this ATPS system: a polyethylene glycol (PEG)-maltodextrin system where the desired c-phycocyanin product reports to the maltodextrin bottom phase. The product containing phase is treated with ammonium sulfate in a train such that the desired c-phycocyanin product is precipitated out of solution. The final procedure of the process is a drying step to remove the excess water from the formulated, precipitated product.

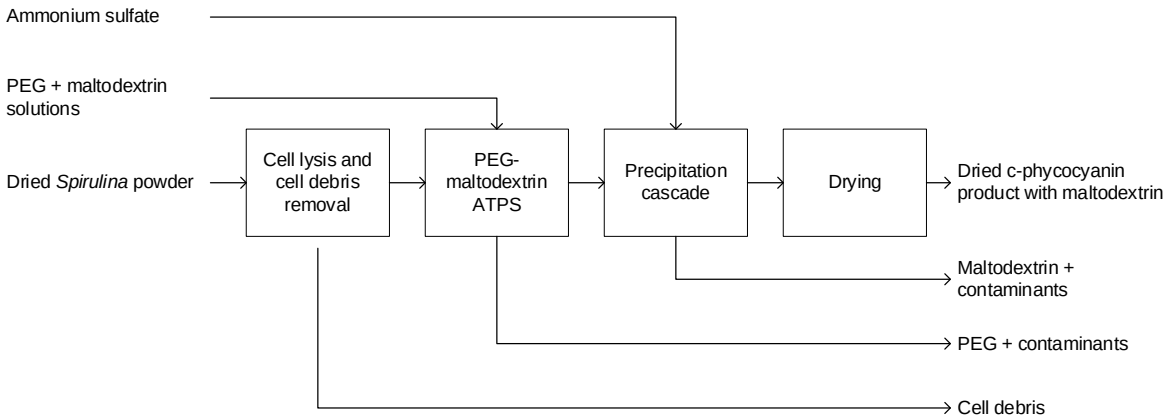

Figure 1. Block flow diagram of the CeBER patented extraction and purification process to obtain c-phycocyanin from *Spirulina*. The diagram has been simplified to only show key chemical streams, excluding more generic components such as water.

ATPS systems for c-phycocyanin purification comprising of a PEG-salt system where the salt is typically phosphate or citrate, have been commonly reported in literature. These PEG-salt systems yield partitioning of the majority of the c-phycocyanin to the PEG phase (Pathil & Raghavarao, 2007). The rationale behind the choice of a PEG-maltodextrin ATPS system for the CeBER patented process is because it is difficult to separate the c-phycocyanin from the PEG phase. The maltodextrin has the additional benefit of helping to stabilize the c-phycocyanin protein such that it has a higher resilience to heat and making it better for long term shelf storage (Agustina, et al., 2019). For food and cosmetic use, the trace compounds in the final product may compromise the safety of the product according to legislature protecting consumer goods. Maltodextrin is, however, considered GRAS (generally recognized as safe) according to the U.S. Food and Drug Administration (2022). Maltodextrin is often used as a supplement for carbohydrates for human consumption (Wilburn, et al., 2020). As such, it is not as important to fully separate the c-phycocyanin from the maltodextrin phase.

Optimization work was performed by Hockey (2020) on the CeBER patented process, with the key findings of their work study presented in the Literature Review. Hockey (2020) recommended having a two-step ATPS, with the first being a PEG-citrate salt system to get good purity and thereafter a PEG-maltodextrin system to get c-phycocyanin out of the PEG phase and into the maltodextrin phase whilst further increasing purity. Hockey (2020) also recommended adding filtration and adsorption options as post- and pretreatments, respectively, to further increase purity. This dissertation will build upon the foundation of the key findings of Hockey (2020), to further the understanding of the process and prepare for the next phase of commercialization, with emphasis on process unit operation parameters and scale-up. A collaboration with an industry partner, anonymized as Company A, commenced following the initial move towards scale-up preparation. Company A has a keen interest in establishing a pilot plant for the CeBER patented process.

1.2 Focus and scope of this project

1.2.1 Focus

The focus of this project will be to explore the downstream processing units of the CeBER patented extraction and purification process to obtain c-phycocyanin from *Spirulina*. The main aim of this project is to investigate the operating conditions for the bead-milling, c-phycocyanin leaching, cell debris removal via centrifugation, ATPS using PEG-citrate and PEG-maltodextrin systems, ammonium sulfate precipitation and filtration downstream processing steps, to yield a c-phycocyanin product of the highest purity ratio possible. Overall, the goal is to achieve a cosmetic grade purity c-phycocyanin product whilst maintaining a high recovery across the entire process.

Experiments at a laboratory scale will be carried out to inform the operating conditions of the individual steps, such that these operating conditions can inform a robust operation of a pilot scale system. The pilot scale system target (as agreed with Company A) is a throughput of 20 kg of dry weight *Spirulina* powder per batch/run.

This project will thus focus on informing the inclusion/exclusion of unit processes, equipment types for these unit processes and operating conditions of said equipment types at the pilot design scale. These decisions will be made whilst considering robust operation and the overarching aim. Generated data at laboratory scale will be used to inform the procurement of equipment for the pilot scale system.

1.2.2 Scope

Although this project will aim to generate data that can inform a more robust pilot scale plant compared to current lab scale process, experimentation will be limited to laboratory scale – no experimental data at an upscale will be included..

To assess the robustness of individual unit processes for this extraction and purification process, this project will make use of three different feedstocks of dried *Spirulina* powder from different suppliers. These suppliers were chosen based on their potential to supply the pilot scale or scale greater than that with dried *Spirulina* powder. Hence, the robustness testing will also allow for us to confirm what type of feedstock is preferred (from amongst the three) and, as such, will give a preliminary indication of which supplier to consider for the upscale of the project. The project will be limited by not using fresh *Spirulina* as a feedstock. Laboratory scale experiments of the full runs of process will be performed at a scale of 100 g of dried *Spirulina* powder per run whereas robustness testing of unit procedures will be performed at similar or smaller scales.

A high-level robustness analysis of unit procedures such as bead-milling and aqueous two-phase separation systems will be performed in this study. This is because their operating parameters have already been established and described during the optimization described by Hockey (2020). As such more optimization is considered to be redundant.

1.3 Structure of dissertation

This Chapter 1 (Introduction) is followed by Chapters covering the Literature Review, Approach to Project and Methodology, Results and Discussion, Conclusions and Recommendations.

Chapter 2, the Literature Review, delves into the details of the target protein (c-phycocyanin) and its properties and value. Thereafter, c-phycocyanin quality control is discussed. The dissertation then covers the overarching main procedures needed to extract and purify c-phycocyanin from *Spirulina*. Following this, the specific unit procedures outlined in the work of Hockey (2020) are discussed as they form the framework upon which this dissertation is based. The key areas of the CeBER process for c-phycocyanin extraction process from *Spirulina* are then explored, namely bead-milling, leaching, cell debris removal, aqueous two-phase separation, ammonium sulfate precipitation and filtration. It is explained what these unit procedures are and findings pertaining to these unit procedures in the context of c-phycocyanin extraction and purification from *Spirulina* and other sources are discussed. Robustness and Process Design are then covered, including what makes a process robust and the importance of having a robust process, especially when there is potential for scale-up. The Literature Review closes with a discussion of the gaps in literature with regards to extraction and purification of c-phycocyanin from *Spirulina*, considering the context of this project and the framework set by Hockey (2020). These gaps inform the problem statement, research objectives and key questions posed to guide the subsequent chapters of this dissertation.

Chapter 3, Approach to Project and Methodology, gives an overview of which methods were used to generate the results presented in the subsequent results sections. It includes a detailed description of experiments performed, with inclusion of experimental conditions, equipment used, and materials used. Chapter 3 justifies how these methods and experiments were used to generate answers to the key questions posed in Chapter 2. It also explains how different experimental blocks relate to each other, thus informing the link between results of different experimental blocks.

Chapter 4, Results and Discussion, is broken up into subchapters pertaining to the different key areas of the CeBER process for c-phycocyanin extraction and purification from *Spirulina*. The results of each subchapter lead on to each other, in the same way as the experimental blocks do since they are also specific to the unit procedures of the extraction and purification process. As such, the discussion for each subchapter refers to the results of the previous subchapter, i.e. cell debris removal results and discussion refers to the results and discussion of the particle size distribution subchapter. The final subchapter is on the overall process, where the results obtained are generated using a methodology that is based on the results yielded in the preceding subchapters. The final subchapter presents a culmination of choices made based on the results of the preceding subchapters, which includes some optimization of operating conditions and revision of process unit procedures.

Chapter 5, Conclusions and Recommendations, contains the final conclusions of the dissertation and discusses recommendations for future work that would help complement this dissertation in terms of understanding of phenomena that was presented in the results of Chapter 4. It also includes recommendations that may further support claims made in the conclusions or provide clarity on unknowns mentioned in the conclusions.

2 Literature Review

2.1 c-Phycocyanin

2.1.1 Phycobiliproteins

c-Phycocyanin is a blue pigment found in cyanobacteria (Ramos, et al., 2010). It falls under a group of proteins called phycobiliproteins (PBPs). PBPs form a subset of light-capturing proteins, and are proteins that are covalently bound to bilin, a biological-pigmented arrangement of tetrapyrroles (Dufossé, 2018). As such, these proteins are known as chromoproteins (colour proteins). Owing to their chemical nature, phycobiliproteins express solubility in water. PBPs are abundantly found in microalgae of the classes *Cryptophyceae*, *Cyanophyceae* and *Rhodophyceae* (Dufossé, 2018) wherein they play the role of primary photoreceptor for photosynthesis (Singh, et al., 2015). PBPs are categorized by the wavelength of light that they are best able to absorb (λ_{max}) (Kuddus, et al., 2013). These subclasses are: phycoerythrin, pink-purple with λ_{max} = 540 – 570 nm; phycoerythrocyanin, orange with λ_{max} = 560 – 600 nm; c-phycocyanin, blue with λ_{max} = 610 – 620 nm; and allophycocyanin, blue-green with λ_{max} = 650 – 655 nm (Kuddus, et al., 2013). Phycobiliproteins perform their function as pigments by harvesting solar energy in the range beyond that of chlorophyll (λ_{max} = 450 nm) absorption (Dufossé, 2018).

The light absorbing properties of phycobiliproteins encourages the application of these proteins in biomedical research, therapeutics and diagnostics – in which they are used as fluorescent markers (Glazer, 1997). There has also been a growing trend in the food and beverage markets to push towards more natural, clean and biologically safe products which has promoted the use of phycobiliproteins which satisfy all of these requirements (Dufossé, 2018). Additionally, colourants in these industries need to exhibit heat and light stable properties (Dufossé, 2018). Microalgal colourants such as c-phycocyanin have been proved to express these characteristics (Dufossé, 2018; Glazer, 1997).

2.1.2 Phycobilisomes

Phycobiliproteins, such as c-phycocyanin, are found in supramolecular units called phycobilisomes (PBSs), typically within proximity of the light harvesting organelle of cells (Kraan, 2013; Dufossé, 2018). PBSs are amalgamations of organic molecules, including phycobiliproteins, comprising of a core molecule with peripheral rods in a fan-like arrangement around the central molecule (Watanabe, et al., 2012; Singh, et al., 2015). The central molecule and surrounding rods are comprised of phycobiliproteins, with linker proteins providing stability (David, et al., 2011).

PBSs are found as particles on the surface of the thylakoid (Kraan, 2013) – a membrane-bound organelle that accommodates photosynthesis in chloroplasts and cyanobacteria (Helmenstine, 2019). This is unlike the non-soluble chlorophyll pigment which is found embedded within the thylakoid membrane (Kraan, 2013).

PBSs make up the majority (approximately 60%) of the total protein content in cyanobacteria (Singh, et al., 2015). These photoautotrophs make use of phycobilisomes to harvest and transduce solar energy before transferring this energy to the photosynthetic reaction centre (Singh, et al., 2015). PBSs also function as an emergency reservoir of nitrogen, sulfur and carbon (Parmar, et al., 2011).

2.1.3 Properties and uses

c-Phycocyanin is a polymer that exists as trimers and hexamers, meaning that molecules of c-phycocyanin comprise of either three or six monomers. These c-phycocyanin molecules have been found to have molecular weights of approximately 113 kDa and 225 kDa, respectively (Stec, et al., 1999). The monomers of c-phycocyanin itself, can be perceived as having two subunits, namely the α- and β-chains whose molecular weights are approximately 19.5 and 21.5 kDa, respectively (Sørensen,

et al., 2013). c-Phycocyanin expresses pH stability in the neutral to weakly acidic range of pH 5.0 to 7.5 measured at a temperature of 9 °C, and it remains stable at temperatures up to 40 °C (Sekar, 2008).

c-Phycocyanin is best able to absorb light with a wavelength of 610 – 620 nm (Kuddus, et al., 2013). The ability of c-phycocyanin to absorb this wavelength of light is responsible for its blue colour. As a result of its blue colour, c-phycocyanin is used in the food and cosmetic industries as a natural alternative to toxic, synthetic dyes and is also used as a colourant in pharmaceutical products (Glazer, 1997; Dufossé, et al., 2005). An example of this is that c-phycocyanin has replaced a synthetic blue dye used in smarties, where that synthetic dye is shown to have contributed towards symptoms of attention deficit hyperactivity disorder (Klein & Buchholz, 2013). It has additionally been ascertained that c-phycocyanin has anti-carcinogenic, anti-inflammatory and anti-oxidative properties (Glazer, 1997; Kuddus, et al., 2013) and is thus extremely lucrative to all three industries. As with other phycobiliproteins, high purity c-phycocyanin can be used in fluorescent marking in immunological studies and in associated diagnostic roles in biomedical research (Glazer, 1997).

The market for c-phycocyanin has been reported to have a compounded annual growth rate of 9.8 % projected for the period between 2023 and 2030 (Verified Market Research ®, 2024). The market forecast suggests that the total global revenue for the c-phycocyanin market will reflect a greater than 2× increase over this period, to 364 million USD (Verified Market Research ®, 2024). The selling price of c-phycocyanin depends on the purity and hence application of the product.

2.1.4 Sources and production

The production of c-phycocyanin by microorganisms can differ depending on the nutritive method of said microorganisms. Autotrophic, heterotrophic and mixotrophic production are all possible routes for the production of c-phycocyanin. The most prolific production method is the autotrophic method, more specifically photoautotrophic production, which is a nutritive system where the light (typically sunlight in nature) provides the energy for the production and atmospheric carbon dioxide is the primary inorganic carbon source (Erikson, 2008). In this photoautotrophic manner, c-phycocyanin producing cyanobacterial species like *Spirulina* can be cultivated at a large-scale outdoors (Erikson, 2008). Heterotrophic production has been achieved in *Galdieria sulfuraria,* where strains requiring only an organic carbon source were used (Sørensen, et al., 2013). Mixotrophic production can be described as the method where photosynthetic microorganisms are cultivated in media with organic carbon sources – this is typically done in sealed photobioreactors (Kuddus, et al., 2013). The organic carbon sources serve as secondary energy and biomass sources for the microorganisms to promote further production of c-phycocyanin and other proteins. This mixotrophic production was reported by Boussiba & Richmond (1979) using *Spirulina platensis*. Table 1 summarizes the naturally occurring c-phycocyanin contents of cyanobacterial and microalgal species most commonly used for c-phycocyanin production. It must be noted that by using recombinant methods, higher c-phycocyanin cell contents may be achieved. c-Phycocyanin content is also a function of light wavelength, light intensity and nitrogen availability (Hsieh-Lo, et al., 2019).

Spirulina species exhibit some of the higher wt % c-phycocyanin content and, as such, it is the most commonly used source of c-phycocyanin. Another reason for this is the ease with which *Spirulina* can be grown outdoors in raceway ponds and the fact that these raceway ponds or other culturing methods can be carried out at a large scale (Kuddus, et al., 2013). This supports the use of *Spirulina* for the feedstock of this extraction process.

Spirulina is also used as a source of lipids and other proteins, with the high protein composition making it a lucrative source material for certain animal feeds, etc.

Table 1. Summary of c-phycocyanin cell contents of microorganisms typically used for c-phycocyanin production

Microorganism	c-phycocyanin content (dry wt %)	Reference
Anabaena sp.	~ 10 %	(Moreno, et al., 1995)
Galdieria sulphuraria	~ 3 %	(Graverholt & Eriksen, 2007)
Nostoc sp.	~ 12 %	(Shukia, et al., 2008)
Phormidium fragile	~ 13 %	(Shukia, et al., 2008)
Spirulina fusiformis	~ 16 %	(Minkova, et al., 2003)
Spirulina platensis	~ 12%	(Boussiba & Richmond, 1979)

2.2 c-Phycocyanin quality control indicators

There are many quality indicators of a protein product like c-phycocyanin. Industrial standards of quality are determined by three principal measurements namely: purity ratio, colour intensity and bacterial loading. This has been included in the Literature Review since it informs the understanding of these principle measurements that are quoted throughout literature pertaining to the concentration and purity of c-phycocyanin.

2.2.1 Purity Ratio

The purity ratio (sometimes referred to as *purity number*) of c-phycocyanin is the ratio of absorbance readings (A) at different wavelengths (Erikson, 2008), as shown in Equation 1:

$$Purity\ ratio = \frac{A_{620}}{A_{280}} \qquad \text{Equation 1}$$

The absorbance at 620 nm wavelength of light is the maximum absorbance of c-phycocyanin. The absorbance at 280 nm is the maximum absorbance for the total present amino acids in solution. This the purity ratio gives a quantification of c-phycocyanin present to other amino acids present in the product sample (Erikson, 2008). This c-phycocyanin purity ratio can be used to compare results across literature as well as to compare results of this dissertation with said literature results.

In section 1, it was mentioned that included in the many uses of c-phycocyanin was the option of using high grade c-phycocyanin for fluorescent marking – this analytical grade c-phycocyanin can be described as having a purity ratio greater than 4.0 (Guan, 2016). Similarly, food, cosmetic and reactive grades have corresponding purity ratios as shown in Table 2.

Table 2. Summary of the purity ratios for different quality grade c-phycocyanin

Grade	Purity ratio	Reference
Food	0.7 ≤	(Song, et al., 2013)
Cosmetic	1.5 – 2.5	(Guan, 2016)
Reactive	3.9 <	(Rito-Palomares, et al., 2001)
Analytical	4.0 <	(Guan, 2016)

2.2.2 Concentration and colour intensity

The chief use of c-phycocyanin is as a colourant. Because of this, companies using c-phycocyanin often have a requirement for the colour intensity of the c-phycocyanin they buy from producers. The colour intensity of c-phycocyanin can be regarded to be a function of the concentration of c-phycocyanin in the product extract which is directly related to the maximum absorbance of c-phycocyanin, absorbance at 620 nm wavelength, as put forth by Bennet and Bogorad (1973):

$$C_{c-PC}\ (mg/mL) = \frac{A_{620} - 0.474 * A_{650}}{5.34} \qquad \text{Equation 2}$$

Su, et al. (2014), used this equation from Bennet and Bogorad (1973) and other authors use the same equation with a <1% difference in wavelengths when quoting concentration of c-phycocyanin. The method used to yield Equation 2 was with extinction coefficients. Bennet and Bogorad (1973) used *Fremyella diplosiphon* as the microbial source of c-phycocyanin. The same methodology was applied by Yoshikawa and Belay (2008) to determine extinction coeffficients and as a result a new equation for the concentration of c-phycocyanin based on the same wavelengths but used *Spirulina* as their microbial source of c-phycocyanin. The equation they derived with the *Spirulina* extinction coefficients was:

$$C_{c-PC} = 0.162 \times A_{620} - 0{,}098 \times A_{650} \qquad \text{Equation 3}$$

Both equations are important since Equation 2 is used widely throughout literature on c-phycocyanin and as such is better for comparison between literature sources, however Equation 3 is more pertinent since it was developed using c-phycocyanin sourced from *Spirulina*. These equations can be used to calculate mass of c-phycocyanin in feed and product streams at various stages of a recovery and purification process and hence recovery across unit procedures can be presented, allowing for recovery comparisons between different process routes in literature and this dissertation.

2.2.3 Bacterial contamination

The bacterial contamination in the final c-phycocyanin product is important to note as there are strict guidelines in place to ensure that any food products are not compromised by the contamination of undesirable microorganisms (Holban & Grumezescu, 2018). Bacterial contamination can be determined using either analytical methods or plate-streaking can be used for preliminary quantification. Bacterial contamination is typically quantified using a measurement of colony forming units (CFU) per unit mass.

For the purpose of quantifying bacterial contamination for a food product, an external laboratory analysis has to be conducted since the speciation information provided is necessary as a supplement when producing a food product (Holban & Grumezescu, 2018). There is no literature on the bacterial contamination allowed in particular products. Instead, this requirement will be specified by potential buyers of a c-phycocyanin product.

2.3 c-Phycocyanin protein extraction and recovery procedures

This subchapter is dedicated to giving a broader understanding which extraction and recovery methods can and were previously used to extract and recover c-phycocyanin. Some downstream configurations are also listed in this subchapter to get an understanding of how broad the variety of options are.

To recover and purify microbial metabolites from cell cultures, different process routes can be taken depending on where the desired metabolite is located (Doran, 1997). Figure 2 shows that when the desired product is located intracellularly, as is the case with c-phycocyanin in *Spirulina*, the downstream recovery process is much more intensive than the cases of an extracellular product or when the cell is the product itself (Doran, 1997). It is, therefore, important to find equipment pieces to carry out these

recovery and purification procedures effectively and efficiently. The cell disruption, cell debris removal, primary isolation, product enrichment and final isolation steps (Figure 2) are the only steps that are relevant to the extraction process in this thesis, since the *Spirulina* feedstock will not be cultivated in the lab for this process but rather purchased as a raw material to the extraction process.

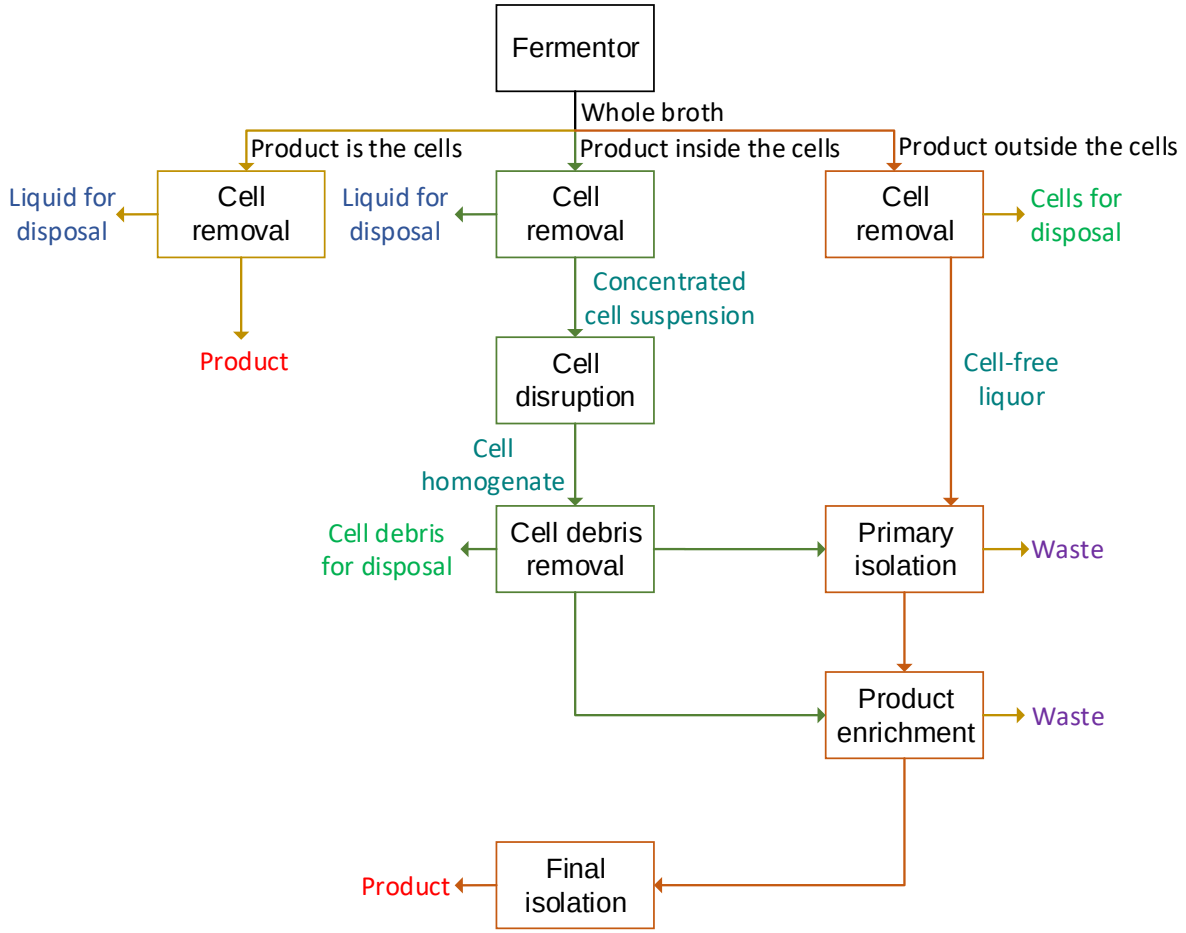

Figure 2. Different downstream processing routes available for recovery of microbial metabolites [adapted from Doran (1997)].

2.3.1 Cell disruption

Since the desired c-phycocyanin product is located intracellularly, the extraction process must include a cell disruption step to liberate the product from within the cells. For the extraction of c-phycocyanin from cyanobacteria like *Spirulina*, which are small in size compared to other eukaryotic algal species, there is no conventional method of cell lysis employed. Figure 3 shows the main methods used in general for cell lysis to liberate intracellular products of microorganisms. For c-phycocyanin liberation specifically, reported methods include freeze-thawing (Minkova, et al., 2003), phosphate buffer leaching of dried cells (Chaiklahan, et al., 2011), ammonium sulfate hypotonicity lysis (Niu, et al., 2007), osmotic shock (Boussiba & Richmond, 1979) and bead-milling (Scheer & Kufer, 1977). Table 3 presents some the purity and recovery results for c-phycocyanin across different recovery and purification process routes for c-phycocyanin from algal sources. Guan (2016) reports that for a poorer cell breakage, the subsequent leaching time can be lengthened to recover all desired product in the liquid phase.

Many of the reported cell lysis techniques used for c-phycocyanin liberation from *Spirulina* are carried out only at a lab scale. When being scaled-up, the use of consumables for chemical or biological methods of cell lysis becomes expensive and increases the operating costs immensely (Seider, et al., 2017). This is one of the reasons why mechanical methods are preferred at a pilot scale (and at larger

scales) for cell lysis. Thus, emphasis on a technoeconomic analysis of the process route needs to be understood at scale. Many studies exist where this type of analysis was performed to inform the unit procedures chosen for their recovery and purification methods for high value products like microalgal metabolites including pigments (Chauton, et al., 2015; Grima, et al., 2003; Kroumov, et al., 2017) . This type of analysis falls out of the scope for this dissertation but is important to note and discuss.

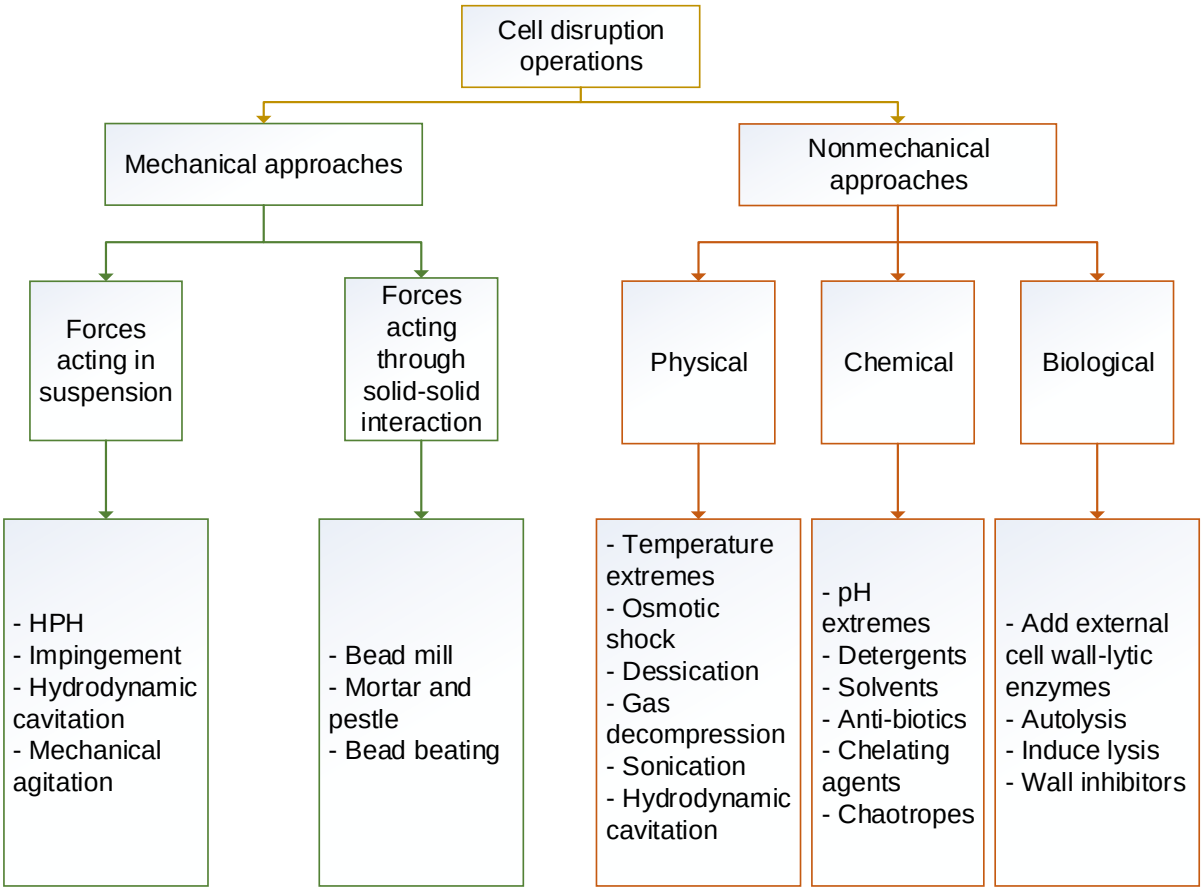

Figure 3. Cell disruption operations for intracellular product liberation [adapted from Harrison (2011)].

2.3.2 Cell debris removal

Cell debris removal is typically the first technique employed in the manner of separation in a downstream processing train for protein products. It is typically a form of solid-liquid separation that removes large cell components like cell wall debris from the process. Centrifugation and filtration are the most used techniques to eliminate cell debris from the liquid extract (Harrison, et al., 2013). These techniques will be reviewed in more detail at a later stage of the dissertation (See Subchapter 2.5)

2.3.3 c-Phycocyanin recovery and purification

Following the disruption of the cells and liberation of the intracellular c-phycocyanin into solution, various purification steps can be used towards preparing the final desired product. Table 3 shows a summary of different methods of c-phycocyanin purification from *Spirulina*, also giving the method of c-phycocyanin extraction from the cells. The most notable trend observed from studies is that the purity of the product increases with the number of extraction and recovery steps included in the downstream processing train. It must be noted that the majority of the studies presented in Table 3 were performed at a lab scale.

Most of the documented research pertaining to c-phycocyanin from *Spirulina* is around the extraction and purification of c-phycocyanin to a high grade – higher than the grade for use in food and cosmetics. Chaiklahan et al. (2011) reported a product purity ratio in the range of food grade c-phycocyanin using a single purification step with a good recovery. What is important to take from this summary is that ATPS operation as part of the downstream processing train offers the possibility of a good recovery, better than most, as reported by Pathil & Raghavarao (2007). With a trade-off between purity and recovery, a process may be obtained that can produce a lot of product at the required (lower) purity specification.

Table 3. Comparison of different extraction and purification processes for c-phycocyanin from literature

Reference	Cell disruption step to extract c-phycocyanin	Main c-phycocyanin purification steps	Overall recovery	Final product purity ratio
(Minkova, et al., 2003)	Freeze-thawing, phosphate buffer	Rivanol, ammonium sulfate precipitation, sephadex gel filtration, final ammonium sulfate precipitation	46 %	4.3
(Chaiklahan, et al., 2011)	Phosphate buffer	Membrane filtration	82 %	1.07
(Niu, et al., 2007)	Ammonium sulfate hypotonicity lysis	Expanded bed chromatography, anion-exchange chromatography	5 %	>3.2
(Ramos, et al., 2010)	Sodium phosphate buffer (3 step)	Expanded bed adsorption chromatography, packed bed chromatography	62 %	>4
(Bhaskar, et al., 2005)	Liquid nitrogen, phosphate buffer and crushing	Ammonium sulfate precipitation, dialysis and gel filtration chromatography	-	4.98
(Pathil & Raghavarao, 2007)	High pressure homogenization	Polyethylene glycol-potassium phosphate ATPS and ultrafiltration	85%	3.52*

*in a single ATPS extraction step, 4.05 was obtained as a purity ratio for multiple steps

A more detailed review of literature concerning relevant extraction and purification methods will follow on later in the dissertation.

2.3.4 Drying formulation

Drying is usually the concluding step in the formulation of a final protein product like c-phycocyanin. Both spray drying and freeze drying have reportedly been used to achieve a desired moisture content in the final product protein (Abdul-Fattah, et al., 2007). This is an important formulation step for processes using precipitation since the preliminary product stream will contains large quantities of water. Freeze drying has been used extensively for the final formulation of reactive grade phycobiliproteins (Herrera, et al., 1989; Patel, et al., 2005; Roman, et al., 2002).

Spray drying uses temperatures typically around 60 °C and operates using evaporation. It is much cheaper than freeze dryers as there is a lower level of control of the extent of drying achieved by a spray dryer. In principle, the spray dryer subjects the wet sample to hot air/gas which passes through the wet sample and carries water out of the sample. The high temperature of spray dryers often causes protein products to denature to some extent and thus some loss is to be expected in this formulation step. However, they can be customised and their operating conditions set to avoid denaturing protein products, such as c-phycocyanin.

Freeze dryers are much more expensive as they require refrigeration and sub-atmospheric pressure for operation. They operate on the principle of sublimation of frozen water particles: The wet sample is frozen, and the pressure of the container is decreased and then the temperature is increased, owing to the low pressure generated the ice sublimes into water vapour.

Owing to the relative cost of spray drying being cheaper it has become conventional for commercial formulation of protein products (Vazquez-Romero, et al., 2022).

2.4 Extraction and purification process from Hockey (2020)

This subchapter is dedicated to the previous work performed by Hockey (2020) on the CeBER extraction and purification process. This will serve as a guide to the rest of the literature review as it contextualizes the framework upon which the results yielded in this dissertation are based on.

2.4.1 Key findings

Hockey (2020) describes a process using bead-milling, leaching, a PEG-citrate ATPS, a PEG-maltodextrin ATPS and finally ammonium sulfate precipitation. The dissertation by Hockey described the process that is being subject to robustness testing and optimization, where applicable in this dissertation. It is therefore important to understand the key findings and from Hockey (2020) to fully grasp the context of the work described in this dissertation. Some of the key findings of Hockey (2020) are as follows.

Bead-milling was found to be relatively unnecessary for their work, due to the *Spirulina* cells in the dried powder used already being in a lysed state. For the *Spirulina* powder used, the leaching was shown to take around 24 hours to reach an equilibrium concentration. The leaching was performed at 4 °C. Multiple ATPS configurations were tested, including PEG-maltodextrin and PEG-citrate systems. The PEG-citrate and PEG-maltodextrin ATPSs performed as expected to further increase the purification factor over the ATPS step. They were optimized in terms of polymer molecular weights and weight percentages of components. PEG 4000 was found to be most optimal for the two-stage ATPS recommended, in which a PEG-citrate ATPS is followed by a PEG-maltodextrin ATPS.

The data generated in terms of recoveries and purities can be considered as reliable up until the ATPS stage since these data were generated through physical experiments and analytical methods. The data generated in terms of recoveries and purities downstream of the ATPS stage were obtained via the use of simulation software.

Hockey proposed that using an adsorption technique in the leaching step will allow for a better purification factor over the further downstream processing steps to be realized. Adsorption using chitosan and/or activated charcoal has been shown to improve c-phycocyanin purity ratio in the crude for c-phycocyanin from *Spirulina* (Fekrat, et al., 2018)

Hockey also suggested that filtration be used as a purification step in the process as many studies have been performed on filtration as a purification method after an aqueous two-phase separation system for c-phycocyanin purification. Ultrafiltration has been shown to perform well with removal of PEG molecules from c-phycocyanin product solution (Rito-Palomares, et al., 2001; Pathil & Raghavarao, 2007; Sørensen, et al., 2013).

2.4.2 Process description

Figure 4 is adapted from Hockey (2020) and serves to illustrate the proposed extraction and purification process for c-phycocyanin from *Spirulina*.

The main feed (900 mL deionized water, 5.6 $g.L^{-1}$ of citrate buffer (92 % trisodium citrate and 8 % citric acid for pH 6) with 111 $g.L^{-1}$ dried *Spirulina* powder) is fed into the bead-mill. The slurry is milled for 15

min before being fed through a sieve of 180 µm aperture. The resultant slurry is left to leach for 2 hours at 4 °C. This slurry is then centrifuged at 7000 g for 40 min and the liquid stream being approximately 400 g is fed into an ATPS system where PEG 4000 and citrate (pH 6, same composition as buffer) is introduced to 20 wt % and 11 wt %, respectively. This mixture is stirred for 20 min before being centrifuged at 7000 g for 30 min. The top phase containing PEG and the product c-phycocyanin is sequestered and introduced into another ATPS system by addition of maltodextrin and deionized water to 22 wt % and 67 wt %, respectively. This mixture is mixed for 20 min at 250 rpm before being centrifuged at 7000 g for 30 min. The resultant bottom phase is sequestered using hydraulic pumping and is subject to ammonium sulfate precipitation using ammonium sulfate addition to a concentration of 298 g/L, the subsequent precipitate pellet is then dissolved in deionized water of 1 L and ammonium sulfate is added again to a concentration of 410 g/L and the pellet sequestered, and spray dried to formulate the final powdered product.

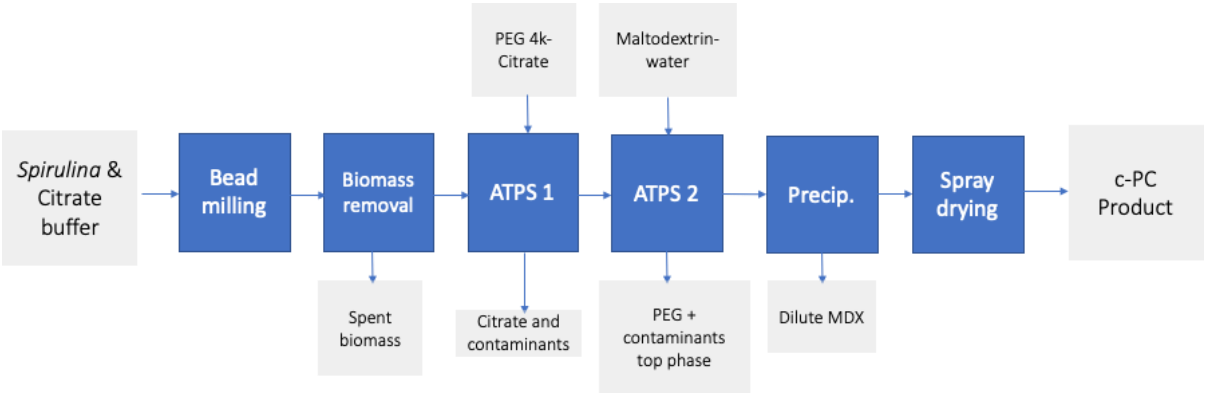

Figure 4. Proposed CeBER extraction process for c-phycocyanin from *Spirulina* completed at lab-scale, as described in Hockey (2020).

2.5 Individual unit processes studied

This subchapter will delve into the unit processes recommended as the way forward from Hockey (2020). The mechanisms of operation for unit processes will be discussed. The section on bead-milling does not go into great detail since this was a major focus of Hockey (2020) and this dissertation does not include significant testing of the bead-milling optimization but rather the downstream implications of the bead-milling conditions recommended by Hockey (2020).

2.5.1 Bead-milling

Bead-milling is a mechanical method of cell disruption in which a cell suspension and glass or metal beads are subject to high-speed agitation by a rotating agitator within the milling chamber (Green & Perry, 2008). The milling is driven by an impeller that mixes the contents of the milling chamber (beads and slurry). Without being well-mixed the cells in the bead mill will not collide with the beads. It is therefore a system partly driven by mixing in a solid-liquid system.

Bead-mills have a controllable residence time (Green & Perry, 2008). There are methods such as that developed by Jorg Schwedes for the selection of the correct grinding media, i.e. bead size that is related to the kinetic energy of the beads and the frequency of collisions (Kwade, et al., 1996). For any type of substance to be subject to milling, there is a critical stress value that needs to be overcome before the effects of the milling can be observed (Green & Perry, 2008).

The extent of bead-milling can be described by the stress intensity and stress frequency. Both of which are representatives of energy input. Stress intensity is given by (Kwade, et al., 1996):

$$SI = (\rho_m - \rho) D_m^3 V_t^2$$ Equation 4

And stress frequency is given by (Kwade, et al., 1996):

$$SF = \omega(\frac{D_m}{D})^2 t$$ Equation 5

Where:

ρ_m	Media density (kg.m^{-3})
ρ	Slurry density (kg.m^{-3})
D_m	Media diameter (m)
D	Diameter of vessel (m)
V_t	Impeller tip speed (m.s^{-1})
ω	Rotational speed (s^{-1})
t	Time milled (s)

In order to see any grinding action, a certain threshold stress intensity must be overcome. The stress intensity is also related to the median of the grinded particles (Green & Perry, 2008). The stress frequency describes the probability that a particle is caught between two grinding beads and is stressed (Kwade, et al., 1996). The stress frequency is a dimensionless number and governs the probability of cell breakage – as such it is an important dimensionless number to consider in the scale-up of a bead mill.

Bead-mills range in size from 1 to 1000 dm^3 volume. Installed power of up to 320 kW is possible for bead-mills. The Reynolds number can be related to the power drawn by the mill (Green & Perry, 2008). The orientation of a bead-mill may be vertical or horizontal, however for a vertically orientated mill, the stirrer speed needs to be high enough to fluidize the system to avoid particles packing the bottom of the milling chamber (Green & Perry, 2008). This typically yields for a higher stirrer speed requirement; however, it allows for easier removal of slurry post milling, especially in continuous operation.

The following variables affect the performance of the bead mill according to Green & Perry (2008): impeller tip speed, size of beads, bead charge, feed concentration, density of beads, temperature, design of blades, shape of mill chamber (or baffles), residence time. For example, impeller tip speed has been shown to increase in the rate of protein released from microorganisms such as baker's yeasts, up to a point (Chisti & Moo-Young, 1986); at a certain tip speed there was no significant increase in the rate of protein release.

2.5.2 Leaching

Leaching is the process of a soluble component being extracted from its carrier into a solvent. The mechanism of leaching is governed by mass transfer between the carrier and the solvent (Seikova, et al., 2004). The rate of leaching is crucial when designing an extraction process, especially within the context of intracellular compounds like c-phycocyanin (Ho, et al., 2005). A higher rate of leaching is preferred as it allows for a shorter time on stream to produce product. Owing to the water-solubility of c-phycocyanin, aqueous solvents have typically been used for the extraction of c-phycocyanin from *Spirulina* (Silveira, et al., 2007). Leaching allows for the liberation of c-phycocyanin from the surface of the thylakoid membrane where phycobilisomes (containing pigments like c-phycocyanin) are located, in cyanobacteria (Kraan, 2013; Harouna-Oumarou, et al., 2007).

In solid-liquid extraction, the solid structure containing the desired soluble compounds can be considered inert, however the morphology of the solid can affect the mass transfer and thus the kinetics

of the leaching (Harouna-Oumarou, et al., 2007). By Fick's law of diffusion, the diffusion of a soluble compound from the solid into the liquid is driven by the concentration gradient between that soluble compound in the solid and in the bulk liquid. During the mass transfer the concentration gradient will tend towards and reach equilibrium (Green & Perry, 2008), at which point mass transfer of the soluble compound is negligible.

When a relatively infinite quantity of substance is being leached into a solvent, a point will be reached where no more substance can be dissolved in the solvent. This is known as the saturation point of the substance in the solvent. This point of saturation is reached when the concentration of solute in the solvent equals the solubility of the solute in that solvent. Solubility can be defined as the maximum amount of solute that can be dissolved in a solution at a fixed temperature. A pseudo-saturation point can be reached when the concentration gradient of solute in the solid and in the bulk liquid is in equilibrium. At both the saturation and pseudo-saturation point, an increase in the solute concentration will no longer be observed. It would be preferred to have the operating conditions set to not reach a point where solubility is the limiting mechanism of leaching and rather equilibrium due to concentration gradient being null, since this equilibrium can be shifted by adding more liquid (Green & Hughes, 1955).

An optimization of leaching can be considered as changing conditions of leaching such that the system reaches the saturation point in the shortest time possible as well as increasing the solubility of the solvent such that the maximum amount of desired solute can be dissolved in the solvent (Green & Hughes, 1955). In the context of leaching intracellular products from disrupted microorganisms, optimizing leaching will result in a shorter time on stream and a higher recovery of the desired intracellular products in the leachate.

The rate of leaching is dependent on the operating conditions of the leaching which affect the mass transfer from the carrier to the solvent. These factors include temperature, type of solvent, solid-liquid ratio, solid particle size and impeller speed (Elgayar, et al., 2016; Su, et al., 2014).

It is important to note that comparison of leaching results across literature sources even for the same leaching conditions cannot be normalized without understanding the starting concentration of c-phycocyanin in the microalgal source. This information is not readily found in literature, and as such the percentage of liberated c-phycocyanin cannot be calculated and compared. Thus, yield of c-phycocyanin per unit mass of microalgae cannot be a true reflection of the percentage c-phycocyanin liberated nor can it be a true reflection of the efficiency of a particular leaching set-up. Only intra-experimental comparisons can be made in terms of efficiency. Table 4 shows that the ranges for c-phycocyanin purity ratio and yield are wide, but this cannot be solely attributed to the differences in process conditions.

Table 4. Summary of c-phycocyanin (c-PC) purity ratios and yield of c-PC per unit mass of microalgae for different cell liberation techniques and leaching times

Extraction method	Leaching time (h)	Crude extract c-PC purity ratio	c-PC yield($mg.g^{-1}$)	Reference
Homogenization	4	0.59	-	(Antelo, et al., 2010)
Microwave assisted	25/60	1.27	57	(Aftari, et al., 2015)
Mechanical shearing; freeze-thawing		0.42; 0.48	-	(Guan, 2016)
Bead-milling	26	0.63	55	(Hockey, 2020)
Bead-milling	1	0.60	82	(Moraes, et al., 2010)
Homogenization	4	0.46	46	(Silveira, et al., 2007)

Leaching kinetics

It is important to predict the rate of leaching under the operating conditions of the extraction process, as such, predictive kinetic models are typically developed for this. Mass transfer kinetics of a leaching system can be described by two theoretical stages. Firstly, the contact between the solid and the liquid which causes the solubilization of soluble compounds. Secondly, transfer of soluble compounds from inside the solid into the bulk liquid through diffusion. Furthermore, a third stage can be described when the concentration of solute in the bulk liquid is decreased by adding more liquid to increase the concentration gradient and allow for more of the desired compound to be leached (Schwartzberg & Chao, 1982).

Ho, et al (2005) shows how solid-liquid extraction can be considered as the reverse of adsorption and as such first order kinetics that describe adsorption can similar be used to describe leaching. Other authors agree with the description of leaching being the reverse of adsorption but describe the kinetics as being 2nd order or a combination of 1st order mechanisms (Harouna-Oumarou, et al., 2007; Su, et al., 2014; Rakotondramasy-Rabesiaka, et al., 2009) . Harouna-Oumarou, et al (2007) describe the leaching of water-soluble bioactive compounds from *Tilia* sapwood particles using a 2nd order kinetic model. The model, which agreed with the experimental data, assumed that two primary phenomena occur during leaching. The first is the dissolution of all water-soluble compounds when they come in to contact with the water. This is the stage of the highest rate of leaching. The second phenomenon is a stage of slower leaching that is controlled by the diffusion of the water-soluble compounds from inside the sapwood particles into the bulk liquid. This slowing down in the leaching rate can be described as the leaching being limited by mass transfer. Rakotondramasy-Rabesiaka et al. (2009) also describes a second order kinetic characteristic for solid-liquid extraction of protopine from *Fumaria officinalis*.

Lagergren et al. (1898) quote a pseudo-first order kinetic model where the rate of leaching is directly proportional to the driving force of a concentration gradient:

$$\frac{dC}{dt} = k_1(C_e - C) \qquad \text{Equation 6}$$

Where:

$\frac{dC}{dt}$	is the rate of leaching of solute (mg.mL^{-1}.min^{-1})
t	is leaching time (min)
C	is the concentration of solute (mg.mL^{-1})
C_e	is the equilibrium concentration of solute (mg.mL^{-1})
k_1	is the first-order leaching rate constant (min^{-1})

Equation 6 was also used by many authors who described leaching with 1st order kinetics including Ho et al. (2005) in their research of leaching of water-soluble compounds in *Tilia* sapwood. Equation 6 is integrated at boundary conditions of t from t = 0 to t = t, and C from C = 0 to C = C. The resulting equation is then linearized, resulting in Equation 7:

$$\log(C_e - C) = \log(C_e) - \frac{k_1}{2.303}t \qquad \text{Equation 7}$$

Using $C(t)$ experimental data, $log(C_e - C)$ vs t can be plotted, and from the gradient the first-order leaching rate constant k_1 can be determined.

Ho et al. (2005) quoted a second order model for solid-liquid extraction:

$$\frac{dC}{dt} = k_2(C_e - C)^2 \qquad \text{Equation 8}$$

Where:

$\frac{dC}{dt}$	is the rate of leaching of solute (mg.mL^{-1}.min^{-1})
t	is leaching time (min)
C	is the concentration of solute (mg.mL^{-1})
C_e	is the equilibrium concentration of solute (mg.mL^{-1})
k_2	is the second-order leaching rate constant (mL.mg^{-1}.min^{-1})

When Equation 8 is integrated at boundary conditions of t from t = 0 to t = t, and C from C = 0 to C = C, Equation 9 is the result:

$$C = \frac{C_e^2 k_2 t}{1 + C_e k_2 t} \qquad \text{Equation 9}$$

Equation 9 can be linearized to Equation 10:

$$\frac{t}{C} = \frac{1}{k_2 C_e^2} + \frac{t}{C_e} \qquad \text{Equation 10}$$

Thus C_e and k_2 can be determined from the intercept and gradient of the straight line generated by plotting $\frac{t}{C}$ vs t.

With reference to Equation 9, an initial extraction rate (IER) can be described when time tends to 0, i.e. at the very incipient of leaching. Thus, the initial extraction rate can be described by:

$$IER = k_2 C_e^2 \qquad \text{Equation 11}$$

This second-order model was also used by Su, et al. (2014) and Rakotondramasy-Rabesiaka, et al. (2009). Su, et al. (2014) found that this second-order model agreed with the experimental data for leaching of c-phycocyanin from *Spirulina* under a variety of operating conditions, with the coeffificent of determination suggested acceptable predicition of leaching concentration of c-phycocyanin (R^2 = 0.98). The operating conditions of leaching and the model outputs are summarized in Table 5.

Table 5. Experimental ranges for operating conditions of a leaching system of c-phycocyanin from *Spirulina,* adapted from Su, et al. (2014)

Operating conditions	**Experimental range**
pH	5 – 7
Temperature (°C)	30 – 50
Spirulina particle size (µm)	<25
Solid-liquid ratio (g.mL^{-1})	0.05 (dried *Spirulina*)
Solvent type	Phosphate buffer

2.5.3 Cell debris removal via centrifugation

Cell debris removal using centrifugation is a common practice at laboratory and commercial scale. Centrifuges are versatile and do not require any consumables like membranes to operate. Further, a simple change in residence time can produce the same separation of solid-liquid for a different size distribution of solid particles.

The separation of a solid and liquid using centrifugation is called sedimentation centrifugation since the solid particles get sedimented by the force of centrifugation into a cluster which allows the liquid to be easily removed from the system with a lower solid concentration (Green & Hughes, 1955). Centrifugation uses circular motion to force matter outward from the axis of rotation. It works on the principle of Stokes' law modified by the centrifugal acceleration in the rotational axis, this is shown in Equation 12 (Green & Perry, 2008; Richardson, et al., 2002):

$$\frac{dr}{dt} = \frac{1}{18\mu}\omega^2 R(\rho_s - \rho_L)d^2 = \frac{v_s R\omega^2}{g} \qquad \text{Equation 12}$$

Where:

$\frac{dr}{dt}$	Settling velocity (m.s^{-1})
μ	Viscosity of liquid (kg.m^{-1}.s^{-1})
ω	Centrifuge speed (s^{-1})
R	Radius of centrifuge (m)
ρ_s	Density of solid (kg.m^{-3})
ρ_L	Density of liquid (kg.m^{-3})
d	Diameter of solid particles (m)
v_s	Settling velocity (m.s^{-1})
g	Acceleration (m.s^{-2})

Equation 12 is based on modelling solid particles as spheres. According Stokes' Law, settling velocity is determined using a force balance on a particle in a fluid. Stokes' Law is modified by substituting the gravity term with the centrifugal equivalent of gravity to yield Equation 12.

The settling velocity term is an indication of the performance of the degree of separation, thus the variables on the right-hand side of Equation 12 are those to be optimized to increase settling velocity to a maximum. For a constant centrifuge and particle distribution the only dependent variable would be the speed of rotation.

To physically observe the extent of separation there a few performance criteria to track (Green & Perry, 2008), for batch operation at lab scale, the following two are of importance:

1. Cake dryness or moisture content
2. Total solids recovery

Cake dryness is a measure of how much moisture is left in the solids' "stream" after centrifugation. The greater the degree of separation in a sedimentation centrifuge, the more tightly packed the solid

particles in the cake would be. This will affect the voidage of the cake wherein liquid is trapped when the supernatant is poured off. For a more compact cake with a lower voidage, less liquid is trapped in the cake, hence more liquid is recovered as the supernatant (Green & Perry, 2008).

A rinsing step is sometimes included post-centrifugation where the cake is rinsed to recover more dissolved product trapped in the cake. This solution would then require further centrifugation to recover the product in the supernatant (Green & Hughes, 1955).

Solids recovery is simply the amount of solids recovered in the solids stream – thus allowing for the determination of how much solids is in the liquid stream giving an indication of the clarity of the liquid stream.

Centrifuge Design

To fully interpret results of cell debris removal using a centrifuge, the principles underpinning the fundamental theory of centrifuge design should be understood. The centrifuge design theory helps understand the thought process towards deciding on a centrifuge type and how to scale this type when increasing throughput.

Stokes' Law from first principles can be used for centrifuge design and scale up (Richardson, et al., 2002).

With reference to Figure 5, integrating Equation 12 between the limits of $r = r_0$ and $r = R$ we can find Equation 13 giving the retention time (t_r) within the centrifuge necessary for any particle greater than d to be deposited on the centrifuge wall (Richardson, et al., 2002).

$$t_r = \frac{18\mu h}{d^2(\rho_s - \rho_L)R\omega^2}$$ Equation 13

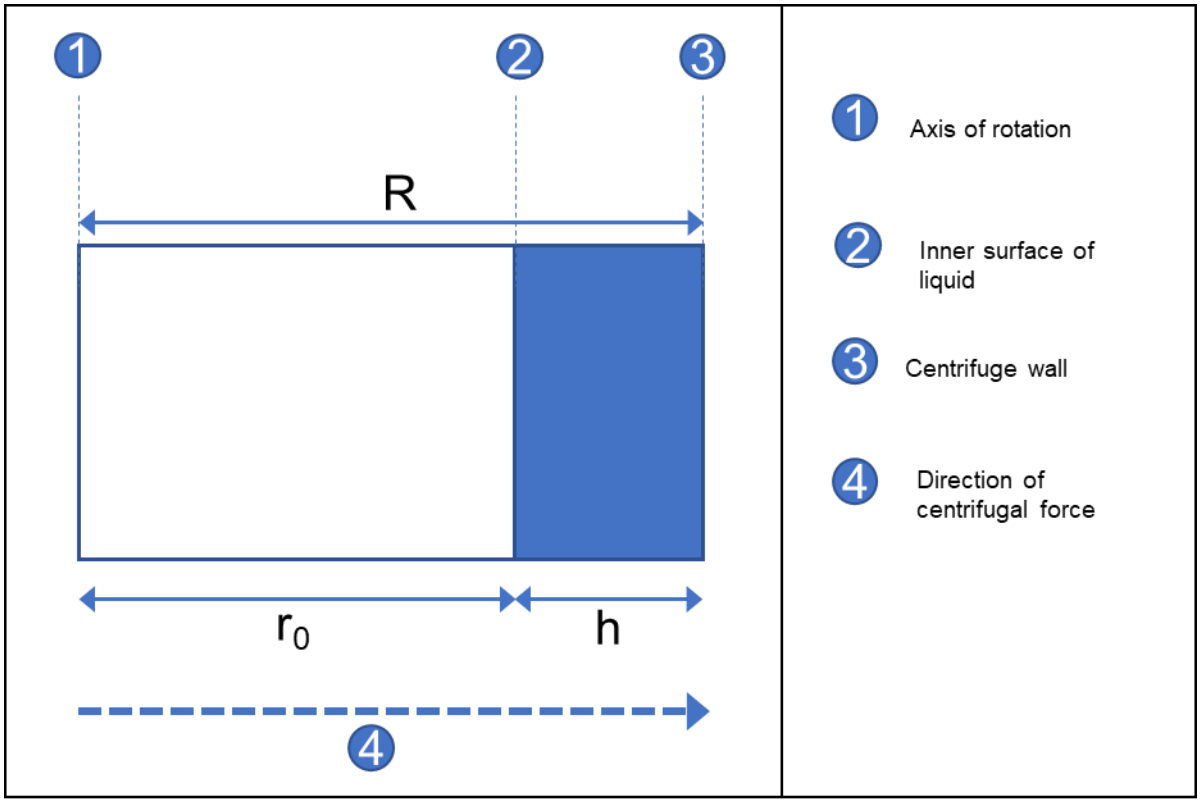

Figure 5. Diagram of a cross-section of a centrifuge, with key variables affecting its operation and design

The maximum throughput (Q) can be calculated from this retention time by dividing the volumetric hold-up (V') in the centrifuge by retention time:

$$Q = \frac{d^2(\rho_s - \rho_L)R\omega^2\, V'}{18\mu h}$$ Equation 14

The volumetric hold-up can be expressed in terms of the dimensions of the centrifuge with H being the axial length:

$$V' = \pi(R^2 - r_0^2)H$$ Equation 15

By substitution of the settling velocity term of Equation 14, this equation becomes:

$$Q = \frac{v_s R\omega^2}{gh} V'$$ Equation 16

Then, by expressing V' in terms of centrifuge dimensions:

$$Q = \frac{v_s R\omega^2}{gh}\, \pi(R^2 - r_0^2)H$$ Equation 17

Finally defining a new term Σ as the quotient of $v_s$over Q results in:

$$\Sigma = \frac{R\omega^2}{gh}\, \pi(R^2 - r_0^2)H$$ Equation 18

When the liquid thickness is < 5 % of the bowl diameter then it can be ignored, and the capacity factor can be expressed as:

$$\Sigma = \pi R(R + r_0)H\frac{\omega^2}{g}$$ Equation 19

Σ is the equivalent cross-sectional area of a gravity settling tank with the same degree of separation of the centrifuge. Σ is independent of the properties of the slurry and is only dependent on the dimensions of the centrifuge, location of overflow exits and speed of rotation (Richardson, et al., 2002). The definition of the capacity factor allows for scaling of the centrifuge. We can use the following to find the equivalent area needed for a scaled-up throughput once the equivalent area and throughput of the current scale is determined:

$$\frac{Q_1}{\Sigma_1} = \frac{Q_2}{\Sigma_2}$$ Equation 20

2.5.4 Aqueous two-phase separation

ATPS intro

Aqueous two-phase separation (ATPS) is a liquid-liquid fractionation technique wherein two immiscible aqueous phases are formed – each with its own properties (Asenjo & Andrews, 2011). Two types of ATPS systems exist: polymer-polymer and polymer-salt. In the polymer-polymer system, the top phase is often polyethylene glycol (PEG) with the bottom phase being either dextran or maltodextrin (Iqbal, et al., 2016). In polymer-salt systems, sulfates, phosphates or citrates are the most commonly used as the salt phase. Citrates have been replacing phosphates and sulfates owing to their relative ease of disposal, attributed to its biodegradability (Murty, et al., 2012).

The two phases are formed when the phase forming components (polymers or polymer and salt) are mixed in quantities greater than the 'critical concentration' of each of these components. This prevents a single phase from forming and instead two phases are observed. The immiscibility between the two polymer phases causes large aggregates to form and steric exclusion will lead to distinct two-phase formation (Asenjo & Andrews, 2011). In a polymer-salt ATPS, the two-phase formation can be attributed to the salt capturing large volumes of the water present that subsequently causes an exclusion phenomenon (Asenjo & Andrews, 2011).

Once the system reaches equilibrium, two phases with distinct composition and density are formed in layers: one top phase and one bottom phase. There is usually a visible boundary between the phases.

It is possible to use the partitioning of the two phases to separate proteins from contaminants like cell debris or to separate out specific proteins from other proteins. Soluble materials usually express a tendency to partition to the more polar phase (the bottom phase) while proteins will move towards the top phase which is usually less polar and hydrophobic (typically rich in PEG) (Asenjo & Andrews, 2011). To separate specific proteins from others, variables such as the ionic strength of the salt, type of ions, and polymer molecular weight can be manipulated to alter the partition coefficient.

ATPS is considered a safe purification technique for proteins since there is little to no denaturation of proteins. This observation is owing to the large relative volumes of water and the lack of disruptive interfacial tension (Asenjo & Andrews, 2011).

Factors influencing ATPS operation

ATPS does not offer perfect purification of desired products but the following are some of the factors affect the partition coefficient (similar to the position of equilibrium of the system) thus affected the protein partitioning and the relative volumes of the two phases.

Polymer concentration and molecular weight

Generally, a higher molecular weight (MW) of the polymer leads to a lower concentration required for two-phase formation. High polymer concentrations result in lower partitioning to the phase with the greater MW (for polymer-polymer systems). For polymer-salt systems, higher concentrations decrease partitioning to the polymer phase (Iqbal, et al., 2016).

Temperature

Temperature is a factor that is essential to control in an ATPS. Both density and viscosity are functions of temperature. Thus, at each temperature the system will have a different equilibrium position i.e. a different phase diagram. It has been reported that lower temperatures favour distinct phase formation in low concentration polymer-polymer systems (Asenjo & Andrews, 2011).

pH

The pH of the ATPS mostly affects the partitioning of proteins. If the pH of the system is higher than the isoelectric point of the protein, the net charge of the protein becomes negative and this increases the partitioning to the PEG phase (Murty, et al., 2012; Iqbal, et al., 2016). This phenomenon is attributed to induced-dipole effects (Iqbal, et al., 2016).

ATPS for c-phycocyanin purification

There are a number of studies in the literature which report PEG-salt systems being used for the purification of c-phycocyanin, some of these studies and their results are summarized in Table 6. High recoveries, of above 85 %, were obtained in the PEG phase across most studies performed. pH of operation tended to be in the range of 6 – 7.2. Typically, polymer molecular weight for PEG was optimized in the studies but no conclusive trends were found. The optimal polymer/salt ratio for prioritizing purification factor and recovery falls within a range of 4 – 12.3 wt % for PEG and 11 – 22 wt % for salts. There was no clear combination of weight fractions that can be considered optimal from the available literature. The highest recovery of c-phycocyanin found was 100 % by Antelo, et al (2015) which was at the lowest polymer weight fraction and highest salt weight fraction. The highest purification factor from the literature reviewed was 2.45 quoted by Sørensen, et al (2013) which occurred at the highest polymer weight fraction and lowest salt weight fraction from the reviewed works. Other authors reported similar findings: increase in polymer weight fraction and decrease in salt weight fraction favouring an increase in the purification factor whereas an increase in salt weight fraction with a decrease in the polymer weight fraction resulting in a higher recovery being observed. Table 6 is a summary of these key literature works studied, with their experimental conditions and c-phycocyanin yield and purification factors.

There has also been evidence of PEG-maltodextrin systems being used for the purification of c-phycocyanin. Fagan-Endres (2019) and Hockey (2020) both report using a PEG-maltodextrin ATPS for the purification of c-phycocyanin from *Spirulina*. It is important to note that Hockey (2020) diluted the crude extract by 10× before the PEG-citrate ATPS and this yielded the results in Table 6.

Table 6. Comparison of experimental conditions and outputs of ATPS for c-phycocyanin purification, from literature

Salt used	Polymer/salt wt %	Purification factor	Yield (%)	pH	Temperature	Reference
Citrate	11 / 20	1.63	96	6	Room	(Hockey, 2020)
-	11/22*	1.43	87	-	Room	(Hockey, 2020)
Phosphate	5 / 18	1.33	87	6	-	(Antelo, et al., 2010)
Phosphate	12.3 / 11.6	2.45	88	7.2	Room	(Sørensen, et al., 2013)
Phosphate	4 / 21	2	100	6	-	(Antelo, et al., 2015)

* 11 wt % PEG and 22 wt % maltodextrin, no salt was used.

2.5.5 Ammonium sulfate precipitation

When an aqueous solution containing dissolved proteins is subject to the addition of ammonium sulfate, the salt ions out-compete the proteins in solution, essentially "taking" the water molecules for their own. Hydrophilic interactions between water molecules and proteins thus decrease significantly, forcing the protein molecules out of solution as precipitate (Song, et al., 2013). This phenomenon is termed "salting out". Salts other than ammonium sulfate may also be used for this; however, ammonium sulfate is a neutral salt making it less likely to induce a localized pH fluctuation that could cause the denaturing of proteins (Bartlett & Birkin, 1993).

Ammonium sulfate precipitation performance is usually reported using saturation percentages or fractions of saturation of ammonium sulfate which gives an indication of the quantity of ammonium sulfate added to the solution to achieve given recoveries, purities, etc.

The conversion between saturation fractions and mass of ammonium sulfate added can be calculated using the following formula from Wingfield (2001):

$$W = \frac{W_{sat}\,(C_2 - C_1)}{1 - (PS_2)}$$ Equation 21

Where:

W	is the quantity, in mass, of ammonium sulfate to be added to a 1 litre solution of concentration S_1 to produce a concentration of S_2.
W_{sat}	is the number of grams of ammonium sulfate that is dissolved in a 1 litre saturated ammonium sulfate solution
C_1	is the initial saturation fraction of complete saturation of ammonium sulfate, e.g., a 30 % saturation would be expressed as 0.3
C_2	is the final saturation fraction of complete saturation of ammonium sulfate at the point where weight (g) is added.
P	is the product of specific volume of saturated solution with W_{sat} divided by 10^3

The W_{sat} term and the specific volume are dependent on the temperature of solution. Table 7 and Figure 6 summarizes ammonium sulfate saturation concentrations and specific volumes of ammonium sulfate.

Table 7. Summary of ammonium sulfate saturation concentrations and specific volumes at different temperatures adapted from Wingfield (2001) and Dawson et al. (2002).

Temperature (°C)	**0**	**10**	**20**	**25**
Ammonium sulfate (g) per liter saturated solution	515.4	524.6	536.5	541.8
Specific volume in saturated solution (ml/g)	0.528	0.536	0.541	0.544

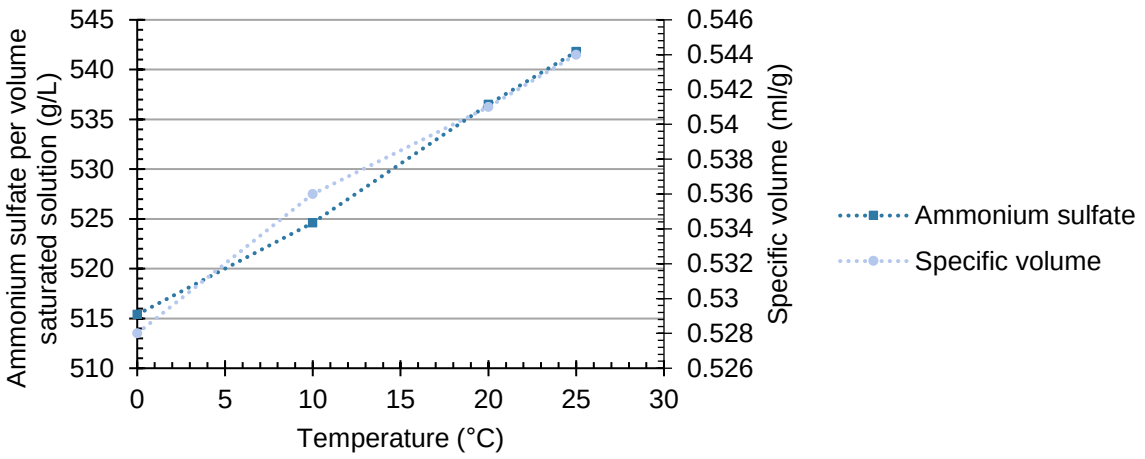

Figure 6. Ammonium sulfate saturation concentrations and specific volumes at different temperatures adapted from Wingfield (2001) and Dawson et al. (2002).

Since each protein has its own unique hydrophilic interactions with water with discrete requirements of ammonium sulfate to induce its precipitation, a fractionation method of ammonium sulfate addition can be employed to selectively precipitate proteins based on the amount of ammonium sulfate added (Song, et al., 2013). As salt is added fractionally, more precipitate will be observed. At the point where the solution is fully saturated with salt, the precipitate should comprise all the protein in the initial solution (Green & Hughes, 1955). Making use of the fractional nature of precipitation; precipitation is often performed in a precipitation train if the initial protein solution contains different proteins. The first precipitation step is performed at a saturation fraction just below the saturation fraction at which the desired protein will begin to precipitate. This will remove some undesired proteins and potentially contaminants from the protein solution since the desired protein will remain in solution in the supernatant and said proteins and contaminants will precpitate out of solution. A second precipitation can then be performed on that supernatant, at a higher fraction of saturation to precipitate the desired protein from the solution. The precipitate pellet containing the desired protein can be resuspended and subject to further precipitation at a fraction of saturation between that of the first two steps to allow for the further removal of unwanted proteins (Song, et al., 2013).

It is important to note the point at which a solution is completely saturated with salt since an oversaturation would be waste of consumables, especially if the process is scaled up. Conductivity is a measure of the mobility of dissolved ions in solution and thus, the point where the conductivity stops increasing is a representation of the saturation point of the salt, ammonium sulfate – this is because the solution reaches equilibrium (Chang, 2007).

Within systems with upstream (preceding precipitation) operating conditions kept constant, the performance of the precipitation can be predicted to some extent. Silva et al. (2009) describe a second order kinetic model was developed for the prediction of extract purity as a function of the ammonium sulfate saturation, the resuspension volume for fractional precipitation, initial volume and the pH. The coefficient of determination was found to be 0.83 which suggests correlation exists but warrants further investigation (Silva, et al., 2009).

Song, Zhao and Suying (2013) reports using a method of ammonium sulfate fractional precipitation to establish a prediction of purity ratio and recovery at different ammonium sulfate saturations whilst maintaining constant cell disruption and leaching methods. Figure 7 shows the results of the fractional precipitation where recovery increases with ammonium sulfate precipitation and purity in the precipitate increases until 30 % and thereafter decreases as more protein is precipitated with increasing ammonium sulfate saturation.

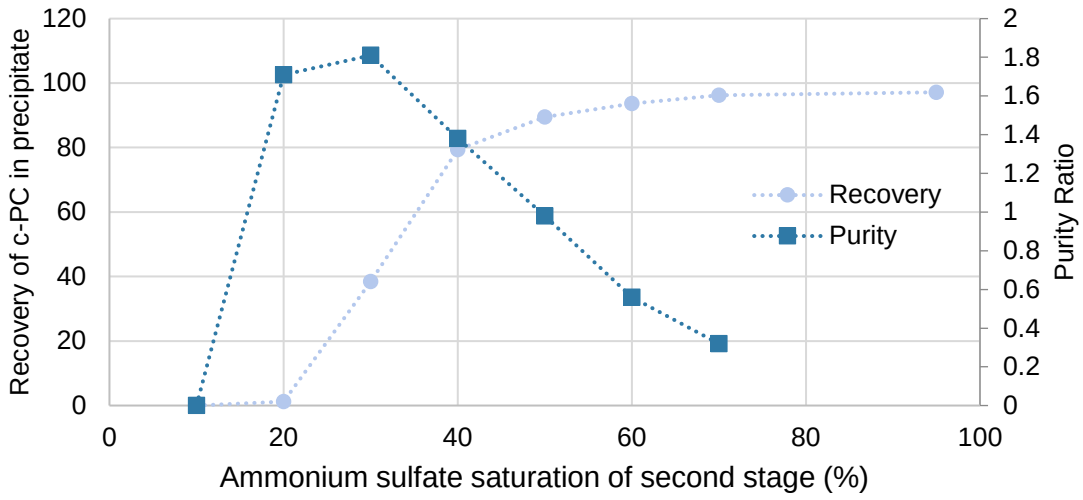

Figure 7. c-Phycocyanin recovery and purity ratio in the precipitate at different fractional ammonium sulfate saturations adapted from Song, Zhao and Suying (2013)

Note that the purity is not at the ammonium sulfate saturation percentages on the axis but rather after a two-stage fractional precipitation, the first being at 10 % lower than the ammonium sulfate saturation at which the purity is plotted in Figure 7. For example; at the point of (40; 1.38) for purity ratio, was yielded from precipitating at 30 % saturation, and then precipitating the resultant supernatant at 40 % saturation. This would give an estimate of the saturation at which most of the c-phycocyanin would precipitate out, i.e., at 50 % which was the saturation used in further studies of Song et al (2013).

Recoveries, purification factors and c-phycocyanin purity ratios do not seem to be consistent for the same ammonium sulfate saturations across different studies of purification that use ammonium sulfate precipitation. Table 8 shows a compilation of ammonium sulfate precipitation performance results and conditions on *Spirulina* crude extract from different studies. The various papers used different methods for cell disruption and leaching. The purification factors of the precipitation steps do not correlate with the saturation fraction used.

Proteins are also sometimes stored in ammonium sulfate solution as it inhibits bacterial growth (Wingfield, 2001). Fagan-Endres et al (2019) showed how sequential precipitation stages can be used to both increase purity of c-phycocyanin and also decrease bacterial contamination of the pellet. This data is summarized in Table 9.

Table 8. Critical experimental conditions of ammonium sulfate precipitation and c-phycocyanin purity and recovery outputs on *Spirulina* crude extracts from different studies

Saturation fraction	Precipitate purity ratio	Purification factor	Recovery of c-phycocyanin (%)	Feedstock	Reference
0.65	1.5	-	80 %	Wet biomass	(Kumar, et al., 2014)
0.5	0.89	1.71	91 %	Wet biomass	(Silva, et al., 2009)
0.3 & 0.5 fractional	1.43	1.47	-	Wet biomass	(Bhaskar, et al., 2005)
0.3 & 0.5 fractional	3.1	2.71	-	Wet biomass	(Zhang & Chen, 1999)
0.5	2.05	2.5	85 %	Dried powder	(Song, et al., 2013)
0.3 & 0.5 fractional	0.61	1.96	-	Wet biomass	(Muthulakshmi, et al., 2012)

Table 9. Purity ratio and bacterial contamination of c-phycocyanin product of precipitation adapted from Fagan-Endres, et al. (2019)

Quality indicator	1 stage	2 stages	3 stages
Purity ratio ($\frac{A_{620}}{A_{280}}$)	0.74	1.69	2.73
Bacterial contamination (CFU/g)	750000	15000	5000

2.5.6 Filtration

Filtration is a separation technique that operates using size-exclusion. It can be used for separating compounds down to 10 Da in molecular particle size (ultrafiltration). The size exclusion can be reconfigured to suit the process by changing the membrane pore size.

Studies have been performed on purifying c-phycocyanin using ultrafiltration. Many authors report using ultrafiltration after an ATPS to exclude the PEG molecules from the product (Rito-Palomares, et al., 2001; Pathil & Raghavarao, 2007; Sørensen, et al., 2013). A summary of some authors conditions and outputs from ultrafiltration can be found in Table 10.

Table 10. Filter pore size and c-phycocyanin purity and recoveries used by and achieved by different studies, respectively

Pore size	Purification factor	Purity after	Recovery	Reference
30 kDa	1.29	3.1	70.5 %	(Rito-Palomares, et al., 2001)
30 kDa	-*	>4	-	(Pathil & Raghavarao, 2007)
50 kDa	1.67	4.5	79 %	(Sørensen, et al., 2013)

*purity already greater than 4 leading into the filter.

Sørensen, et al. (2013) describes diluting the feed to the ultrafiltration unit to allow for the feed to pass through the filter since the viscosity of the PEG can affect the performance of the filtration. Sørensen, et al. (2013) also describes using this greater pore size to remove smaller proteins in the filtrate. However, the source of c-phycocyanin was *G. sulfuraria*, hence we do not know if this would work well for the protein composition of *Spirulina*. If c-phycocyanin is the smallest protein present to the filter it would not prove to increase the purity of the product.

Filtration can also be used for desalting by method of size exclusion, i.e, the pore size will not allow any of the dissolved particle to pass through except for the salt in solution. This will result in the retentate being desalted (Phillips & Signs, 2005).

2.6 Robustness and process design

The quality of a product being produced in a manufacturing sense may be dependent on many factors such as raw materials used, operating conditions of the process, environmental conditions, amongst others (Mondal, et al., 2014). In the space of process engineering and within more specific context of the c-phycocyanin extraction and purification process described in Section 2.4, it is difficult to guarantee perfect reproducibility of product quality (i.e. c-phycocyanin purity and colour intensity) with every production batch.

Thus, thresholds of quality, pre-determined based on the potential application of the product, are typically determined and process is required to meet these product specifications (Mondal, et al., 2014)

Several of the factors contributing to product quality can be controlled, but others cannot be controlled. A process that will still meet the product specifications with a fluctuation in uncontrollable factors is called a robust process (Mondal, et al., 2014). In the design of a process, it is important to identify the uncontrollable factors and ensure the operation of the process under influence of these factors is sufficient to yield a product of desired standards.

Since robustness is not tangible there have been attempts made to express robustness in terms of other things such as process capability index (Kazmer & Roser, 1999). Existing robustness modelling approaches have been developed, for the design of robust systems, such as those by Taguchi (1986), Nelder and Lee (1991) for single stage process and Suri and Otto (2001) and Yuangyai, et al (2012) for multi-stage processes.

The most uncontrollable variable for the c-phycocyanin extraction and purification process is the dried *Spirulina* powder feedstock. To produce the dried *Spirulina*, there are many uncontrollable and variable factors. The first are production environmental conditions since open raceway ponds are most commonly used for the large-scale cultivation of *Spirulina* (Ma, et al., 2019). The *Spirulina* strain as well as the method and degree of drying will also determine the particle size distributions of the dried powder. These factors will result in a variability of the product with respects to c-phycocyanin composition, cell (or cell debris) size distribution and integrity of cell structure.

Robustness to controlled variables can usually be tested using a sensitivity approach where a variable is controlled and fluctuated to note the “knock-on” effect it has on the performance of the process and the effect on the product (Mondal, et al., 2014). Using different feedstocks, we can use a sensitivity-based approach since each feedstock would be different in composition and thus see the effect these feedstocks have on the performance of key areas of the extraction and purification and final product, under identical operating conditions of the process.

2.7 Summary and gaps of literature & previous work

This subchapter will discuss how the literature review informs decisions on the current process and future developments of the process. It will also discuss the gaps in knowledge surrounding the process and thus inform the key questions for the research performed in this study. This subchapter will be focused on the gaps in the previous work by Fagan-Endres et a (2019) and Hockey (2020) and how the literature bridges the gaps and informs potential work for this dissertation.

The previous work in Hockey (2020) has full data available for each processing step tested. However, for the downstream processes after the ATPS, the data is limited to a computed mass balance results for c-phycocyanin purity, recovery and concentration in place of physical experimental results. Physical experimental work results are necessary to optimize operating conditions based on these factors. Operating conditions for all downstream processing need to be established so that the project can move onto a larger scale – once the operating conditions are set the scale-up of equipment can be performed such that at the larger scale the equipment should aim to achieve the same performance as the lab scale at these newly established operating conditions. Table 11 summarizes the key operating parameters from Hockey (2020) and gives an indication of which unit procedures require robustness testing and/or optimization.

Table 11. Summary of the gaps in the work performed by Hockey (2020) in terms of the parameters calculated in the unit procedures of the recommended process route by Hockey (2020)

Stage	Parameters	Optimization/Robustness testing required
Bead-milling	Time; bead-loading; solvent to biomass ratio; agitation speed	Robustness testing
Leaching	Time	Both
Centrifugation	Time; centrifuge speed; Temperature	Both
PEG-Citrate ATPS	PEG wt %; Citrate wt %	Robustness testing
Maltodextrin-PEG ATPS	Maltodextrin wt %; PEG wt%	Robustness testing
Ammonium sulfate precipitation	Number of stages; ammonium sulfate concentration	Both

Leaching times were tested in Hockey (2020), however prediction models were not considered and only a single source of *Spirulina* was tested. From the work performed by Su, et al. (2014), it is thought that c-phycocyanin from microalgae follows similar leaching patterns to other bioactive componds from organic matter. However, there is not much available research on the leaching patterns of c-phycocyanin from dried *Spirulina* powder. This suggests that it is of importance to understand the difference in leaching patterns between fresh and dried *Spirulina*.

Limited research has been published on the cell debris removal step which is of great importance since if the solid-liquid separation here is inefficient the process will have a low recovery of c-phycocyanin which is in the supernatant at this junction in the downstream. Thus, centrifuge design for the upscale process is important to allow for the scalability of recovery of the crude product from lab-scale through to the potential upscale.

A lot of data exists for the purification of c-phycocyanin from *Spirulina* using an ATPS system using PEG and citrate. However, most papers do not quote all their operating conditions, and reported work has been at lab scale which is at a volume < 10 % of the projected lab scale of this project. This suggests that it will be difficult to compare results well to literature with confidence – since we do not know how much scale affects performance. Literature sources pertaining to the upscale of an ATPS process exist but many do not explain how it was performed in terms of which variables were scaled, e.g., the use of dimensionless numbers or simple upscaling of all measured dimensions.

There is no available literature on the use of a maltodextrin and PEG ATPS for the purification of c-phycocyanin except for the previous work done under CeBER. Literature regarding purification of proteins in general using a maltodextrin-PEG system do exist (Rao, et al., 1991; Ramyadevi, et al., 2012; Alves, et al., 2000), however this dissertation is considering Hockey (2020) as the most relevant literature on this system for c-phycocyanin since an optimization procedure was performed. It is noted that Hockey (2020) showed an intricate understanding of the maltodextrin-PEG system.

The previous work performed has focused on the ATPS of the process without much new research performed on the ammonium sulfate precipitation since the inception of the patent (Hockey, 2020; Fagan-Endres et al., 2019). Literature also does not have much available information on fractional precipitation of c-phycocyanin using ammonium sulfate besides that reported by Song et al. (2013). The available literature like Song et al. (2013) also suggests that to predict the c-phycocyanin recovery and purity ratios in the precipitate, constant leaching and cell disruption conditions are required. Thus, it is important to carry out the fractional precipitation in this study to establish the trends of recovery and purity with ammonium sulfate saturation.

Literature did not describe the knock-on effects of using precipitation before ATPS or vice versa. It did seem, however, that precipitation was performed first for an unexplained reason – different to the

CeBER extraction and purification process. There may be some good in performing a precipitation on the crude product instead of after the ATPS, as the product containing PEG phase may not respond to precipitation as expected. This gap is something that was considered and noted for future work, the effect of changing the purification mechanism order will not be addressed in this dissertation as it is considered as out of scope for this study.

There is current work being performed on the process upstream to the extraction and purification process: culturing fresh *Spirulina* as a feed. This current work will not be covered in this dissertation as it is being performed by a co-researcher in the same department working towards the same overarching c-phycocyanin project. For now, the extraction process has been limited to a feed of dried *Spirulina* powder. If the extraction and purification process is reliant on an external supplier for its feed, a variability in the composition of the feed owing to the nature of microbial cultures is unavoidable. Furthermore, there is no guarantee of permanent supply of feed from a single supplier – especially in the case of upscaling where a delay in feedstock may be costly to the process as a business. In such cases a back-up supplier would be required. This suggests that the process needs to capable of utilising a varying feedstock of *Spirulina* to produce a suitable product of c-phycocyanin, i.e., the process needs to be robust. Literature does not describe the effect of different feedstocks on an extraction process or c-phycocyanin, nor does it describe the effect of different feedstocks on a particular extraction method, e.g., ATPS or ammonium sulfate precipitation. This further emphasizes the need for robustness testing of the existing process to ensure it can process variability in the feed successfully.

To assist in bolstering the overall robustness of the process, the configuration and choice of downstream processes will be critical. Thus, it is important to note the robustness of specific unit processes as an important quality aside from that unit's ability to produce a pure product stream. In the context of the CeBER c-phycocyanin extraction and purification process, at the current stage of development unit operations have been chosen and some optimized, thus the need for robust process design is not necessary at this point. However, from Hockey (2020), it is recommended that the ATPS step be rendered obsolete based on purification performance and in its place include a filtration step for the purification of the c-phycocyanin product. Thus, a robustness study on both the filtration and ATPS ought to be performed to allow for the better choice of unit procedure for that purification step. In the event that the ATPS is more robust than filtration, it would make more sense to include the ATPS since we have more of a need for robustness – to meet product specification with different feedstocks – rather than for higher purification since the ATPS does purify the product, just not to the extent that filtration is reported to achieve (Hockey, 2020).

The recommendation from Hockey (2020) to consider removing the two ATPS steps will allow for less uncontrollable factors to influence the performance of the extraction process such as fluctuations in ATPS composition (which also affect ATPS performance by nature of the ATPS mechanism). Two downstream processes will effectively be replaced by one. This will also have an effect on the overall recovery of c-phycocyanin, as recovery is based on a product law where the greater the number of downstream processes with individual recoveries the lower the overall recovery for identical recoveries of less than 100 %. ATPS recovery over the two-stage ATPS was 83 %. The ATPS forms a major part of the CeBER patent and as such there is a large emphasis on attempting to include the ATPS in the final design of the process route. Ultrafiltration, on the other hand, tends to have a recovery of around 70-80 % over the filtration step (Rito-Palomares, et al., 2001; Sørensen, et al., 2013) . However, this recovery was using ultrafiltration after an ATPS system. There is no available literature on the use of ultra- or microfiltration after precipitation for the purification of c-phycocyanin from *Spirulina*. Thus, testing of the robustness of the two whilst considering the impact on recovery would be the best route forward.

2.8 Defining the research project

This subchapter has the purpose of presenting the problem statement being addressed, the research project objectives and the key research questions that will guide the experimental design. Answering these key questions is the purpose of this dissertation.

2.8.1 Problem statement

The CeBER process for c-phycocyanin extraction and purification from *Spirulina* has multiple aspects that have not yet been fully optimized, nor has the process been assessed for robustness. In particular, leaching kinetics for *Spirulina* samples need to be understood to predict c-phycocyanin concentrations for a given time of leaching. Further, a better choice of operating conditions of the various unit operations need to be established, and the ability for the process to handle a variation in feed type needs to be assessed. Through addressing these factors, a final process recommendation can be established to enable the development of a mass balance of the process with accompanying equipment choices to inform the pilot plant design and the technoeconomic feasibility of the CeBER process.

2.8.2 Research project objectives

1. Observe the particle size distributions of different dried *Spirulina* powder samples with and without prior bead-milling.
2. Observe and understand the c-phycocyanin leaching kinetics from different dried *Spirulina* powder samples.
3. Determine whether or not bead-milling is a necessary step in the extraction process for dried *Spirulina* powder samples.
4. Determine the optimum centrifugal speed for cell debris removal.
5. Observe how the ATPS steps handle different samples of *Spirulina* leachate.
6. Determine the optimum ammonium sulfate saturation percentages for a protein precipitation train for prioritizing purity and recovery of c-phycocyanin.
7. Determine the ability of micro-filtration to purify the c-phycocyanin further, post precipitation.
8. Establish the process recoveries, per extraction and purification steps, for different dried *Spirulina* powder samples.

2.8.3 Key research questions

Particle size distribution

- What are the particle size distributions for the different *Spirulina* powders?
- How do the particle size distributions of the different *Spirulina* powders compare?
- How does milling affect the cut sizes and particle size distributions of the different *Spirulina* powders?

Leaching

- Is bead-milling a necessary precursor to improve the leaching time required for c-phycocyanin to reach an equilibrium concentration when leaching at room temperature in a citrate (pH 6) buffer?
- Can we predict the c-phycocyanin concentration in the leachate at any point during the leaching, using the standard models available in the leaching literature?
- Consequently, does c-phycocyanin from dried *Spirulina* powder follow first order or second order leaching kinetics, or neither?
- How long should the leaching stage be, considering all potential *Spirulina* powders?
- Do all *Spirulina* powders leach in the same way, or are different behaviours observed?

Cell debris removal

- How does g-force in centrifugation affect the recovery of c-phycocyanin over the cell debris removal stage?
- At what g-force should the pilot plant be operated at and why?
- Consequently, what type of centrifuge is best suited for this operation?
- How consistent is the centrifugation performance for different *Spirulina* powders?

ATPS

- What is the c-phycocyanin recovery and c-phycocyanin purity achieved for a single stage PEG-citrate ATPS for the different *Spirulina* powder feeds?
- What is the c-phycocyanin recovery and c-phycocyanin purity achieved for a single stage PEG-maltodextrin ATPS for the different *Spirulina* powder feeds?
- What is the c-phycocyanin recovery and c-phycocyanin purity achieved for a two-stage ATPS system of PEG-citrate ATPS followed by a PEG-maltodextrin ATPS for the different *Spirulina* powder feeds?
- Considering the operating conditions identified to be best for the pilot plant process, how robust is the ATPS step in terms of recovering and purifying c-phycocyanin from the different *Spirulina* powder feeds?

Precipitation

- How does ammonium sulfate saturation percentage affect the recovery of c-phycocyanin in the precipitate?
- At what ammonium sulfate saturation does the supernatant in the precipitation realize its highest purity?
- At what ammonium sulfate saturation does the precipitate in the precipitation stage realize its highest purity?
- What is a plausible combination of ammonium sulfate saturation percentages for consecutive precipitation stages? How does using two stages of precipitation improve the c-phycocyanin purity ratio?
- Considering the operating conditions identified to be best for the pilot plant process, how robust is the precipitation step in terms of recovering and purifying c-phycocyanin from the different *Spirulina* powder feeds?

Overall process

- Considering the operating conditions identified to be best for the pilot plant process, how robust is the overall c-phycocyanin extraction and purification process in terms of recovering c-phycocyanin and purifying c-phycocyanin?

3 Approach to Project and Methodology

3.1 Research methodology

Owing to the quantitative objectives of this dissertation, laboratory experiments were the primary source of data collection. Secondary data sourcing stemmed from laboratory work that was followed up by modelling, e.g. fitting existing kinetic models to experimental data, using software to determine particle size distribution from laboratory-sourced microscopic images of feedstocks. Primary quantitative methods of data sourcing were rejected since most conjecture on the problem statement would not prove to be beneficial towards achieving research objectives owing to their lack of accuracy, e.g. it would not be preferred to guess a value of an optimum operating conditions when it was possible to determine the optimum conditions through experimental work.

3.2 Experimental approach

The key blocks of experiments were:

1. Characterisation of dried *Spirulina* powders
2. Leaching kinetics tests
3. Cell debris removal tests
4. ATPS tests
5. Ammonium sulfate precipitation tests
6. Full runs of process

The results of all experimental blocks (1-5) informed the methodology of block 6. The results from block 1 helped explain observation of the results from block 2 and 3.

3.3 Experimental methods

3.3.1 Materials

Three different dried *Spirulina* powder samples were used. The purpose of using different sources of dried *Spirulina* powder was to assess the robustness of the individual unit procedures and to observe the effect it has on the key performance indicators of the process (c-phycocyanin recovery and c-phycocyanin purity across each unit procedure).

The three dried *Spirulina* powder samples used in this experimental are as follows:

- Carbocraft *Spirulina* sourced from Carbocraft (Pty) Ltd, South Africa, Batch no. FKDS-0014080001
- Brenntag *Spirulina* sourced from Brenntag South Africa (Pty) Ltd, a product from China, Batch no. ZA01005125 (food grade)
- *Spirulina* of Indian origin, sourced from a local health foods company
- For the ammonium sulfate precipitation experiments, an additional *Spirulina* powder was used. This was Green Create Nutra *Spirulina* sourced from Green Create Nutra in L Escalier, Mauritius, batch no. unknown

Sources for chemicals used for the experimental work differed, and are named in the subsequent methodologies. All the deionised water used in the experimental work was type 2, <15MΩ.CM sourced from a Millipore Elix 3 unit, using reverse osmosis and electro-deionisation.

3.3.2 *Spirulina* powder feed size distribution

The aim of these experiments was to characterise the different dried *Spirulina* powder samples, with emphasis on the particle size distributions (PSDs) and the morphology of the cells. This included analysis of the powders before and after they were bead-milled.

For this analysis, 1 mL samples of a 111 $g.L^{-1}$ of dried *Spirulina* powder in 5.6 $g.L^{-1}$ citrate buffer (92 wt% trisodium citrate dihydrate and 8 wt% citric acid monohydrate, pH 6) were pipetted into 2 mL Eppendorf tubes before and after bead-milling (as per section 3.3.3). 20 µL of each Eppendorf sample tube was diluted to 50× using deionized water (type 2, <15MΩ.CM) and placed on glass microscope slides with a cover slip. These slides were then subject to microscopy using an Olympus BX40 microscope. The Phase 2 contrast setting was used to view the cells under 10× magnification. A Dino-Lite digital microscope was inserted into the eyepiece of the BX40 microscope and connected to a laptop to capture images of the focused magnification of the *Spirulina* cells.

In the DinoXcope software for Macintosh OS, the images were scaled by inputting the degree of magnification, as shown in Figure 8.

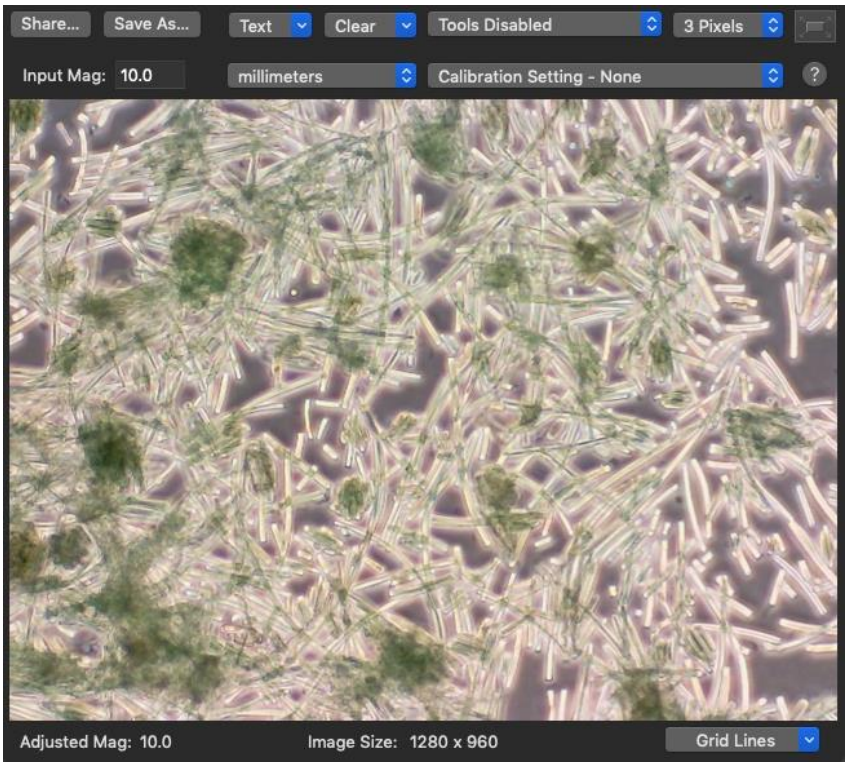

Figure 8. Screenshot of the DinoXcope software interface

These images were then processed using ImageJ to determine the size distribution and shape of the cells. The following method was used to prepare the image for the distribution determination after opening the ImageJ software:

> "File" → "Open.." → select desired image → "Image" → "Adjust" → "Color Threshold..." → Hue, Saturation and Brightness of the image was adjusted to the point at which only the cells are red. → "Analyze" →"Set scale…" → the scale was then adjusted to match that of the magnification used →"Analyze" →"Analyze particles" → the inputs summarized in Table 12 were entered →"Analyze" → "Distribution…" → the inputs summarized in Table 13 were entered → the data generated was then exported to Microsoft Excel for further analysis.

The images generated after the "Colour Threshold…", "Analyze particles" and "Distribution…" functions were all saved.

Table 12. Summary of inputs for "Analyze" tab in ImageJ software

“Analyze particles” Item	**Input**
Size (mm^2)	0.05 – Infinity
Circularity	0.00 – 1.00
Show	Outlines
Check boxes	Display results, clear results

Table 13. Summary of inputs for "Distribution" tab in ImageJ software

“Distribution” Item	**Input**
Parameter	Area
Specify bins	1000
Range	0 - 500

3.3.3 *Spirulina* cell disruption via bead-milling

The *Spirulina* cells were disrupted using the cell disruption method proposed by Hockey (2020). In later sections of this dissertation, “milled *Spirulina*” refers to a stock sample of *Spirulina* that was subjected to the methodology described here.

The *Spirulina* cells in the dried powders were disrupted as follows. 1 kg of 1 mm diameter borosilicate glass beads (purchased from MilliporeSigma) were added to a 3 L bucket. 900 mL of deionised water (type 2, <15MΩ.CM) was poured into this 3 L bucket. 100 g of dried *Spirulina* powder was weighed and added to the bucket. The slurry was stirred using an overhead stirrer (Rexon ® RDM-100A 14”) at 250 rpm. 5.6 $g.L^{-1}$ of citrate buffer was weighed out and added after the overhead stirrer RDM-100A was turned on. The citrate buffer was made up of 92 wt% trisodium citrate and dihydrate and 8 wt% citric acid monohydrate, pH 6 confirmed using Lasec pH 50+ DHS probe. Citric acid (99.5% purity) was sourced from Merck (Pty) Ltd. Batch no. 1048884 and trisodium citrate dihydrate (mb grade) was sourced from Merck (Pty) Ltd. Batch no. 3226531. Masses were weighed using a Radwag PS 4500.R2 balance. Following the addition of the citrate buffer, the slurry was left to be milled for 15 min at room temperature. The slurry was then poured into a 1 L Erlenmeyer flask through a 180 µm aperture sieve tray and funnel. This allowed for the separation of the glass beads from the slurry.

3.3.4 c-Phycocyanin leaching tests

c-Phycocyanin leaching tests were performed on the different feedstocks of dried *Spirulina* powder (as supplied as well as milled). This was to gauge the c-phycocyanin leaching patterns across the different feedstocks under the leaching conditions proposed by Hockey (2020). These tests also aimed to determine the average c-phycocyanin content in the different dry *Spirulina* powders and the time required to reach the equilibrium concentration of c-phycocyanin in the leachate.

Leaching was performed in a 3 L bucket, with 100 g dry weight *Spirulina* powder (with or without milling as per 3.3.3) suspended in 900 mL of a 5.6 $g.L^{-1}$ citrate buffer. Citrate buffer was made up of 92 wt% trisodium citrate and dihydrate and 8 wt% citric acid monohydrate, pH 6 confirmed using Lasec pH 50+ DHS probe. Citric acid (99.5% purity) was sourced from Merck (Pty) Ltd. Batch no. 1048884 and trisodium citrate dihydrate (mb grade) was sourced from Merck (Pty) Ltd. Batch no. 3226531. Masses were weighed using a Radwag PS 4500.R2 balance. The mixture was left to be stirred under an overhead stirrer (Rexon ® RDM-100A 14”) at 250 rpm for 24 hours at room temperature.

2 mL samples were drawn (via pipette) from the mixture at regular intervals over the 24-hour period. The samples were pipetted into 2 mL Eppendorf tubes. The samples were centrifuged at the time of the sample being taken, using a Eppendorf Minispin Plus benchtop centrifuge at 10 000 g for 8 min. 1 mL of the supernatant was pipetted and used to determine the c-phycocyanin purity ratio, total protein

concentration and c-phycocyanin concentration at that point in the leaching time using spectroscopy methods (explained in the *Analytical methods* section).

3.3.5 Cell debris removal

The aim of these experiments was to determine recovery of product-containing supernatant at different centrifugation conditions. The independent variable investigated was centrifugation speed as opposed to centrifugation time as there is a minimum settling velocity for particles and it was important to ensure this minimum settling velocity was overcome with the centrifugation speeds used in the process. The dependent variable investigated was recovery of supernatant as this would be directly proportional to the recovery of the desired protein c-phycocyanin as it is a water-soluble protein and is thus found in the supernatant at this point in the process.

This set of experiments was performed on a stock mixture of 111 $g.L^{-1}$ of milled (as per 3.3.3) or non-milled *Spirulina* powder in a citrate buffer (5.6 $g.L^{-1}$: 92 wt% trisodium citrate dihydrate, 8 wt% citric acid monohydrate, pH 6). Citric acid (99.5% purity) was sourced from Merck (Pty) Ltd. Batch no. 1048884 and trisodium citrate dihydrate (mb grade) was sourced from Merck (Pty) Ltd. Batch no. 3226531. Masses were weighed using a Radwag PS 4500.R2 balance.

2 mL samples of the stock mixture were then pipetted into the 2 mL Eppendorf tubes of known mass, which were again weighed. The stock mixture was kept under an overhead stirrer RDM-100A at 250 rpm throughout the sampling process.

Samples were centrifuged for 8 min at relative centrifugal forces (g) over the range of 1000 g to 10 000 g using an Eppendorf Minispin Plus benchtop centrifuge. After centrifugation, the supernatants (referred to as crude extract from here onwards) were poured into 2 mL Eppendorf tubes of known mass by turning the initial tubes upside down for 10 seconds. The initial Eppendorf tubes were weighed again before being left in a Labotec EcoTherm drying oven at 80 °C for 24 hours to dry the cell debris. After drying, the Eppendorf tubes were weighed again. The Eppendorf tubes containing the crude extracts were used to determine the c-phycocyanin purity ratio and c-phycocyanin concentration using spectroscopy (methods explained in the Analytical methods section).

For subsequent experiments, after the crude extract was poured off, the Eppendorf tubes containing the cell debris were supplemented with 1 mL of citrate buffer (5.6 $g.L^{-1}$: 92 wt% trisodium citrate, 8 wt% citric acid, pH 6), allowed to leach at room temperature for 5 hours, and centrifuged for a second time. This second centrifugation used the same benchtop centrifuge, but was operated at 7000 g relative centrifugal force for 8 minutes. The crude extract was poured off into 2 mL Eppendorf tubes of known mass. Both the initial tubes and the tubes containing the crude extract were weighed. The tubes containing the cell debris were left in a drying oven at 80 °C for 24 hours to dry the cell debris. After 24 hours the tubes were removed from the oven and weighed. The Eppendorf tubes containing the supernatants were used for determining the c-phycocyanin purity ratio and c-phycocyanin concentration using spectroscopy (methods explained in Analytical methods section).

3.3.6 Aqueous two-phase separation (ATPS)

The ATPS experimental block was performed to determine the robustness of this separation system. The conditions recommended by Hockey (2020) were used to determine if those optimized conditions were applicable over the range of different *Spirulina* feedstocks.

Figure 9 describes the general ATPS experimental procedure, followed for all ATPS types. A 10 mL sample of the stock solution at different dilutions ranging from 1× to 4× was poured into a 50 mL centrifuge tube of known mass and weighed. Components necessary to obtain the correct weight percentages for the ATPS were measured out and added to the centrifuge tube. Masses were weighed using a Radwag PS 4500.R2 balance. The centrifuge tube contents were mixed for 20 seconds by placing the tube on a benchtop vortex (Scientific Industries Vortex Genie 2) running at maximum speed. The centrifuge tube was then centrifuged using a Hettich Zentrifuge Universal 320 benchtop centrifuge for 15 min at 2640 g relative centrifugal force at room temperature.

The volume distribution between the two phases formed was measured. The top phase was siphoned off using a syringe into a 50 mL centrifuge tube of known mass. A 1 mL sample of both phases were pipetted into a 2 mL Eppendorf tubes of known mass to calculate the densities of the phases. These samples were then also used to determine the c-phycocyanin purity ratio and c-phycocyanin concentration using spectroscopy (methods explained in the *Analytical methods* section).

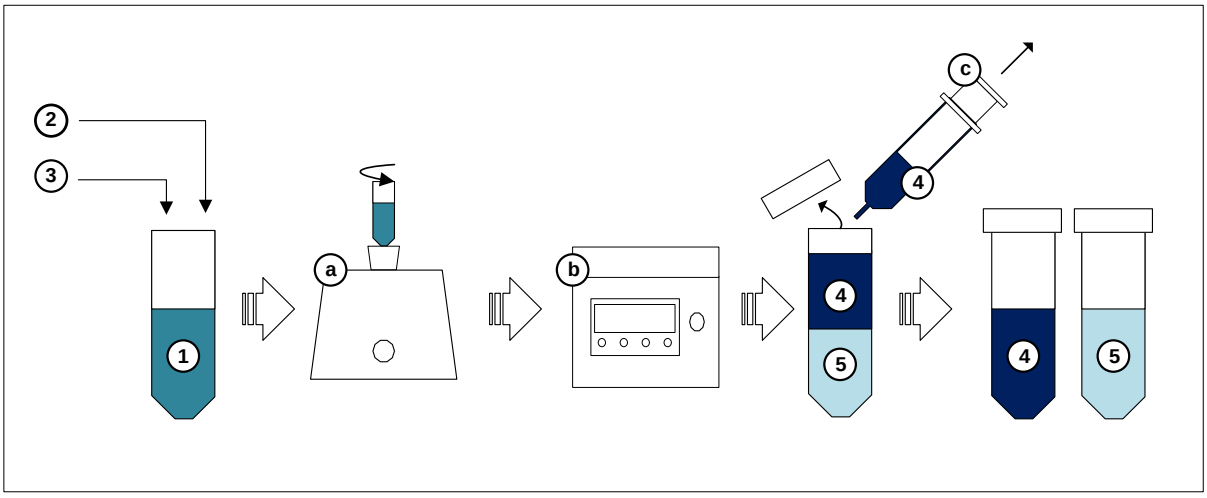

Figure 9. Diagram of ATPS experimental procedure, with numbers and letters in the figure referring to: (1) Initial c-phycocyanin containing stock solution; (2) PEG 4000/deionized water; (3) Citrate salts/maltodextrin; (4) Top phase; (5) Bottom phase; (a) Benchtop vortex; (b) Centrifuge; (c) Syringe.

PEG-citrate (single-stage) ATPS

For a single-stage PEG-citrate ATPS, the methodology described in Figure 9 was performed using a stock solution of crude extract (1), post cell debris removal of 111 $g.L^{-1}$ of milled dried *Spirulina* powder in a 5.6 $g.L^{-1}$ citrate buffer. The citrate buffer was made up of 92 wt% trisodium citrate and dihydrate and 8 wt% citric acid monohydrate, pH 6 confirmed using Lasec pH 50+ DHS probe. Citric acid (99.5% purity) was sourced from Merck (Pty) Ltd (Batch no. 1048884) and trisodium citrate dihydrate (mb grade) was sourced from Merck (Pty) Ltd (Batch no. 3226531). PEG 4000 (2) sourced from Sigma Aldrich (Batch no. BCCH1629) and citrate salts (3) (92 wt% sodium citrate and 8 wt% citric acid) were measured out and added to the crude extract (1) to allow for a mixture composition of the first ATPS system, summarized in Table 14.

Table 14. Mass fractions of components used for PEG-citrate ATPS procedure, adapted from Hockey (2020)

Component	**Mass fraction**
Crude extract	0.69
Citrate salts	0.2
trisodium citrate dihydrate	*0.184*
citric acid monohydrate	*0.016*
PEG 4000	0.11
Total	**1**

PEG-maltodextrin (single-stage) ATPS

For a single-stage PEG-citrate ATPS, the methodology described in Figure 9 was performed using a stock solution of crude extract (1), post cell debris removal of 111 $g.L^{-1}$ of milled dried *Spirulina* powder

in a 5.6 g.L^{-1} citrate buffer. The citrate buffer was made up of 92 wt% trisodium citrate and dihydrate and 8 wt% citric acid monohydrate, pH 6 confirmed using Lasec pH 50+ DHS probe. Citric acid (99.5% purity) was sourced from Merck (Pty) Ltd (Batch no. 1048884) and trisodium citrate dihydrate (mb grade) was sourced from Merck (Pty) Ltd (Batch no. 3226531). PEG 4000 (2) (sourced from Sigma Aldrich, Batch no. BCCH1629) and maltodextrin (3) (sourced from Supplement World, South Africa) were measured out and added to the crude extract (1) to allow for a mixture composition of the first ATPS system, summarized in Table 15.

Table 15. Mass fractions for components used for PEG-maltodextrin ATPS procedure, adapted from Hockey (2020)

Component	Mass fraction
Crude extract	0.67
Maltodextrin	0.22
PEG 4000	0.11
Total	**1**

PEG-citrate & PEG-maltodextrin (two-stage) ATPS

For a two-stage ATPS using a PEG-citrate combination followed by PEG-maltodextrin combination, the methodology described in Figure 9 is followed using chemicals as per “PEG-citrate (single-stage). Thereafter, the methodology described by Figure 9 is followed again using the PEG phase (4) from the PEG-citrate (single-stage) as (1), deionized water as (2) and maltodextrin as (3). Mass fractions for the second stage are summarized in Table 16.

Table 16. Mass fractions for components used for PEG-maltodextrin ATPS procedure for a two-stage ATPS system, adapted from Hockey (2020)

Component	Mass fraction
Deionized water	0.67
Maltodextrin	0.22
PEG (top) phase	0.11
Total	**1**

3.3.7 Ammonium sulfate precipitation

For the ammonium sulfate precipitation experiments, an additional *Spirulina* powder was used. This was Green Create Nutra *Spirulina* sourced from Green Create Nutra in L Escalier, Mauritius, batch no. unknown.

The first aim of the ammonium sulfate precipitation experiments was to find the optimum ammonium sulfate saturation percentage for removal of contaminating proteins without significant loss of the desired protein, c-phycocyanin – i.e. to achieve the highest possible c-phycocyanin purity in the supernatant without significant loss in recovery of c-phycocyanin. A second aim was to find the optimum ammonium sulfate saturation percentage that yields the highest c-phycocyanin purity ratio in the precipitate pellet. Finally, a third aim of these experiments was to determine how different samples of *Spirulina* performed in an ammonium sulfate precipitation step, and thereby assess the robustness of the ammonium sulfate precipitation procedure.

The following methods were performed on stock solutions of different *Spirulina* crude extracts containing c-phycocyanin, and other intracellular macromolecules. These stock solutions had undergone cell disruption (*Spirulina* cell disruption via bead-milling) and leaching in citrate buffer (5.6 g.L^{-1}: 92 wt% trisodium citrate dihydrate, 8 wt% citric acid monohydrate, pH 6) for 24 hours, followed

by cell debris removal. The ammonium sulfate precipitation experiments were carried out at room temperature.

Single stage ammonium sulfate precipitation

Ammonium sulfate salt (analysis grade) sourced from Merck (Pty) Ltd (Batch no. AM1297217) was used to precipitate proteins out of the starting solution. Ammonium sulfate was added to volumes of the crude extracts at salt saturation percentages ranging from 10 to 99 %. The calculation of the salt saturation percentages can be found in the Appendix section A.3.1. Figure 10 describes the single stage ammonium sulfate precipitation procedure. Masses were measured using Radwag PS 4500.R2 balance.

The single stage ammonium sulfate precipitation was performed by taking 20 mL of the starting solution and pouring it into a 50 mL centrifuge tube of known mass. A pre-determined specific mass of ammonium sulfate salt was weighed out and added to the centrifuge tube. The tube was then weighed, and the mass recorded. The solution within the centrifuge tube was mixed using a desktop vortex spinner (Scientific Industries Vortex Genie 2) for 20 seconds. The centrifuge tube was then centrifuged for 15 min at 2640 g using a Hettich Zentrifuge Universal 320 desktop centrifuge. After centrifugation, the supernatant was poured out of the centrifuge tube into another centrifuge tube (of known mass) to isolate the precipitate which remained in the original tube. The centrifuge tube containing the precipitate and the tube containing the supernatant were weighed and the volume read off the graduated markings.

The conductivity of the supernatant was measured using a benchtop conductivity meter. The precipitate was resuspended in 20 mL of deionized water. Both the supernatant and the resuspended precipitate were analysed for their c-phycocyanin purity ratio and concentration of c-phycocyanin using spectroscopy (method described in the "*Analytical methods*" section).

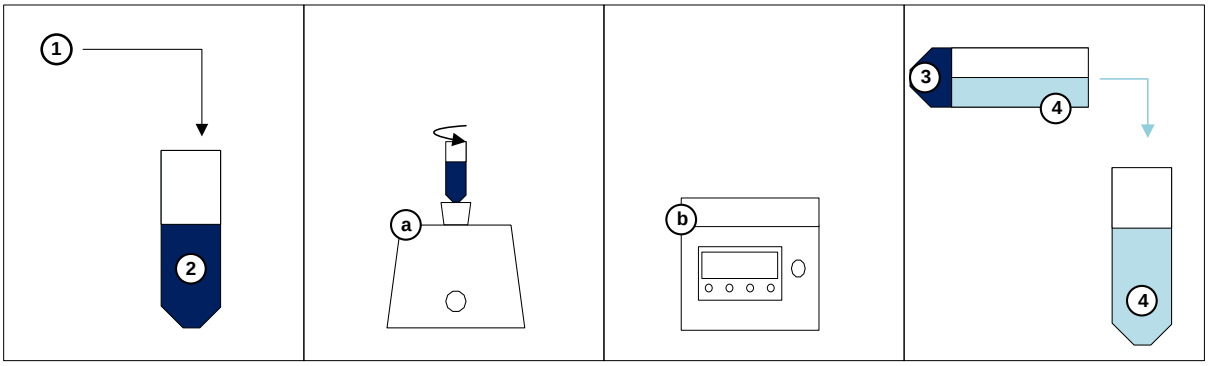

Figure 10. Diagram describing experimental procedure for a single stage ammonium sulfate precipitation, with numbers and letters in the figure referring to: (1) Ammonium sulfate crystals; (2) Stock solution of *Spirulina* leachate; (3) Precipitate pellet; (4) Supernatant; (a) Benchtop vortex; (b) Benchtop centrifuge.

Two-stage ammonium sulfate precipitation

Ammonium sulfate salt (analysis grade) sourced from Merck (Pty) Ltd (Batch no. AM1297217) was used to precipitate proteins out of the starting solution of crude extract. The first stage of the ammonium sulfate precipitation aims to remove impurities and unwanted proteins from the crude extract. Once these unwanted proteins and impurities were precipitated out, the supernatant of the first stage was treated with more ammonium sulfate aiming to precipitate out the desired protein of c-phycocyanin whilst potentially improving its purity ratio. The ammonium sulfate saturation percentages used for the first and second stage were determined from the results of the single-stage ammonium sulfate precipitation experiments (the explanation of this choice is found in section 4.5).

Figure 11 describes the two-stage ammonium sulfate precipitation procedure. A 20 mL stock solution of crude extract was poured into a 50 mL centrifuge tube. Ammonium sulfate was weighed out and added to a saturation percentage of 22 %. This centrifuge tube was centrifuged using the same method

as before (for the single precipitation). The supernatant was sequestered, and more ammonium sulfate was weighed out and added to the supernatant to reach a cumulative saturation percentage of 45 %. The centrifuge tube was then centrifuged (same conditions as for the single precipitation). After centrifugation, the supernatant was poured off and the pellet resuspended in 20 mL of deionized water. Both the supernatant and the resuspended precipitate were analysed for their c-phycocyanin purity ratio and concentration of c-phycocyanin using spectroscopy (method described in the "*Analytical methods*" section).

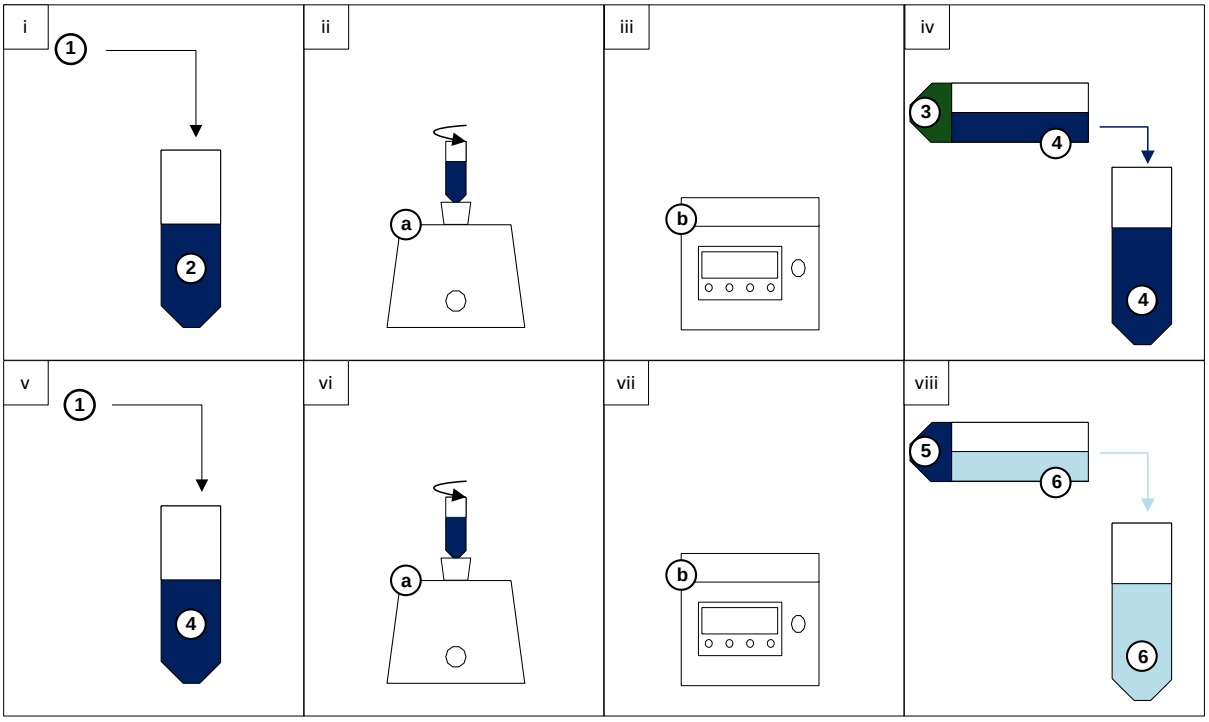

Figure 11. Diagram describing the experimental procedure used for a two-stage ammonium sulfate precipitation, with numbers and letters in the figure referring to: (1) Ammonium sulfate crystals; (2) Stock solution of *Spirulina* leachate; (3) Precipitate pellet after 1st precipitation; (4) Supernatant after 1st precipitation; (5) Precipitate pellet after 2nd precipitation; (6) Supernatant after 2nd precipitation; (a) Benchtop vortex; (b) Benchtop centrifuge.

3.3.8 Microfiltration

This set of experiments were performed on the final c-phycocyanin precipitate pellet (post two-stage ammonium sulfate precipitation) as part of the full runs of the process. The purpose of including microfiltration is to remove any microorganisms and other impurities from the c-phycocyanin protein product through size exclusion.

The precipitate pellet containing the c-phycocyanin was diluted 3× by mass with deionized water (type 2, <15MΩ.CM) and vacuum filtered using a benchtop vacuum filter set-up. The filters and their details are summarized in Table 17. The procedure used for the vacuum filtration is described in Figure 12.

Table 17. Filter membranes in order and with pore size used for the micro-filtration procedure

Order	Name	Pore size(μm)
1	Carl Schleicher & Schüll Marke Selecta Nr. 604	12
2	Whatman glass microfibre GF/A 1820-047	1.6
3	LASEC FLAS31103047 Glass fibre	1.2
4	FILTER-LAB® Gridded MCE Membrane	0.45

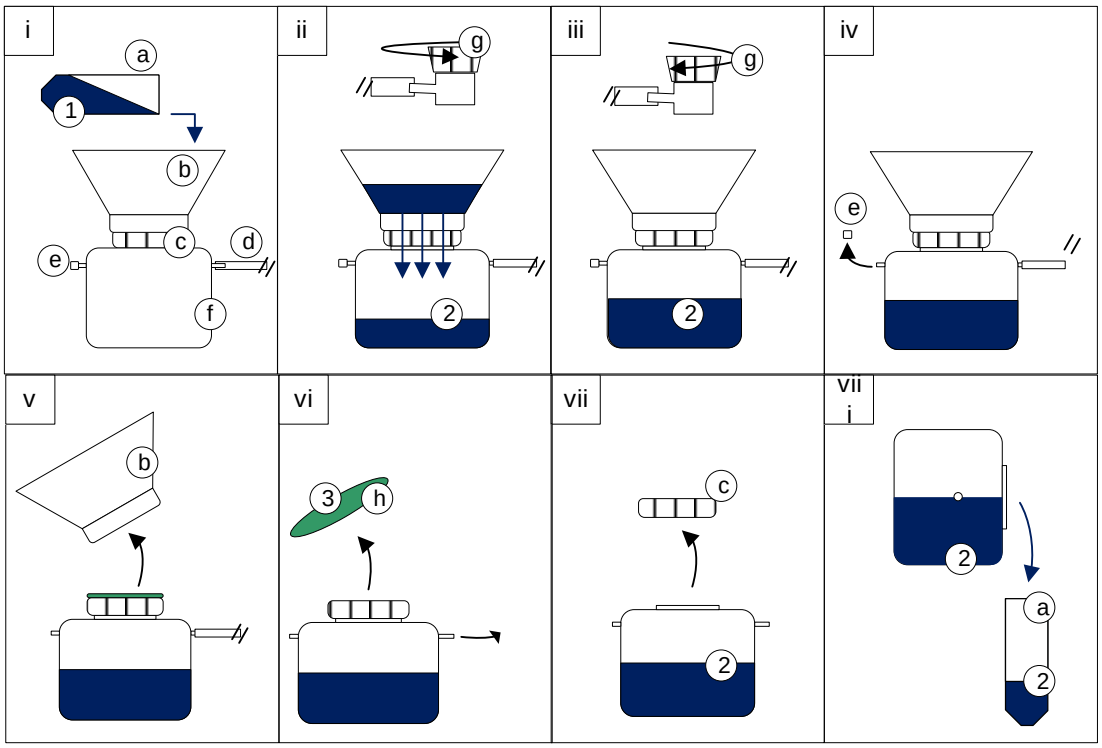

Figure 12. Diagram describing the procedure of using a benchtop vacuum filtration system, with numbers and letters in the figure referring to: (1) Feed solution; (2) Filtrate; (3) Filter retentate cake; (a) centrifuge tube; (b) Filter funnel; (c) Membrane base; (d) Port to vacuum; (e) Vacuum release port; (f) Filter base; (g) Valve for vacuum; (h) Filter membrane.

With reference to Figure 12, the desired filter paper (1) was placed onto the base of the vacuum filter (2). The lid was then screwed on until it catches (3). Thereafter, the tube (4) connected to the vacuum pump was connected to the vacuum filter base (2a). Then, the solution (5) was poured into the filter. The valve was then opened by twisting the handle (6) to create a vacuum within the vacuum filter. This pulled the liquid and all solubilized components smaller than the filter paper pore size through the filter and into the base of the vacuum filter. After closing the valve, the stopper (2b) was opened to release the vacuum in the base. The lid was then unscrewed, and the filter paper was removed. The filtrate was poured into a 50 mL centrifuge tube and the vacuum filter base and lid was rinsed and dried. The next filter paper, with smaller pore size than the previous, was then placed on the vacuum filter base and the process was repeated by pouring the filtrate from the previous filtration into the funnel of the lid. 1 mL of the filtrate after each consecutive filter was pipetted into a 2 mL Eppendorf tube. The samples taken in the Eppendorf tubes were analysed for their c-phycocyanin concentration and c-phycocyanin purity ratio (method described in the "*Analytical methods*" section).

3.3.9 Full runs of process

Full runs of the process were performed to assess the overall performance of the process when subject to the different dried *Spirulina* powder samples. The runs were conducted operating at the newly established best conditions from the preceding experiments. As well as determining the overall process performance, the aim of these experiments was to determine c-phycocyanin purity and recovery after each unit procedure.

Based on the results of the previous experimental blocks, the final process that was assessed excluded any ATPS procedures and included a microfiltration procedure following the ammonium sulfate precipitation train. Microfiltration was used as a method of further purifying the product stream of the final precipitation step. Microfiltration was used to filter out unwanted bacteria and larger protein and other contaminants that reduce c-phycocyanin purity. The full runs experiments were carried out at room temperature.

The details of the full run of the process are as follows.

Cell disruption and leaching

The *Spirulina* powder was disrupted as follows. 1 kg of 1 mm diameter glass beads were added to a 3 L bucket. 900 mL of de-ionized water type 2, <15MΩ.CM sourced from CeBER laboratories, was poured then poured into this 3 L bucket. 111 $g.L^{-1}$ of dried *Spirulina* powder was weighed out and added to the bucket. The slurry was stirred using an overhead stirrer Rexon ® RDM-100A 14" at 250 rpm. 5.6 $g.L^{-1}$ of the citrate buffer (92 % trisodium citrate dihydrate and 8 % citric acid monohydrate, pH 6) was weighed out and added after the overhead stirrer RDM-100A was turned on. Citric acid (99.5% purity) was sourced from Merck (Pty) Ltd. Batch no. 1048884 and trisodium citrate dihydrate (mb grade) was sourced from Merck (Pty) Ltd. Batch no. 3226531. Masses were measured using Radwag PS 4500.R2 balance.

Following the addition of the citrate buffer the slurry was left to be milled for 15 min at room temperature. The slurry was then poured into a 1 L Erlenmeyer flask through a 180 µm aperture sieve tray and funnel. This allowed for the separation of the glass beads from the slurry.

After cleaning the 3 L bucket with municipal water (sourced from City of Cape Town) and drying it with paper towel, the mixture was poured from the Erlenmeyer flask back into the 3 L bucket and put back under the overhead stirrer to leach for 24 hours.

Cell debris removal

After being left to leach and the bucket weighed, three 2 mL samples were pipetted into separate 2 mL Eppendorf tubes before the mixture was poured into 500 mL Beckmann centrifuge bottles and centrifuged at 10 000 g for 20 min using a Beckmann Avanti-J25 standing centrifuge at room temperature. After centrifugation, the centrifuge bottles were removed and the supernatant poured into another 3 L bucket of known mass. The bucket filled with the supernatant was weighed.

Precipitation

Ammonium sulfate was added to the bucket to achieve an ammonium sulfate saturation percentage of 22 %. This mixture was put under an overhead stirrer x for 10 min. Once mixed, the solution was poured equally into 50 mL centrifuge tubes of known mass and centrifuged at 2640 g for 15 min using a Hettich Zentrifuge Universal 320 benchtop centrifuge after three 2 mL samples of solution was pipetted into separate 2 mL Eppendorf tubes. After centrifugation the supernatant was poured into a 3 L bucket of known mass. The 50 mL centrifuge tubes containing the precipitate were weighed. More ammonium sulfate was added to the supernatant to achieve 45 % ammonium sulfate saturation. This solution was mixed for 10 min using a Rexon ® RDM-100A 14" overhead stirrer with 6-paddle impeller at 250 rpm.

Thereafter poured equally into 50 mL centrifuge tubes of known mass and centrifuged at 2640 g for 15 min using a Hettich Zentrifuge Universal 320 benchtop centrifuge after three 2 mL samples of solution was pipetted into separate 2 mL Eppendorf tubes. After centrifugation the supernatant was poured into a 500 mL Erlenmeyer flask of known weight and weighed. Three 2 mL samples of solution were pipetted into separate 2 mL Eppendorf tubes and used.

Microfiltration

Following the precipitation, the pellet containing the c-phycocyanin was diluted 3× by mass with deionized water type 2, <15MΩ.CM, sourced from CeBER laboratories and vacuum filtered using a benchtop vacuum filter set-up. The filters and their details are summarized in Table 17. The procedure used for vacuum filtration is described in Figure 12.

The samples taken in the Eppendorf tubes were subject to spectroscopy methods explained in the *Analytical methods* section to determine c-phycocyanin concentration and purity ratio.

3.3.10 Analytical methods

Spectroscopy

Photospectroscopy was used to analyze the c-phycocyanin purity and concentration in the various feed and product streams. For this, a FLUOstar Omega spectrophotometer was used to measure the absorbance of the samples at various wavelengths. In each instance, 200 µL of appropriately diluted samples were pipetted into a 96-well multi-well plate and the plate inserted into the FLUOstar Omega spectrophotometer. "Absorbance Endpoint" was the assay function inputted to generate the absorbance OD at 280, 620 and 650 nm light wavelengths.

c-Phycocyanin purity ratio was determined using the absorbances at wavelengths of 620 nm and 280 nm according to Equation 1 (Erikson, 2008):

$$Purity\ ratio = \frac{A_{620\ nm}}{A_{280\ nm}} \qquad \text{Equation 1}$$

c-Phycocyanin concentration was determined using absorbances at wavelengths of 620 nm and 650 nm, according to Equation 3 (Yoshikawa & Belay, 2008):

$$c - phycocyanin\ \left(\frac{mg}{mL}\right) = 0.162 \times A_{620\ nm} - 0.098 \times A_{650\ nm} \qquad \text{Equation 3}$$

A calibration to find the linear ranges of absorbance readings was performed to understand the extent to which the samples needed to be diluted to allow for the absorbance readings to be a trustworthy representation of the composition of the sample. A sample stock of crude extract of *Spirulina* powder in citrate buffer was diluted in the range of 1× to 300× and subject to spectroscopy. Absorbance readings were recorded at wavelengths of 280 nm, 620 nm and 650 nm. Figure 13 was generated from this data. The linear ranges of the absorbance readings were found for each wavelength tested by using linear regression on Microsoft Excel for the best fit of linearity between at least 3 data points. The results of the linear regression are summarized in Table 18.

Table 18. Summary of the linear ranges for absorbance (OD) at 280, 620 and 650 nm with the coefficient of determination for that range

Light wavelength (nm)	Linear absorbance range (OD)	Coefficient of determination
280	1.1 – 3.34	0.985
620	0.48 – 1.03	0.932
650	0.25 – 0.6	0.903

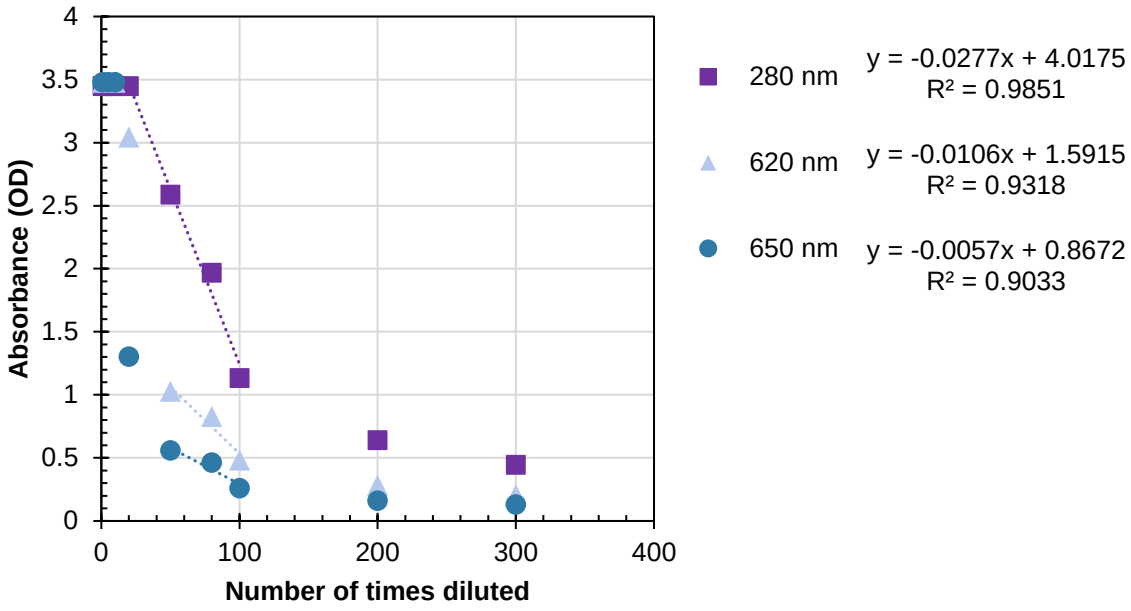

Figure 13. Plot of dilution vs absorbance (OD) at 280, 620 and 650 nm using the FLUOstar Omega spectrophotometer.

Performance indicators

c-Phycocyanin purity ratio

The purity of c-phycocyanin is typically reported as a purity ratio. It is a ratio of the maximum absorbance of c-phycocyanin to the maximum absorbance for total amino acids in solution. The absorbances from the spectrophotometer were used to calculate this purity ratio as described above. The ratio is quoted as Equation 1 from Erikson (2008).

$$Purity\ ratio\ = \frac{A_{620}}{A_{280}}$$ Equation 1

c-Phycocyanin concentration

In the results of this dissertation, the c-phycocyanin concentration of a sample was determined by Equation 3 (Yoshikawa & Belay, 2008):

$$C_{c-PC}(\mathrm{mg.mL^{-1}}) = 0.162\ \times\ A_{620} - 0.098\ \times A_{650}$$ Equation 3

Purification factor

The purification factor is the ratio of purity ratios before and after a particular purification method. It gives an indication of the extent of purification of that method on the sample. The purification factor is the ratio of c-phycocyanin purity of the product stream out of a purification process to the c-phycocyanin purity of the feed to that process, described by Equation 22:

$$Purification\ factor\ = \frac{c-phycocyaninPurity\ ratio_B}{c-phycocyanin\ Purity\ ratio\ _A}$$ Equation 22

Where B is the product stream and A is the feed stream.

c-Phycocyanin recovery

c-Phycocyanin recovery is calculated based off the c-phycocyanin concentration in the feed and product streams over an entire system or over a particular extraction/purification step in the system. The concentration and the volume of the streams are multiplied to determine the c-phycocyanin mass in that stream (Equation 23):

$$c-PC\ concentration\ \times\ volume\ of\ sample = mass\ of\ c-PC \qquad \text{Equation 23}$$

c-Phycocyanin recovery over a process can therefore be described by the following Equation 24:

$$Rec_{c-PC}\ (\%) = \frac{mass\ of\ c-PC_{out}}{mass\ of\ c-PC_{in}} \times 100\ \% \qquad \text{Equation 24}$$

Solution densities

All solution densities reported or used were determined by pipetting 1 mL of the respective solution into a 2 mL Eppendorf tube of known mass and then weighed. The weighing was performed in triplicate using an Ohaus Adventurer Analytical fine balance.

Statistical analysis

Experimental error

Experimental error was estimated and standard deviation between experimental and analytical repeats was calculated and used to represent this experimental error. In text and in tables, the standard deviation is presented as the uncertainty in the quoted figure, notated with "±". In figures, the standard deviation is depicted using error bars. Experimental error was propagated, where applicable.

Experimental data plotting

For all general calculations and for all graphs generated, Microsoft Excel 2019 was used.

For the methodology described in 3.3.2, DinoXcope and ImageJ software were used to generate images and subsequently particle size distribution data. Said data was then exported to Microsoft Excel and Excel was used to generate the graphs and data found in Chapter 4 Results and Discussion.

Experimental data fitting

Where applicable for fitting existing literature models to experimental data, weighted least squares straight line fitting method and linear regression was used (Shine, 2006). These methods were used on the experimental data generated from 3.3.4 c-Phycocyanin leaching tests methodology to fit Equation 7 and Equation 8 from 2.5.2 of the Literature Review onto said data.

Experimental data interpretation

To help statistically validate interpretation of experimental data, statistical analysis methods were used. To evaluate the significance of the difference between two data sets, a t-test was used. To evaluate the significance of the difference trends in more than two data sets, a method of linear regression followed by t-tests on the linear model generated was used. These statistical analyses were performed on Python using the statsmodels library.

4 Results and Discussion

4.1 *Spirulina* powder size distributions

This section presents the results of the size distribution of the *Spirulina* powder samples used in this project, both prior to and after milling. The milling tests in particular were required to understand the robustness of the milling setup and to ensure that breakage of *Spirulina* cells occurred, to facilitate leaching of the intracellular c-phycocyanin product. Establishing the size distributions of the different samples used will also help in discussion of other results in this chapter, as the size distributions are anticipated to potentially influence leaching patterns and the effectiveness of cell debris removal.

The results were generated using the DinoXcope and ImageJ software, following the methodology described in 3 Approach to Project and Methodology. Examples of the images used to generate the size distribution graphs can be found in Appendix B.1 Size distribution for the *Spirulina* powder samples tested.

Table 19 presents key values describing the particle size distribution and median values for the different *Spirulina* powders, in both their original states and after milling. The d_{80} is the representative diameter for a distribution such that 80% of the population of particles have a diameter smaller than the d_{80} value. The d_{50} is the representative diameter for a distribution such that 50% of the population of particles have a diameter smaller than the d_{50} value, where d_{50} is considered the median diameter of a population. The d_{ave} is the representative diameter for a distribution that is the average (mean) diameter of the population of particles. Table 19 also presents standard deviation from the mean diameter for all the *Spirulina* powder samples before and after milling, this data informs the width of the distribution of particle diameters which are visually depicted in Figure 14, Figure 15 and Figure 16.

The Brenntag and Carbocraft powders in their original states showed similar cut sizes in d_{80}, d_{ave}, but not d_{50}. For the Carbocraft powder sample, the d_{50} and d_{80} were less than 10% apart, at 0.50 ± 0.01 mm and 0.54 ± 0.02 mm respectively. The Indian powder was much smaller than the Brenntag and Carbocraft powder samples, with most measurements of diameter being less than half the size of the Brenntag and Carbocraft diameters. This confirms that there can be significant differences in the *Spirulina* powder particle sizes from different suppliers.

It was thought that milling of the powders for the same residence time, with the same milling media for the same mill loading, would result in the same, if not similar, median diameters in all samples, since the stress intensity of the mill is directly related to the median of the size distribution of the particles (Green & Perry, 2008). This would be the case if the threshold milling residence time is overcome. Data supporting this would be beneficial to the process since it would allow for distributions of equal median diameters across all *Spirulina* powders in the product stream after the milling. Equal distributions would, in turn, would allow for a simpler design procedure for centrifuges used for cell debris removal and allow for better comparison between the leaching patterns of different *Spirulina* powder samples. This is due to solid-liquid separation being more predictable, since most classification methods use size and density as the driving force for separation (Green & Perry, 2008).

From Table 19, we see that though the Brenntag and Carbocraft samples had different median diameters prior to milling (0.33 ± 0.04 mm and 0.50 ± 0.01 mm, respectively), they had the same median diameters after milling (0.25 ± 0.02 mm and 0.25 ± 0.03 mm, respectively). This supports the assumption that the threshold milling residence time had been overcome to allow for similar distributions of particle diameters across these two *Spirulina* powder samples. The d_{80} and d_{ave} for the Brenntag and Carbocraft samples prior to milling were within 10% of each other, and were still within 10% of each other post-milling, albeit significantly smaller. This suggests that the milling setup and dependent parameters allowed for similar distributions of diameter in the post-milling product stream for the Brenntag and Carbocraft samples.

The Indian sample, prior to milling, had a median diameter smaller than that of the milled Carbocraft and Brenntag samples. For d_{50}, d_{80} and d_{ave}, the Indian sample did not yield significant changes after milling (all changed less than 15%). Thus, little breakage occurred. This suggests that because the particle size distribution is dependent on the milling loading, residence time and milling media, either the threshold stress intensity was not overcome during milling for the Indian sample to yield smaller diameters after milling, or the residence time was not long enough to see a significant change in the distribution of the sample diameter. Further experiments on increasing residence time would help to understand the observation made from the Indian sample, however since this dissertation focuses on robustness testing of current conditions this was considered out of scope but should be considered for future work. Hlabangana et al. (2018) showed how the size distributions for the same feed changes with residence time, tending towards a smaller average particle diameter, smaller d_{80} and smaller d_{50} with increase in milling residence time. They also concluded that control of the particle size distribution in the feed is of utmost importance to improve efficiency of the mill. The data therefore suggests that to achieve a similar distribution after milling for all *Spirulina* powder samples, the residence time for milling should be longer or the media changed to increase the stress intensity.

Table 19 shows that the particle diameters of the Brenntag and Carbocraft samples prior to milling were widely distributed (high standard deviation from the average diameter) and after milling were still widely distributed. This means that there were many particle diameters that did not lie close to the representative diameters of the distribution. Therefore, the predictability of subsequent leaching and solid-liquid separation processes is potentially not well informed by the size distribution data.

From Figure 14 for the Brenntag sample, the milling shifted the bulk of the data in the PSD left. This indicates that the central tendency of the dataset became smaller in general without impacting the minimum and maximum observed particle sizes much. From Figure 15 it can be observed that the Carbocraft sample followed the same pattern as observed for Brenntag. With the actual representative diameters for the Carbocraft and Brenntag samples within 6 % of each other post-milling (see Table 19) it is suggested, based on size of particles, that the leaching patterns for Carbocraft and Brenntag will be similar. Figure 16 shows the very slight left shift in the PSD of the Indian sample from non-milled to milled. This suggests that the leaching patterns for the Indian sample milled and non-milled will be similar.

Based on the data generated, although it can be said that the current milling setup processed the Carbocraft and Brenntag *Spirulina* powder robustly (to produce particle size distributions that are significantly similar, within a 10% confidence interval), it cannot be said that the milling setup used is robust overall since it did not perform the same for significantly smaller particle sizes, i.e. the Indian sample (for which the representative diameter measurements were significantly different and no significant difference in representative diameters were observed after milling, with a 15% confidence interval). Simply put, the current setup of the mill is not robust enough to yield similar distributions of diameter across all samples tested. The change in representative diameter over the milling was considered a degree of breakage of cells since the degree of breakage caused by the drying methods are unknown. The degree of breakage and particle diameter will influence surface area exposed to the solvent which will influence the rate of leaching experienced downstream (Elgayar, et al., 2016; Su, et al., 2014; Harouna-Oumarou, et al., 2007).

Table 19. Representations of the size distributions for *Spirulina* samples, milled and non-milled. The uncertainty is notated using "±" and was calculated as the standard deviation of triplicate measurements. The STD values indicate the average standard deviation from the mean for the different powder diameter sizes – indicating the width of the particle size distribution.

	d_{80} (mm)	d_{50} (mm)	d_{ave} (mm)	Overall STD (mm)	Overall STD (% of mean)	95 % confidence interval of d_{ave} (mm)
Brenntag	0.51 ± 0.05	0.33 ± 0.04	0.41 ± 0.03	0.40	97	0.385 – 0.435
Brenntag milled	0.41 ± 0.04	0.25 ± 0.02	0.34 ± 0.02	0.37	108	0.317 – 0.363
Carbocraft	0.54 ± 0.02	0.50 ± 0.01	0.42 ± 0.02	0.42	101	0.394 – 0.446
Carbocraft milled	0.40 ± 0.02	0.25 ± 0.03	0.36 ± 0.02	0.39	110	0.336 – 0.384
Indian	0.25 ± 0.01	0.10 ± 0.01	0.24 ± 0.01	0.35	147	0.218 – 0.262
Indian milled	0.23 ± 0.01	0.10 ± 0.01	0.21 ± 0.01	0.30	144	0.191 – 0.229

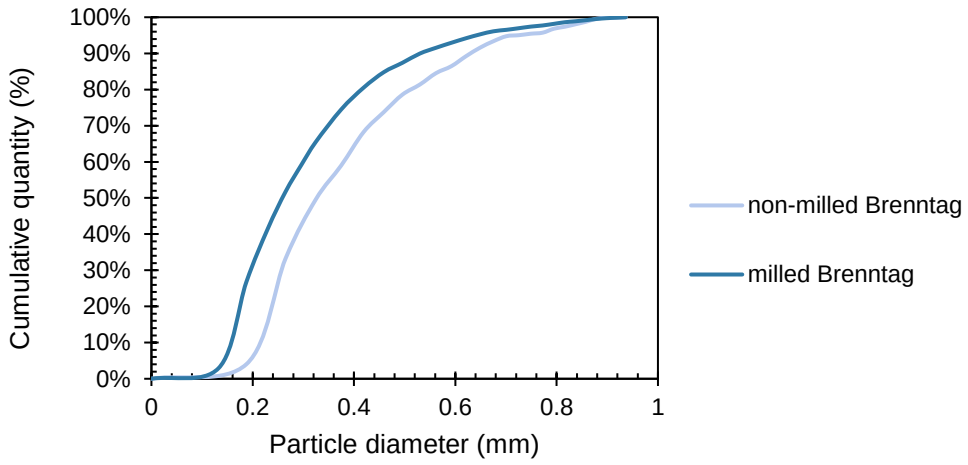

Figure 14. Cumulative particle size distributions for Brenntag milled and non-milled Spirulina powder samples

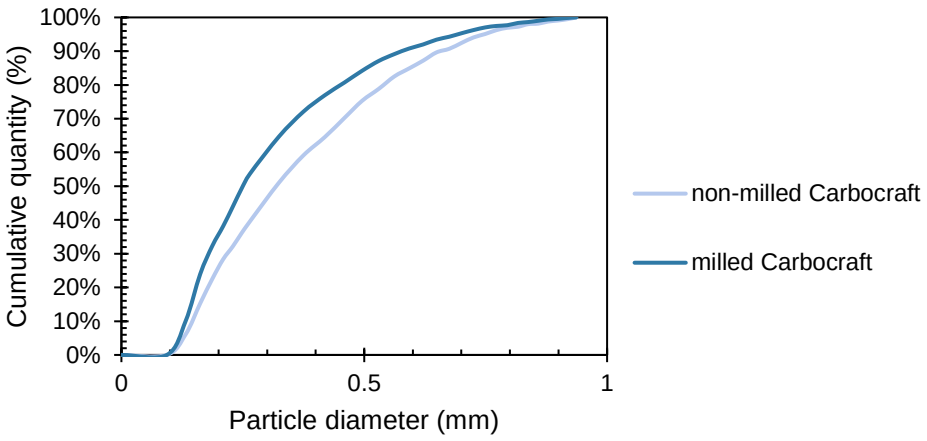

Figure 15. Cumulative particle size distributions for Carbocraft milled and non-milled Spirulina powder samples

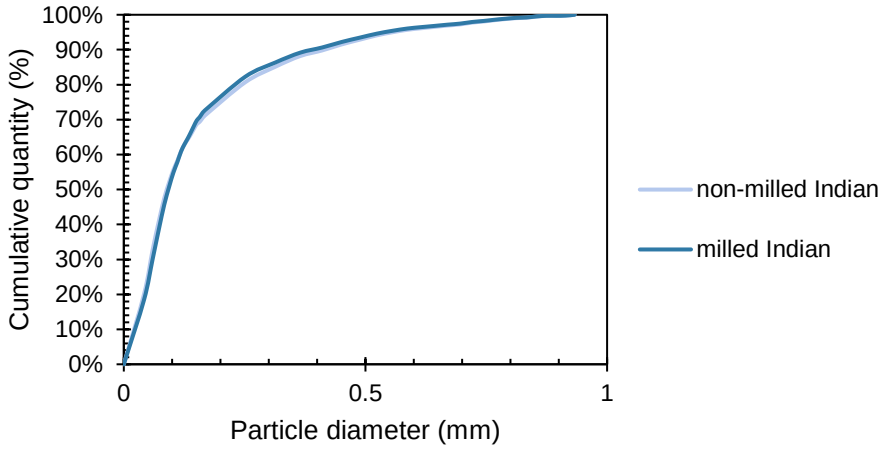

Figure 16. Cumulative particle size distribution for the Indian milled and non-milled Spirulina powder samples

For reference and future comparisons, the stress intensity and stress frequency of the milling was calculated using Equation 4 and Equation 5 from section 2.5.1 of the Literature Review. The calculated values are summarized in Table 20.

The stress intensity is directly proportional to the square of the tip speed so for an increase in agitator speed the stress intensity can be increased. There may be a point of speed for the same loading, feed and bead size and residence time where the median of all three *Spirulina* samples post-milling will be significantly similar in size. This would be ideal to contribute towards the robustness of the system – that it can take a large variance in size of *Spirulina* powder particles and mill them all to roughly the same distribution. This would be beneficial to the solid-liquid separation steps that follow, whose efficiency are particle size dependent. Full optimization on all relevant variables was not performed as part of this study and hence a conclusion on the most effective setup for the milling cannot be made from the data generated here.

Table 20. Milling stress factors calculated for the bead-milling process

Variable	Value
Stress frequency (-)	1.57
Stress intensity (Nm)	1.8×10^{-5}

4.2 c-Phycocyanin leaching from Spirulina

Leaching tests were carried out to determine the rates at which c-phycocyanin and other cellular components leached into solution and the end c-phycocyanin concentration and purity ratio after 24 hours of leaching for all available *Spirulina* samples. The purpose of these experiments was firstly to compare the feedstocks in terms of the achievable maximum c-phycocyanin concentration and purity ratio. The second purpose was to determine the kinetics of c-phycocyanin leaching from the different samples to establish predictive kinetic models to allow for the concentration at any given point of the leaching to be known. This is required for optimizing the leaching time, ideally shortening it to allow for a shorter time on stream for the process. Experiments were performed on milled and non-milled dried *Spirulina* powder samples.

4.2.1 Leaching profiles

Leaching tests centering on the c-phycocyanin concentration in the leachate were performed to determine the time at which the equilibrium concentration of c-phycocyanin in the solution would be reached and what that concentration would be. It was expected that the c-phycocyanin concentration would increase until an equilibrium concentration was achieved and thereafter no change in concentration would be observed (Rakotondramasy-Rabesiaka, et al., 2009).

Figure 17 shows the leaching profiles of the milled samples of Carbocraft, Brenntag and Indian *Spirulina* powders. The Carbocraft sample had an almost instantaneous increase in c-phycocyanin concentration to approximately 4 $mg.mL^{-1}$ from time 0 to 0.65 h. Thereafter the concentration increased linearly ($R^2 = 0.96$) until time 7.3 h, after which the concentration remained at around 10.8 ± 0.69 $mg.mL^{-1}$. The Brenntag sample also showed an instantaneous increase in c-phycocyanin concentration to 3.69 ± 0.67 $mg.mL^{-1}$ from time 0 to 0.63 h. The c-phycocyanin concentration thereafter stayed approximately the same until 8 h, at which time the concentration started to increase approximately linearly ($R^2 = 0.96$) until 18.6 h, finally reaching an equilibrium concentration of 11.1 ± 1.54 $mg.mL^{-1}$. The Indian sample showed an instantaneous increase in c-phycocyanin concentration to 0.56 ± 0.01 $mg.mL^{-1}$ from 0 to 0.6 h, followed by a stagnant phase until 8 h during which time the concentration remained at approximately 0.59 ± 0.03 $mg.mL^{-1}$, thereafter the concentration increased suddenly from 8 to 9 h to a concentration of 1.31 ± 0.06 $mg.mL^{-1}$. This equilibrium concentration was maintained until the 24 h point, at which the experiment was concluded. The change in the Indian sample concentration at 8 h was only significant when compared to the initial concentration of the Indian sample, but was not significant when compared to the concentration changes that occurred for the Brenntag and Carbocraft samples.

The Brenntag and Carbocraft samples had similar equilibrium c-phycocyanin concentrations of 11.1 ± 1.54 $mg.mL^{-1}$ and 10.8 ± 0.69 $mg.mL^{-1}$ respectively, with the variance meaning that both final concentrations were effectively the same. However, the Carbocraft leachate reached its equilibrium concentration after 7.3 h and Brenntag only after 18.6 h. This indicates that though equivalent amounts of c-phycocyanin may be present in the powders, they become liberated at different rates. The milled Indian sample reached its lower equilibrium concentration after 9 h, somewhere in-between the Brenntag and Carbocraft times.

The yields of c-phycocyanin per mass dry weight *Spirulina* at the equilibrium concentration of c-phycocyanin of milled Brenntag and Carbocraft samples were 111 ± 15.4 $mg.g^{-1}$ and 108 ± 6.9 $mg.g^{-1}$ respectively. These yields of c-phycocyanin were superior to the c-phycocyanin yields from the *Spirulina* leached by Aftari et al. (2015) (56.75 $mg.g^{-1}$), Silveira et al. (2007) (46 $mg.g^{-1}$), Moraes et al. (2010) (82.48 $mg.g^{-1}$) and Hockey (2020) (55 $mg.g^{-1}$). The extraction method and time allowed for leaching differed between these literature studies though. For example, Aftari et al. (2015) used microwave assisted leaching with a leaching time of 25 min. Other studies, such as Moraes et al. (2010), used dried, frozen biomass as preparation for leaching before milling. It is important to note that these values cannot be normalized and compared since the starting microalgal c-phycocyanin content actually contained in their respective feeds is unknown, and therefore a percentage of liberated c-phycocyanin cannot be accurately determined.

The equilibrium concentration and yield of c-phycocyanin per mass dry weight *Spirulina* for the milled Indian sample was 1.31 ± 0.06 $mg.mL^{-1}$ and 13.1 ± 0.6 $mg.g^{-1}$ respectively. This final concentration and yield were much lower than most values found in literature. Since the Indian sample reached equilibrium faster than the other two samples, it is suggested that the c-phycocyanin concentration is highly dependent on the *Spirulina* feed composition since for the same leaching conditions the c-phycocyanin solubility is constant and as such if more c-phycocyanin was present in the Indian sample an increase in concentration would be observed over time in the leachate and equilibrium would be reached later. Thus, it can be said that the equilibrium is reached due to a lack of concentration gradient after 10.7 h for the Indian sample, rather than because of c-phycocyanin solubility limitations.

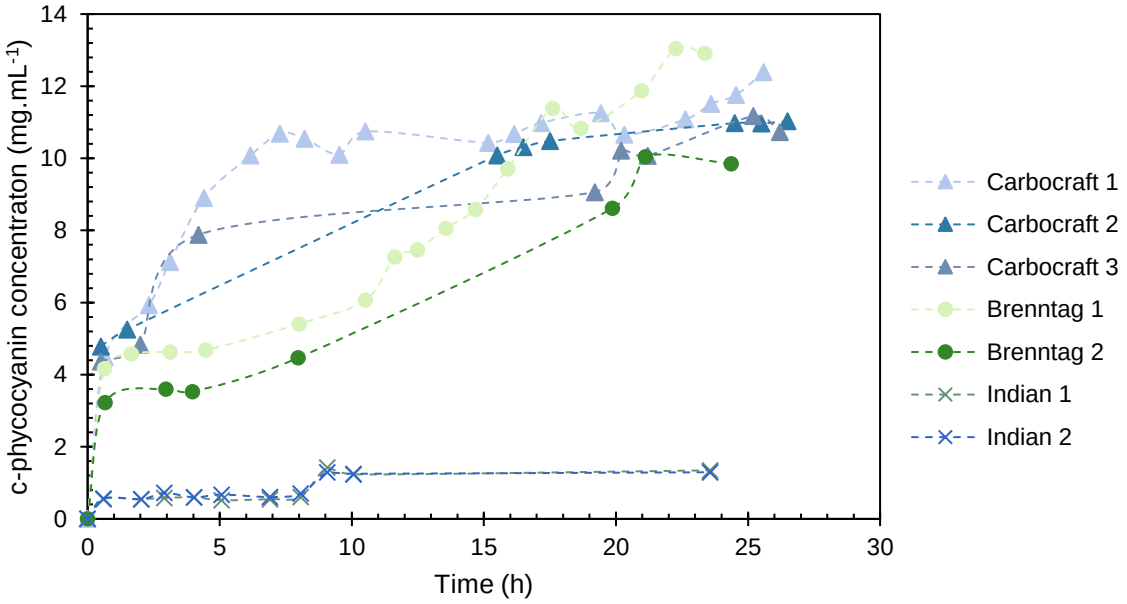

Figure 17. c-Phycocyanin concentration over leaching time for multiple runs of Carbocraft, Brenntag and Indian milled samples. The numbers (1, 2 and 3) appearing after the *Spirulina* sample name, i.e. Carbocraft, Brenntag and Indian, refer to repeats of the same experiment with sampling performed at different time intervals. Repeats were sampled in triplicate.

Trends in the purity number of the leachates with respect to leaching time was also tracked for the milled *Spirulina* samples. This was to assess if there would exist a local maximum of purity owing to different proteins leaching at different rates out of the powder particles. This would allow for the ascertainment of the leaching time required to reach this maximum of purity for each of the samples – which would contribute towards a final c-phycocyanin product of a higher purity ratio.

Figure 18 shows that the milled Indian sample leachate started at a purity of around 0.065 until 4 h. The purity ratio increased to 0.12 from 5 h and hovered around that for the remainder of the experimental leaching time. The milled Brenntag sample's purity ratio averaged at 0.38 before 8 h and thereafter increased to 0.47 by 10.5 h, after which it held steady at an average of approximately 0.46. The milled Carbocraft leachate increased in purity ratio only after the first 10 h of leaching to above the starting purity, thereafter it steadied out at 15 h at an average of approximately 0.41 purity ratio.

Therefore, no significant single point of maximum purity ratio was found for the Indian, Brenntag and Carbocraft samples. A minimum time of leaching, however, can be inferred from the data for which any time after this minimum time the leachate would be at its final maximum purity. These times are in the region of 5 h, 10.5 h and 15 h for the Indian, Brenntag and Carbocraft samples respectively.

c-Phycocyanin purity ratios quoted in literature have quite a large range, like the range of purity ratios found between the three samples used in this study. Silveira et al. (2007) achieved a purity ratio of 0.46 in the crude extract using water as an extractant. Antelo et al. (2010) achieved a 0.59 purity ratio in the crude extract using the same methodology described by Silveira et al. (2007). Aftari et al. (2015) quotes a 1.27 purity ratio in the crude extract using a microwave assisted extraction. Guan (2016) found a

purity ratio of 0.42 in the crude extract when using a mechanical shearing method and found a purity ratio of 0.48 when using the freeze-thaw method. Wang et al. (2016) achieved a 0.89 purity ratio when using a freeze-thaw method of extraction. The literature and the results of the leaching tests performed in this study suggest that the purity ratio of the crude extract may vary significantly depending on the composition of the feed used and the extraction method. Literature sources such as Aftari et al. (2007) and Antelo et al. (2010), amongst others, describe methods of optimizing the extraction process based on a stable feed composition. The results do suggest that a similar extraction feed composition is critical if similar results of purity is desired in the crude extract. The overarching aim of this study is to allow for the extraction process to be robust and thus we cannot optimize the extraction to be tailored to a specific feed compositon but rather need to ensure that the process can handle feeds with varying composition.

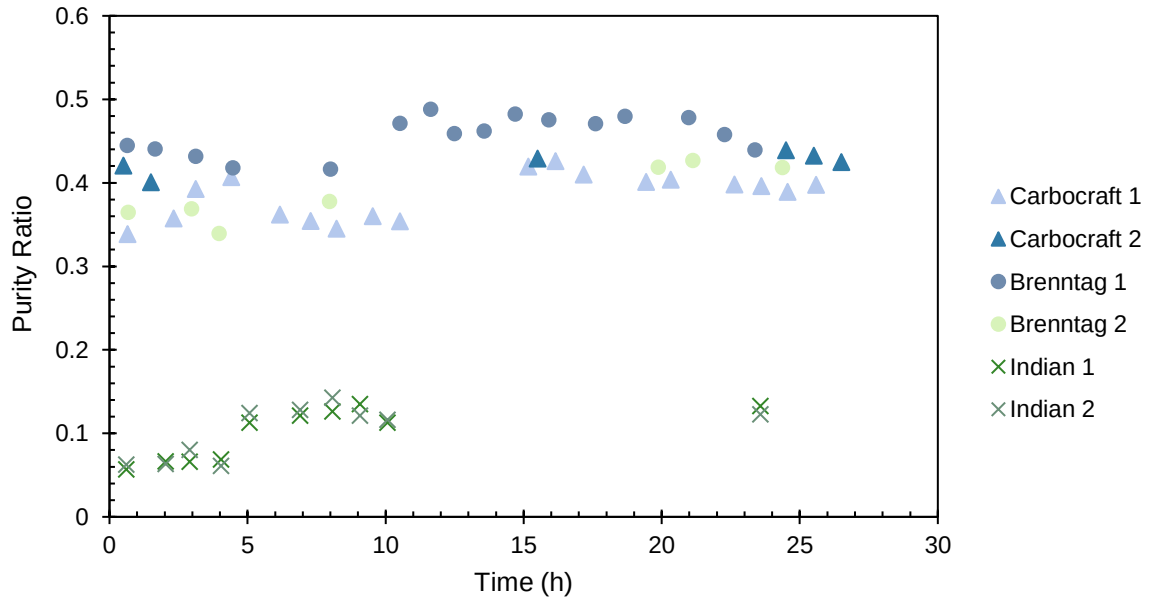

Figure 18. c-Phycocyanin purity ratio over leaching time for multiple runs of Carbocraft, Brenntag and Indian milled samples. The numbers (1, 2 and 3) appearing after the *Spirulina* sample name, i.e. Carbocraft, Brenntag and Indian, refer to repeats of the same experiment with sampling performed at different time intervals. Repeats were sampled in triplicate.

Figure 19 and Figure 20 show the c-phycocyanin concentrations measured in the leachate for milled and non-milled samples of the Brenntag and Carbocraft *Spirulina* powders, respectively. Note that the error bars in Figure 19 and Figure 20 indicate the variance of a triplicate run for the non-milled samples. The milled sample experiments were performed in three separate runs for Carbocraft and two runs for Brenntag, but not at the same time intervals which meant that error bars could not be calculated for each time point. Absorbance readings used for calculation of the c-phycocyanin concentrations were measured in triplicate. However, this standard error is not shown in the figures as it may cause confusion with the error bars for variance of for the non-milled sample runs. The standard error was within 2 % of the average reading and can be regarded as insignificant for this interpretation.

During the drying processes used by the suppliers of the dried *Spirulina* powder samples, it is possible that the *Spirulina* cells had been sufficiently broken to not require a cell disruption of the powder (i.e. bead-milling) for the c-phycocyanin to leach out of solution (Pohndorf, et al., 2016). If this was the case, the non-milled samples would be expected to leach equally as well as the milled sample in terms of time taken to reach the same equilibrium concentration. Results supporting this hypothesis would be beneficial to the extraction process as it would render the bead-milling step, an energy- and capital-intensive process, redundant.

Figure 19 shows the initial leaching of the non-milled Brenntag sample was slower than the Brenntag milled samples. However, by the 8 h mark, it had seemingly caught up with the milled sample in terms of c-phycocyanin concentration. The period of no significant change in concentration observed in both

runs 1 and 2 of milled Brenntag *Spirulina* leaching was not present in the non-milled experiment. The final c-phycocyanin concentration was lower in the non-milled *Spirulina* leachate, with 8.9 ± 0.13 mg.mL^{-1} being the final and highest concentration found in the non-milled sample after 24.3 h. At the same time, the milled sample had reached an equilibrium concentration of 11.1 ± 1.54 mg.mL^{-1}.

Figure 20 shows that the Carbocraft non-milled sample exhibited a relatively slow initial leaching rate when compared to its milled counterpart – like the Brenntag non-milled sample when compared to Brenntag milled. After the slow initial leaching rate, at 3.8 h of leaching, the Carbocraft non-milled *Spirulina* had a similar c-phycocyanin concentration magnitude to the Carbocraft milled runs. From 3.8 h onwards, the Carbocraft non-milled sample followed the same leaching pattern of its milled counterpart, with concentrations being the same. The Carbocraft non-milled concentration profile flattened out at around 7.5 h compared to a 7.3 h for Carbocraft milled. The equilibrium concentration achieved by the Carbocraft non-milled was 10.1 ± 0.62 mg.mL^{-1}, with the Carbocraft milled achieving 10.8 ± 0.69 mg.mL^{-1}. Taking the error measurement into account, the equilibrium concentration of Carbocraft milled and non-milled are comparable.

Hockey (2020) observed similar trends in c-phycocyanin concentration profiles when comparing milled and non-milled dried *Spirulina* powder leaching in the same citrate buffer as used in this study. Hockey (2020) stated that for the *Spirulina* sample used in their study, the milling had no significant effect on the c-phycocyanin concentration profile observed in the leachate over the leaching period. Similarly, for the Carbocraft sample in this study, no significant difference was observed, however for the Brenntag sample there was a notable difference. Thus, the results confirm part of the conclusions from Hockey (2020) that milling is not required to observe c-phycocyanin leaching dried *Spirulina* powders, though further cell disruption via milling may be required to maximize the amount of c-phycocyanin leached.

Additionally, the data from Figure 19 and Figure 20 indicate that there was a significant difference in the initial leaching rate of c-phycocyanin, such that there was a significant difference observed in the concentration at shorter leaching times for milled versus non-milled *Spirulina* powders. Therefore, milling would be beneficial if a leaching time of less than 3.8 h is required, for example due to contamination concerns.

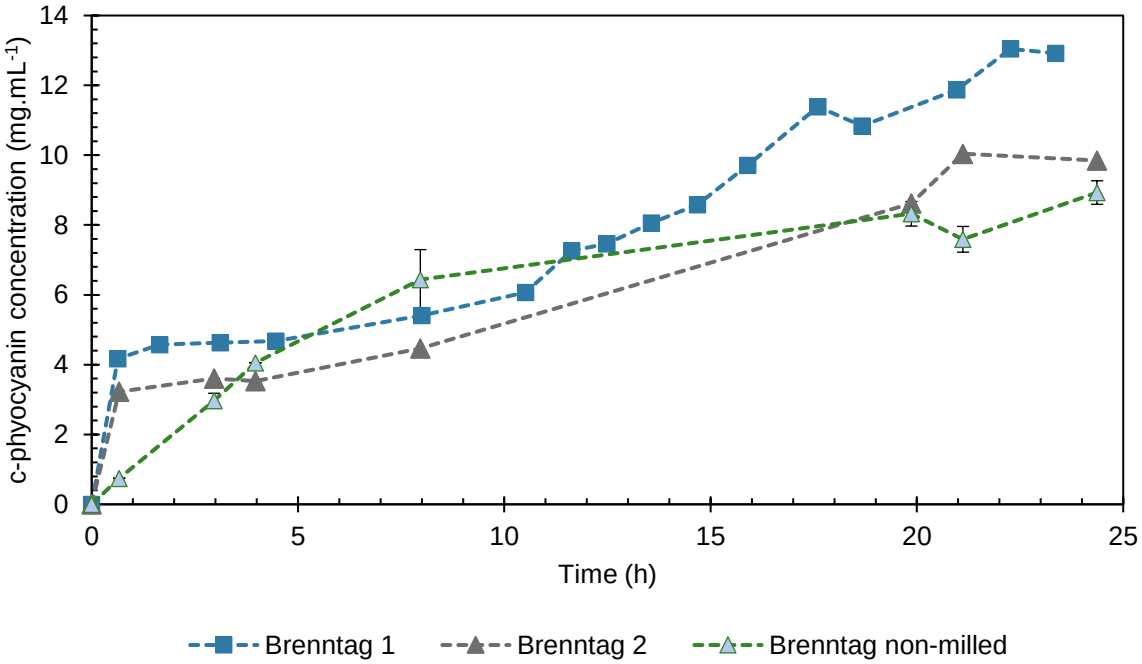

Figure 19. c-Phycocyanin concentration in the leachate over time for Brenntag milled and non-milled runs. Brenntag 1 and 2 refer to repeats of the experiment performed with different time intervals of sampling. Error bars indicate variance from triplicate runs.

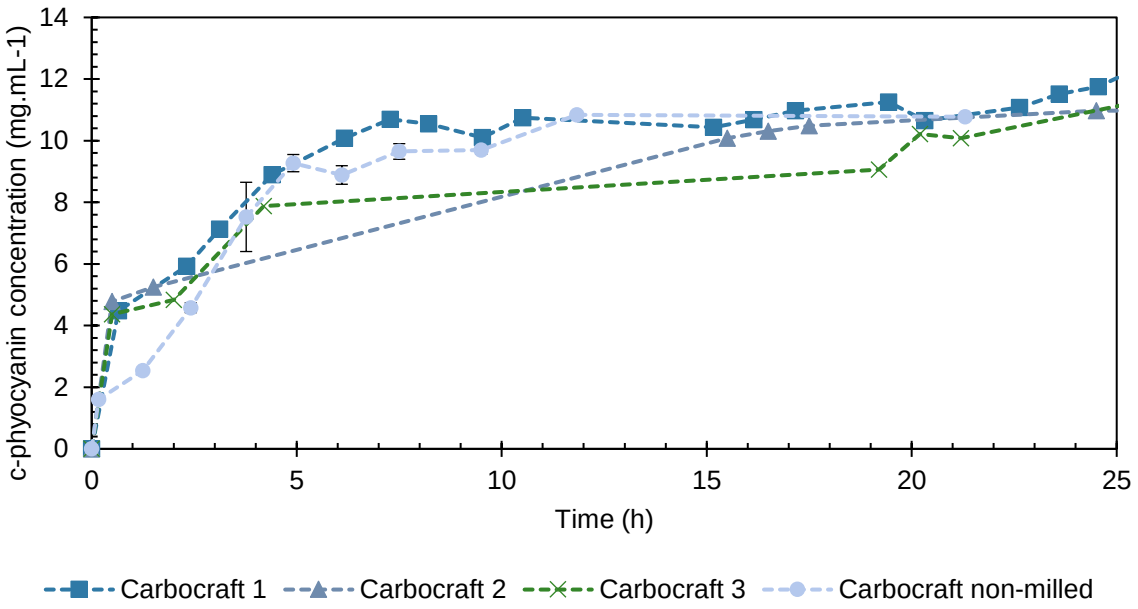

Figure 20. c-Phycocyanin concentration in the leachate over time for Carbocraft milled and non-milled runs. Carbocraft 1, 2 and 3 refer to repeats of the experiment performed with different time intervals of sampling. Error bars indicate variance from triplicate runs

4.2.2 Leaching kinetics analysis

The purpose of the kinetic analysis was to determine the viability of using a predictive method for estimating the c-phycocyanin concentration in the leachate at any given point during the leaching time. The kinetic modeling method described in section 2.5.2 of the Literature Review was used to fit the generated data points from the concentration profiles previously presented in section 4. For the analysis, the c-phycocyanin concentration profiles for the milled and non-milled Carbocraft and Brenntag *Spirulina* samples were fitted to 1st and 2nd order kinetic models, the results of which are presented in this section.

The literature on the leaching of bioactive compounds from organic material, including c-phycocyanin from *Spirulina*, describe good fits for 2nd order kinetics. Should this also be found to be the case for the data in this study, this would allow for the comparison of *Spirulina* powders based on a quantitative measurement of leaching performance. A threshold of 85%, corresponding to a coefficient of determination of 0.85 in the linearization step of the kinetic modeling methods described in section 2.5.2 was chosen to be the minimum requirement for acceptance of a kinetic model. It was decided that only looking at the R^2 value would be enough as acceptance criteria for the linearization step of the kinetic modeling. Although the p-value would be a good indicator of the fit of the linearized data, the resulting uncertainty in the final model resulting from a high p-value with low coefficient of determination was considered to be undesired for the purpose of predicting accurate c-phycocyanin concentrations.

Kinetic performance indicators such as equilibrium concentration, initial leaching rate and leaching constants are defined in section 2.5.2 of the Literature Review.

Carbocraft Spirulina leaching – first order

Figure 21 shows that the linearization of the Carbocraft leaching profile did not have a high correlation to first order kinetics, with the goodness of fit as measured by R^2 being only 0.69. Therefore, the first order kinetic model was not fitted to the experimental data for the Carbocraft milled leaching profile. The upper bound of the equilibrium concentration (10.8 ± 0.69 mg.mL^{-1}) was used for the linearization step.

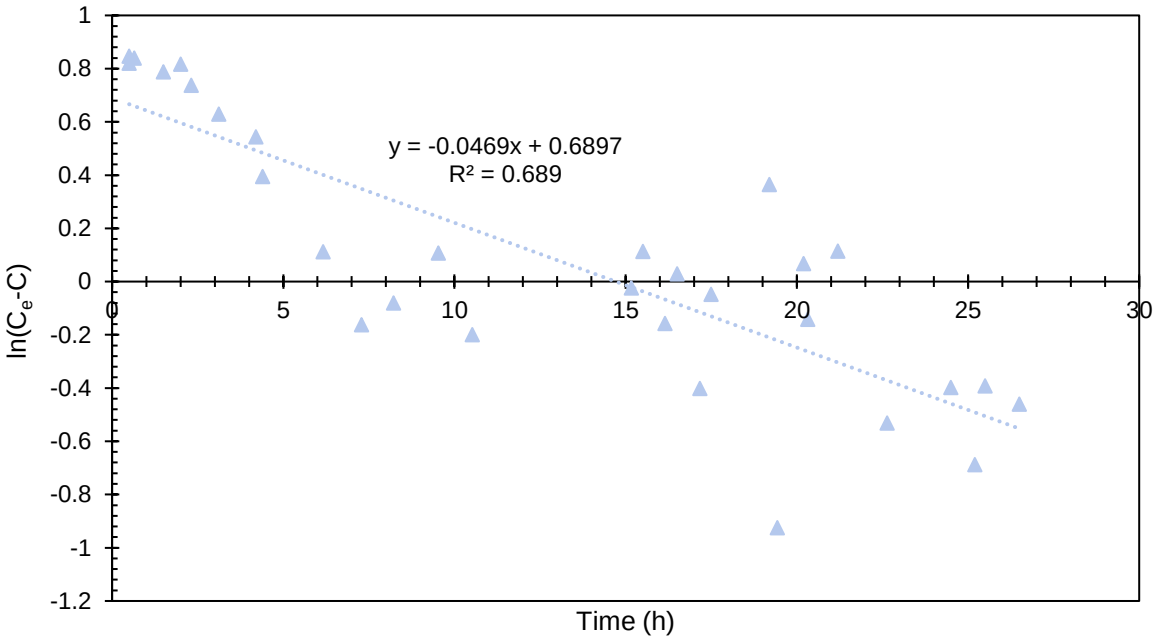

Figure 21. Linearized Carbocraft milled data, for first order leaching kinetics analysis

Figure 22 shows that the linearization of the Carbocraft non-milled leaching profile had a higher and more acceptable correlation (R^2 = 0.92) to first order kinetics. Thus, the data was fitted to a first order kinetic model (see Appendix B.2 for sample calculations). The upper bound for the equilibrium concentration of 10.1 ± 0.62 mg.mL^{-1} was used for the linearization step. The first order leaching constant that resulted was 0.204 h^{-1}. Figure 23 shows how the data from the non-milled Carbocraft sample fits the first order kinetic model. The 1st order model form is:

$$C_{Cnm}\left(\frac{mg}{mL}\right) = 10.1 - 10^{log(10.1)-(0.204/2.303)t} \qquad \text{Equation 25}$$

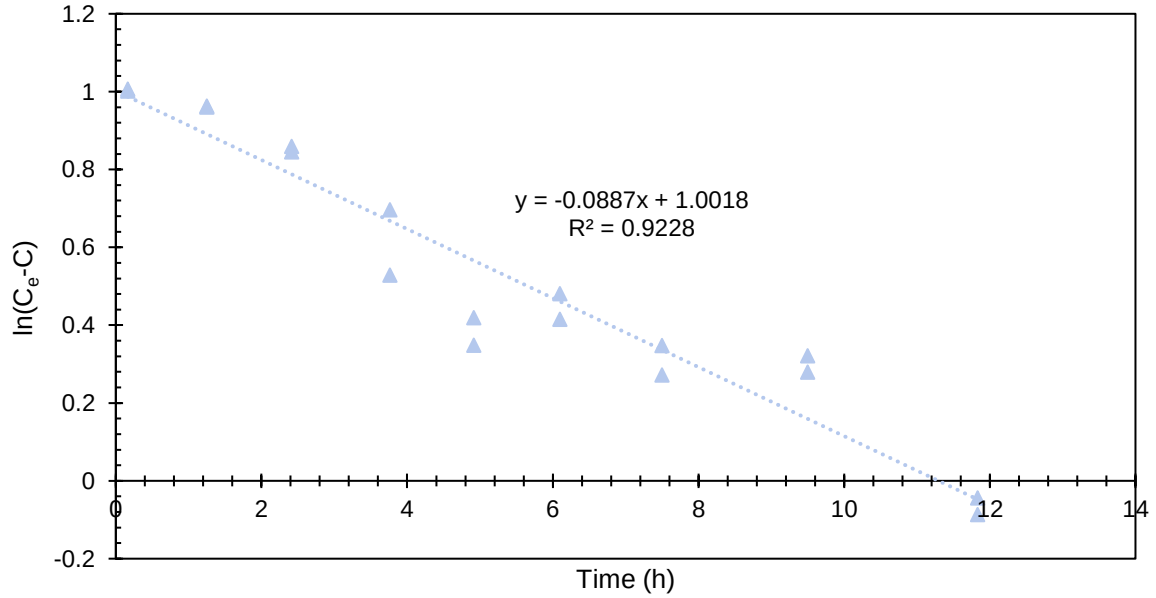

Figure 22. Linearized Carbocraft non-milled data, for first order leaching kinetics analysis

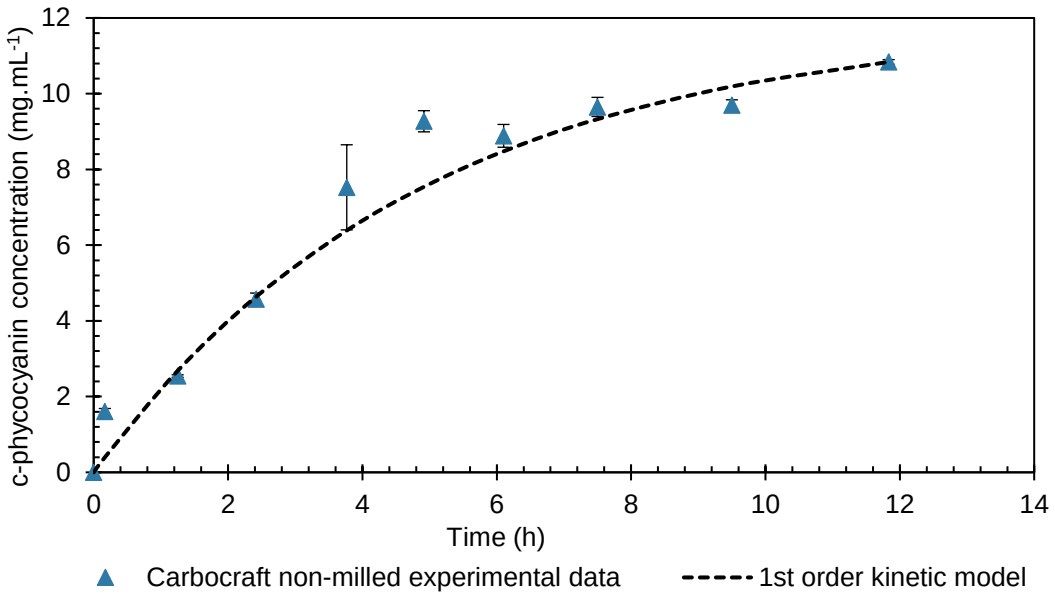

Figure 23. Carbocraft non-milled experimental data fitted to the first order kinetic model

Carbocraft Spirulina leaching – second order

Figure 24 and Figure 25 show that the milled and non-milled Carbocraft leaching experimental data correlated well with a linear trendline when subjected to a second order kinetic linearization, with coefficients of determination of R^2 = 0.98 and R^2 = 0.96 found respectively – well above the chosen minimum acceptable R^2. Figure 24 and Figure 25 also show how accounting for the recorded error of measurement altered the linear trendline. This weighted linear regression was used to develop the second order kinetic model in place of the linear trendline to the linearized data points, as it accounted for the propagation of error from the spectroscopy. The intercept and the slope of the weighted linear regression was used to determine the equilibrium concentration, initial extraction rate and the 2nd order kinetic coefficient of leaching: 11.16 ± 1.18 mg.mL^{-1}, 10.2 mg.mL^{-1}.h^{-1} and 0.08 ± 0.003 mL.mg^{-1}.h^{-1} respectively for the milled Carbocraft sample and 10.8 ± 1.62 mg.mL^{-1}, 9.85 mg.mL^{-1}.h^{-1} and 0.084 ± 0.005 mL.mg^{-1}.h^{-1} for the non-milled Carbocraft sample.

Figure 26 and Figure 27 respectively, show how the milled and non-milled Carbocraft leaching experimental data fitted to the 2nd order kinetic model developed using weighted linear regression. The model forms for the milled and non-milled Carbocraft are as follows:

$$C_{Cm}\left(\frac{mg}{mL}\right) = \frac{(11.16^2)(0.08)t}{1+(11.16)(0.08)t} \qquad \text{Equation 26}$$

$$C_{Cnm}\left(\frac{mg}{mL}\right) = \frac{(10.8^2)(0.084)t}{1+(10.8)(0.084)t} \qquad \text{Equation 27}$$

The 2nd order kinetic model correlated well with the individual runs of the Carbocraft milled samples, with an average R^2 of 0.95. For the non-milled Carbocraft samples, the 2nd order kinetic model and experimental data correlated with an R^2 of 0.9. Though the coefficient of determination is above 0.9, the fit of the data is not in the same curve as the model especially at values prior to time 4 h. Based on a visual inspection, the model only seemed to fit at the very beginning of the leaching time and after the equilibrium concentration has been achieved in the experimental data.

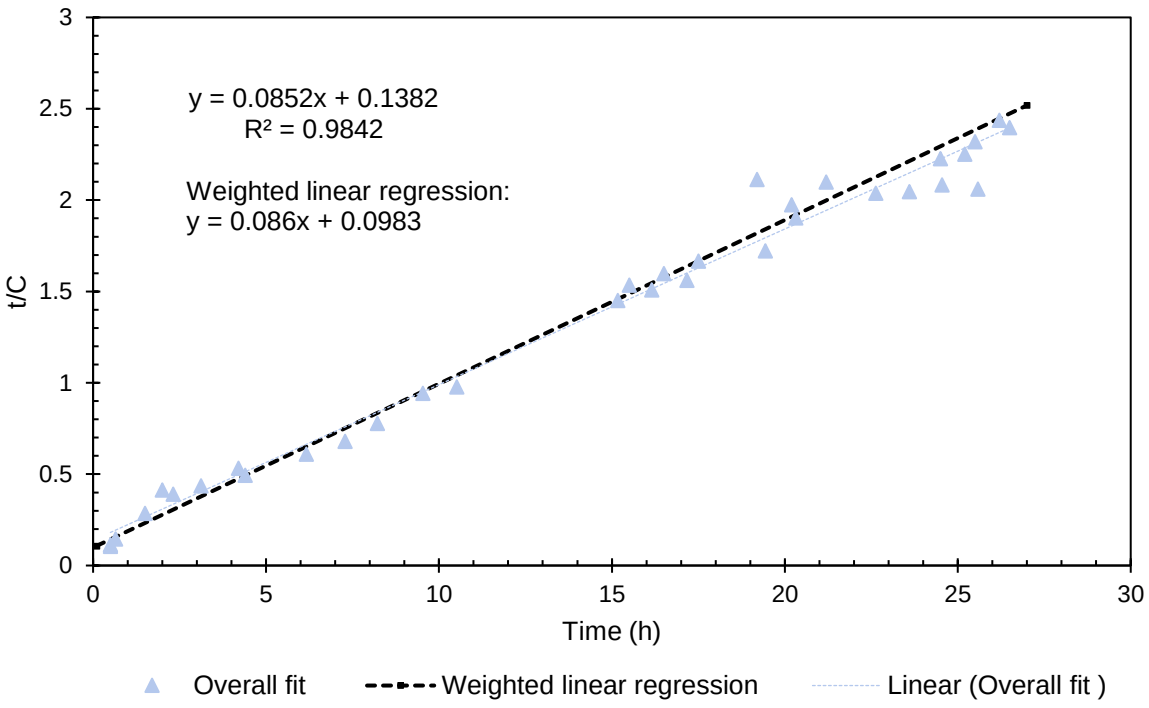

Figure 24. Carbocraft milled experimental data linearized according to second order kinetics

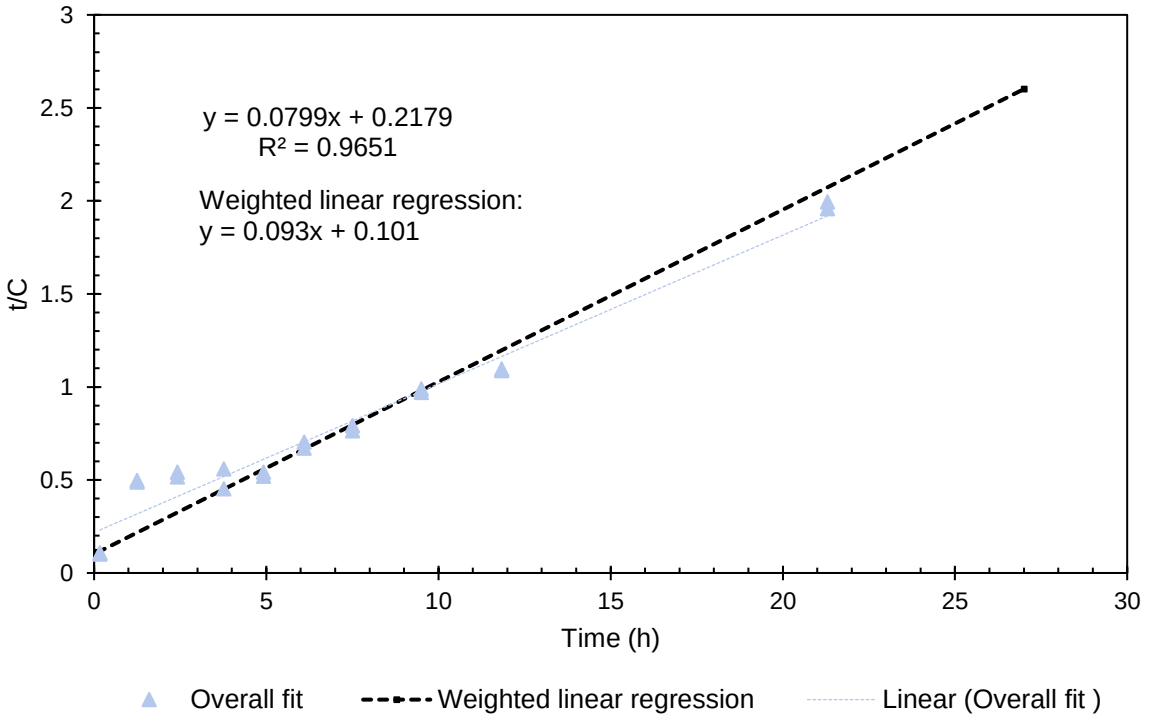

Figure 25. Carbocraft non-milled experimental data linearized according to second order kinetics

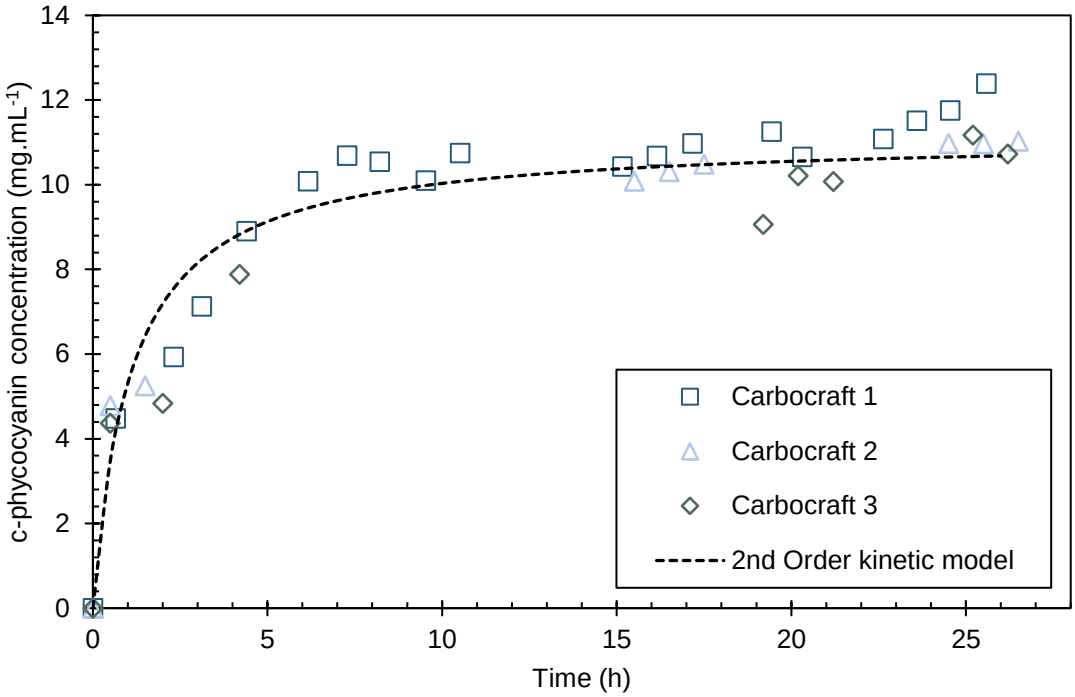

Figure 26. Carbocraft milled experimental data fitted to the second order kinetic model

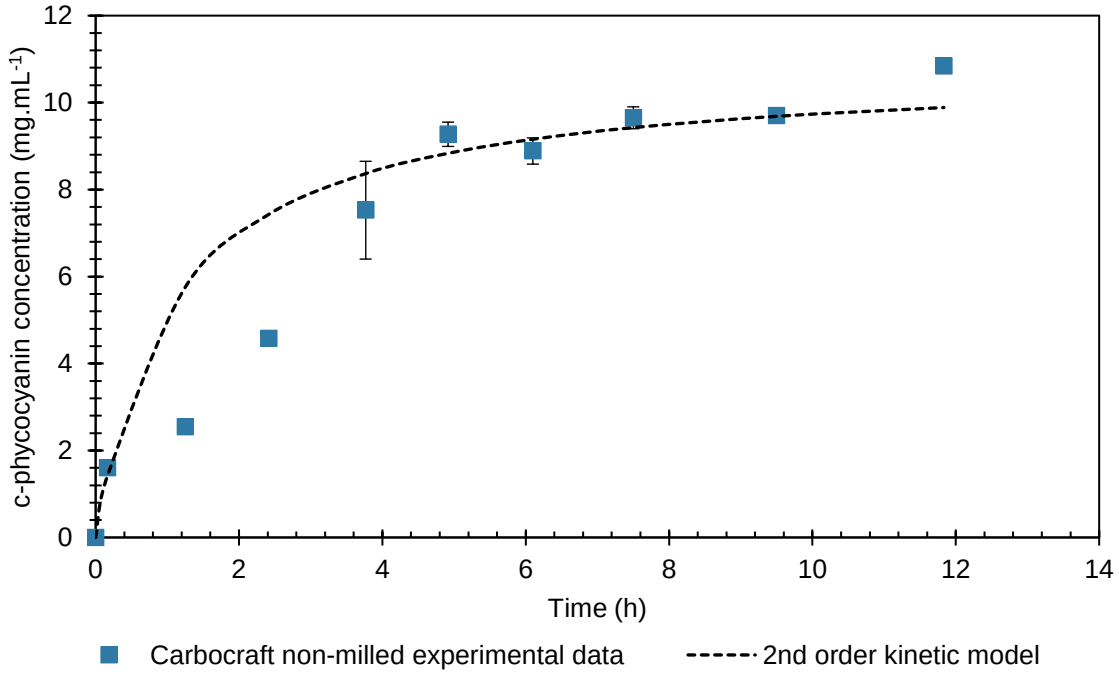

Figure 27. Carbocraft non-milled experimental data fitted to the second order kinetic model

Brenntag Spirulina leaching – first order

Figure 28 shows that the linearization of the milled Brenntag leaching profile did not have a high correlation to first order kinetics, with an R^2 of only 0.75 obtained. Therefore, the first order kinetic model

was not fitted to the experimental data for the Brenntag milled leaching profile. The upper bound of the equilibrium concentration of 11.1 ± 1.54 mg.mL^{-1} was used for the linearization step.

However, a visual inspection of the data indicated that the poor goodness of fit was largely because of the later time data. Figure 28 shows that between 7.9 h and 19 h, the Brenntag milled *Spirulina* leaching profile correlates within the previously defined the acceptable range of R^2 to the first order kinetic linearization. The first order leaching constant was 0.118 h^{-1} for Brenntag milled in this period.

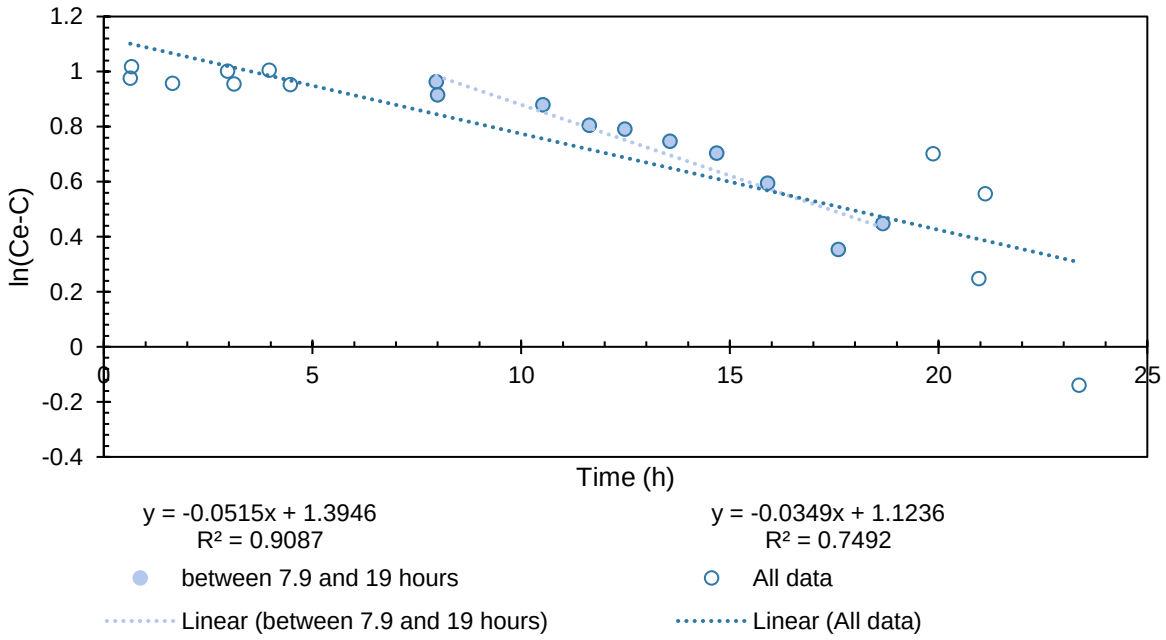

Figure 28. Linearized Brenntag milled data, for first order leaching kinetics analysis

Figure 29 shows that the linearization of the Brenntag non-milled *Spirulina* leaching profile did meet the requirement of 0.85 R^2 of correlation to first order kinetics achieving R^2 = 0.88. Therefore, a first order kinetic model was fitted to the experimental data for the Brenntag non-milled leaching profile. The upper bound of the equilibrium concentration of 8.8 ± 1.54 mg.mL^{-1} was used for the linearization step.

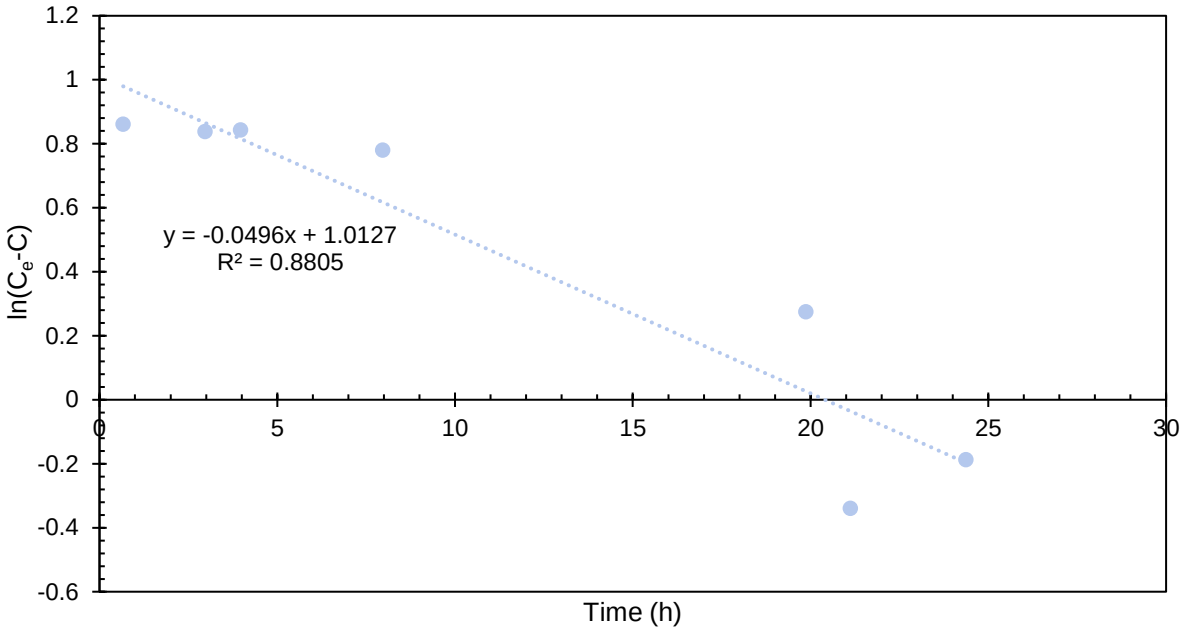

Figure 29. Linearized Brenntag non-milled data, for first order leaching kinetics analysis

Figure 30 shows the first order kinetic model with the leaching experimental data for the Brenntag milled *Spirulina* between 7.9 and 19 h. The first order leaching constant was 0.118 h^{-1} and the first order model form is given by Equation 4. The coefficient of determination (R^2) was 0.93 which is relatively high, meaning the model accurately predicts the shape of the data. However, from a visual inspection, it is clear the data does not fit around the model very well. Consequently, the first order kinetic model does not well-predict the behaviour of the leaching of c-phycocyanin in the Brenntag milled sample, despite the relatively high R^2 value.

$$C_{Bm}\left(\frac{mg}{mL}\right) = 11.1 - 10^{log(10.1) - (0.118/2.303)t} \qquad \text{Equation 28}$$

Figure 31 shows the first order kinetic model with the experimental data for the Brenntag non-milled *Spirulina*. The coefficient of determination (R^2) was 0.93 over the entire period. Once again, the coefficient of determination was relatively high and met the previously defined threshold of correlation, which should indicate a good model prediction. However, as with the milled Brenntag sample, a visual inspection of the plots yields that the experimental data does not fit on the first order kinetic model well, with the model underestimating most of the concentration values.

$$C_{Bnm}\left(\frac{mg}{mL}\right) = 8.8 - 10^{log(8.8) - (0.06/2.303)t} \qquad \text{Equation 29}$$

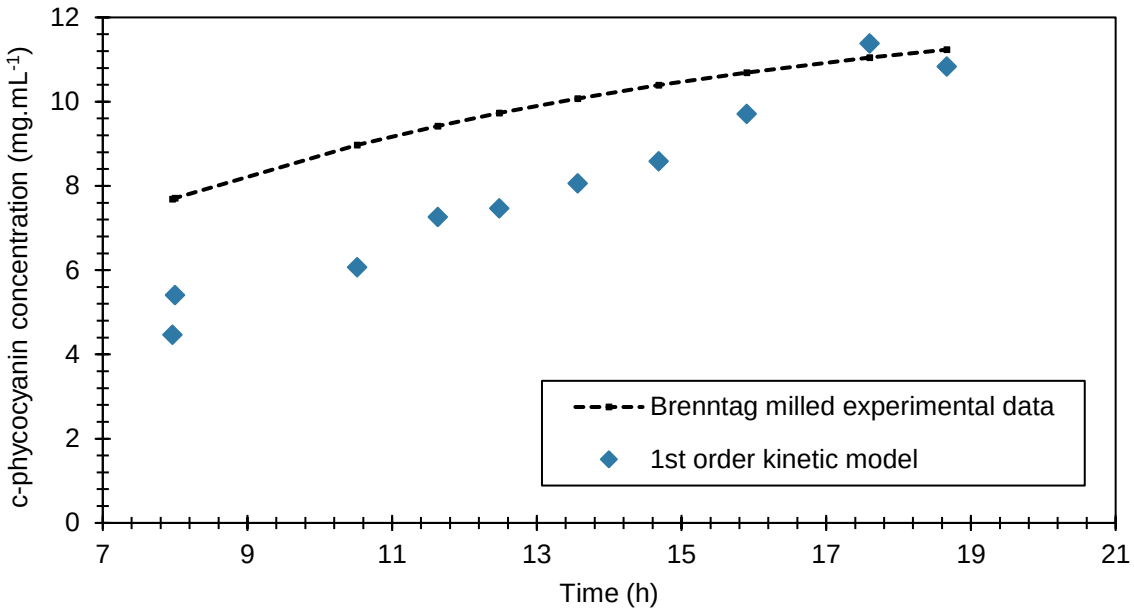

Figure 30. Brenntag milled experimental data fitted to the first order kinetic model between 7.9 and 19 hours

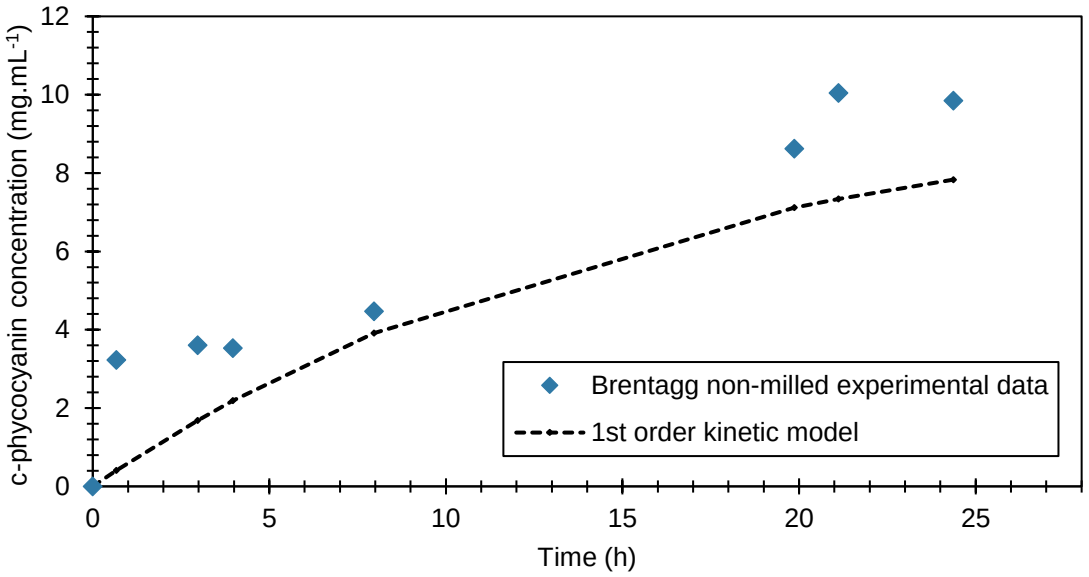

Figure 31. Brenntag non-milled experimental data fitted to the first order kinetic model

Brenntag Spirulina leaching – second order

Figure 32 shows that the linearization of the Brenntag milled leaching profile does not have a high correlation to second order kinetics, with an R^2 of only 0.73 resulting for the linear fit. Therefore, the second order kinetic model was not fitted to the experimental data for the Brenntag milled leaching profile.

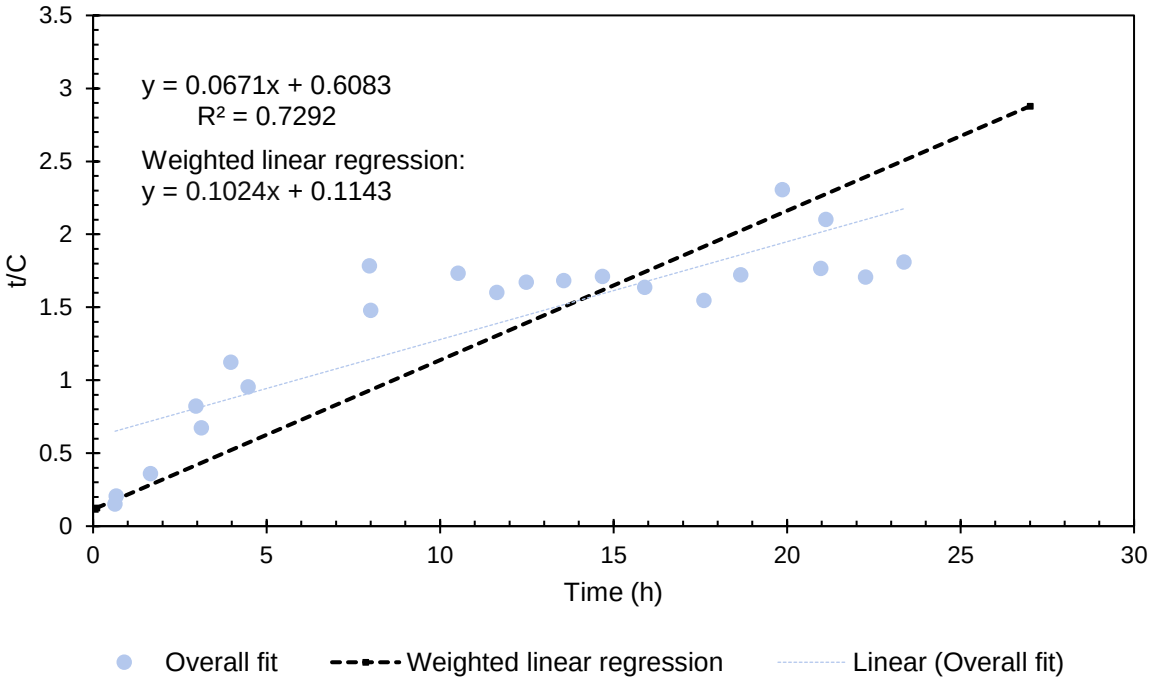

Figure 32. Brenntag milled experimental data linearized according to second order kinetics

Figure 33 shows that the linearization of the Brenntag non-milled leaching profile had a higher correlation (R^2 = 0.86) to second order kinetics compared to the milled sample. Therefore, the second order kinetic model was fitted to the experimental data for the Brenntag non-milled leaching profile. Figure 33 also shows how accounting for the recorded error of measurement alters the linear trendline. This weighted linear regression was used to develop the second order kinetic model in place of the linear trendline to the linearized data points, as it accounted for the propagation of error from the spectroscopy. The intercept and the slope of the weighted linear regression was used to determine the equilibrium concentration, initial extraction rate and the 2nd order kinetic coefficient of leaching: 10.3 ± 1.78 mg.mL^{-1}, 6.37 mg.mL^{-1}.h^{-1} and 0.06 ± 0.003 mL.mg^{-1}.h^{-1} respectively. Thus, the model form is:

$$C_{Bnm}\left(\frac{mg}{mL}\right) = \frac{(10.3^2)(0.06)t}{1 + (10.3)(0.06)t} \qquad \text{Equation 30}$$

Figure 34 shows how the Brenntag non-milled leaching experimental data fits on the 2nd order kinetic model developed using weighted linear regression. The 2nd order kinetic model and experimental data correlate with an R^2 of 0.78. This R^2 indicates that the model does not accurately predict the leaching of this sample, confirmed by a visual inspection of the model fit.

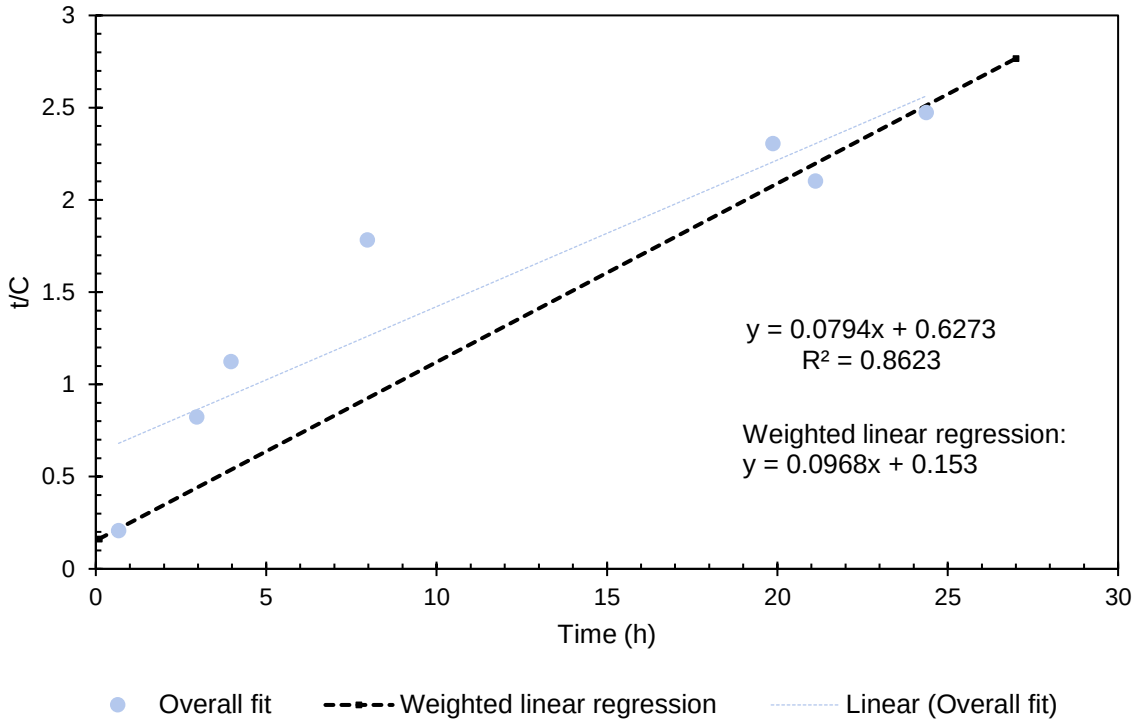

Figure 33. Brenntag non-milled experimental data linearized according to second order kinetics

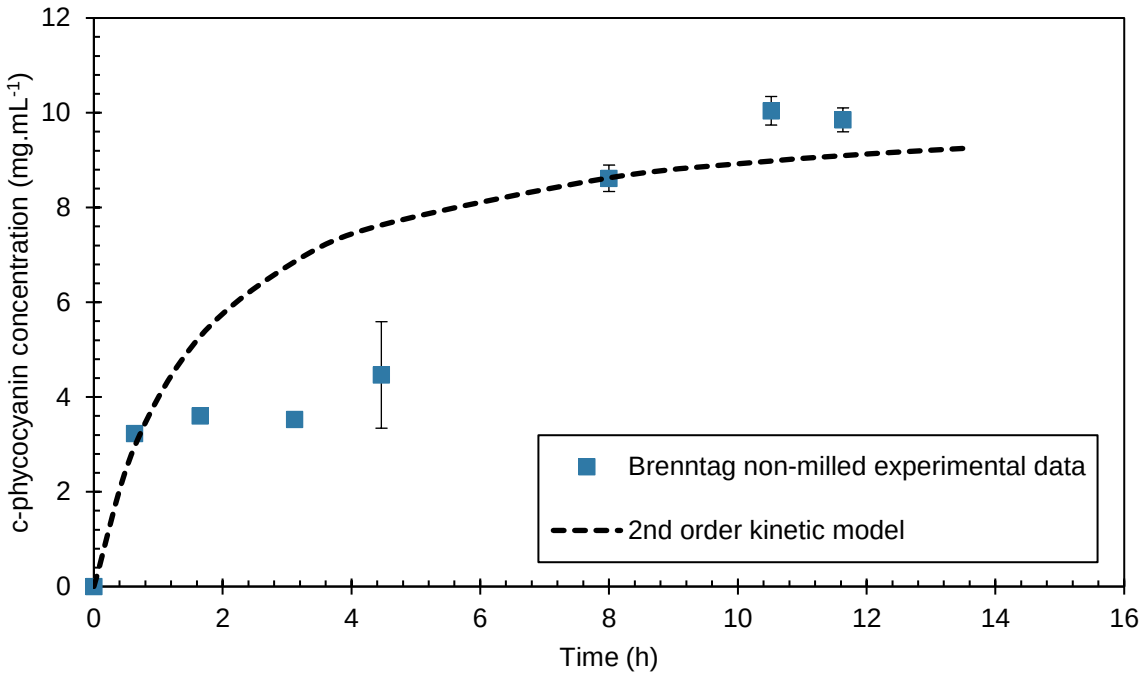

Figure 34. Brenntag non-milled experimental data fitted onto the second order kinetic model

Indian Spirulina leaching – first order

Figure 35 shows that the linearization of the milled Indian sample leaching profile did not have a high correlation to first order kinetics ($R^2 = 0.56$). Therefore, the first order kinetic model was not fitted to the

experimental data for the milled Indian sample leaching profile. The upper bounds for the equilibrium concentration 1.31 ± 0.06 mg.mL^{-1} was used for the linearization step.

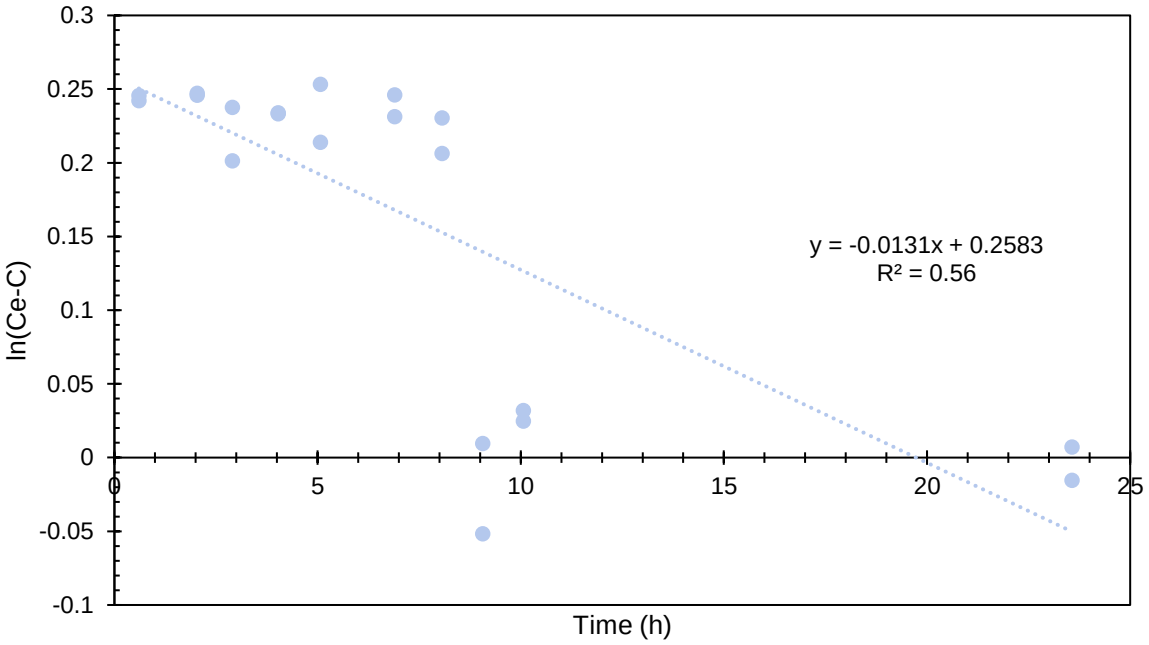

Figure 35. Linearization of milled Indian sample leaching data according to first order leaching kinetics

Indian Spirulina leaching – second order

Figure 36 shows that the linearization of the Indian leaching profile did not have a high enough correlation to second order kinetics (R^2 = 0.74). Therefore, the second order kinetic model was also not fitted to the experimental data for the Indian milled leaching profile.

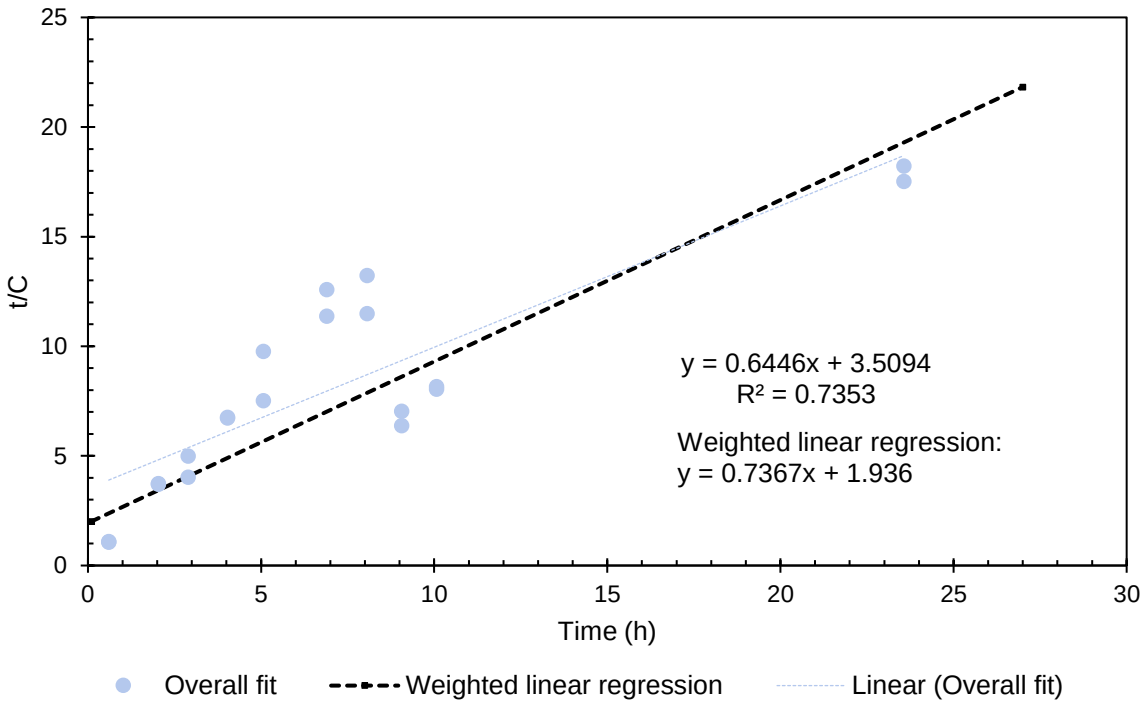

Figure 36. Linearization of milled Indian sample leaching data according to second order leaching kinetics

4.2.3 Leaching discussion

The different samples tested in the leaching studies showed varying concentration profiles in terms of shape. The Carbocraft milled and non-milled samples both appeared to follow the conventional leaching patterns described by literature with a logarithmic shaped concentration profile over time; indicating that the fastest leaching occurred at the beginning, followed by a deceleration in the rate of leaching over time until the equilibrium concentration was reached. By contrast, the milled Brenntag concentration profiles (see Figure 17) had a long period of no significant change in concentration at the beginning of the leaching time, after the initial solubilization phase, and then experienced an almost instantaneous increase in concentration before the rate of leaching decelerated as the system reached equilibrium. Similarly, the milled Indian sample experienced the same period of no significant concentration change at the beginning of the leaching. The non-milled Brenntag did not have a period of no change in concentration at the beginning of the leaching, but rather appeared to increase in concentration steadily before the rate of leaching decelerated as equilibrium was approached, not unlike both the milled and non-milled Carbocraft samples.

The phase of no change in concentration at the beginning of the leaching depicted for the samples of milled Indian and Brenntag samples was not expected based on the available literature on c-phycocyanin leaching kinetics from dried powders. The location of c-phycocyanin, on the surface of rather than inside thylakoid membrane, means that it should be readily available to be leached out into solution compared to other pigments like chlorophyll (Helmenstine, 2019; Kraan, 2013). However, literature has shown how drying methods can affect the c-phycocyanin content within algal species and it is thought that drying methods could affect the rate of leaching too (Guroy, et al., 2017). In the second phase of mass transfer, post instantaneous solubilization, mass transfer could have been limited by the tortuous path within the particle for soluble particles to enter the bulk fluid (Ho, et al., 2005). This might be represented in the bulk fluid concentration profile of that soluble substance as a period of no observed change before a sharp increase as the concentration would take time to be registered in the bulk fluid. This could be what was observed in the Indian and Brenntag milled samples concentration profiles. Therefore, differences in the drying methods used in the preparation of *Spirulina* powders could account for the different behaviour seen here. This is often an unknown quality, though, as it is a step done by the powder providers. It is also often not reported in the literature either – for example, Song,

Zhao and Wang (2013) performed leaching kinetics studies on dried *Spirulina* powders but did not mention the method used for the drying of said *Spirulina* samples.

The Carbocraft sample seemed to have a very short period of no observed concentration change, suggesting that the c-phycocyanin was readily available to leach into the bulk fluid. This implies that the morphology of the Carbocraft dried cells was the most conducive to product liberation. When studying the cells under a microscope at 10× magnification, however, the Carbocraft and Brenntag samples both appeared to have the same shape. This suggests that there was a structural difference in the Brenntag sample, possibly within the cells, that could not be observed easily under the microscope and that caused a more complex diffusion pathway for the c-phycocyanin to move from the cell into the bulk fluid (Pohndorf, et al., 2016). The Carbocraft and Brenntag *Spirulina* powders did have comparable equilibrium concentrations of c-phycocyanin though.

The kinetics model outputs for the Carbocraft *Spirulina* (Table 21) show that the initial leaching rate for the non-milled *Spirulina* was slower than the milled samples and that the coefficient of leaching was slightly higher for the non-milled sample. This is plausible since the leach solution from the non-milled sample reached equilibrium around the same time as the milled, and the non-milled profile still caught up to the milled even given that it had a lower initial leaching rate.

Table 21. Summary of the model outputs for leaching performance of the milled and non-milled Carbocraft Spirulina samples.

Leaching output	**Milled**	**Non-milled**
Initial extraction rate ($mg.mL^{-1}.h^{-1}$)	10.2	9.85
Kinetic coefficient ($mL.mg^{-1}.h^{-1}$)	0.08 ± 0.003	0.08 ± 0.005
Equilibrium concentration ($mg.mL^{-1}$)	11.2 ± 1.18	10.8 ± 1.62

Both the milled and non-milled Carbocraft samples followed second order kinetics and thus, it does not seem that milling affects the kinetics of leaching in terms of order but only the initial rate of leaching. This is supported by the data where the concentrations at equilibrium were comparable when accounting for error and that the initial leaching rate of the milled sample was higher than that of the non-milled sample. The two phenomena causing the Carbocraft to be of a second order in terms of kinetics would be the initial solubilization of c-phycocyanin upon contact with the bulk fluid (water) and the equilibrium concentration of c-phycocyanin in the water (Schwartzberg & Chao, 1982).

The Brenntag non-milled sample had a very short or no initial solubilization stage of mass transfer (Figure 19), which is seen by the slow increase in the concentration in the first few hours of the leaching time compared to its milled counterpart. The Brenntag non-milled sample had a lower initial solubilization concentration to its milled counterpart. This indicates that for this *Spirulina* powder, the milling of the sample did further break down the cells and thus allowed for more readily soluble c-phycocyanin to be exposed to the bulk fluid. This is corroborated by the results in section 4.1 *Spirulina* powder size distributions, with the milled Brenntag d_{80} being lower than the non-milled. The non-milled Brenntag *Spirulina* leachate increased in c-phycocyanin concentration from the start of the leaching time until the end of the phase of no change in concentration the milled sample. The Brenntag non-milled samples followed second order kinetics loosely, whereas the milled sample seemed to follow the first order kinetics more closely. The period of no change in concentration is where the milled sample leaching deviated most from following second order kinetics. Thus, the effect of the milling to increase the initial solubilization concentration may have caused the tortuosity of the c-phycocyanin's path out of the cell fragments to limit the mass transfer until such time that the equilibrium concentration becomes enough of driving force for the mass transfer of c-phycocyanin into the bulk fluid.

The Indian *Spirulina* powder did not seem to follow first or second order leaching kinetics, however the pattern of leaching seemed to be similar (from a qualitative standpoint) to the Brenntag leaching – with a stagnant phase before an increase in the concentration. The increase in concentration happened in such a short span of time relative to the stagnant phase of concentration that it is difficult to fit the data to a kinetic model. This does suggest that the data could fit a first order model – similarly to the Brenntag *Spirulina* leaching from the time of the increase of concentration to when it plateaus around the final equilibrium concentration. However, it is important to note that compared to literature values for

concentration of c-phycocyanin (such as those from Aftari et al. (2015), Hockey (2020), Antelo et al. (2010) quoted in the 4.2 c-Phycocyanin leaching *from* Spirulina section), the amount of c-phycocyanin that leached from the Indian sample is very low and as such is it not possible to assess the kinetics in much depth. This low concentration of c-phycocyanin is quite unexpected for a *Spirulina* sample. However, this unexpectedly low yield c-phycocyanin content could be attributed to the age of the Indian sample (with its batch number/date of manufacture/storage time being unknown), which was in storage for at least three years before the other samples were obtained. Furthermore, the c-phycocyanin may have been damaged during the drying process used to prepare the Indian *Spirulina* powder (Guroy, et al., 2017).

The variability in the leaching profiles for the different samples and the different kinetic fits that resulted indicates that a better understanding of the effect of the drying methods on the powders would be needed to help explain the inner workings of the kinetics. The variability overserved also indicates that leaching tests should be performed on all new *Spirulina* powders procured during production as an assessment to determine the c-phycocyanin of that particular batch. This assessment will be more critical in the event of a new supplier being used. It is clear, however, that milling allows for a faster initial rate of leaching, but the fact that milling of the Brenntag and Carbocraft samples did not seem to change the time needed to reach the equilibrium concentration significantly, indicates that it may not be a necessary step to include in the overall process. This is further supported by literature where equilibrium c-phycocyanin concentration was achieved at around the same time for milled and non-milled samples of dried crushed biomass (Rakotondramasy-Rabesiaka, et al., 2008). Other literary sources note that bead-milling increased yield of intracellular microalgal products from to 5.6 % to 18.8 % (Shen, et al., 2009) and 100 % increase in yield (Baldev, et al., 2014). These microalgal samples were not dried, however, and as such they cannot be used for direct comparison with the results obtained in this dissertation nor from Hockey (2020).

4.3 Cell debris removal

4.3.1 Cell debris removal results

The purpose of the cell debris removal tests was to assess the ability of centrifugation to perform the separation of the *Spirulina* cell debris from the c-phycocyanin containing leachate after the leaching stage for both milled and non-milled samples. Thus, both milled and non-milled samples were used to further investigate the downstream effects of bead-milling to support the inclusion or exclusion of the cell disruption step. The performance of the cell debris removal was measured in terms of liquid recovery, since the liquid was the product containing phase. The cell debris removal tests were performed in a dead-end centrifuge using a batch operation approach. The solid cell debris was collected in a pellet form and the clarified liquid stream was drawn off as the product stream.

According to literature, the higher the relative centrifugal force, the higher the recovery of product-containing liquid in the liquid stream out of the centrifuge. This relationship is expected to be linear (Green & Perry, 2008). However, beyond a certain g force, it was anticipated that any increase in the extent of separation would become insignificant because the solid cake would become as packed as possible and minimal additional liquid separation would occur (Green & Perry, 2008). Thus, data interrogating this was needed to determine the centrifugal force above which the increase in liquid recovery becomes insignificant. This would inform the choice of an optimal g force for operation of the centrifuge. It was expected that the sample with the largest particles would have the best recovery since those particles should in theory settle the fastest (Green & Perry, 2008).

Figure 37 shows that as the g force increased, the recovery of the product-containing liquid increased across all the milled samples. However, the recovery did not seem to plateau at the higher g forces tested. Instead, over the range 1000 – 10 000 g, the increase in recovery remained linear. The milled Carbocraft sample had the best extent of separation, reaching a 77 % recovery of the total crude liquid at 10 000 g. The Indian sample performed the second best, reaching 72 % recovery of liquid at 10 000 g. The Brenntag sample reached 62 % recovery at 10 000 g, and therefore had the worst separation of the milled samples. Overall, considering all conditions tested, the Carbocraft *Spirulina* had the highest

recovery, and the Brenntag *Spirulina* had the lowest recovery at every g force tested. All three milled samples showed indications of linear increase in recovery with time, with the R^2 values being 0.91, 0.82 and 0.98 for the milled samples of Brenntag, Carbocraft and Indian, respectively. The Indian sample showed an increase of 16 % in recovery of the liquid as the centrifugal force was increased from 1000 g to 10 000 g. Carbocraft showed an increase of 18 % over this range and Brenntag a 15 % increase.

An Ordinary Least Squares (OLS) regression analysis was performed on the data shown in Figure 37 to help quantify the significance of the difference in trends between the samples tested. From centrifuge theory (Green & Perry, 2008), the effect of centrifuge speed on recovery data should be linear until such a point that the sedimentation cake cannot be further compressed for the same centrifuge residence time. As such linear and logarithmic regression models were fitted to the recovery data found in Figure 37. However, it was found that linear regression fitted better to all sets of data and was used to ensure consistent comparison of trends between samples. The OLS regression was performed using the OLS regression function from the statsmodels library in Python.

The regression analysis test results are shown in Table 22. The probability of the p-values of each line fitted for each samples' data are all above the 0.05 threshold value, rejecting the null hypothesis and quantifying a 95 % confidence that the variables in the model improve the fit and that the model is statistically significant. The relative linearity provided by the R^2 values all being greater than 0.75 suggest that the residuals are normally distributed for all 3 samples. Using this, t-tests were performed to compare the significance of the trends suggested by the slopes generated from the linear regression. A Python script was used to perform the t-tests. The difference in the slopes of Carbocraft and Indian samples is 0.000295 and the t-statistic is 1.55. This t statistic is less than the critical value from the t distribution at 95 % (1.96) and therefore the null hypothesis could not be rejected. Thus, the slopes for the Carbocrft and Indian samples are not significantly different at the 95 % confidence level. This suggests that the Carbocraft and Indian samples behave similarly across the centrifuge speeds tested. The difference in the slopes of the Indian and Brenntag samples is 0.00447 and the t statistic is 3.72. This t statistic is greater than the critical value from the t distribution for a 95 % confidence level and so the null hypothesis that the slopes are equal was rejected. Thus, the slopes for Indian and Brenntag samples are significantly different at the 95 % confidence level. This suggests that the Brenntag sample behaves differently to the Indian and Carbocraft samples across the centrifuge speeds tested.

It is interesting to note that the Carbocraft and Indian samples behave similarly to each other and differently to the Brenntag, since the Brenntag and Carbocraft samples have similar morphology and are similar in size. This contrast was not further investigated and remains unexplained.

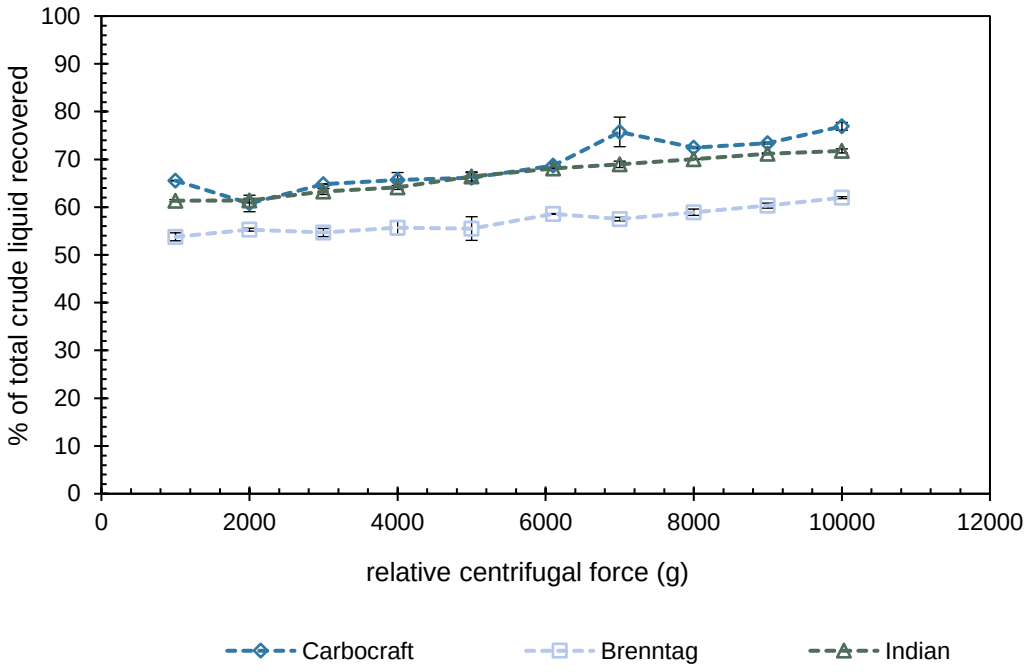

Figure 37. Recovery of the crude liquid leachate following centrifugation over the range of 1000 to 10 000 g force for milled Brenntag, Carbocraft and Indian Spirulina samples after leaching. The error bars indicate variance in the measured recovery for triplicate runs of the samples.

Table 22. Summary of the outputs of the OLS regression analysis performed on the milled *Spirulina* samples liquid recovery data in Figure 37 with linear regression model (Model), coefficient of determination (R^2), probability associated with the F-statistic [Prob(F-statistic)]

Sample	***Model***	***R^2***	***Prob(F-statistic)***
Brenntag	$y = 8.4 \times 10^{-4} + 52.6$	0.78	2.47×10^{-7}
Carbocraft	$y = 1.6 \times 10^{-3} + 60.3$	0.76	5.69×10^{-7}
Indian	$y = 1.3 \times 10^{-3} + 59.6$	0.97	1.22×10^{-14}

It was hypothesized that the non-milled samples would allow for a greater recovery of liquid across the centrifugation stage since milling results in smaller cell debris particles (shown in section 4.1 *Spirulina* powder size distributions), which decreases the terminal settling velocity of the debris particles, meaning a lesser extent of separation for the same operating conditions of the centrifuge (Green & Perry, 2008). Data supporting this hypothesis would support the removal of the milling step – an energy- and capital-intensive step of the extraction process.

Figure 38 shows that at low relative centrifugal forces, the separation of the milled Carbocraft biomass from the liquid was better or equal to the non-milled samples in terms of clarified liquid recovery from the centrifuge. However, at forces of 7 000 g and higher, the non-milled Carbocraft biomass was separated better in terms of liquid recovery when compared to the milled sample. Table 23**Error! Reference source not found.** shows the t-test performed on the data for the Carbocraft milled versus non-milled to statistically quantify the significance of the difference between the two scatter plots in Figure 38. The results of the t-test show that there was a significant difference in the slopes of the linearized Carbocraft and Carbocraft non-milled data for the 95 % confidence level. The slopes being statistically significantly different suggests that the milling influenced the trend of the recovery observed. This suggests that we can be confident (95 %) that the Carbocraft sample did perform differently than the Carbocraft non-milled sample.

Figure 39 shows that for all relative centrifugal forces tested, the non-milled Brenntag sample had better liquid recovery compared to its milled counterpart for every g-force tested. Table 24 summarizes the t-test for the comparison of milled versus non-milled Brenntag data. The results of the t-test show that there was not a significant difference in the slopes of the linearized Brenntag and Brenntag non-milled data for the 95 % confidence interval level. Thus, it is suggested that the trend in the recovery data is the same and thus we can be confident at the 95 % confidence level from a combination of the linear coefficients of determination and the results of the t-test that the milling of the Brenntag sample caused a decrease in the efficiency of the cell debris removal via centrifugation. This is because for the same trend (slope) the Brenntag non-milled sample outperformed its milled counterpart. This should be attributed to the smaller PSD representative diameter of the milled Brenntag resulting in a lower sedimentation rate in the centrifuge as expected from centrifuge theory (Green & Perry, 2008). The difference in efficiency can be quantified by an 8-9 % increase observed in the liquid recovery at every g-force tested when Brenntag was not milled.

Therefore, the results for the Brenntag sample are as expected when compared to literature and the performance of this solid-liquid separation is in line with the first principles that govern centrifugation whereby a larger particle will separate out easier than a smaller particle (Green & Perry, 2008; Richardson, et al., 2002).

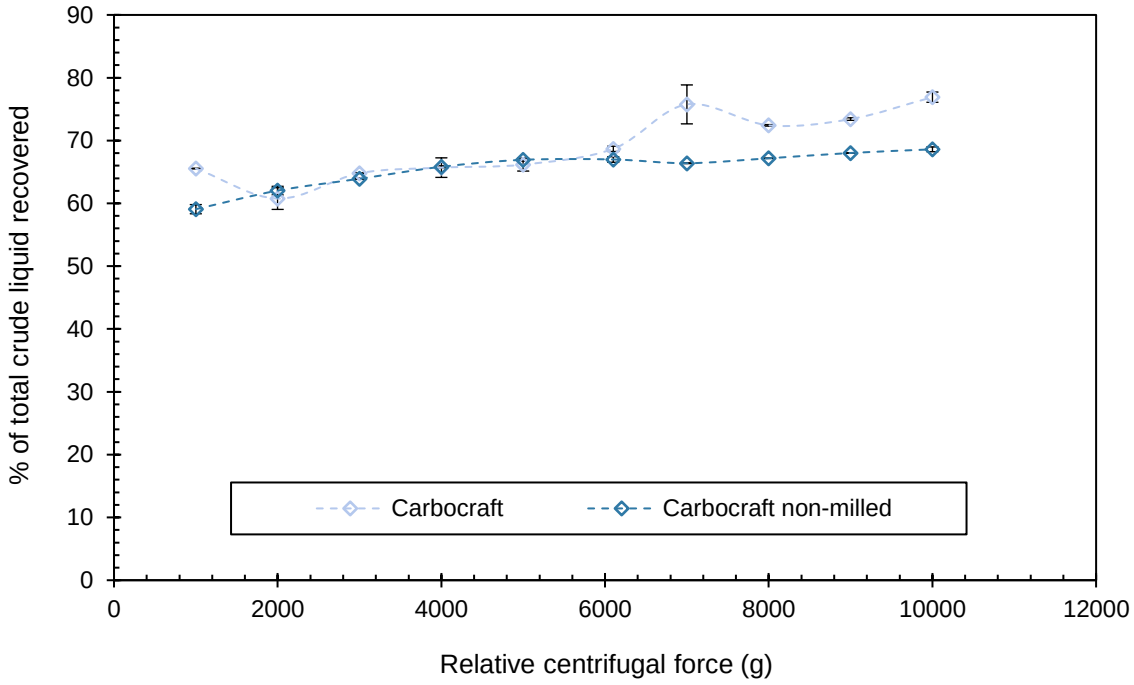

Figure 38. Recovery of crude liquid leachate out of centrifuge over the range of 1000 to 10 000 g force for milled and non-milled Carbocraft Spirulina samples after leaching. The error bars indicate variance in the measured recoveries across triplicate runs.

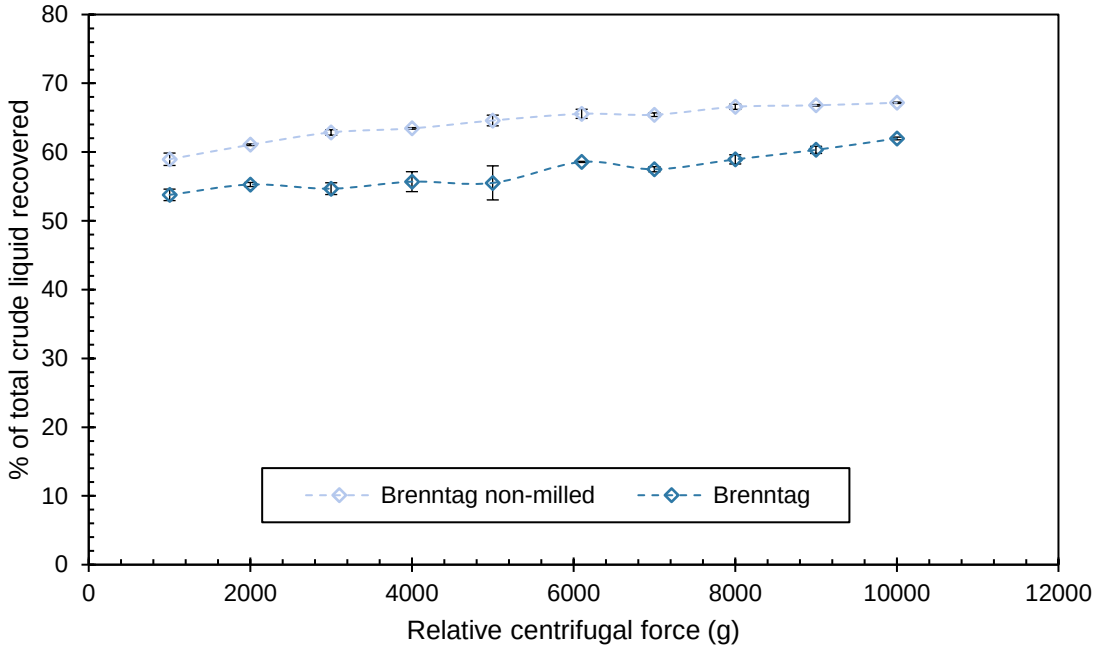

Figure 39. Recovery of crude liquid leachate out of centrifuge over the range of 1000 to 10 000 g force for milled and non-milled Brenntag Spirulina samples after leaching. The error bars indicate variance in the measured recoveries across triplicate runs.

Table 23. Summary of the regression analysis and t-test statistical significance results performed on the milled and non-milled Carbocraft Spirulina leachate recovery data from Figure 38

Sample	***Model***	***R^2***	***Prob(F-statistic)***
Carbocraft	$y = 1.6 \times 10^{-3} + 60.3$	0.76	5.69×10^{-7}
Carbocraft non-milled	$y = 8.8 \times 10^{-4} + 60.6$	0.80	1.3×10^{-7}
	t-test		
Difference in slopes	***Std Error Difference***	***t-statistic***	***Null hypothesis rejection***
7.0×10^{-4}	2.4×10^{-4}	2.97	Yes

Table 24. Summary of the regression analysis and t-test statistical significance results performed on the milled and non-milled Brenntag *Spirulin*a leachate recovery data from Figure 39

Sample	***Model***	***R^2***	***Prob(F-statistic)***
Brenntag	$y = 8.4 \times 10^{-4} + 52.6$	0.78	2.47×10^{-7}
Brenntag non-milled	$y = 8.4 \times 10^{-3} + 59.6$	0.89	5.74×10^{-7}
	t-test		
Difference in slopes	***Std Error Difference***	***t-statistic***	***Null hypothesis rejection***
6×10^{-6}	1.27×10^{-4}	4.5×10^{-2}	No

The c-phycocyanin purity in the leachate was also measured before and after the centrifugation. This data is presented in Figure 40. It was anticipated that the purity would remain the same across different

g forces of centrifugation, as the leachate should remain homogeneous. Correspondingly, the figure shows that no significant changes in purity appeared in the data, though the variances across the triplicate runs were quite large. To note, the original purity (prior to centrifugation) was influenced by the time taken to leach each sample. All samples were centrifuged for these tests not long after being milled, with the centrifuge time also being short compared to the full leaching time.

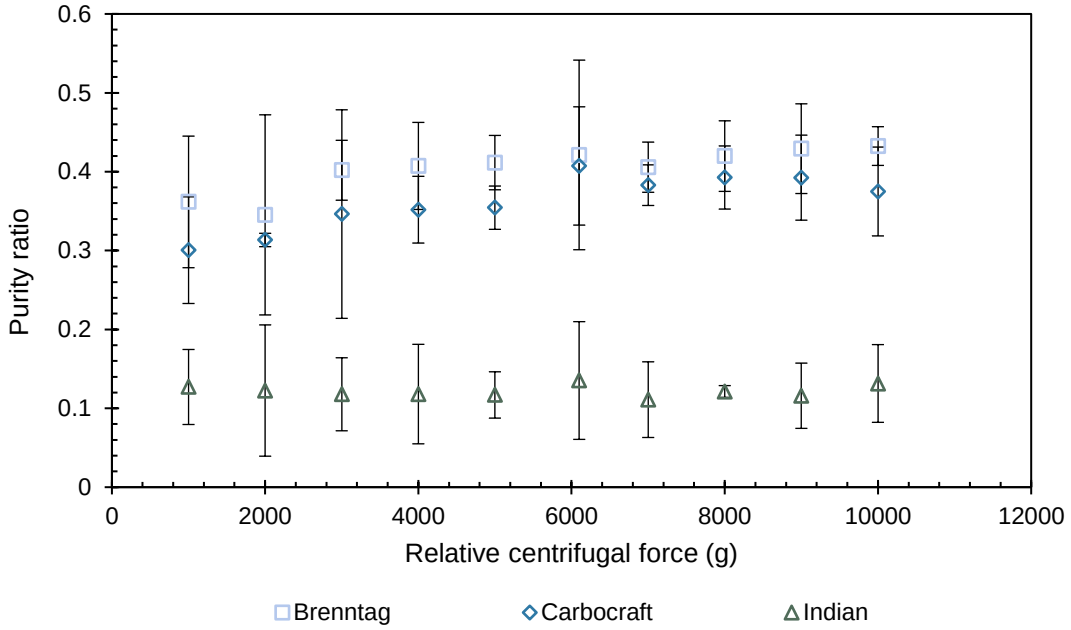

Figure 40. Purity ratio of the crude liquid leachate recovered out of centrifuge over the range of 1000 to 10 000 g force for Brenntag, Carbocraft and Indian Spirulina samples after leaching. The error bars indicate variance for triplicate runs.

It was thought that rinsing of the cell debris pellet would allow for the overall recovery of more c-phycocyanin, as the c-phycocyanin in the leachate that was entrained with the pellet could be recovered. It is also possible that more c-phycocyanin could be leached from the cell debris into the fresh buffer solution due to the lower c-phycocyanin concentration in the liquid driving a subsequent mass transfer of c-phycocyanin into the bulk liquid (Janin, et al., 2009). Therefore, a resuspension of the milled Carbocraft *Spirulina* cell debris pellet in buffer solution followed by a second centrifugation step at 7 000 g was tested. This resuspension was allowed to leach for 5 hours as per the methodology in section Cell debris removal. Figure 41 shows that before the pellet rinsing step, with an increase in the g force of centrifugation a higher c-phycocyanin recovery was yielded. This is because the higher the g force the more leachate was recovered and thus more c-phycocyanin. After the rinsing step, the overall recovery of c-phycocyanin was consistently higher than that of the first step. **Error! Reference source not found.** summarizes the results of a t-test performed on the recovery before rinsing and after rinsing. The results of the t-test ($p<0.05$) indicate that there was a significant difference in the recoveries yielded before and after the rinsing step. The data therefore suggests that a rinsing step could be used to increase the overall c-phycocyanin recovery. However, the cost-benefit of employing an extra rinsing step must also be considered. For example, at 10 000 g the recovery was 76.9 ± 3.4 % before rinsing and 85.5 ± 3.8 % after rinsing, and so, considering variability, it is possible that there is a difference of only few percent, which may be insignificant. This possible insignificant improvement was yielded using additional buffer as a consumable along with additional leaching time and an additional centrifugation step. Thus, the techno-economics would need to be performed to check the viability of using the rinsing step. The highest recovery achieved post rinsing was 85.5 ± 3.8 % at 10 000 g. The recovery at a first spin of 1000 g and second spin of 7 000 g after rinsing is 85.0 ± 12.3 %. This suggests that similar recoveries could be achieved at 1000 g and 10 000 g first centrifugations if the rinsing step is applied. However, the variance in the reading at 1000 is much larger than the other data point so it is not the most reliable. The overall c-phycocyanin recoveries after rinsing for all g forces of first spin are very similar, suggesting that for a rinsing step a lower g force of first spin could be used. No final

conclusions can be made on the viability of the rinsing step at this stage as there is still scope to alter the rinsing time or the second centrifugation step g force, however the data does suggest that there is promise for an increase in c-phycocyanin recovery when incorporating a rinsing step. These results were found for a dead-end centrifugation system which has better liquid clarifying capabilities than other systems. As such, if a different type of centrifugation was used it may require the additional rinsing step to achieve comparable recoveries.

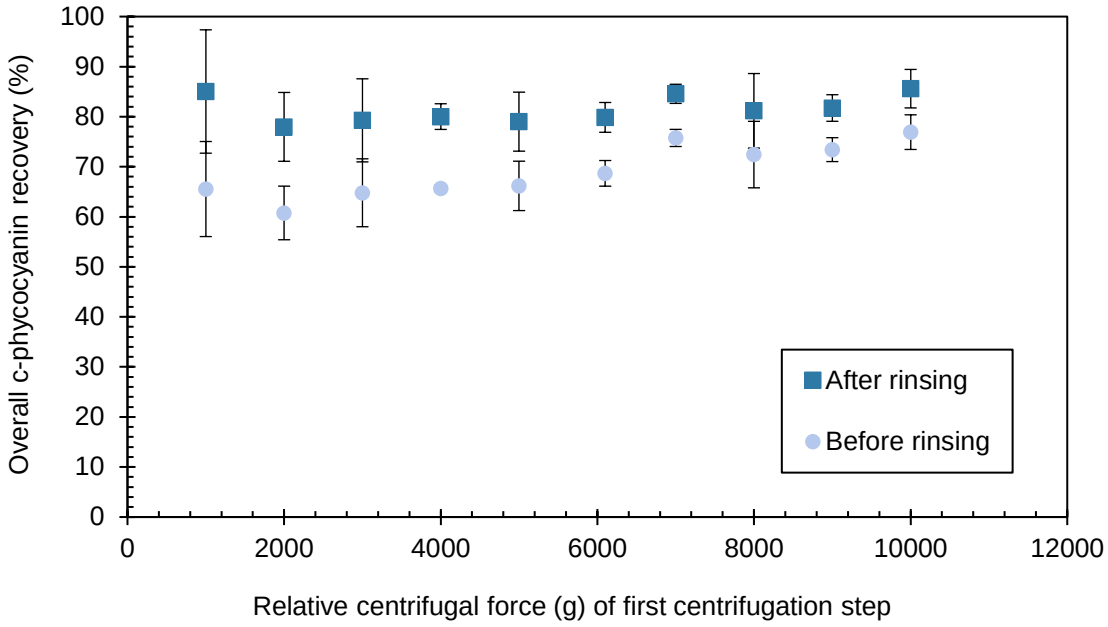

Figure 41. Recovery of the milled Carbocraft crude liquid after a first and second centrifugation, i.e. with and without additional cell debris rinsing, at different g forces for the initial cell debris removal centrifugation and 7 000 g for the second centrifugation. The error bars indicate the variance across triplicate runs.

4.3.2 Discussion on cell debris removal

Literature sources for cell debris removal of *Spirulina* do not go into much detail regarding the reasons behind their centrifugation method. Not much literature is available on the recovery of c-phycocyanin or liquid post centrifugation. The general principles of centrifugation can be applied to interrogate the data acquired. To discuss the performance of a sample of *Spirulina* powder being centrifuged, we must understand the physical properties of that slurry being centrifuged. One of the major influences on the performance of solid-liquid separation by centrifugation is the size of the solid particles in the slurry. This links directly to the terminal settling velocity of the solids. For the same density, the greater the size of a particle, the higher the terminal settling velocity of a particle and hence the faster that solid particle settles.

The highest recovery of liquid in the liquid product stream was found for the milled Carbocraft samples (see Figure 37). The milled Carbocraft samples had the most tightly packed solids cake (moisture content was calculated in determining liquid recovery, see 3.3.5 Cell debris removal) – implying that a greater extent of solids separation from the liquid was achieved compared to the other milled samples whose cakes would, therefore, have contained more entrained liquid. This ties in when considering the particle sizes of the milled samples. When comparing the milled samples, the milled Carbocraft *Spirulina* had the largest d_{80}, d_{50} and d_{ave}, meaning that the terminal settling velocity would have been the highest of the milled samples if the densities of the powders were assumed to be approximately equal, and therefore it was expected that it would settle the fastest.

The worst liquid-solid separation in terms of recovery of crude liquid of the milled samples was observed for the Brenntag samples. However, the particles were bigger than the Indian sample for d_{80}, d_{50} and d_{ave} – suggesting that the Brenntag biomass separation should have performed better than the Indian samples. This inconsistency could possibly be due to a density difference between the powders, which was assumed to be insignificant considering all samples are of the same species. This inconsistency could also be a result of a difference in morphology (see microscope images in Appendix B.1). The cell fragments of the Indian sample were more spherical in shape than the Brenntag cell fragments which were more spiral-shaped. Both cell fragment populations were irregular, however. Furthermore, all of the milled samples had wide particle size distributions, and the Indian powder had a much wider distribution compared to the Brenntag powder. The Brenntag powder had a mean particle size of 0.34 mm with a standard deviation of 0.36 mm whereas the Indian sample had a mean particle size of 0.21 mm with a standard deviation of 0.35 mm. Thus, though similar standard deviations from the mean within a sample of milled powders were observed, the milled Indian sample had a comparatively larger percentage difference in the standard deviation from the mean compared to the milled Brenntag sample. This also means that the milled Indian sample had much finer particles present in the PSD than the milled Brenntag sample. It has been shown that a wider spread PSD and higher fine particle content can yield a tighter packed cake since the smaller particles fill the voids between the larger particles (Mehdipour & Khayat, 2017). This phenomenon could have allowed the milled Indian solids cake to be more tightly packed, decreasing the voidage and so resulting in less room for product-containing liquid to be retained between the particles of cell debris.

The relatively larger particle sizes of the non-milled samples suggest that the non-milled cell debris should separate better from the liquid than their milled counterparts since they would be expected to have a higher settling velocity. However, since size is not the only variable affecting centrifugation (as previously explained), the PSD of the particles can alter how packed the cell fragments become in the cake which will in turn affect how much liquid can be recovered. Looking at Figure 38, centrifugation of the milled and non-milled Carbocraft crude extract yielded the same magnitude of recovery at lower centrifugation speeds but at higher speeds the milled outperformed the non-milled, albeit that the non-milled had a greater d_{80}, d_{50} and d_{ave}. When looking at the size distributions, the Carbocraft non-milled had a 101 % standard deviation from the mean whereas the milled had a 110 % standard deviation from the mean (see Table 19 and Figure 15).). It appears that even with a greater than 10% reduction in size across d_{80}, d_{50} and d_{ave} when milling, the increase in PSD width (represented by the standard deviation from the mean) post-milling did significantly alter the filter cake packing, such that the trend in liquid recovery was statistically different to the non-milled case. It has been shown that a wider spread PSD and higher fine particle content can yield a tighter packed cake since the smaller particles fill the voids between the larger particles (Mehdipour & Khayat, 2017) .

For the Brenntag samples, the milling decreased the uniformity of the distribution, with the standard deviation increasing from 97 % to 108 % of the mean, see Table 19 and Figure 14. Figure 39 shows that the non-milled sample separated better than the milled sample. This is as expected since the non-milled particles were bigger and thus the settling velocity would have been expected to be higher (Green & Perry, 2008). Therefore, it seems that milling the Brenntag sample, and the resulting 20 % reduction in the d_{80} and a 17 % reduction in the d_{ave}, was enough to decrease the efficiency of the cell debris removal, despite the increase in PSD width.

From the data at hand, we see that the particle size distribution of the *Spirulina* powders can have a significant effect on the efficiency of the cell debris removal. This suggests that for a given *Spirulina* powder it may be possible to identify a milled PSD that permits the benefits of an increased the initial leaching rate, but that can also contribute towards better or at least equivalent of non-milled powder packing of cell debris, thereby resulting in a higher recovery of liquid in the cell debris removal stage. However, from the data that was generated, it can only be said that for this particular setup (dead-end centrifuge operating between 1000 and 10 000 g for 10 min), that the higher g-force will result in better separation and that milling may have a negative effect on the liquid recovery depending on the *Spirulina* powder used in the feed.

For the current set-up used for the two-stage centrifugation with the rinsing step included between consecutive centrifugations, to obtain the results shown in Figure 41, a much longer time-on-stream will

be incurred, prior to time optimization of the rinsing. This is owing to the fact that the 10 hours was used to leach the c-phycocyanin prior to the second centrifugation step. A better conclusion of this proposed rinsing can be developed upon revision of the techno-economics of this step. A more informed decision can be made on the inclusion or exclusion of this rinsing step once we can quantify the increase in recovery in terms of profit on the c-phycocyanin product. Concerning the operation conditions of this step; the higher the g force of the first spin, the lower the percentage increase of recovery is what is observed – thus, to maximize recovery, greater electricity demands are required. The operation parameters of this step would also best be concluded upon once the techno-economic implication of the rinsing is understood.

What is clearly observable from the results in Figure 37 is that for a higher g force, a higher recovery of liquid is yielded. Therefore, the most optimal operating conditions for the process overall will need to consider the tradeoff between recovery of product and the additional energy cost associated with operating at a higher g force. Determining the optimal operating conditions will also need to consider the capital cost required for a centrifuge capable of operating at higher g forces. When prioritizing recovery, the centrifugation step should be operated at the highest g force available (10 000 g for this specific setup, since we only tested up to this) if this speed is available, and the process should also include a rinsing step to maximize recovery. This conclusion is well documented by the theory of centrifugation described in Perry's Handbook and Coulson and Richardson (Green & Perry, 2008; Richardson, et al., 2002).

Since the increase in recovery with increase in g force appears linear to 10 000 g, an increase in centrifugation time could also or could alternatively be implemented to allow for better recovery – if g force is not increased further. The tradeoff between holding time and increase g force would need to be optimized taking process economics into account. For this project, for the full runs of the process, the centrifugation time would be increased to increase liquid recovery since the centrifuges used for the experimental could not exceed much more than 10 000 g. Sørensen, et al. (2013) used a higher force of 25 000 g to centrifuge *Spirulina* cell debris and sequester the supernatant, supporting that there may still be an increase in recovery possible above 10 000 g. This does depend on the size of the cell fragments being centrifuged, however. For example, Song et al. (2013) also used dried *Spirulina* powder and operated their cell debris removal centrifugation at 10 000 g for 15 min – similar operating conditions to the conditions tested in this project. Critially, the techno-economics will play an important role in determining the best operating conditions for this cell debris removal area of the process since the liquid recovery, even at the lowest g force, is not much lower than the recovery at the highest g force. Thus, the economics will better inform the decision to tradeoff between recovering more product at a higher operating cost (energy for a higher operating speed).

Based on the recommended centrifuge speed, type of slurry and potential capacities for scale-up, it is recommended that the centrifuge used for an upscale of the process be a disk stack nozzle discharge centrifuge (Green & Perry, 2008). The centrifuge design parameters have not been quoted since these would be heavily dependent on the economics. With the results presented in this section, a multi-dimensional techno-economic model cannot be generated since the effect of centrifuge speed compounded with centrifugation time has not been investigated.

4.4 Aqueous two-phase separation

The purpose of the aqueous two-phase separation (ATPS) experiments was to check how robust the operation of the ATPS system is at the operating conditions proposed by Hockey (2020). Different dilutions of the feedstock were used as an additional check of robustness since it would change the protein concentration of the feed.

Figure 42 shows the ATPS phase formation for the three different *Spirulina* crude extract samples at different dilutions when fed into the citrate-PEG 4000 system at the recommended salt and polymer concentrations from Hockey (2020). Phase formations are presented as the bottom phase's volume as a percentage of the total volume. At 1× dilution (i.e. the proposed operating condition from Hockey (2020)) the Brenntag sample showed no dual phase formation. A single aqueous phase remained. As

the dilution of the crude extract increased to 2.4 times, two phases were seen forming. At 2.4× dilution and above, the citrate bottom phase volume was roughly stabilized at 34 ± 5.3 % of the total ATPS volume. At 1× dilution the Indian crude extract yielded a citrate bottom phase volume of 80 % of total volume. At 1× diluted, the Carbocraft crude extract unexpectedly formed three distinct phases, as shown in Figure 45. The bottom phase of the Carbocraft sample had a volume of 60 % of total volume. This is a 40 % variability across the three samples showing poor robustness at the proposed component weight fractions of 20 wt% citrate salts and 11 wt% PEG. Both the Indian and Carbocraft crude extracts showed a similar trend to the Brenntag sample of decreasing the bottom phase % of total volume with an increase in number of times diluted in the citrate-PEG ATPS. The observation of the bottom phase volume becoming roughly stabilized above 2× dilution was also observed for Indian and Carbocraft crude extracts. The bottom phase volume was roughly stable at 54 ± 4 % of total volume and 41 ± 6 % of total volume for the Indian and Carbocraft crude extracts, respectively.

Figure 43 shows the effect of the dilution of the crude extract of the three *Spirulina* sample crude extracts on the purification factor over the citrate-PEG ATPS system. The purification factor over the citrate-PEG ATPS is the ratio of the purity in the top PEG-phase over the purity of the crude extract preceding the ATPS. The Indian and Carbocraft samples both yielded a 1.2 purification factor at the recommended operating conditions (1× dilution). The Brenntag sample did not obtain a purification factor at 1× dilution since no phase formation was observed and hence the top PEG-phase could not be sampled. An increase in dilution saw the Indian sample decrease in purification factor to 0.5 at 4× dilution. The increase in dilution saw the Carbocraft purification factor staying roughly the same at 1.25 ± 0.06 across all dilutions tested. For the Brenntag sample, the increase in dilution also seemed to have no significant effect with the purification factor averaging at 1.23 ± 0.05 across 2.4× to 5.4× diluted.

Figure 44 shows the recovery of c-phycocyanin in the top PEG-phase of the citrate-PEG ATPS for the three different *Spirulina* sample crude extracts at different dilutions. At 1× diluted, the Indian sample achieved the highest recovery of c-phycocyanin in the top PEG-phase of 85 %. At 1× diluted, the Carbocraft sample achieved 8 % recovery of c-phycocyanin and the Brenntag sample achieved 0 % recovery since no phases were formed at 1× diluted. As dilution increased, the Indian sample experienced a drop in the recovery of c-phycocyanin in the top PEG-phase with recovery dropping to approximately 4 % at a 4× diluted crude extract. The increase in dilution of the crude extract for the Carbocraft sample saw an increase in recovery of c-phycocyanin in the top PEG-phase that roughly stabilized at 36.5 ± 0.71 % from 3.6× diluted to 5.4× diluted. As dilution increased, the Brenntag sample yielded an increase in recovery, before tapering off to 24 ± 4.2 % after being 3.6× diluted.

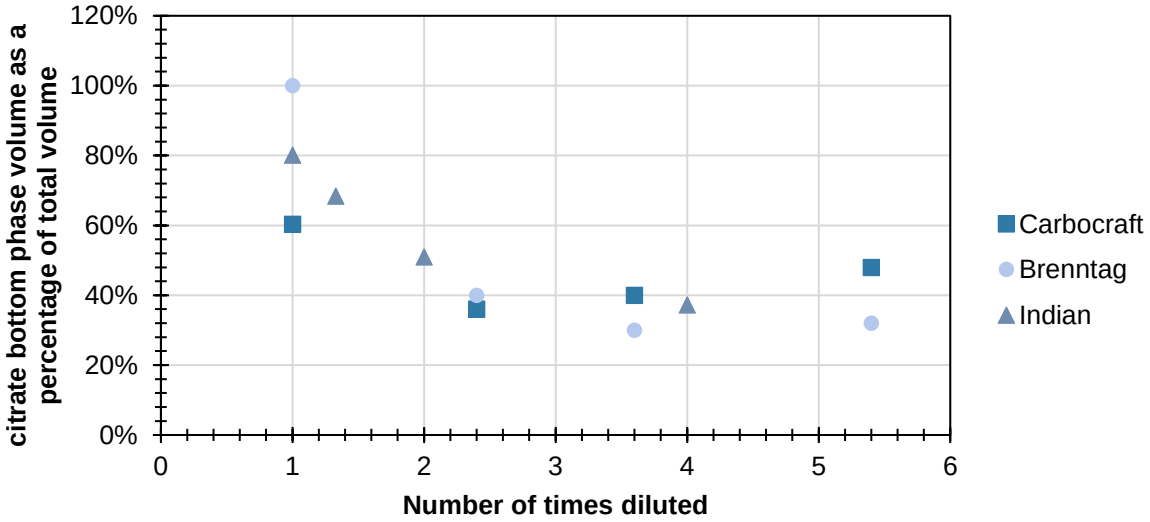

Figure 42. Citrate-PEG 4000 ATPS citrate bottom phase volume as a percentage of total volume at different concentrations of crude extract feed for the Brenntag, Carbocraft and Indian *Spirulina* crude extract samples

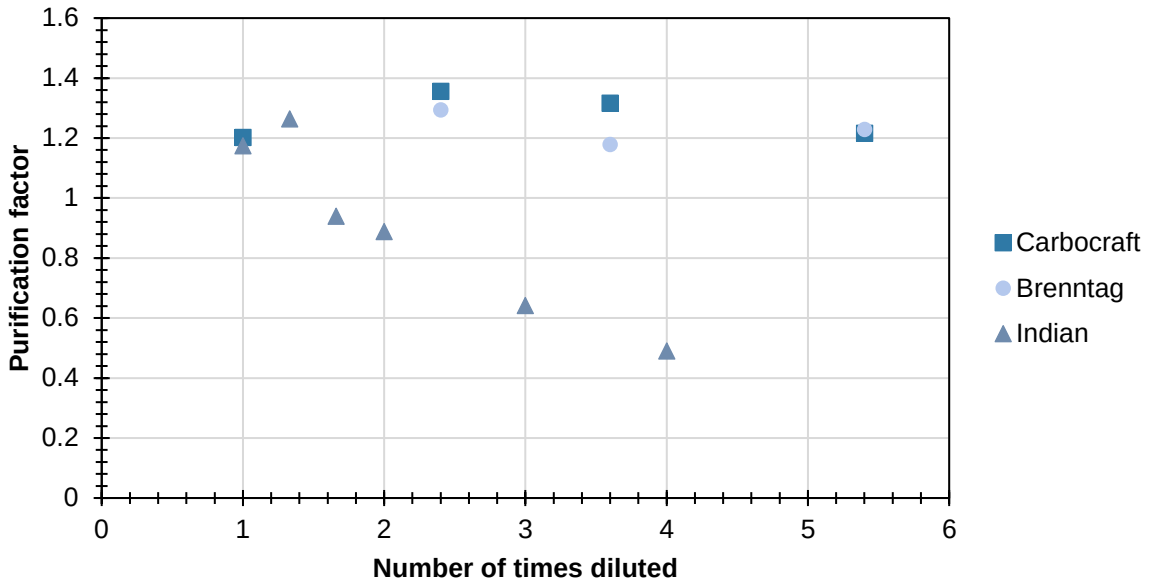

Figure 43. Purification factor in the top PEG phase of the citrate-PEG 4000 ATPS at different crude extract feed concentrations for the Brenntag, Carbocraft and Indian *Spirulina* crude extract samples

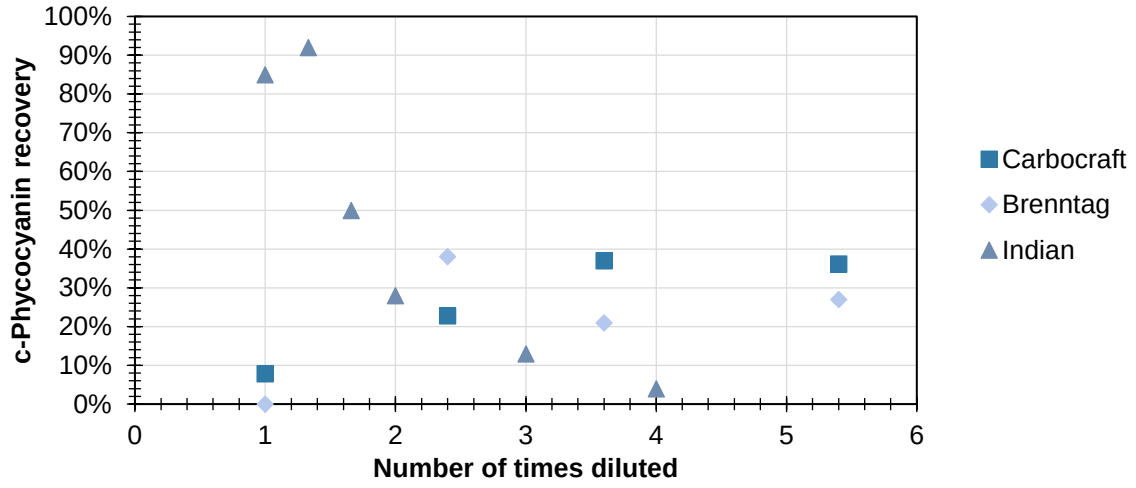

Figure 44. c-Phycocyanin recovery in the citrate-PEG 4000 ATPS top PEG phase for Brenntag, Carbocraft and Indian *Spirulina* crude extract samples

It was thought that a possible reason for the poor ATPS formation was that the viscosity of the mixture was too high and that this may have inhibited the interaction between the ATPS components such that no clear phase formations could occur. Another possible explanation for the unexpected phase formation is that something present in the crude extract was affecting the partitioning and if diluted the effect of this component would be reduced. This is the reason why experiments using diluted crude extract were performed. With dilution of the crude extract, more distinct phase separation occurred that allowed for the purification factors to be established. The dilution also served to change the crude extract macromolecule concentration by a known amount to observe the effects this had on the ATPS performance. The starting c-phycocyanin concentrations for the three samples tested were not the same as that used in the experiments described by Hockey (2020), ~5 $mg.mL^{-1}$, at 1.31 ± 0.06 $mg.mL^{-1}$, 11.1 ± 1.54 $mg.mL^{-1}$ and 10.8 ± 0.69 $mg.mL^{-1}$ for the Indian, Brenntag and Carbocraft samples, respectively. This suggests that the protein concentration may also have been different which also could have influenced the phase formation. This could have been confirmed using a protein assay. This was not tested, however, as the key aim of these experiments was to test the robustness of this ATPS

system and see if it could handle a fluctuation in feed composition. It is important to note, however, that the Indian sample was the same as the sample used in Hockey (2020) and it was unexpectedly not behaving similarly to the results described in Hockey (2020) – this could be attributed to protein degradation during storage. Furthermore, the maltodextrin used was of a food grade in both studies, however a different batch was used in this study when compared to Hockey (2020), this difference could also have influenced the performance of the ATPS.

From Figure 42 and Figure 44 it would be logical that the recoveries increased as the dilutions increased since for all three *Spirulina* sample crude extracts tested the top PEG-phase volume increased however, this was not the case. For the Indian sample, the recovery of c-phycocyanin in the top PEG-phase decreased as that phase increased in volume. This suggests that with an increase in dilution of the crude extract for the Indian sample, the c-phycocyanin was partitioning more to the bottom citrate-phase. This is further supported by the purification factor decreasing with increased dilution, as shown in Figure 43. This was only observed for the Indian sample. For the Carbocraft and Brenntag sample crude extracts, as the top PEG-phase increased and stabilized with increasing dilution, the recovery of c-phycocyanin in that phase increased and stabilized too. This suggests that the partitioning of the c-phycocyanin was not affected by the increased dilution of the crude extracts for Carbocraft and Brenntag. This is further supported by the results presented in Figure 43 where the purification factors remained roughly constant for all dilutions tested.

At a 1× diluted crude extract, Hockey (2020) reports an expected 1.63 c-phycocyanin purification factor in the top PEG-phase with a 95.6 % recovery of c-phycocyanin over the citrate-PEG ATPS. These values are in stark contrast to the results presented in Figure 42, Figure 44 and Figure 43, with purification factors of 1.2, 1.2, 0 as well as c-phycocyanin recoveries of 85 %, 8 % and 0% found for the Indian, Carbocraft and Brenntag samples, respectively. Another reason behind the low recovery observed for the Carbocraft crude extract was that at 1× diluted, the ATPS did not form two phases, but instead formed three phases, as shown in Figure 45.

Of the factors that influence the performance of an ATPS (namely polymer concentration and weight, temperature and pH (Asenjo & Andrews, 2011; Iqbal, et al., 2016; Murty, et al., 2012)), all were kept constant between Hockey (2020) and this study. Thus, this disparity between ATPS results was unexpected. The only potential difference between the citrate-PEG ATPS set-up from Hockey (2020) is the composition of the crude extract. This is likely, as Hockey (2020) used a different *Spirulina* powder to those used in this study. This would have resulted in the macromolecule ratio and concentration being different to that of Hockey (2020). It can be observed that a dilution of the crude extract does impact the partitioning of the ATPS greatly from the trends seen in Figure 42. As such, it is postulated that the composition of the crude extracts used in this study were significantly different to that used by Hockey (2020) and each other. Although crude extract from all *Spirulina* samples should yield water soluble compounds, the ratio of the macromolecules in said extract can be different depending on growth conditions, and this could influence phase formation since protein concentration affects partitioning (Asenjo & Andrews, 2011; Iqbal, et al., 2016; Murty, et al., 2012). Furthermore, this difference affected the partitioning and hence the performance of the citrate-PEG ATPS yielding the vastly different purification factors and recoveries. From the results it can clearly be seen that the citrate-PEG ATPS system using the recommended operating conditions from Hockey (2020) is not robust.

Upon repeats of certain experiments, three phases forming was observed, similarly to the Carbocraft at 1× diluted. This was also not expected but could be because of remnant cell debris in the system causing the ATPS to function differently.

With regards to the PEG-maltodextrin ATPS, the results of preliminary experiments also showed it to be a non-robust system. This coupled with the conclusion from Hockey (2020) that the PEG-maltodextrin ATPS yielding low c-phycocyanin purification factors it was considered not suitable for use.

For these reasons as well as other undocumented experiments to further troubleshoot, it was decided by the research group that the ATPS systems would be removed from the CeBER extraction and purification process for c-phycocyanin from *Spirulina* as it was unreliable in producing consistent results and the consistent results it did yield were unfavourable or redundant. The aqueous two-phase

separation for citrate-PEG and PEG-maltodextrin were not carried out to the full extent of which was planned for the research due to the ATPS having been proved to be non-robust.

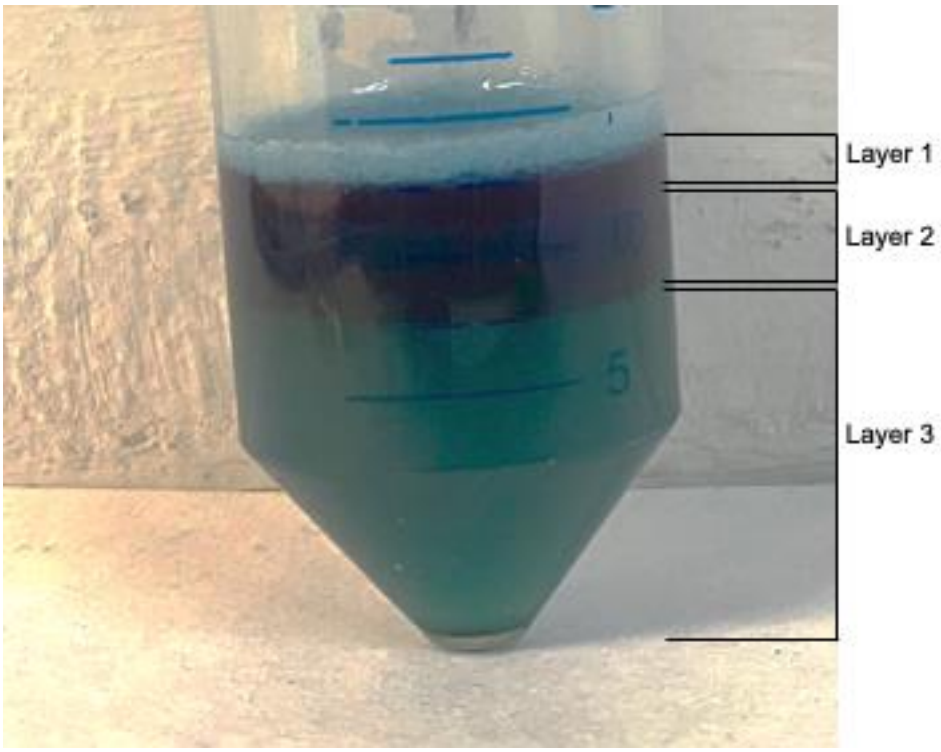

Figure 45. An unexpected three phases forming in the citrate-PEG 4000 ATPS for Carbocraft crude extract at 1× dilution

4.5 Ammonium sulfate precipitation

The primary purpose of the precipitation experiments was to determine operating conditions for a precipitation train of two stages that would allow for good purity and recovery across all *Spirulina* sample crude extracts tested. The first stage was to target the removal of impurities in the precipitate with retention of the c-phycocyanin in the supernatant, followed by a second precipitation of the resulting supernatant to obtain a precipitate of high c-phycocyanin purity.

4.5.1 c-Phycocyanin recovery and purity in the precipitate pellet

c-Phycocyanin recovery in the precipitate pellet

It was hypothesized that c-phycocyanin would begin to precipitate out of solution at a specific solution conductivity (associated with the ammonium sulfate saturation percentage) and that recovery of c-phycocyanin would increase with an increase in ammonium sulfate saturation fraction and would reach 100 % recovery before, or at the point of complete saturation of starting solution (Green & Hughes, 1955). This would allow for the determination of a saturation fraction to be considered the end point of recovery of c-phycocyanin and would allow the process to be able to achieve near to 100 % recovery of c-phycocyanin – if necessary.

Figure 46 shows the recovery of c-phycocyanin in the precipitate as a function of the ammonium sulfate saturation fraction, as determined for the different *Spirulina* sample crude extracts. Figure 46 shows that all of the crude extracts follow the same precipitation trend; when a certain ammonium sulfate saturation threshold was overcome, the c-phycocyanin recovery increased approximately linearly with

saturation and tended towards a final value of 100 %. For the Indian *Spirulina* crude extract sample, the recovery of c-phycocyanin reached 100 % at an ammonium sulfate saturation fraction between 0.5 and 0.6. Similarly, the Brenntag *Spirulina* crude extract sample reached 100 % c-phycocyanin recovery between 0.5 and 0.6 of ammonium sulfate saturation. The Carbocraft crude extract did not reach 100 % recovery within the experimental range of ammonium sulfate saturations but did achieve a 91 ± 4.4 % recovery at 0.85 times saturation. The Green Create Nutra (GCN) crude extract also did not reach 100 % recovery within the experimental range of ammonium sulfate saturations but did achieve 75 ± 4.3 % recovery at 0.77 of ammonium sulfate saturation. However, for both the GCN and Carbocraft crude extracts, at the maximum saturation fractions tested recovery still appeared to be increasing linearly with saturation fraction. This suggests that 100 % of c-phycocyanin may still be possible at even higher degrees of saturation. The data suggests an agreement with the hypothesis; where it can be confidently claimed that at 100 % saturation we can achieve a full recovery of the c-phycocyanin product in the pellet for the Indian *Spirulina* powder sample and for the Brenntag *Spirulina* powder sample, and based on the trends, it is likely that this can also be achieved for the other two *Spirulina* sources. Song et al. (2013) shows the recovery does not reach 100 % but does tend towards it, with accounting for the confidence interval in this study the data does agree with the results from Song et al. (2013).

Based on literature information, it was anticipated that c-phycocyanin would begin to precipitate out of solution at a specific conductivity at which the salt ions begin to out-compete the c-phycocyanin (Song, et al., 2013), allowing for a particular saturation fraction of ammonium sulfate to be considered as the incipient point of c-phycocyanin precipitation. Knowing this point will aid in establishing optimal process operating conditions. Figure 46 shows that all samples began to precipitate c-phycocyanin between 0.11 and 0.22 saturation, apart from the GCN sample for which c-phycocyanin was only observed in the pellet at saturations above 0.42. According to Song et al. (2013), c-phycocyanin starts precipitating out between 0 and 0.2 saturation, which agrees for the runs with all *Spirulina* samples except the GCN sample. Based on these results, it therefore cannot be concluded that a specific saturation fraction will induce the precipitation of c-phycocyanin for all crude extracts.

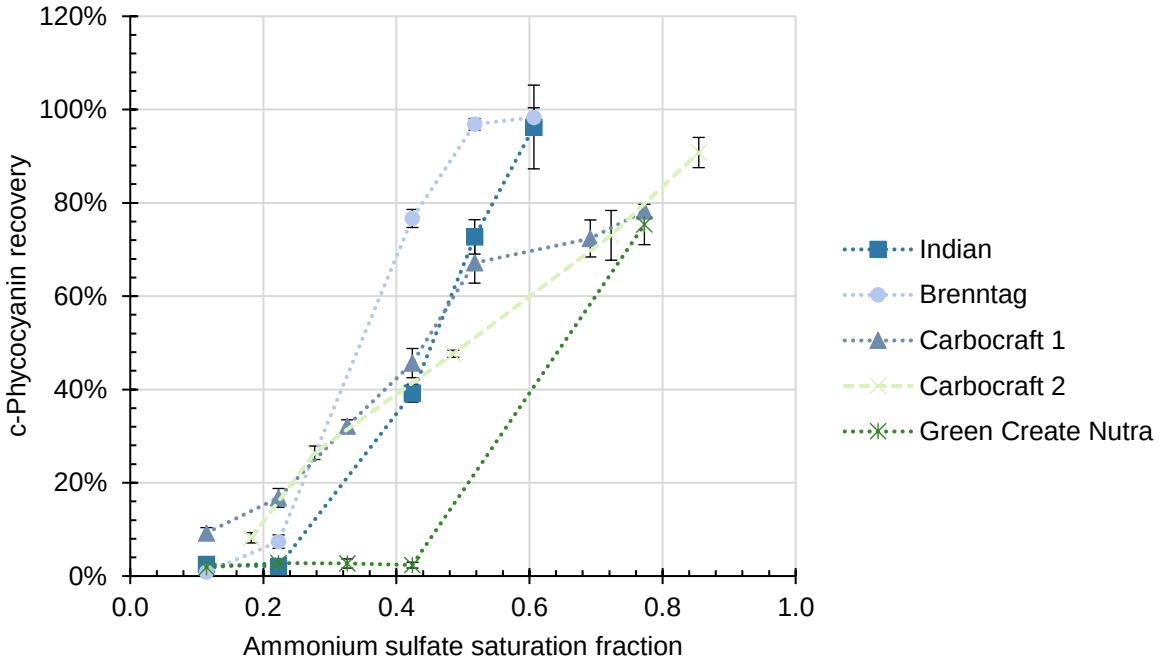

Figure 46. Effect of ammonium sulfate saturation fraction on the recovery of c-phycocyanin in the precipitate pellet for Brenntag, Carbocraft (two leachates tested), Indian and Green Create Nutra *Spirulina* powder crude extracts. Error bars in this figure indicate the variance for triplicate runs of the experiment.

Figure 47 shows how the mass of the precipitate increases with an increase in ammonium sulfate. From Figure 47 we can see that the Carbocraft 1 crude extract's precipitate pellet has a greater mass than that of the Indian crude extract at all ammonium sulfate fractions tested.

The mass of the Indian precipitate remained the same for the first two ammonium sulfate saturation fractions tested before increasing with increasing ammonium sulfate saturation. This trend is the same as the recovery of c-phycocyanin for the Indian sample as seen in Figure 46. Similarly, the recovery of the c-phycocyanin for Carbocraft 1 in Figure 46 increased with increasing ammonium sulfate saturation fraction and the mass of precipitate for Carbocraft 1 follows the same trend as in Figure 47. The increase in the precipitate pellet mass with increasing ammonium sulfate saturation was expected as it is aligned with the theory of fractional precipitation. Fractional addition of ammonium sulfate to a protein containing solution will see more protein being precipitated out as the increase in salt ions present reduce the solubility of the proteins in solution (Green & Hughes, 1955).

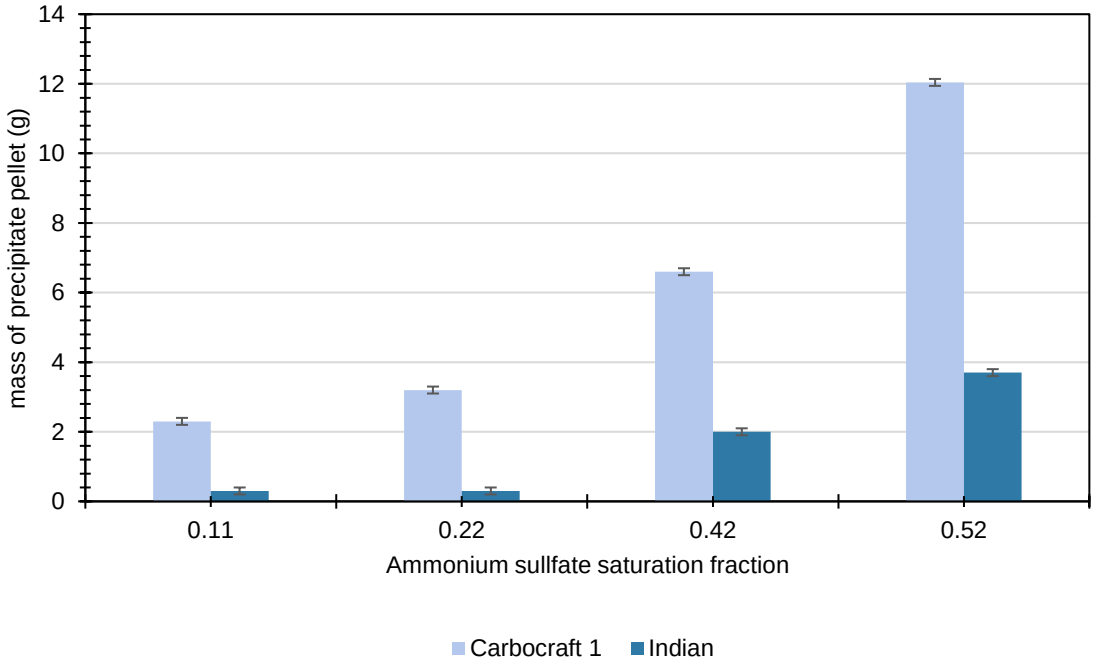

Figure 47. Mass of precipitates at lower ammonium sulfate saturations for Carbocraft 1 and Indian samples. Error bars in the figure indicate the variance generated from triplicate runs.

c-Phycocyanin purity in the precipitate pellet

Based on literature, it was expected that the fractional addition of ammonium sulfate to a starting solution of *Spirulina* crude extract will yield a decrease in the purity ratio of the pellet before a steady increase in the purity ratio to a maximum, and then a decrease back to the starting purity (Green & Hughes, 1955; Song, et al., 2013). This suggests that there is an optimal ammonium sulfate saturation fraction that yields a maximum purity ratio in the pellet. This value would be the desirable operating condition for the second precipitation stage.

Figure 48 shows the purity ratios from which the purification factors in Figure 49 are calculated. Figure 49 shows the precipitation pellet purification factor as a function of the ammonium sulfate saturation fraction. With reference to Figure 49, the precipitation pellet purification factor for all samples did not reach much above 1.5 with a confidence interval of less than 15 % for any of the ammonium sulfate saturation percentages tested. The best performing system in terms of purification factor was the precipitate pellet of the Indian *Spirulina* sample which reached a purification factor of 2.6 ± 0.3 at an

ammonium sulfate saturation fraction of 0.4 – indicating a 160 % increase in the purity number when compared to the crude extract used for these precipitation experiments. The worst performing system was Carbocraft 2 which reached its highest purification factor of 1.3 ± 0.1 at a 0.49 ammonium sulfate saturation fraction.

From Figure 48, it can be seen that although the Indian *Spirulina* sample crude extract performed the best in terms of purification factors, the sample only reached its highest purity ratio of 0.32 ± 0.05 in the pellet at a 0.4 ammonium sulfate saturation fraction – the lowest maximum purity ratio in the pellet of all the crude extract samples tested. The highest purity ratio (0.52 ± 0.02) reached from all samples tested was yielded by the Brenntag *Spirulina* crude extract precipitated at 0.61 ammonium sulfate saturation. For Carbocraft 1, Carbocraft 2 and Indian *Spirulina* crude extracts, the purity in the pellet as well as the purification number increased with ammonium sulfate saturation and reached a maximum at around 0.4 – 0.5 ammonium sulfate saturation and then began to decrease with an increase in ammonium sulfate saturation percentage. Up to a saturation fraction of 0.6, the purity of the pellet for the Brenntag *Spirulina* crude extract sample continued to increase with ammonium sulfate saturation. It seems that for a further increase in the saturation, the Brenntag *Spirulina* crude extract sample would follow the same trend as the other samples. The GCN *Spirulina* crude extract sample reached a purity ratio local maximum at 0.22 saturation before decreasing with an increase in ammonium sulfate saturation to a local minimum at 0.42 and then increased linearly with saturation. Carbocraft 1 and 2 *Spirulina* crude extract samples achieved their purity ratio maximums of 0.46 ± 0.07 and 0.40 ± 0.01 at 0.42 and 0.49 ammonium sulfate saturation fractions, respectively.

Therefore, the highest purity number was achieved for the different samples in the range of 0.4 – 0.6 ammonium sulfate saturation fraction, with the exception of the GCN sample. An ammonium sulfate saturation within this range can be considered an optimal saturation fraction for the purification and recovery of c-phycocyanin in the precipitation process.

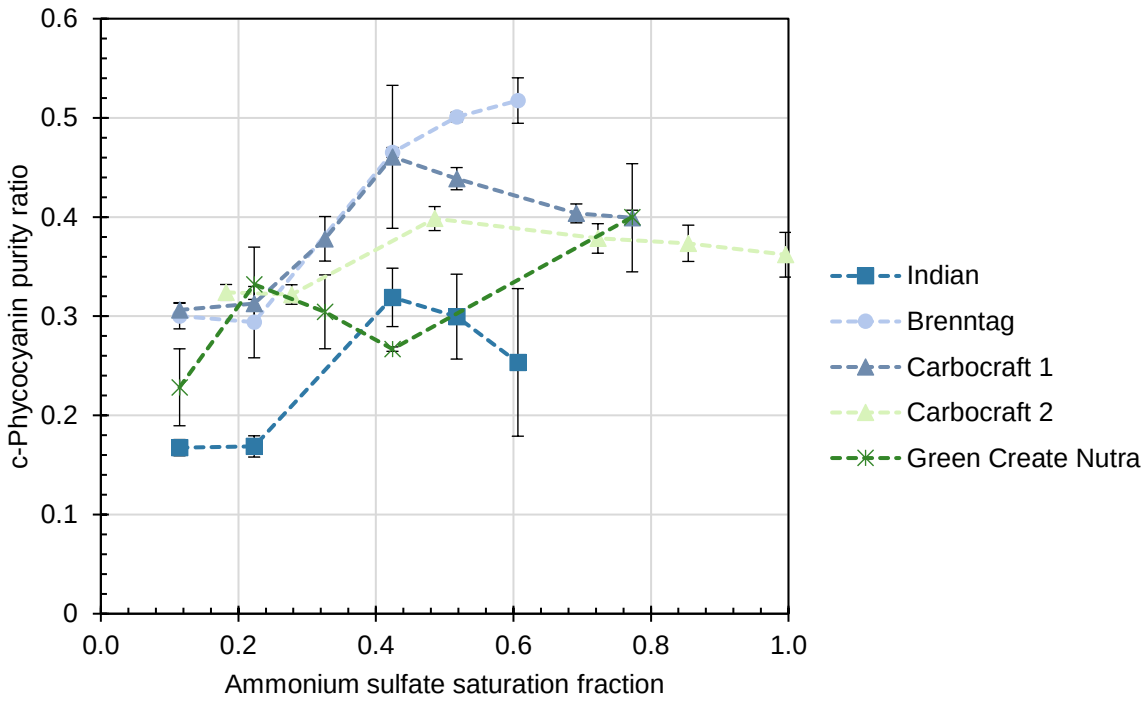

Figure 48. Effect of ammonium sulfate saturation fraction on the c-phycocyanin purity ratio of the precipitate pellet of Brenntag, Carbocraft (two leachates tested), Indian and Green Create Nutra *Spirulina* crude extracts. Error bars in the graph indicate the variance for triplicate runs of the experiment.

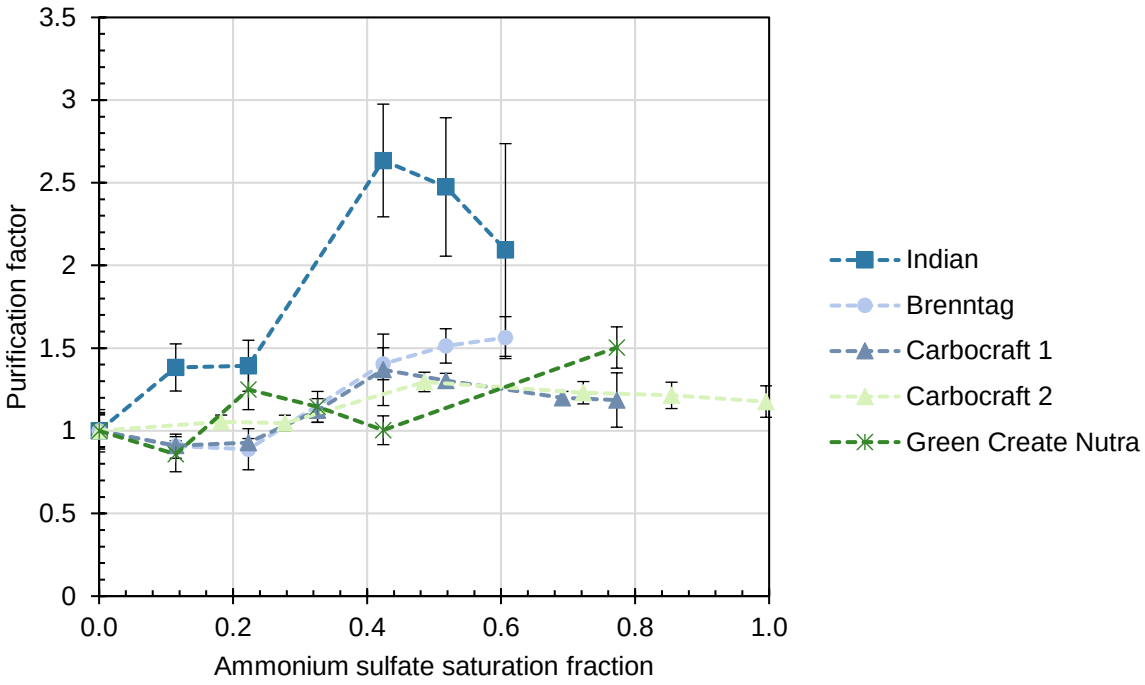

Figure 49. Effect of ammonium sulfate saturation fraction on the c-phycocyanin purity ratio of the precipitate pellet of Brenntag, Carbocraft (two leachates tested), Indian and Green Create Nutra *Spirulina* crude extracts. Error bars in the figure indicate variance for triplicate runs of the experiment.

4.5.2 c-Phycocyanin purity in supernatant

Based on literature (Song, et al., 2013; Chang, 2007; Green & Hughes, 1955), it was anticipated that the fractional addition of ammonium sulfate would allow for some protein and contaminants to be removed from the solution in the precipitate, increasing the c-phycocyanin purity of the supernatant and with further fractional addition, decrease the purity of the supernatant to below that of the starting solution when c-phycocyanin starts to precipitate out of solution (Song, et al., 2013). This would allow for the establishment of an optimal ammonium sulfate saturation at which the supernatant would be at its highest c-phycocyanin purity, enabling this to be set as an operating condition for the first stage of precipitation to remove contaminants and some undesired protein from the system.

Figure 51 shows the purification factor in the precipitate pellet as a function of the ammonium sulfate fraction for the different *Spirulina* sample crude extracts. The purification factor is the ratio of the purity of the precipitate to the purity of the crude extract. With reference to Figure 51, the supernatant purification factor for all samples did not go above 1.14 for any of the ammonium sulfate saturation percentages tested. The best performing system in terms of purification factor achieved in the supernatant was the Carbocraft 2 run, in which a purification factor of 1.13 ± 0.03 was achieved at 0.28 ammonium sulfate saturation fraction – indicating a 13 % increase in the purity number when compared to the crude extract used for the precipitation experiments. All samples, apart from the GCN, seemed to follow the same trend with a seemingly unchanging purification factor between 0 and 0.28 saturation fraction. The purification factor thereafter dropped off steadily, almost linearly, approaching 0. This drop off corresponded with when c-phycocyanin itself started to precipitate.

Figure 50 contains the same results as Figure 51 however it shows the actual purity ratios achieved in the supernatant for each of the samples. We can see that the Carbocraft 1 system reached its maximum supernatant purity of 0.36 ± 0.01 at 0.22 saturation fraction. The Carbocraft 2 system reached a purity of 0.35 ± 0.01 at 0.28 saturation fraction. The Indian *Spirulina* supernatant reached its maximum purity ratio of 0.13 ± 0.01 at 0.17 saturation. The Brenntag supernatant reached its maximum purity ratio of

0.33 ± 0.02 at 0.17 saturation. Finally, the GCN reached its maximum purity ratio of 0.28 ± 0.02 at 0.11 saturation fraction.

Therefore, there was no significant increase in the purity of the supernatant observed compared to the starting solution, with Carbocraft 2 being the exception. This indicates that c-phycocyanin is one of the first proteins to be precipitated out of solution. As a result, there isn't an ammonium sulfate saturation fraction that can be used to obtain a significantly higher purity of c-phycocyanin in the supernatant. There was however cell debris and other contaminants removed from the systems, observed as a physical sludge precipitate, the mass of which increased with ammonium sulfate saturation fraction as shown in Figure 45. This implies that there could still be a benefit to an initial low saturation precipitation step.

To note, purity ratios and purification factors cannot be compared to literature since no results of a similar study were found. However, Song et al. (2013) describe a system using a two-stage precipitation in which the first stage will alter the overall result of purity and purification factor and as such cannot be compared to the single stage fractional precipitation carried out in this experiment.

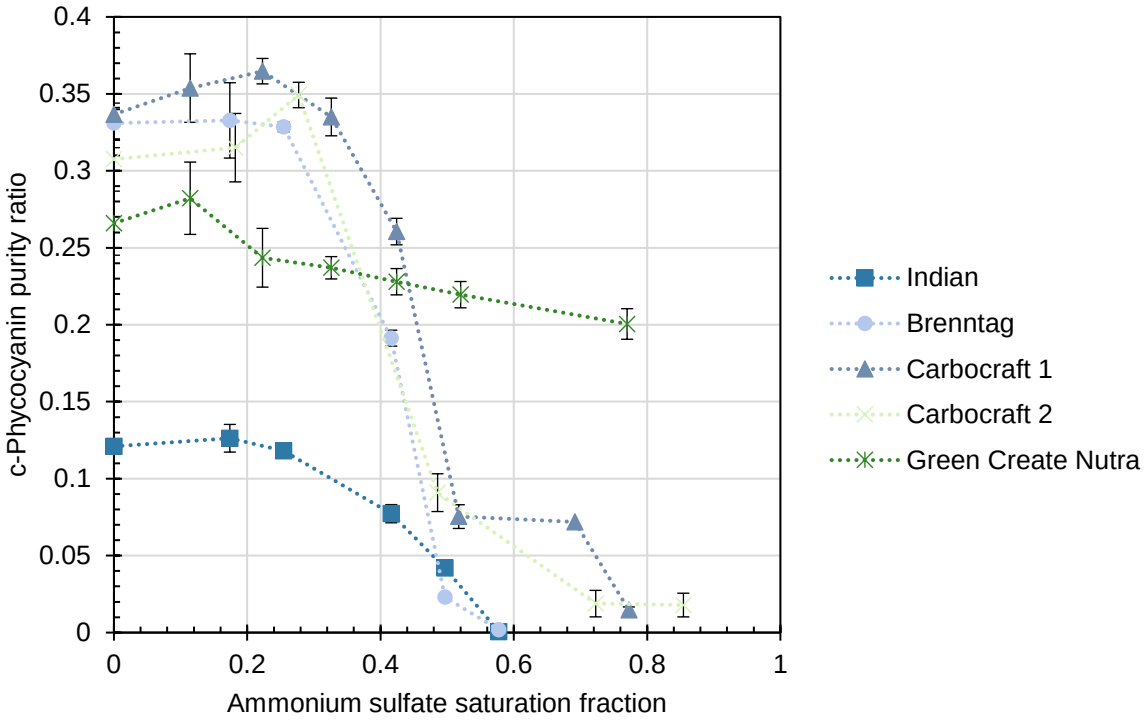

Figure 50. Effect of ammonium sulfate saturation fraction on the c-phycocyanin purity ratio of the precipitation supernatant of Brenntag, Carbocraft (two crude extracts tested), Indian and Green Create Nutra *Spirulina* crude extracts. Error bars in the figure indicate variance for triplicate runs of the experiment.

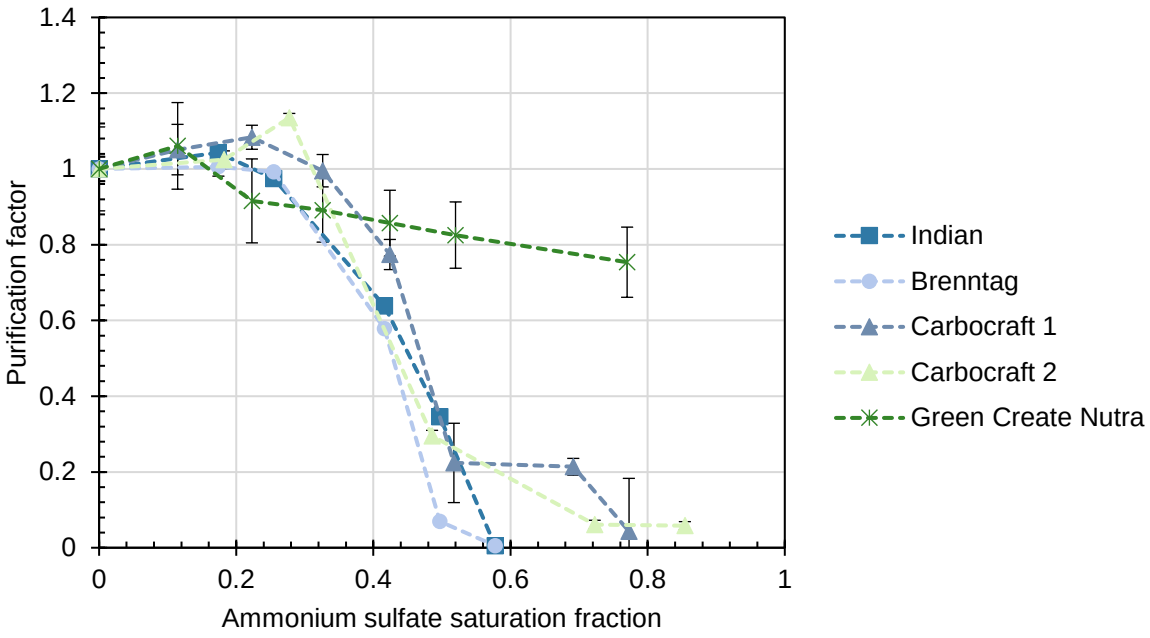

Figure 51. Effect of ammonium sulfate saturation fraction on the c-phycocyanin purification factor of the precipitation supernatant of Brenntag, Carbocraft (two crude extracts tested), Indian and Green Create Nutra Spirulina crude extracts. Error bars in the figure indicate variance for triplicate runs for the experiment.

4.5.3 Discussion on ammonium sulfate precipitation

The purpose of the precipitation experiments was to establish operating conditions for a precipitation train of two stages of ammonium sulfate precipitation in the form of ammonium sulfate saturation fractions for each stage. A point of note is that, from Figure 46, the data suggests that full recovery of c-phycocyanin is possible. The data suggests that 100 % recovery of c-phycocyanin to the precipitate should happen before complete ammonium sulfate saturation is reached. The saturation fraction at which this 100 % recovery will be observed cannot conclusively be stated, however, with variations observed with the different crude extracts. For a two-stage system, with some undesired protein being removed by the first stage of precipitation, and the second stage being operated at complete saturation we can still recover approximately 100 % of the c-phycocyanin at a higher purity than the starting solution if 100 % recovery is desired.

If the techno-economics of the process does allow for less than 100 % recovery of c-phycocyanin across the precipitation train, however, it can be confidently said that we can achieve purification factor of at least 1.3 ± 0.32. This is only beneficial, however, if the 1.3 ± 0.32 purification factor does span a purity ratio of above 1.5 – since the overarching aim of this extraction and purification process is to achieve cosmetic grade c-phycocyanin.

With reference to Figure 50 and Figure 51, the hypothesized increase in the supernatant purity at lower saturations before decreasing, cannot be confirmed by the data for all samples. This suggests that a two-stage precipitation may not be the best approach if the aim is to increase the purity ratio, because a purer supernatant to be used as the starting solution for the second precipitation stage will not be achieved. However, even though no increase in purity was observed at saturations lower than that needed for c-phycocyanin precipitation, pellets of a significant mass formed, as shown in Figure 47.This suggests that the first precipitation step is still removing contaminants of some sort, e.g. persisting cell debris, proteins not picked up by the spectroscopic assays, etc. This evidence suggests that the two-stage precipitation will be better than the single-stage since if this significant mass of contaminants is not removed it will persist downstream. Below the c-phycocyanin precipitation threshold of ammonium sulfate saturation for an increase in saturation an increased pellet mass is observed suggesting that a

saturation of just below the threshold of c-phycocyanin precipitation would be best for removal of contaminants, including microbial. Microbial plating could be performed to further corroborate this necessity of a first step, since ammonium sulfate precipitation has been shown to remove bacterial loading (Fagan-Endres, et al., 2019). A key motivation for the inclusion of a multi-stage ammonium sulfate precipitation train in the patent for this process was its ability to remove microbial contaminants from the desired c-phycocyanin product (Fagan-Endres, et al., 2019). Fagan-Endres et al. (2019) reported a bacterial loading reduction from 750 000 CFU/g after a single-stage ammonium sulfate precipitation to 15 000 CFU/g after a two-stage ammonium sulfate precipitation. This further supports the inclusion of a two-stage ammonium sulfate precipitation system for this process.

A saturation fraction of 0.22 is therefore recommended for the first precipitation stage, as it is safely beneath the threshold value of c-phycocyanin precipitation for all samples and it allows for an increase in purity in the supernatant or the same purity ratio as the initial crude with a noticeable precipitate of contaminants like cell debris.

With reference to Figure 48 and Figure 49, it can be observed that the greatest c-phycocyanin purity in the pellet will be achieved when precipitating in the range of 0.4 to 0.6 ammonium sulfate saturation. The optimal saturation fraction is relative to the sample of *Spirulina* used and therefore the weighted mean of the range is recommended to be used. This is approximately 0.45.

These operating conditions can be altered to increase purity or recovery depending on what is needed by the purification process at a given time.

4.6 Conclusions on individual unit operation testing

Based on the testing of the individual unit operations, the following is a summary of the key take-aways that should be used to inform the process going forward and inform the full runs of the process for the robustness testing.

- The leaching data suggests that bead-milling is not always necessary to shorten the time taken to extract all the c-phycocyanin in dried *Spirulina* powder. The minimum time needed to leach all *Spirulina* samples tested to achieve an equilibrium concentration in the leachate is 19 h.
- For separation of the cell debris from the c-phycocyanin containing supernatant using centrifugation, the higher the g force, the higher the recovery of the supernatant across the cell debris removal area. This would suggest operating at a minimum of 10 000 g, the highest g force tested at the laboratory scale. A second centrifugation step combined with rinsing of the cell debris pellet in between spins is a good strategy to increase the overall c-phycocyanin recovery. The best performing sample in terms of crude liquid recovery was the Carbocraft *Spirulina* sample which reached 77%. The Brenntag and Indian *Spirulina* samples reached 62 % and 72 % recovery, respectively.
- The ATPS system, especially the citrate-PEG ATPS is not robust and as such it is recommended that the ATPS step be excluded from the pilot process.
- A two-stage ammonium sulfate precipitation will yield a purer c-phycocyanin product compared to a single stage, if not in terms of purity ratio, then in terms of cell debris content or both. The saturation fraction recommended to be used for the first stage (in which c-phycocyanin is retained in the supernatant) is 0.22. At higher saturations, c-phycocyanin starts precipitating. The Indian, Carbocraft and Brenntag *Spirulina* samples achieved the highest purity ratios in the pellet at 40 %, 42 % and 60 % ammonium sulfate saturation, respectively. Therefore, 45 % ammonium sulfate saturation is recommended, as a starting point for further optimization at a higher scale, for the second precipitation to purify and recover c-phycocyanin in the pellet.
- Considering the removal of the ATPS system from the process, it is recommended that micro- and/or ultrafiltration be added as an additional purification step after the precipitation (recommended internally from process route owner and from Hockey (2020), Sørensen et al (2013) and Rito-Palomares et al. (2001). The inclusion of filtration aims to purify the product stream, using size exclusion, based on the removal of cell debris, larger proteins and microorganisms.

4.7 Full runs of the process

4.7.1 Full run configuration

Following on from the optimization work performed on the leaching, cell debris removal and precipitation procedures, full runs of the extraction process using the identified “best” operating conditions were performed. The purpose of the full runs was to see the compounded effect of the chosen operating conditions on the recovery and purity ratio of the c-phycocyanin containing phases throughout the steps of the process. Another purpose was to assess the robustness of the entire process at the recommended operating conditions. The robustness testing also informs which of the *Spirulina* powder samples should be recommended as the most suited for use in a pilot scale operation using this process.

Due to the ATPS purification steps having been excluded, the full runs included two microfiltration steps after the precipitation procedures, in the form of a 0.45 μm aperture filter followed by a 0.22 μm aperture filter. The alterations to the configuration of the process can be seen in Figure 52. Operating conditions of the key unit procedures in the new configuration are summarized in Table 25. The operating conditions in Table 25 are the alterations of operating conditions, other key operating conditions are omitted from the table as they remain the same from the initial methodology descriptions for the individual unit procedures. The key reason for the inclusion of the microfiltration was to reduce microbial contamination in the final c-phycocyanin stream, as this is a critical concern for food and cosmetic grade product. Both 0.45 μm and 0.22 μm sizes are chosen since these are the smallest sizes for microfiltration that will size exclude bacteria and other cell fragments and components that could contaminate the c-phycocyanin product. *Spirulina* is known to be contaminated since it is grown in open ponds (Molina, et al., 2019). Anti-biotics can also not be used since *Spirulina* is a cyanobacteria However, it should be noted that microbial plating was not performed to confirm the degree of contamination (probability increased owing to a non-sterile process route), as this was seen as outside the scope of this thesis.

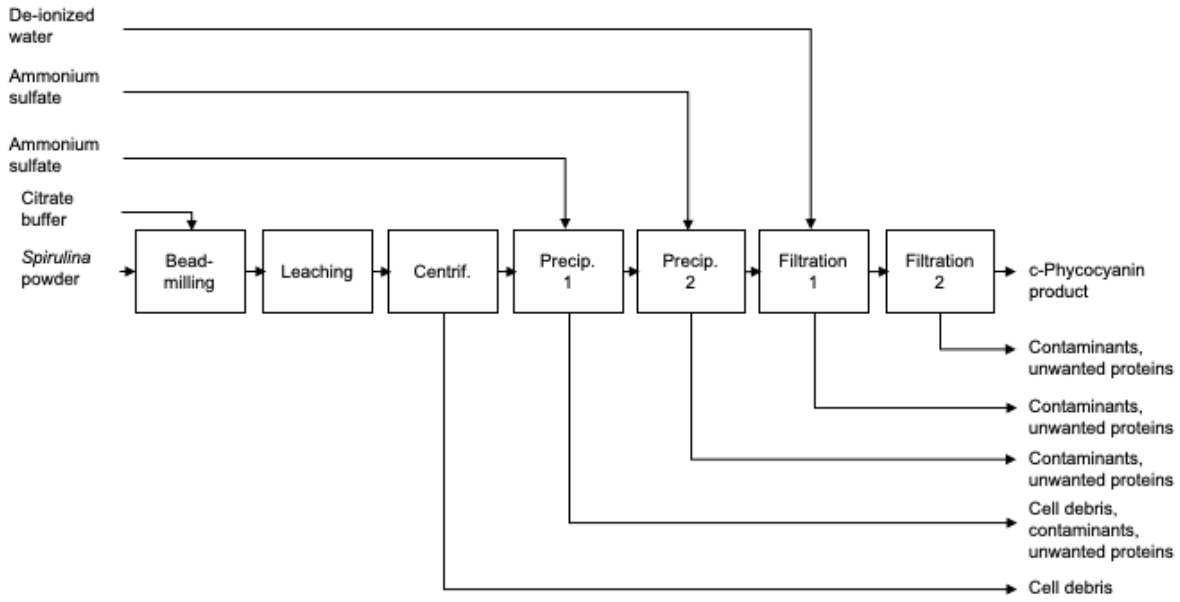

Figure 52. Block flow diagram of the new configuration for the CeBER process for extraction and purification of c-phycocyanin from *Spirulina*

Table 25. Table summarizing key operating conditions for the unit procedures of the newly configured CeBER process

Key unit procedure	"Best" operating conditions	Unit
Bead-milling	15	min
Leaching	19	h
Cell debris removal via centrifugation	20, 10 000	min, g
Precipitation 1	0.2	Ammonium sulfate saturation fraction
Precipitation 2	0.45	Ammonium sulfate saturation fraction
Filtration 1	0.45	μm aperture size
Filtration 2	0.22	μm aperture size

4.7.2 c-Phycocyanin purity and recovery for full runs

Figure 53 presents the purity ratio of the c-phycocyanin containing phases following each step in the downstream process. The data shows that after the bead-milling and leaching, the purity ratio in the crude extract for the Indian *Spirulina* powder was 0.10 ± 0.01, it was 0.35 ± 0.01 for the Brenntag *Spirulina* powder and it was 0.35 ± 0.01 for the Carbocraft *Spirulina* powder. The purities achieved here were not expected. From the Leaching results (Section 4.2 c-Phycocyanin leaching from Spirulina), it was expected that the purity ratios for Carbocraft and Brenntag after 19 h of leaching would be close closer to 0.40 and 0.45 respectively. However, it was shown that there were no real predictive trends with purity ratio and time of leaching. This could also be a result of different bags of Brenntag and Carbocraft powders used for the full runs compared to the leaching (the composition may not have been the same).

In the case of the Indian crude extract, the first precipitation at an ammonium sulfate saturation of 0.22 showed minimal influence on the purity ratio. Therefore, no other proteins were precipitated out or the proteins precipitated out included c-phycocyanin in the same ratio as in the crude extract. The second precipitation at an ammonium sulfate saturation of 0.45 almost tripled the purity to 0.34 ± 0.01.

The Carbocraft *Spirulina* powder crude extract was similarly affected by the first precipitation step with no significant change in the purity ratio, followed by an increase to a purity of 0.43 ± 0.02 after the second precipitation step. This is in line with what was found in the original precipitation experiments where, for a similar crude extract purity ratio at 0.42 saturation, a 0.46 purity ratio was achieved and at 0.5 saturation a 0.43 purity ratio was achieved (see Section 4.5).

The Brenntag *Spirulina* crude extract performed the best in the first and second precipitation with an almost doubling in purity to 0.64 ± 0.03 after the second precipitation. Accounting for experimental error, it cannot for sure be said that the Brenntag *Spirulina* powder crude extract showed a significant increase in purity across the first precipitation stage.

For both the Indian and Carbocraft *Spirulina* powder crude extracts it appears as though the first precipitation did not contribute towards the final purity after precipitation, however when we consider the Brenntag *Spirulina* powder sample, the first precipitation increased the purity ratio by a small amount, but this allowed the second precipitation to outperform the best performing single stage precipitation for Brenntag *Spirulina* powder, as was presented previously in Figure 50. The value of the first precipitation can also be qualitatively observed in the lingering cell debris removal forming a pellet.

This 2-stage precipitation train therefore yielded a purification factor of 1.86, 1.23 and 3.4 for the Brenntag, Carbocraft and Indian *Spirulina* powder samples, respectively. From the literature reviewed and presented in Table 8, these purification factors are within the expected range for a 2-stage precipitation. Bhaskar et al. (2005), Zhang & Chen (1999) and Muthulakshmi et al. (2012) quoted 1.47, 2.71 and 1.96 purification factors for 2-stage ammonium sulfate precipitation for c-phycocyanin purification, respectively.

Subsequent microfiltration at 0.45 μm aperture size (Filtration 1) of all three *Spirulina* samples' resuspended precipitate increased the product purity. The purity for the samples' precipitate increased by approximately 0.2 for the Brenntag *Spirulina*, by approximately 0.28 for the Carbocraft *Spirulina* and by 0.12 for the Indian *Spirulina* to 0.85 ± 0.01, 0.71 ± 0.01 and 0.45 ± 0.03, respectively. This suggests that the Carbocraft *Spirulina* crude extract had more larger proteins that could be removed by the 0.45 μm aperture microfiltration step, whereas the Indian *Spirulina* powder had the least amount.

The second microfiltration step (Filtration 2) used a 0.22 μm aperture filter. The missing data for the Indian *Spirulina* for Filtration 2 was because its resuspended precipitate was found to not pass through the filter. Thus, the c-phycocyanin extraction process ended at Filtration 1 for the Indian *Spirulina*. The purity ratio of the Carbocraft *Spirulina* filtrate from Filtration 1 increased by 0.08, and the Brenntag *Spirulina* filtrate from Filtration 1 increased by 0.05. This further supports that the Carbocraft *Spirulina* powder contained more proteins that are smaller than c-phycocyanin when compared to the Brenntag *Spirulina* powder. The ratio of c-phycocyanin to other proteins increased more for Carbocraft than for Brenntag. It is difficult to compare the microfiltration results to those of literature since literature mostly contained results of processes that used ultrafiltration to purify c-phycocyanin.

The final purity ratios achieved using the three different feed samples were 0.90 ± 0.02, 0.79 ± 0.03 and 0.46 ± 0.03 for Carbocraft, Brenntag and Indian powders, respectively. With food grade c-phycocyanin requiring a purity ratio of above 0.7, the c-phycocyanin purified from the Brenntag and Carbocraft *Spirulina* powders meet the threshold to be considered food grade. The purification process using Indian *Spirulina* powder as the feed did not yield c-phycocyanin of food grade. The aim of the initial patent and subsequent development of the process by CeBER was to produce cosmetic grade c-phycocyanin. Cosmetic grade c-phycocyanin has a purity ratio of > 1.5, which at this point is still not met.

It was thought that the higher the purity ratio in the crude extract, the higher the final purity ratio after filtration. It was also thought that the Brenntag and Carbocraft *Spirulina* powder samples would perform the same since the crude extracts for these two samples were similar in purity ratio at 0.35 ± 0.01. It was expected that the Indian *Spirulina* powder would perform best in precipitation in terms of overall purification factor – as supported by the precipitation experiments. The data does not fully support the hypothesis posed as the Brenntag *Spirulina* powder sample outperformed the Carbocraft *Spirulina* powder by over 10 % in the final purity. Therefore, we cannot conclude that the purity ratio in the crude is the only thing that affects the purity ratio of the final product for the c-phycocyanin extraction and purification process. The Indian sample did have the greatest overall purification factor of 4.4, meaning it was purified the most compared to its starting purity in the crude extract, however this purification was still not enough to meet food grade c-phycocyanin criteria. The Brenntag *Spirulina* powder performed second best in terms of purification factor at 2.6 and Carbocraft at 2.2.

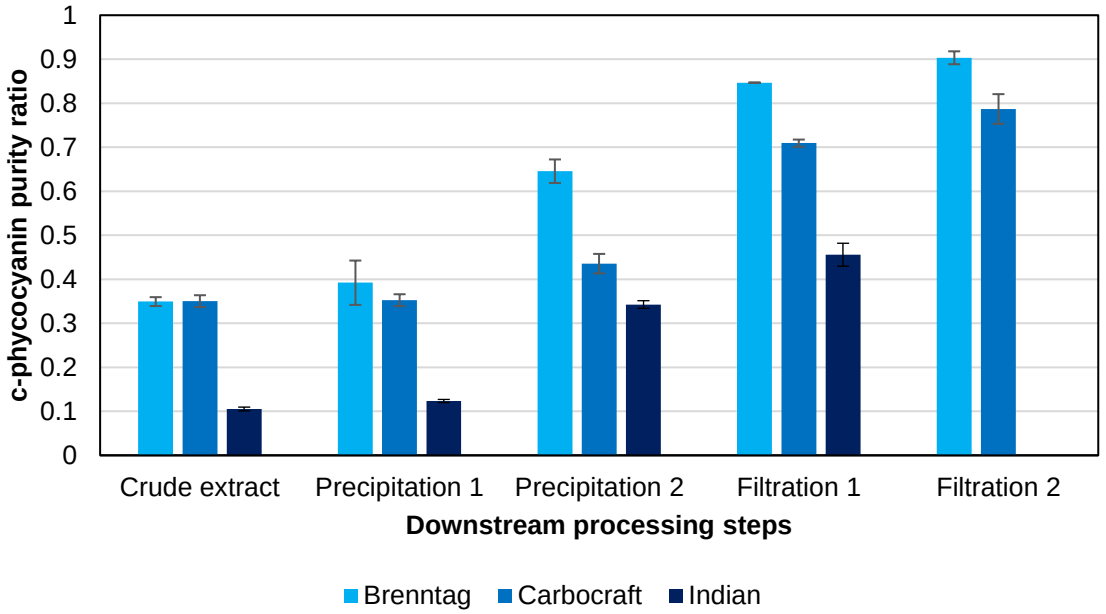

Figure 53. c-Phycocyanin purity ratio after each downstream processing step for Brenntag, Carbocraft and Indian *Spirulina* sample feeds. Error bars in the figure indicate variance for triplicate runs of the experiment.

With reference to the methodology (Section 3.3.9), the purpose of increasing the centrifugation time from 10 min to 20 min for the full runs was to allow for easier separation of the cell debris and supernatant. Figure 54 presents the c-phycocyanin recovery over each downstream processing step in this extraction and purification process. It shows how the increase in centrifugation holding time from 10 min to 20 min increased the recovery for across all *Spirulina* powder samples to above 90 % in the crude. The Indian *Spirulina* powder yielded the highest c-phycocyanin recovery over the centrifugation step into the crude extract. In the cell debris removal results section (Section 4.3), it is seen that Carbocraft showed its best performance in terms of recovery at 77 % at the same g force (10 000 g). This shows that the increase in centrifugation time allowed for the Indian sample to outperform the Carbocraft in terms of c-phycocyanin recovery. This indicates that an investigation into varying the centrifugation time will provide worthwhile insight into cell debris removal performance.

From the precipitation experiments, the recoveries across all samples were within the range of expectance with the Indian *Spirulina* powder sample showing the highest recovery of c-phycocyanin in the supernatant after Precipitation 1 at 0.22 ammonium sulfate saturation. Figure 54 shows that the recovery for the first stage of precipitation was 99 ± 5 %, 93 ± 11 % and 83 ± 5 % for the Indian, Carbocraft and Brenntag *Spirulina* samples, respectively. This is within the expected range of recovery for a single stage precipitation, with Kumar et al (2014), Silva et al (2009) and Song et al (2013) having quoted 80 %, 91 % and 85 % recoveries of c-phycocyanin over a single stage ammonium sulfate precipitation at 0.65, 0.5 and 0.5 ammonium sulfate saturation fractions, respectively.

The recoveries across Precipitation 2 were lower on average than that of Precipitation 1. The Carbocraft sample performed the best with 79 ± 7 % recovery achieved. The Indian *Spirulina* samples' supernatant from Precipitation 1 achieved 67 ± 5 % recovery of c-phycocyanin across Precipitation 2. Across Precipitation 2, the Brenntag *Spirulina* powder sample recovery dropped off substantially more than expected for the precipitation stage, down to 32 ± 5 %. It is unclear as to what caused this, as this low recovery was observed across triplicate runs. It is difficult to compare results over a two-stage ammonium sulfate precipitation of c-phycocyanin with literature results since literature sources like Bhaskar et al. (2005) and Zhang & Chen (1999) that do describe a two-stage precipitation do not quote their overall recovery over the two-stage process.

The recoveries across the filtration steps for all the *Spirulina* samples were close to 100 %, as expected given the nature of the separation method. As previously mentioned, since this system used

microfiltration, comparison to literature sources was not possible, since those literature sources that do describe using filtration (such as Rito-Palomares et al (2001) and Sørensen et al (2013)) used ultrafiltration. These sources quote 70.5 % and 79 % recovery of c-phycocyanin over their ultrafiltration systems.

The overall recoveries of the Carbocraft and Indian *Spirulina* powder samples were comparable at 65 ± 14 % and 66 ± 8 %, respectively. The overall recovery of the Brenntag *Spirulina* powder was 24 ± 8 %. This low recovery observed for the Brenntag *Spirulina* powder was owing to the extremely low recovery over the Precipitation 2 stage. These recoveries are well within range for c-phycocyanin extraction and purification processes reported in literature. Minkova et al. (2003) report an overall recovery 46 % for a four stage process albeit for a final c-phycocyanin purity ratio of 4.3. Ramos et al. (2010) report a 62 % recovery for a two stage system yielding a final c-phycocyanin purity ratio of > 4. Chaiklahan et al. (2011) report a 82 % recovery over a single stage process for a final c-phycocyanin purity ratio of 1.07. Niu et al. (2007) report a 5 % recovery for a two stage process yielding a final c-phycocyanin puriy ratio of > 3.2. The literature mostly reported final c-phycocyanin purity ratios that are higher than that achieved by any of the *Spirulina* powders in this process, with many of them having better recovery too.

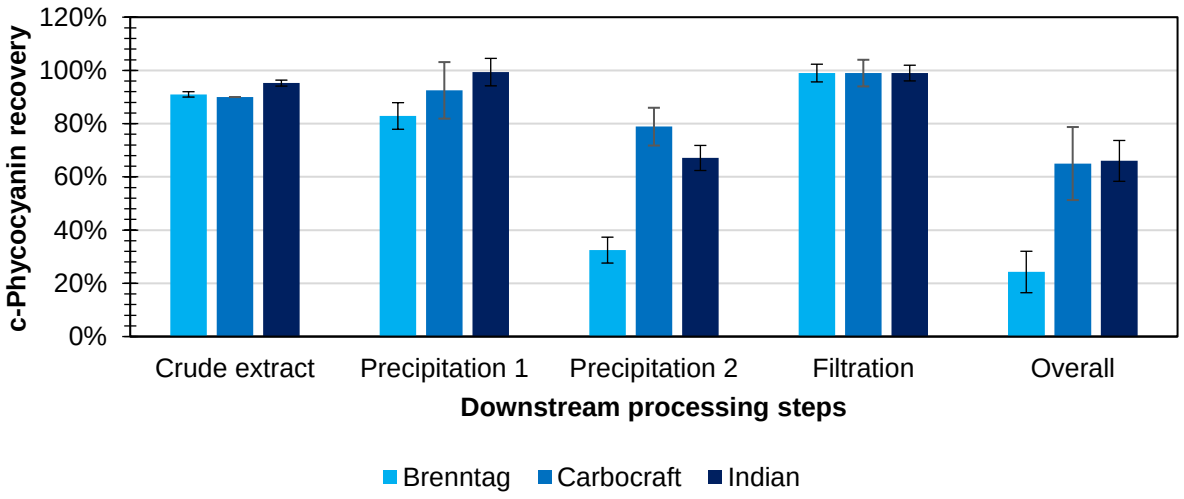

Figure 54. c-Phycocyanin recovery across each of the downstream processing steps, as well as the overall process recoveries for Carbocraft, Brenntag and Indian *Spirulina* sample feedstocks. Error bars in the figure indicate variance for triplicate runs of the experiment

4.7.3 Key performance indicators of full runs

Table 26 summarizes the key outputs of the c-phycocyanin extraction and purification process for all three feed samples tested. The Brenntag *Spirulina* powder reached a final purity ratio of 0.90 ± 0.02, which was the highest purity achieved by any of the *Spirulina* powders used. Both the Brenntag and Carbocraft *Spirulina* powders managed to meet the requirement for food grade c-phycocyanin in this extraction and purification process.

The best overall recovery was found with the Carbocraft *Spirulina* powder sample. The Carbocraft *Spirulina* powder sample achieved over quadruple the yield of c-phycocyanin compared to the Brenntag *Spirulina* powder per mass raw materials used. Considering the original feed material, the Carbocraft *Spirulina* powder had the highest c-phycocyanin content at 7 wt% of total weight, while the Indian powder had the lowest at 1 wt% and the Brenntag powder had 5 wt %.

Table 26. Key performance indicators for Brenntag, Carbocraft and Indian *Spirulina* feedstocks across the extraction and purification process

	Brenntag	**Carbocraft**	**Indian**
c-PC content of powder (wt %)	5	7	1
Purity of crude extract	0.35 ± 0.01	0.35 ± 0.01	0.11 ± 0.00
Purity of the final product	0.90 ± 0.02	0.79 ± 0.03	0.46 ± 0.03
Overall yield (g/kg *Spirulina*)	11.29 ± 1.14	46.9 ± 4.84	3.70 ± 0.31
Overall recovery (%)	24 ± 7.8	66 ± 7.7	65 ± 13.7
Overall purification factor	2.6	2.2	4.4

The overarching aim of the c-phycocyanin extraction and purification process is to produce cosmetic grade c-phycocyanin (purity ratio of > 1.5) – this is not achieved in this study performed. However, the study does demonstrate a robust process to handle feed with a variance in size and c-phycocyanin content and most probably drying methods used to prepare the *Spirulina* powder, whilst improving the purity of the crude extract with each step to between 0.46 and 0.90, thus achieving food grade for some samples tested. This study has shown that a stepwise increase of the purity ratio is possible. Therefore, a feed that has a higher c-phycocyanin content than those used in this study would yield a greater crude extract purity than those achieved in this study, by nature of its higher c-phycocyanin content. Furthermore, by optimization of the leaching step with respects to c-phycocyanin purity in tandem with c-phycocyanin recovery, would yield a higher crude extract purity for the samples used in this study. As such, for a higher crude extract purity with similar purity upgrades throughout the individual unit procedures, a higher purity ratio in the final product can be expected.

One key takeaway is that the purity ratio in the crude extract was seemingly low compared to literature values. Niu et al. (2007) reports using dried powdered *Spirulina* and used various methods of extraction obtaining purity ratio between 0.59 to 0.72 in the crude extract. Other literature sources reported crude extracts from dried powder and fresh biomass boasting c-phycocyanin purity ratios of above 0.89 (Song, et al., 2013; Bhaskar, et al., 2005). This indicates that the *Spirulina* used in the experiments for this dissertation had low c-phycocyanin content or that the leaching methodology did not prioritize c-phycocyanin extraction. The latter is unlikely, given that the leaching methodology is a standard practice reported on in literature.

Work is currently being performed by CeBER on using adsorption via activated charcoal and/or chitosan to improve the purity ratio of the crude extract. If similar purification factors as reported in this dissertation can be obtained over the downstream processes, with a higher crude extract purity ratio, cosmetic grade c-phycocyanin should be achievable.

If we can consider the equilibrium concentrations of the leaching tests as the maximum amount of c-phycocyanin in the *Spirulina* powders tested, then the highest c-phycocyanin content of the powders by weight is 7 % in the Carbocraft sample. However, literature shows that for *Spirulina*, c-phycocyanin content can be up to approximately 12 % by weight (Boussiba & Richmond, 1979). *Spirulina* with a higher c-phycocyanin content would be preferred for this process as it should result in a higher purity ratio of the crude extract and a larger mass of c-phycocyanin product per run of the process for the same recoveries per downstream step.

Literature also shows that drying of *Spirulina* can cause a loss of up to 46 % of c-phycocyanin content depending on the method used (Guroy, et al., 2017). Previous reports have stated that the drying of fresh *Spirulina* can cause a loss of protein up to 20 % of total protein content (Desmorieux & Hernandez, 2004). This suggests that for the same *Spirulina*, the fresh material would have had a higher purity ratio in the crude extract when compared to that same *Spirulina* when dried. This is because c-phycocyanin is more prone to damage by drying than the total protein content in *Spirulina* (Chaiklahan, et al., 2011). Freeze-dried and sun-dried *Spirulina* reportedly keeps c-phycocyanin content the best out of the drying methods tested – this should therefore be a specification of the preferred feed to this process (Chaiklahan, et al., 2011). Drying can also affect the morphology of the cells and as such can change the way the c-phycocyanin leaches from the cell – choosing the correct method of drying to specify the

feed with may allow for a shorter leaching time to reach equilibrium concentration, thus improving the process by shortening the time on stream required to produce mass unit of c-phycocyanin.

5 Conclusions and Recommendations

The focus of this dissertation was to determine better operating conditions of unit procedures for the CeBER extraction and purification process developed to obtain cosmetic grade c-phycocyanin from *Spirulina.* This included both the process patented by CeBER and subsequent developments. An investigation was also performed into the robustness of the current process and potential alterations that can be made to the process in the case of weak robustness.

Prior to this dissertation, the CeBER process had not been not fully optimized nor was it previously assessed for robustness. Particularly: the c-phycocyanin leaching kinetics for *Spirulina* under the process conditions had not been investigated and, as such, c-phycocyanin concentrations for given leaching times could not be predicted. Unit procedures were not yet operating at optimized operating conditions, with the effect of changing the operating conditions of each operation unknown. Further, the ability of the process to handle variation in the feed material and composition was unknown. These aspects needed to be addressed to inform pilot plant design and upscale of the c-phycocyanin extraction and purification process from the laboratory scale as well to inform a mass balance and subsequent technoeconomic feasibility of the CeBER process.

To address these issues, experiments at different operating conditions and using different dried *Spirulina* powder samples were performed to determine optimized operating conditions for the bead-milling, leaching, aqueous two-phase separation, ammonium sulfate precipitation and microfiltration steps. From the interpretation of the results presented in Chapter 4, the following conclusions can be drawn.

Bead-milling, employed to disrupt the *Spirulina* cells, does affect the particle size distribution of the *Spirulina* biomass in solution but not in a uniform manner for all powders. This may be linked to the drying method used in the preparation of the powders by the suppliers. The bead-milling and resulting increased degree of cell disruption was shown to increase the rate of the extraction of the c-phycocyanin, as is expected to be the case for intracellular products from algal microorganisms (Pohndorf, et al., 2016). However, only an increase in the initial rate of extraction was observed. A comparable amount of time was taken to reach the equilibrium concentration of c-phycocyanin for both the milled and non-milled samples. The cell debris removal results suggest that milling has either a negative or no significant effect on the recovery of c-phycocyanin containing supernatant out of the cell debris removal area using centrifugation. The combined effect of these findings suggest that bead-milling may not be required and may even be undesirable for a process that only uses dried *Spirulina* powder for its feed. This is presumably because sufficient cell disruption had occurred during the powder drying. However, since the process is projected to eventually reach a stage where it can be fed with fresh *Spirulina*, the bead-milling step cannot totally be excluded from consideration.

The c-phycocyanin concentration during a leach of *Spirulina* biomass (milled or non-milled) in a citrate buffer of pH 6 could not be modelled reliably nor accurately using standard first or second order kinetics. It is postulated that the morphology of the *Spirulina* feedstocks differs from each other – most likely caused by both growth conditions and the drying methods used to prepare the *Spirulina* powder. Within samples, trends could be found but across samples no real trend was observed. The only exception was that the leaching of both the Brenntag and Carbocraft *Spirulinas* were affected in the same manner by milling, with an increase in the initial extraction rate observed as expected. However, between the milled samples Carbocraft appeared to leach according to expected leaching kinetics with the profile appearing logarithmic (Ho, et al., 2005). The Indian and Brenntag samples appeared to have a stagnant period of no real concentration change past the initial contacting stage of leaching, this was unexpected.

The minimum leaching time to reach the equilibrium c-phycocyanin concentration for all samples was quite long at 19 h. A long leaching time is of concern as it increases the likelihood of microbial contamination especially since the leaching is carried out in a non-sterile, room temperature environment. 19 h is also quite high compared to the rest of the processing time. If the leaching step requires optimization, it is recommended that a study be performed into the effect of temperature on c-phycocyanin leaching kinetics. It is also recommended that a study be performed into an intermittent

removal of c-phycocyanin containing leachate throughout the leaching time and replenishment of solvent as this would increase the concentration gradient increasing the driving force for c-phycocyanin leaching. A further future consideration is to carry out the leaching using a higher buffer to dried *Spirulina* ratio as this could increase the initial leaching rate of c-phycocyanin and may result in a shorter leaching time required to reach a desired c-phycocyanin concentration or equilibrium concentration in the leachate.

From the results of this study, a disk stack centrifuge is proposed as best suited to the needs of this process based on centrifuge speed, type of slurry and potential capacities for scale-up (Green & Perry, 2008). Disk stack centrifuge is well documented for its use in cell debris removal (Green & Perry, 2008). The at the centrifugal force proposed is at least 10 000 g since this has been shown to produce the highest recovery of c-phycocyanin. It is recommended that this be calibrated against the different physical configurations of a disk stack centrifuge versus the dead-end centrifuge used in the lab scale tests. It is recommended that a study be performed in which both centrifuge speed and centrifugation time are varied in the experimental design to ascertain their interactive impact on the extent of solid-liquid separation. This would help to inform a techno-economic assessment of the cell debris removal step to aid in an optimized scaling of this unit area.

A two-stage centrifugation with pellet rinsing in between each stage is recommended to maximize the c-phycocyanin leachate recovery. The highest increase in recovery found in this study was an increase from 76.9 ± 3.4 % before rinsing to 85.5 ± 3.8 % after rinsing at 10 000 g first centrifugation speed and 7 000 g second centrifugation speed. However, the rinsing would require the process run time to increase, and so the time and effort (cost) of this additional leaching step would need to be weighed against the benefit of the small percentage increase in recovery. More research into scheduling and leaching studies on the rinsing step would need to be performed for a better conclusion to be drawn.

The aqueous two-phase separation system was shown to deliver variable results. The composition of the feed to the ATPS system affected the performance. This included the formation of three phases at times, the lack of separate phases forming at other times, and inconsistencies arising in the volume percentages of the phases when two phases did form. The phase formation was also found to be highly dependent on the concentration of the crude extract, which was not expected. The data suggests that the ATPS system would need to be optimized for each different feed used to the CeBER process to yield a desired result, and that the ATPS may not be suitable for use at all for some feeds. It is therefore recommended that the ATPS step be excluded from the overall process design for translation.

For the ammonium sulfate precipitation cascade, it was proposed that a low saturation fraction (0.22) first precipitation would allow for an increase in the c-phycocyanin purity in the protein component of the supernatant compared to the crude extract; however, this was not observed. This could be a result of all the *Spirulina* samples not containing any proteins that would precipitate out at those lower saturations below 0.22. This initial precipitation was still found to be beneficial though, as it removes other impurities from the process stream. The highest c-phycocyanin purity in the precipitate pellet was observed at different saturations for different samples. As such, a saturation of 0.5 was chosen for the second precipitation step as it was close to the saturations at which most of the samples experienced their peak in purity and it still ensured a c-phycocyanin recovery of above 60 % in the precipitate pellet for all of the samples tested. It was thought that a set ionic charge of solution corresponding to a set ammonium sulfate saturation fraction would exist, at which c-phycocyanin starts to precipitate out of solution. However, this was not corroborated by the results. The data does suggest some sort of trend between *Spirulina* samples though. It is thus recommended that the precipitation experiments are performed again at lower concentrations of crude extract to allow for better mixing of ammonium sulfate such that we can be more confident in a localized concentration/ionic charge measurement being a representative of the average solution measurement.

The process was newly configured using the following order of unit procedures: bead-milling, leaching, cell debris removal via centrifugation, two-stage ammonium sulfate precipitation and microfiltration. From the results of the full process run which incorporated the findings of the individual unit operation tests, the process was found to be robust enough to handle the three *Spirulina* powder samples used up to the point of the last 0.22 μm microfiltration step. The robustness referred to is robustness in terms of putting a feed into the system and achieving an increase in the purity ratio in the product stream. All

steps of the process are robust individually. One could argue that the initial precipitation at 0.22 saturation of ammonium sulfate does not increase the purity ratio, but we see the knock-on effect that this has on the purity out of the second precipitation step at 0.45 saturation. The removal of contaminants in the first precipitation allowed for better purification in the second step. This may be a result of better interaction on a chemical level between the proteins and the ammonium sulfate following the removal of contaminants from the system. In future experiments, it is recommended that microbial loading be measured between consecutive precipitation stages to confirm the degree of microbial loading removal over the ammonium sulfate precipitations.

The primary aim of the CeBER extraction and purification process is to produce c-phycocyanin of cosmetic grade. From the results of the full runs conducted in this study, the highest reported purity ratio achieved was 0.9, substantially lower than the target purity ratio of > 1.5 for cosmetic grade. From the full runs it was determined that the c-phycocyanin content of the samples were relatively low compared to that of *Spirulina* quoted in literature. Furthermore, it has been previously shown that drying methods can cause severe loss of c-phycocyanin, exhibiting a higher rate of denaturation than other proteins (Chaiklahan, et al., 2011). As such it is recommended that fresh *Spirulina* be used for the process as it would have a higher purity ratio in the crude extract. Alternatively, efforts should be made to source *Spirulina* powders with a higher initial c-phycocyanin concentration. With similar purification factors as those obtained in the full runs results, with a higher crude extract purity ratio, it is probable that the process achieves cosmetic grade product c-phycocyanin. Another recommendation is to include chitosan and/or activated charcoal pre-treatment of the crude extract to further increase the purity ratio of the crude extract fed to the subsequent purification steps as recommended by Hockey (2020) and tested by Payne (2023). This has been shown to significantly improve the c-phycocyanin purity ratio of crude extract from *Spirulina* and thus could help ensure that the process is able to achieve a final c-phycocyanin purity of at least 1.5.

References

Abdul-Fattah, A., Kalonia, D., & Pikal, M. (2007). The challenge of drying method selection for protein pharmaceuticals: Product quality implications. *Journal of Pharmaceutical Sciences, 96*(8), 1886-1916.

Aftari, R. V., Rezaei, K., Mortazavi, A., & Bandani, A. R. (2015). The Optimized Concentration and Purity of Spirulina platensis C-Phycocyanin: A Comparative Study on Microwave-Assisted and Ultrasound-Assisted Extraction Methods. *Journal of Food Processing and Preservation, 39*(6), 3080-3091.

Agustina, S., Aidha, N. N., & Oktarina, E. (2019). Effect of maltodextrin concentration on the characteristic of phycocyanin powder as a functional food. *AIP Conference proceedings, 2175*(1).

Ahn, J.-W., & Lim, M. (2009). Characteristics of Wastewater from the Pulp.Paper Industry and its Biological Treatment Technologies. *Journal of the Korean Institute of Resources Recycling , 18*(2).

Alves, J., Chumpitaz, L. D., da Silva, L. H., Franco, T. T., & Meirelles, A. J. (2000). Partitioning of whey proteins, bovine serum albumin and porcine insulin in aqueous two-phase systems. Journal of Chromatography B: Biomedical Sciences and Applications, 743(1-2), 235-239.

Antelo, F. S., Anchau, A., Costa, J. A., & Kalil, S. J. (2010). Extraction and Purification of C-phycocyanin from Spirulina platensis in conventional and integrated aqueous two-phase systems. *Journal of the Brazilian Chemical Society, 21*(5), 921-926.

Antelo, F. S., Costa, J. A., & Kalil, S. J. (2015). Purification of C-phycocyanin from Spirulina platensis in aqueous two-phase systems using an experimental design. *Brazilian archives of biology and technology, 58*(1), 1-11.

Asenjo, J., & Andrews, B. (2011). Aqueous two-phase systems for protein separation: A perspective. *Journal of Chromatography A, 1218*(49), 8826-8835.

Bailey, J., & Ollis, D. (1986). *Biochemical engineering fundamentals.* New York: McGraw-Hill Book Co.

Baldev, E., Mubarak Ali, D., Dhivya, M., Kanimozhi, M., Shakena-Fathima, T., Alharbi, N., . . . Thajuddin, N. (2014). Facile and Novel Strategy for Methods of Extraction of Biofuel Grade Lipids from Microalgae - an Experimental Report. *International Journal of Biotechnology for Wellness Industries, 3*(1), 121-127.

Bartlett, P. N., & Birkin, P. R. (1993). The application of conducting polymers in biosensors. *Synthetic metals, 61*(1-2), 15-21.

Bennett, A. (1979). Complementary Chromatic Adaptation in a Filamentous Blue-Green Alga. *The Journal of Cell Biology, 58*(2), 419-435.

Bhaskar, S. U., Gopalaswamy, G., & Raghu, R. (2005). A simple method for efficient extraction and purification of C-phycocyanin from Spirulina platensis Geitler. *Indian Journal of Experimental Biology, 43*, 277-279.

Boussiba, S., & Richmond, A. (1979). Isolation and characterization of phycocyanins from the blue-green alga Spirulina platensis. *Archives of Microbiology, 120*, 155-159.

Breach, M. (2009). *Dissertation Writing for Engineers and Scientists.* Harlow, UK: Pearson Education.

Chaiklahan, R., Chirasuwan, N., Loha, V., Tia, S., & Bunnag, B. (2011). Separation and purification of phycocyanin from Spirulina sp. using a membrane process. *Bioresource Technology, 102*.

Chakraborty, D., Dahiya, S., Kotamraju, A., & Srivastav, K. V. (2019). Valorization of paper and pulp waste: Opportunities and prospects of biorefinery. In *Industrial and Municipal Sludge* (pp. 623-656). Hyderabad: CSIR-IICT.

Chang, R. (2007). *Chemistry* (9, revised ed.). McGraw-Hill Higher Education.

Chauton, M., Reitan, K., Norsker, N., Tveteras, R., & Kleivdal, H. (2015). A techno-economic analysis of industrial production of marine microalgae as a source of EPA and DHA-rich raw material for aquafeed: research challenges and possibilities. *Aquaculture, 436*.

Chavan, R., Saxena, K., & Tigote, D. (2015). Optimization of Acid Hydrolysis Process for Free Glucose Recovery From Starch. *International Journal of Innovative Science, Engineering & Technology, 2*(12).

Chisti, Y., & Moo-Young, M. (1986). Disruption of microbial cells for intracellular products. *Enzyme and Microbial Technology, 8*(4), 194-204.

Columbia Universtiy. (n.d.). *How to Write a Thesis Proposal*. Retrieved January 08, 2016, from http://www.ldeo.columbia.edu/~martins/sen_res/how_to_thesis_proposal.html

Cromie, S., & Doelle, H. (1982). Limitations in substrate utilization efficiency by Zymomonas mobilis. *European journal of applied microbiology and biotechnology*, 69-73.

David, L., Marx, A., & Adir, N. (2011). High-resolution Crystal Structures of Trimeric and Rod Phycocyanin. *Journal of Molecular Biology, 405*(1), 201-213.

Desmorieux, H., & Hernandez, F. (2004). Biochemical and Physical Criteria of Spirulina after Different Drying Processes. Sao Paulo: 14th International Drying Symposium.

Doran, P. (1997). *Bioprocess Engineering Principles.* Academic Press.

Dufossé, L. (2018). *Microbial Pigments From Bacterial, Yeasts, Fungi, and Microalgae for the Food and Feed Industries.* Saint-Denis, France: University of Reunion Island.

Dufossé, L., Galaup, P., Yaron, A., Malis, S., Blanc, P., Murthy, N., . . . Durand, G. (2005). Microorganisms and microalgae as sources of pigments for food use: a scientific oddity or an industrial reality? *Food science and technology*, 1-14.

Elgayar, D. A., Konsowa, A. H., El-Taweel, Y. A., Farag, H., & Sedahmed, G. H. (2016). Intensification of the rate of diffusion controlled catalytic and electrochemical reactions in a new stirred tank reactor with a multi cylindrical blade impeller. *Chemical Engineering Research and Design, 109*(1), 607-617.

Erikson, N. T. (2008). Production of phycocyanin - A pigment with applications in biology, biotechnology, foods and medicine. *Applied Microbiology and Biotechnology, 80*(1), 1-14.

Fagan-Endres, M., Burke, M., Pott, R., & Harrison, S. (2019). *World Intellectual Property Organization Patent No. WO2019034955A1.*

Fekrat, F., Nami, B., Ghavanati, H., Ghaffari, A., & Shahbazi, M. (2018). Optimization of chitosan/activated charcoal-based purification of Arthrospira platensis phycocyanin using response surface methodology. *Journal of Applied Phycology, 31*, 1095-1105.

Fuchino, K., Chan, H., Hwang, L., & Bruheim, P. (2020). *Cell biological studies of ethanologenic bacterium Zymomonas mobilis.* Trondheim: Department of Biotechnology and Food Science, NTNU Norwegian University of Science and Technology.

Future Market Insights. (2018). Phycocyanin Market Growing at a CAGR of 7.6% During the Forecast Period, 2018-2028. *Cision PR Newswire*. Retrieved July 3, 2020, from https://www.prnewswire.com/news-releases/phycocyanin-market-growing-at-a-cagr-of-7-6-during-the-forecast-period-2018-2028-821423288.html

Glazer, A. (1997). Phycobiliproteins - a family of valuable, widely used fluorophores. *Scanning, 19*.

Graverholt, O. S., & Eriksen, N. T. (2007). Heterotrophic high-cell-density fed-batch and continuous-flow cultures of Galdieria sulphuraria and production of phycocyanin. *Applied Microbiology and Biotechnology, 77*(1), 69-75.

Green, A. A., & Hughes, W. L. (1955). Protein solubility on the basis of solubility in aqueous solutions of salt and organic solvents. *Methods Enzymol., 1*, 67-90.

Green, D. W., & Perry, R. H. (2008). *Perry's Chemical Engineers' Handbook* (8th Edition ed.). McGraw-Hill.

Griffiths, M., Harrison, S. T., Smit, M., & Maharajh, D. (2016). *Major commercial products from micro- and macroalgae.* Cape Town.

Grima, E. M., Fernandez, F. A., Medina, A. R., & Christi, Y. (2003). Recovery of microalgal biomass and metabolites: process options and economics. *Biotechnology Advances, 20*, 491-515.

Guan, S. (2016). *Extracting phycocyanin from spirulina and hydrothermal liquefaction of its residues to produce bio-crude oil.* University of Illinois.

Guroy, B., Karadal, O., Mantoglu, S., & Cebeci, O. I. (2017). Effects of different drying methods on C-phycocyanin content of Spirulina platensis powder. *Journal of Fisheries and Aquatic Sciences, 34*(2), 129-132.

Hall, S., & Hall, S. M. (2012). *Rules of Thumb for Chemical Engineers.* Butterworth-heinemann.

Harouna-Oumarou, H. A., Fauduet, H., Porte, C., & Ho, Y.-S. (2007). Comparison of kinetic models for the aqueous solid-liquid extraction of tilia sapwood in a continuous stirred tank reactor. *Chemical Engineering Communications, 194*(1), 537-552.

Harrison, R., Todd, P., Rudge, R., & Petrides, D. (2013). *Bioseparations Science and Engineering.* Oxford University Press.

Harrison, S. (n.d.). The Research Proposal (Module 18). *CHE 5055 Research Communication and Methodology*. Department of Chemical Engineering, University of Cape Town.

Hellendoorn, L., van den Heuvel, J., & Ottengraf, S. (1996). Kinetics of a co-immobilised system. *Progress in Biotechnology*, 479-485.

Helmenstine, A. (2019). *Thylakoid Definition and Function*. Retrieved May 19, 2020, from https://www.thoughtco.com/thylakoid-definition-and-function-4125710

Herrera, A., Boussiba, S., Napoleone, V., & Hohlberg, A. (1989). Recovery of c-phycocyanin from the cyanobacterium Spirulin maxima. *Journal of applied phycology, 1*, 325-331.

Ho, Y.-S., Harouna-Oumarou, H. A., Fauduet, H., & Porte, C. (2005). Kinetics and model building of leaching of water-soluble compounds of Tilia sapwood. *Separation and Purification Technology, 45*(3), 169-173.

Hockey, J. (2020). *Improving an aqeuous two-phase process for C-phycocyanin extraction from Spirulina.* Cape Town: University of Cape Town.

Holban, A. M., & Grumezescu, A. M. (2018). *Microbial Contamination and Food Degradation A volume in Handbook of Food Bioengineering.* Academic Press.

Hsieh-Lo, M., Castillo, G., Ochoa-Becerra, M. A., & Mojica, L. (2019). Phycocyanin and phycoerythrin: Strategies to improve production yield and chemical stability. *Algal Research, 42*.

Hussain, A., Mukhtar, H., & ul Haq, I. (2015). Optimization of fermentation medium for L-lysine production by Corynebacterium glutamicum. *Pak. J. Bot., 47*(SI).

Iqbal, M., Tao, Y., Xie, S., Chen, D., Wang, X., Huang, L., . . . Yuan, Z. (2016). Aqueous two-phase system (ATPS): an overview and advances in its applications. *Biological Procedures Online, 18*.

Janin, A., Blais, J.-F., Mercier, G., & Drogui, P. (2009). Optimization of a chemical leaching process for decontamination of CCA-treated wood. *Journal of Hazardous Material, 169*(1-3), 136-145.

Jeon, J.-M., Rajesh, T., Song, E., Lee, H.-W., Lee, H.-W., & Yang, Y.-H. (2013). Media optimization of Corynebacterium glutamicum for succinate production under oxygen-deprived condition. *JMB, 23*(2).

Kazadi Mbamba, C., Harrison, S., Franzidis, J.-P., & Broadhurst, J. (2012). Mitigating acid rock drainage risks while recovering low-sulphur coal from ultrafine colliery wastes using froth flotation. *Minerals Engineering, 29*, 13–21.

Kazmer, D., & Roser, C. (1999). Evaluation of Product and Process Design Robustness. *Research in Engineering Design, 11*, 20-30.

Klein, B., & Buchholz, R. (2013). 20 - Microalgae as sources of food ingredients and nutraceuticals. In B. McNeil, D. Archer, I. Giavasis, & L. Harvey (Eds.), *Microbial Production of Food Ingredients, Enzymes and Nutraceuticals.* Woodhead Publishing Limited.

Klein, J., & Lee, D. (1978). Biological treatment of aqueous water from usual conversion processes. *Biotechnolory and Bioengineering Symposium 8*, (pp. 379-390).

Kraan, S. (2013). Pigments and minor compounds in algae. In H. Domínguez, *Functional Ingredients from Algae for Foods and Nutraceuticals.* Elsevier.

Kroumov, A., Scheufele, F., Triqeuros, D., Modenes, A., Zaharieva, M., & Najdenski, H. (2017). Modeling and Technoeconomics Analysis of Algae for Bioenergy and Coproducts. In R. P. Rastogi, & M. Datta (Eds.), *Algal Green Chemistry* (pp. 201-241). Elsevier.

Kuddus, M., SIngh, P., Thomas, G., & Al-hazimi, A. (2013). Recent Develoments in Production and Biotechnological Applications of C-Phycocyanin. *BioMed Research International*.

Kumar, D., Dhar, D. W., Pabbi, S., Kumar, N., & Walia, S. (2014). Extraction and purification of C-phycocyanin from Spirulina platensis (CCC540). *Indian Journal of Plant Physiology, 19*(1), 184-188.

Kwade, A., Blecher, L., & Schwedes, J. (1996). Motion and stress intensity of grinding beads in a stirred media mill. Part 2: Stress intensity and its effect on comminution. *Powder technology, 86*, 69-76.

Langford, C. H., & Beebe, R. A. (1995). *The Development of Chemical Principles.* New York: Dover.

Lawford, H., & Rousseau, J. (1993). A comparative study of glucose conversion to ethanol by Zymomonas mobilis and a recombinant Escherichia coli. *Biotechnology Letters*, 499-504.

Ma, Z., Ahmed, F., Yuan, B., & Zhang, W. (2019). Fresh living Arthrospira as dietary supplements: Current status and challenges. *Trends in Food Science & Technology, 88*(1), 439-444.

Mehdipour, I., & Khayat, K. H. (2017). Effect of particle-size distribution and specific surface area of different binder systems on packing density and flow characteristics of cement paste. *Cement and Concrete Composites, 78*, 120-131.

Minkova, K., Tchernov, A., Tchorbadjieva, M., Fournadjieva, S., Antova, R., & Busheva, M. (2003). Purification of C-phycocyanin from Spirulina (Arthrospira) fusiformis. *Journal of Biotechnology, 102*.

Miranescu, M. (2011). Investigations on wastewaters at potato processing and starch recovery and characterisation. *Journal of Agroalimentary Processes and Technologies, 17*(2).

Mokomele, T., Callanan, L., & Clarke, K. (2013). *Ethanol production from xylose and glucose by Zymomonas mobilis for the development of a membrane bioreactor.* Stellenbosch: DST-NRF Centre of Excellence in Catalysis.

Mondal, S. C., Ray, P. K., & Maiti, J. (2014). Modelling robustness for manufacturing processes: a critical review. *International Journal of Production Research, 52*(1), 521-538.

Moraes, C. C., Fernandes De Medeiros Burket, J., & Kalil, S. J. (2010). c-Phycocyanin extraction process for large-scale use. *Journal of Food Biochemistry, 34*(1), 133-148.

Moreno, J., Rodriguez, H., Vargas, M., Rivas, J., & Guerrero, M. (1995). Nitrogen-fixing cyanobacteria as source of phycobiliprotein pigments. Composition and growth performance of ten filamentous heterocystous strains. *Journal of Applied Phycology, 7*(1), 17-23.

Murty, R., Rajasekar, V., Raja, S., Thivaharan, V., & Ramesh, V. (2012). Aqueous Two Phase Systems for the Recovery of Biomolecules - A Review. *Science and Technology, 1*(1), 7-16.

Muthulakshmi, M., Saranya, A., Sudha, M., & Selvakumar, G. (2012). Extraction, partial purification, and antibacterial activity of phycocyanin from. *Journal of Algal Biomass Utilization, 3*(3), 7-11.

Niu, J., Wang, G., Lin, X., & Zhou, B. (2007). Large-scale recovery of C-phycocyanin from Spiruina platensis using expanded bed adsorption chromatography. *Journal of Chromatography, 880*.

Novák, P., & Havlíček, V. (2013). Protein Extraction and Precipitation. In *Proteomic Profiling and Analytical Chemistry.* Elsevier.

Parmar, A., Singh, N. K., Kaushal, A., Sonawala, S., & Madamwar, D. (2011). Purification, Characterization and Comparison of Phycoerythrins From Three Different Marine Cyanobacterial Cultures. *Bioresource Technology, 102*(2), 1795-1802.

Patel, A., Mishra, S., Pawar, R., & Gosh, P. (2005). Purification and characterization of C-Phycocyanin from cyanobacterial species of marine and freshwater habitat. *Protein Expression and Purification, 40*, 248-255.

Pathil, G., & Raghavarao, K. (2007). Aqueous two phase extraction for purification of C-phycocyanin. *Biochemical Engineering Journal, 34*, 156-164.

Phillips, A. T., & Signs, M. W. (2005). Desalting, Concentration,and Buffer Exchange by Dialysis and Ultrafiltration. *Current Protocols in Protein Science*.

Pohndorf, R. S., Camara, A. S., Larrosa, A. P., Pinheiro, C. P., Strieder, M. M., & Pinto, L. A. (2016). Production of lipids from microalgae Spirulina sp.: Influence of drying, cell disruption and extraction methods. *Biomass and Bioenergy, 93*, 25-32.

Rakotondramasy-Rabesiaka, L., Havet, J. -L., Porte, C., & Fauduet, H. (2009). Solid-liquid extraction of protopine from fumaria officinalis L. - Kinetic modelling of influencial parameters. *Industrial crops and products, 29*(1), 516-523.

Rakotondramasy-Rabesiaka, L., Havet, J.-L., Porte, C., & Faudet, H. (2008). Solid-liquid extraction of protopine from Fumaria officinalis L. - Experimental study and process optimization. *Separation and Purification Technology, 59*(3), 253-261.

Ramos, A., Acien, F., Fernandez-sevilla, J., Gonzalez, C., & Bermejo, R. (2011). Development of a process for large-scale purification of c-phycocyanin from Synechocystis aquatilis using expanded bed adsorption chromatography. *Journal of Chromatography B, 879*(7-8), 511-519.

Ramos, A., Acien, R., Fernandez-Sevilla, J., Gonzalez, C., & Bermejo, R. (2010). Large-scale isolation and purification of C-phycocyanin from the cyanobacteria Anabaena marina using expanded bed adsorption chromatography. *Wiley Interscience*.

Ramyadevi, D., Subathira, A., & Saravanan, S. (2012). Aqueous two-phase poly (ethylene glycol) - Maltodextrin system for protein partitioning from shrimp waste: Influence of molecular weight and pH. International Journal of Environmental Sciences, 2(4), 2642-6469.

Rao, K., Szlag, D. S., Sikdar, S. K., Joshi, J., & Sawant, S. (1991). Protein extraction in a spray column using a polyethylene glycol-maltodextrin two-phase polymer system. The Chemical Engineering Journal, 46(3), B75 - B81

Richardson, J., Harker, J., & Backhurst , J. (2002). *Coulson's and Richardson's Chemical Engineering Particle Technology and Separation Processes* (Vol. 2). (J. Coulson, & J. Richardson, Eds.) Oxford: Butterworth Heinemann.

Rito-Palomares, M., Nuez, L., & Amador, D. (2001). Practical application of aqueous two-phase systems for the development of a prototype process for c-phycocyanin recovery from Spirulina maxima. *Journal of Chemical Technology and Biotechnology, 76*(12), 1273-1280.

Rogers, P., Lee, K., Skotnicki, M., & Tribe, D. (1982). *Microbial reactions: Ethanol Production by Zymomonas mobilis.* New York: Springer-Verlag.

Roman, R., Alvarez-Pez, J., Fernandez, F., & Grima, E. (2002). Recovery of pure B-phycoerythrin from the microalga Porphyridium cruentum. *Journal of Biotechnology, 93*, 73-85.

Scharathow, R. (2012). *Driving the evolution of plastics-bioplastics markets and framework.* Berlin: Germany: European Bioplastisc.

Scheer, H., & Kufer, W. (1977). Conformational Studies on C-Phycocyanin from Spirulina platensis. *Journal of Biosciences, 32*, 513-519.

Schwartzberg, H. G., & Chao, R. Y. (1982). Solute Diffusivities in Leaching Processes. *Food Technology, 36*(2), 73-86.

Seider, W. D., Lewin, D. R., Seader, J., Widagdo, S., & Gani, R. (2017). *Product and process design principles : synthesis, analysis, and evaluation* (4th Edition ed.). New York: John Wiley & Sons, Inc.

Seider, W. D., Seader, J. D., & Lewin, D. R. (2009). *Product & Process Design Principles: Synthesis, Analysis and Evaluation 2nd Edition.* Wiley India Pvt. Limited.

Seikova, I., Simeonov, E., & Ivanova, E. (2004). Protein leaching from tomato seed—experimental kinetics and prediction of effective diffusivity. *Journal of Food Engineering, 61*(2), 165-171.

Sekar, S. (2008). Phycobiliproteins as a commodity: trends in applied research, patents and commerciaization. 113-136.

Shen, Y., Pei, Z., Yuan, W., & Mao, E. (2009). Effect of nitrogen and extraction method on algae lipid yield. *International Journal of Agriculture and Biological Engineering, 2*(1), 51-57.

Shine, A. D. (2006). Fitting Experimental Data to Straight Lines (Including Error Analysis). Student Everything Page Chemical Engineering.

Shukia, S. P., Singh, J. S., Kashyap, S., Giri, D. D., & Kashyap, A. K. (2008). Antarctic cyanobacteria as a source of phycocyanin: An assessent. *Indian Journal of Marine Sciences, 37*(4), 446-449.

Silva, L. A., Kuhn, K. R., Moraes, C., & Burkert, C. (2009). Experimental Design as a Tool for Optimization of C-Phycocyanin Purification by Precipitation from Spirulina platensis. *Journal of the Brazilian Chemical Society, 20*(1), 5-12.

Silveira, S. T., Burket, J. F., Costa, J. A., Burket, J. A., & Kalil, S. J. (2007). Optimization of phycocyanin extraction from Spirulina platensis using factorial design. *Bioresource Technology, 98*(1), 1629-1634.

Singh, N., Sonani, R., Rastogi, R., & Madamwar, D. (2015). The phycobilisomes: an early requisite for efficient photosynthesis in cyanobacteria. *EXCLI Journal Experimental and Clinical Sciences, 14*, 268-289.

Smith, F., & Harvey, A. H. (2007). Avoid Common Pitfalls when using Henry's Law. *American Institute of Chemical Engineering, 36*.

Solent Univeristy. (n.d.). *Dissertation proposals*. Retrieved January 08, 2016, from http://mycourse.solent.ac.uk/mod/book/view.php?id=2744&chapterid=1270

Song, W., Zhao, C., & Wang, S. (2013). A Large-Scale Preparation Method of High Purity C-Phycocyanin. *International Journal of Bioscience, Biochemistry and Bioinformatics, 3*(4).

Sørensen, L., Hantke, A., & Eriksen, N. T. (2013). Purification of the photosynthetic pigment C-phycocyanin from heterotrophic Galdieria sulphuraria. *Journal of the Science of Food and Agriculture, 93(12), 2933-2938.*

Stec, B., Troxler, F., & Teeter, M. (1999). Crystal Structure of C-Phycocyanin from Cyanidium caldarium Provides a New Perspective on Phycobilisome Assembly. *Biophysical Journal, 76*(6), 2912-2921.

Su, C.-H., Liu, C.-S., Yang, P.-C., Syu, K.-S., & Chiuh, C.-C. (2014). Solid–liquid extraction of phycocyanin from Spirulina platensis: Kinetic modeling of influential factors. *Separation and Purification Technology, 123*(1), 64-68.

Turton, R., Bailie, R. C., Whiting, W. B., Shaeiwitz, J. A., & Bhattacharyya, D. (2001). *Analysis, Synthesis and Design of Chemical Processes fourth edition.* Upper Saddle River, NJ: Prentice Hall.

Vazquez-Romero, B., Perales, J. A., Pereira, H., Barbosa, M., & Ruiz, J. (2022). Techno-economic assessment of microalgae production, harvesting and drying for food, feed, cosmetics, and agriculture. *Science of the total environment, 837*.

Verified Market Research ®. (2024). *Global Phycocyanin Market Size By Product Type, By Application, By Source, By Geographic Scope and Forecast*. Retrieved 2024, from https://www.verifiedmarketresearch.com/product/phycocyanin-market/#:~:text=Phycocyanin%20Market%20size%20was%20valued%20at%20USD%20173.29,CAGR%20of%209.77%25%20during%20the%20forecast%20period%202024-2030.

Vernes, L., Granvillain, P., Chemat, F., & Vian, M. (2015). Phycocyanin from Arthrospira Platensis. Production, Extraction and Analysis. *Current Biotechnology, 5*.

Watanabe, M., Momoko, S., Kondo, K., Narikawa, R., & Ikeuchi, M. (2012). Phycobilisome model with novel skeleton-like structures in a glaucocystophyte Cyanophora paradoxa. *Biochimica et Biophysica Acta (BBA) - Bioenergetics*, 1428-1435.

Wilburn, D. T., Machek, S. B., Cardaci, T. D., Hwang, P. S., & Willoughby, D. S. (2020). Acute Maltodextin Supplementation during Resistance training. *Journal of Sports Science Medicine, 19*(2), 282-288.

Wingfield, P. T. (2001). Protein Precipitation Using Ammonium Sulfate. *Pubmed Central*. doi: 10.1002/0471140864.psa03fs13

Yoshikawa, N., & Belay, A. (2008). Single-labaratory validation of a method for the determination of c-phycocyanin and allophycocyanin in Spirulina (Arthrospira) supllements and raw materials by spectrophotometry. *National Library of Medicine National Center for Biotechnology Information, 91*(3), 524-259.

Zhang, Y.-M., & Chen, F. (1999). A simple method for efficient separation and purification of c-phycocyanin and allophycocyanin from Spirulina platensis. *Biotechnology Techniques, 13*(1), 601-603.

Appendix A: Approach to Project and Methodology Appendix

A.1 General sample calculations

A.1.1 Performance indicators

c-Phycocyanin purity ratio

The c-phycocyanin purity ratio of a sample is simply the ratio of the absorbances of the sample at two different wavelengths of light *viz*. Absorbance at 620 nm over absorbance at 280 nm (Bennett, 1979).

All absorbance readings were performed in triplicate so the calculation of the purity ratio would be as follows:

Using the absorbance readings at 620 nm and 280 nm as below:

Absorbance at 620 nm	Absorbance at 280 nm
1.01	2.034
1.34	2.080
1.13	2.069

The average absorbance at 620 nm = 1.16, the average absorbance at 280 nm = 2.061, therefore using Equation 1:

$$Purity\ ratio\ = \frac{A_{620}}{A_{280}}$$ Equation 1

$$Purity\ ratio = \frac{1.16}{2.061}$$

$$Purity\ ratio = 0.56$$

Typically, samples are produced in triplicate for the same reading, in that instance the purity ratio will be calculated three times and the average presented as the purity ratio with the standard deviation being quoted in the final answer.

e.g., 0.56, 0.58, 0.61 then the purity will be quoted as: “0.583 ± 0.025”.

c-Phycocyanin concentration

In the results of this dissertation, the c-phycocyanin concentration of a sample was determined by Equation 3 (Yoshikawa & Baley, 2008):

$$C_{c-PC}(\mathrm{mg.mL^{-1}}) = 0.162\ \times\ A_{620} - 0.098\ \times A_{650}$$ Equation 3

All absorbance readings are performed in triplicate so the calculation of the c-phycocyanin concentration would be as follows:

Using the absorbance readings at 620 nm and 280 nm as below:

Absorbance at 650 nm	Absorbance at 620 nm
1.01	2.034
1.34	2.080
1.13	2.069

The average absorbance at 650 nm = 1.16, the average absorbance at 620 nm = 2,061, therefore:

$$C_{c-PC} = 0.162 \times 2.061 - 0.098 \times 1.16$$

$$C_{c-PC} = 0.22\ (\mathrm{mg.mL^{-1}})$$

Typically, samples were produced in triplicate for the same reading, in that instance the c-phycocyanin concentration of the sample was calculated three times and the average presented as the c-phycocyanin concentration with the standard deviation being quoted in the final answer.

e.g., 0.56, 0.58, 0.61 then the c-phycocyanin concentration will be quoted as: "0.583 ± 0.025 mg.mL^{-1}".

Purification factor

The purification factor is the ratio of purity ratios before and after a particular purification method. It gives an indication of the extent of purification of the method on the sample.

For Figure 55 , the purification factor is the quotient of the purity ratio at "B" over the purity ratio at "A".

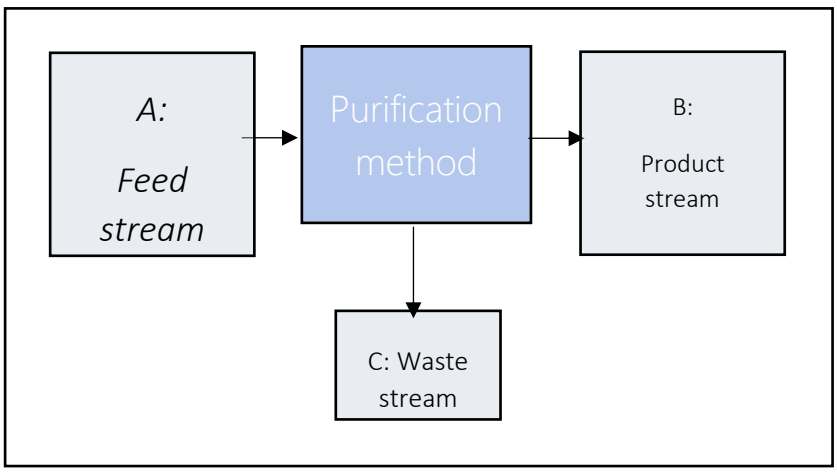

Figure 55. An example purification method

For a c-phycocyanin purity ratio of 0.5 at A and a c-phycocyanin purity ratio of 0.9 at B, the purification factor over the purification method in Figure 55 is given by:

$$Purification\ factor = \frac{Purity\ ratio_B}{Purity\ ratio_A} \qquad \text{Equation 31}$$

Equation 31 becomes:

$$Purification\ factor\ = \frac{0.9}{0.5}$$

$$Purification\ factor\ = 1.8$$

c-Phycocyanin recovery

c-Phycocyanin recovery is calculated based off the c-phycocyanin concentration in the feed and product streams over an entire system or over a particular extraction/purification step in the system. The concentration and the volume of the streams are multiplied to determine the c-phycocyanin mass in that stream:

$$c - PC\ concentration\ \times\ volume\ of\ sample = mass\ of\ c - PC \qquad \text{Equation 32}$$

c-Phycocyanin recovery over a process can therefore be described by the following Equation 33:

$$Rec_{c-PC}\ (\%) = \frac{mass\ of\ c - PC_{out}}{mass\ of\ c - PC_{in}} \times 100\ \% \qquad \text{Equation 33}$$

Thus, if the mass of c-phycocyanin into a system is 800 mg and the product stream contains 40 mg, the c-phycocyanin recovery would be:

$$Rec_{c-PC}\ (\%) = \frac{40}{800} \times 100\ \%$$

$$Rec_{c-PC}\ (\%) = 5\ \%$$

A.2 Aqueous two-phase separation

A.2.1 Sample calculation for PEG-citrate ATPS

1. Weigh the 50 mL centrifuge tube:

$$Empty\ \text{centrifuge}tube\ =\ 13.2\ g$$

2. Add 20 mL of sample stock solution, and weigh the filled centrifuge tube:

$$Filled\ \text{centrifuge}tube\ =\ 23.2\ g$$

3. Calculate the mass of the liquid inside the centrifuge tube:

$$33.2\ g\ -\ 13.2\ g\ =\ 10\ g$$

4. The stock solution within the centrifuge tube has to make up 69 % of the final ATPS mass.

$$Therefore, 1\ \%\ of\ the\ final\ ATPS\ mass\ =\ (10\ g\ )/69\ =\ 0.144\ g$$

5. The required mass of PEG 10 000 and Citrate salts can therefore be calculated by:

$$0.144\ g\ \times\ 11\ =\ 1.59\ g\ and\ 0.144\ \times\ 20\ =\ 2.88\ g, respectively.$$

6. Since PEG 10 000 makes up 11% of the final ATPS mass and citrate salts make up 20 %.

$$Thus\ 1.59\ g\ of\ PEG\ 10\ 000\ is\ required.$$

7. 92 % of the citrate salts is sodium citrate, thus:

$$0.92 \times\ 2.88\ g\ =\ 2.65\ g\ of\ sodium\ citrate\ needs\ to\ be\ added.$$

8. 8 % of the citrate salts is citric acid, thus:

$$0.08\ \times\ 2.88\ g\ =\ 0.23\ g\ of\ citric\ acid\ needs\ to\ be\ added.$$

A.2.2 Sample Calculation for PEG-maltodextrin ATPS

PEG-maltodextrin ATPS calculation corresponding to the mass fraction in Table 15:

- After sequestering the PEG phase from the first ATPS weigh the centrifuge tube with the PEG phase in it.

$$Filled\ \text{centrifuge}\ tube\ with\ PEG\ phase\ contained\ =\ 18.2\ g$$

- Knowing the mass of the centrifuge tube = 13.4 g, the mass of the PEG phase can be calculated:

$$18.2\ g\ -\ 13.4\ =\ 4.8\ g$$

- The PEG top phase makes up 11% of the final ATPS mass.

$$Therefore, 1\ \%\ of\ the\ final\ ATPS\ mass\ =\ (4.8\ g)/11 = 0.43\ g$$

- The required mass of maltodextrin and deionized water can therefore be calculated by:

$$0.43\ g\ \times\ 22\ =\ 9.46\ g\ and\ 0.43\ g\ \times\ 67\ =\ 28.8\ g, respectively$$

- Since maltodextrin makes up 22 % of the final ATPS mass and deionized water makes up 67 %.

$$Thus, 9.46\ g\ of\ Maltodextrin\ is\ required\ and\ 28.8\ g\ of\ deionized\ water\ is\ required.$$

A.3 Precipitation

A.3.1 Ammonium sulfate saturation determination

Because protein precipitation is dependent on the charge of the solution (Song, et al., 2013), a calibration was performed using ammonium sulfate to find the relationship between ammonium sulfate saturation percentages and the conductivity of the solution. Conductivity is a measure of the dissolved ions in solution and thus is a representation of the saturation of the salt, ammonium sulfate. Saturation percentage is affected by the temperature and the temperature of the deionized water fluctuated between 18 ºC and 21 ºC during the calibration.

To establish this calibration, 20 ml of de-ionized water was poured into a glass beaker. Increments of 1 gram of ammonium sulfate from 0 to 15 g was added to this glass beaker and stirred until all salt was dissolved. At each increment, after the salt in solution had dissolved, the conductivity of the solution was tested using a benchtop conductivity meter. The cumulative ammonium sulfate mass added to the beaker, at the point at which the conductivity stopped increasing, was considered the saturation mass for the total volume – including the volume of the salt added – at that point. Figure 56 shows the conductivity of the solution as a function of the salt added to the 20 ml starting volume of deionized water. The conductivity stopped changing at the point where 11 g of ammonium sulfate was added.

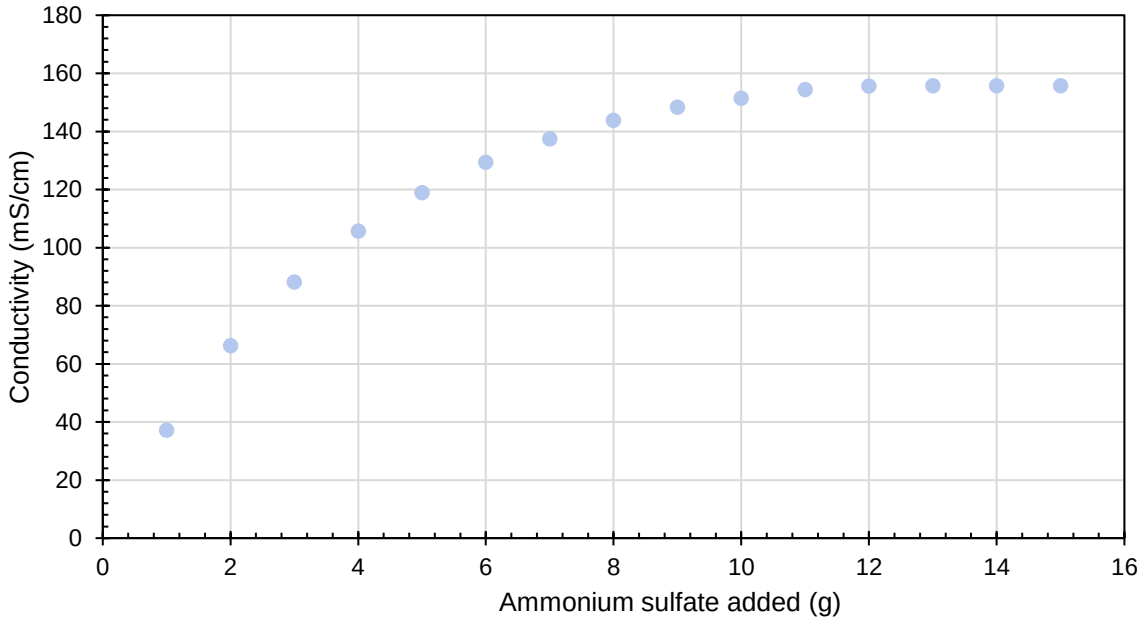

Figure 56. Conductivity of solution as a function of ammonium sulfate added

The saturation percentages for each increment interval were then calculated using the following formula (Equation 21) (Wingfield, 2001):

$$W = \frac{W_{sat}\,(C_2 - C_1)}{1 - (PS_2)}$$ Equation 21

Where:

W is the quantity, in mass, of ammonium sulfate to be added to a 1 litre solution of concentration S_1 to produce a concentration of S_2.

W_{sat} is the number of grams of ammonium sulfate that is dissolved in a 1 litre saturated ammonium sulfate solution

C_1 is the initial saturation fraction of complete saturation of ammonium sulfate, e.g., a 30 % saturation would be expressed as 0.3

C_2 is the final saturation fraction of complete saturation of ammonium sulfate at the point where weight (g) is added.

P is the product of specific volume of saturated solution with W_{sat} divided by 10^3

The correlation between the saturation percentages and the conductivity of the solution was found. Thus, the saturation percentages shown are calculated based on the saturation of ammonium sulfate found using this calibration and not values from literature. W_{sat} corresponds to the 11 g added to a 20 mL volume of deionized water. Thus, via Equation 21, W_{sat} is 425 g/L of saturated solution. The specific volume was taken as 0.545 mL/g from Wingfield (2001).

The more salt is dissolved in solution the greater number of ions in solution, this would suggest that the relationship between salt concentration or salt saturation and conductivity is linearly proportional, but this is not the case. The increase in the salt concentration is independent of the mobility of the ions. The greater the concentration of ions in solution, the lower the mobility of the ions. Thus, the conductivity of a solution is directly proportional to the square root of the salt saturation percentage (Langford & Beebe, 1995). Figure 57 shows this relationship with a coefficient of determination $R^2 = 0.98$.

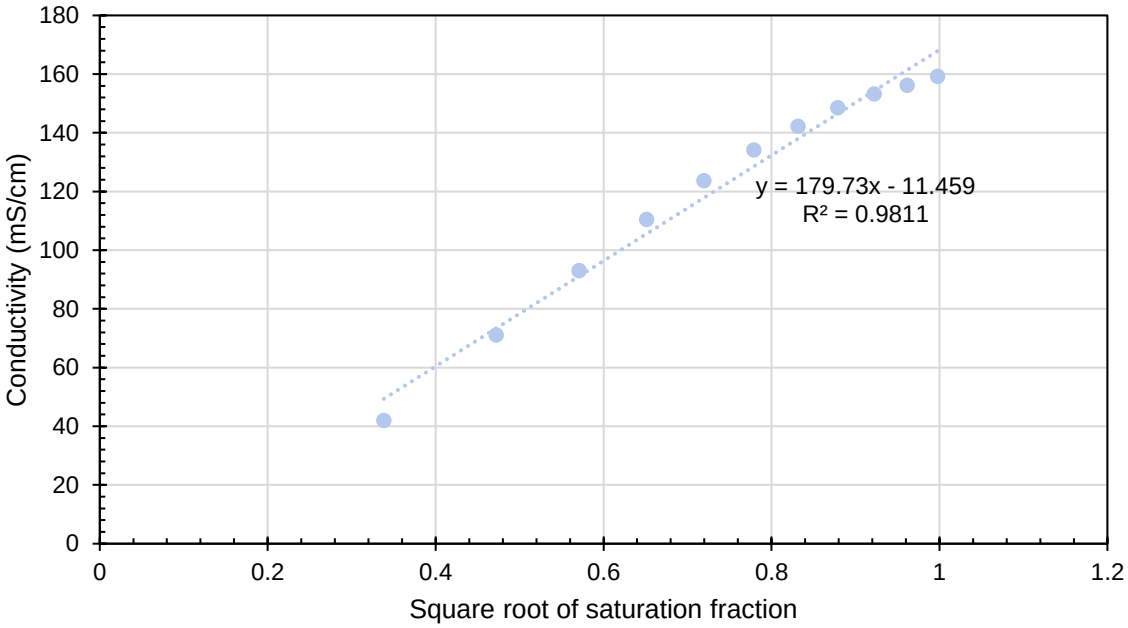

Figure 57. Conductivity in solution as a function of the square root of the ammonium sulfate saturation fraction

The correlation between salt added and conductivity was thus expressed as a relationship between salt added and ammonium sulfate saturation percentage. This relationship, Figure 58, was used to determine the mass of salt needed to achieve a specific saturation percentage for the precipitation experiments. A sample calculation is shown below.

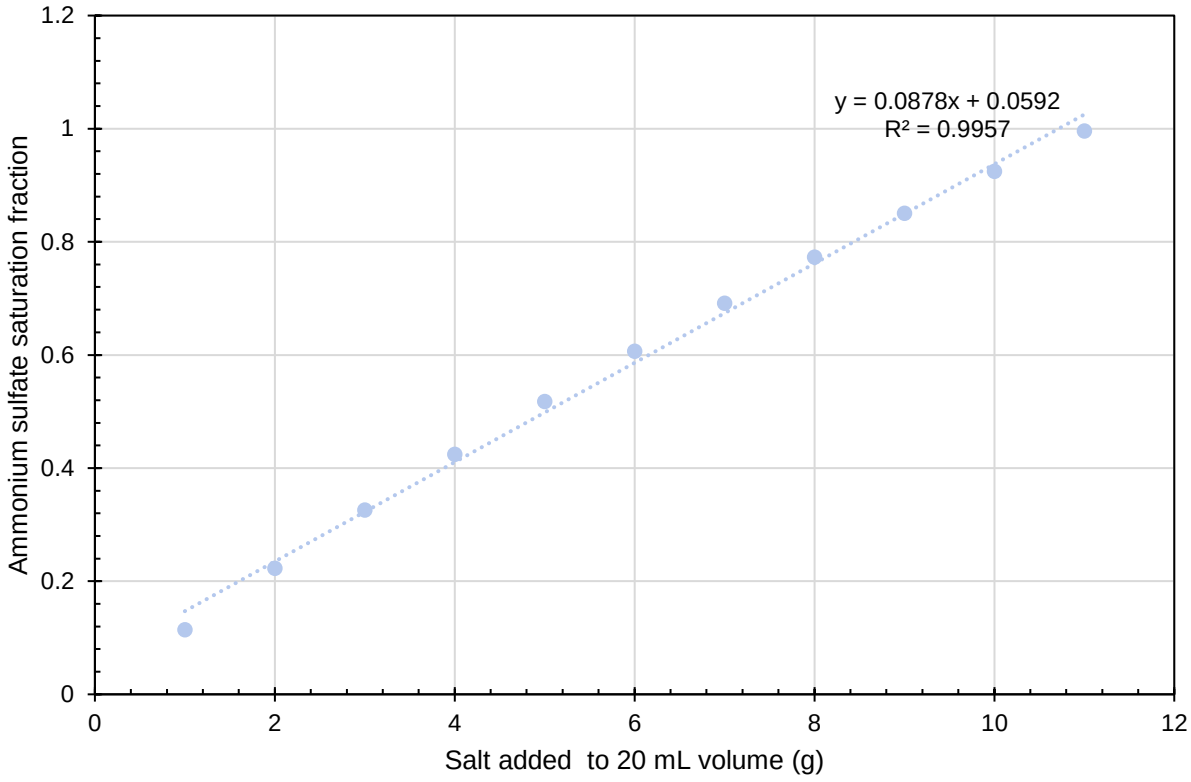

Figure 58. Calibration of ammonium sulfate saturation fraction to mass of ammonium sulfate in grams added to a 20 mL volume

The conductivity calibration could not be performed on the sample stock solution since it would cause foaming that occurs during mixing before the precipitation happens. Data of the calibration was compared to the conductivity measured in the supernatant after precipitation at different salt percentages.

To achieve 20 % saturation in a 20 mL stock solution. We look at the equation for the correlation, from Figure 58:

$$Saturation\ fraction\ =\ 0.0878(Salt\ added\ in\ grams)\ +\ 0.0592.$$

Changing the subject of the formula to be salt added:

$$Salt\ added\ in\ grams\ =\ (saturation\ fraction\ -\ 0.0592)/0.0878.$$

Substituting 0.2 in for y, gives 1.6 g of ammonium sulfate needed to be added to a 20 mL volume of stock solution.

For a two-step precipitation, with the first stage being at 20 %, the previous explanation is followed and once the supernatant is sequestered, the following calculation is followed:

If the second stage precipitation is at 0.4 saturation then we can tell from:

$$Salt\ added\ in\ grams\ =\ (saturation\ fraction\ -\ 0.0592)/0.0878.$$

that 3.88 g per 20 mL stock solution is required to achieve that 0.4 saturation.

With the specific volume of ammonium sulfate being 0.545 mL/g, the 0.4 saturation corresponds to:

$$0.545 \times 3.88 = 2.12\ mL$$

$$Therefore, total\ volume = 20 + 2.12 = 22.12\ mL$$

$$Mass\ of\ salt = 3.88\ g$$

$$Therefore\ concentration = 3.88/22.12 = 0.1754\ g/mL$$

For a 15 mL supernatant at 0.2 saturation, the concentration is:

$$1.6\ g\ added\ to\ 20\ mL, therefore, 0.545\frac{mL}{g} \times 1.6\ g = 0.872\ mL$$

$$Total\ volume = 0.872\ mL + 20\ mL = 20.872\ mL$$

$$Total\ salt = 1.6\ g$$

$$Concentration = 1.6\ g/20.872\ mL = 0.077\ g/mL$$

$$15\ mL, therefore\ 0.077\ g/mL \times 15\ mL = 1.15\ g\ of\ salt$$

Need to get to;

$$0.1754\ g/mL \times (15\ mL + 0.545x) = x\ g\ ammonium\ sulfate$$

$$x = 2.9\ g\ ammonium\ sulfate$$

15 mL of supernatant at 0.2 already contains 1.15g:

$$2.9 - 1.15 = 1.75\ g\ Ammonium\ sulfate\ to\ be\ added.$$

Appendix B: Results and Discussion Appendix

The following link can be followed to view the data sets used for the creation of the figures in the Results section:

- https://figshare.com/s/6eb1843f82e8f3fdfa2b

B.1 Size distribution

This section of the Appendix contains the contrasted images at 10× magnification of the *Spirulina* powder samples after contrasting and saturation adjustment as well as after the drawing function of ImageJ software as described in the Methodology. These images are used to obtain the particle size distributions and cut sizes described in the Results.

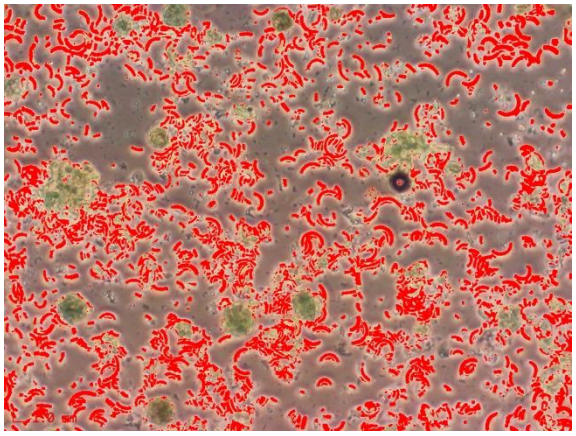

Figure 59. Non-milled Carbocraft Spirulina powder 10× magnification with contrast and saturation adjustment

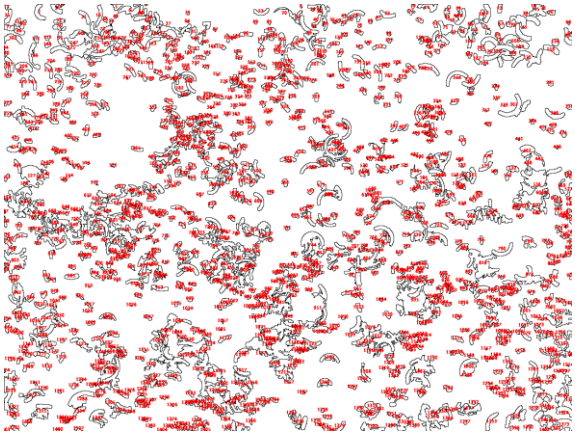

Figure 60. Non-milled Carbocraft Spirulina powder 10× magnification with ImageJ drawing function applied

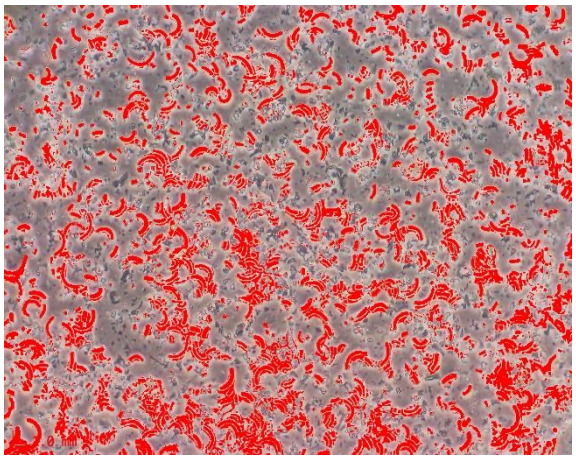

Figure 61. Milled Carbocraft Spirulina powder 10× magnification with contrast and saturation adjustment

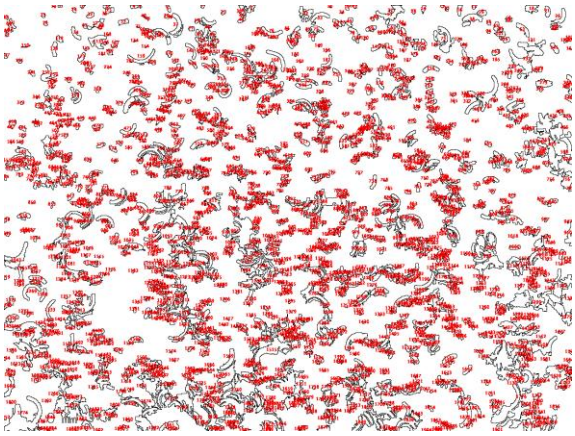

Figure 62. Milled Carbocraft Spirulina powder 10× magnification with ImageJ drawing function applied

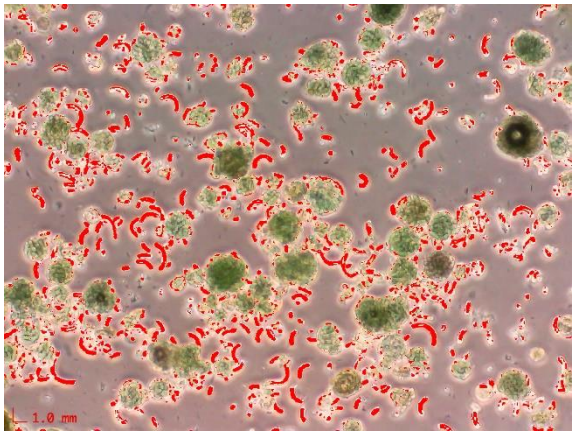

Figure 63. Non-milled Brenntag Spirulina powder 10× magnification with contrast and saturation adjustment

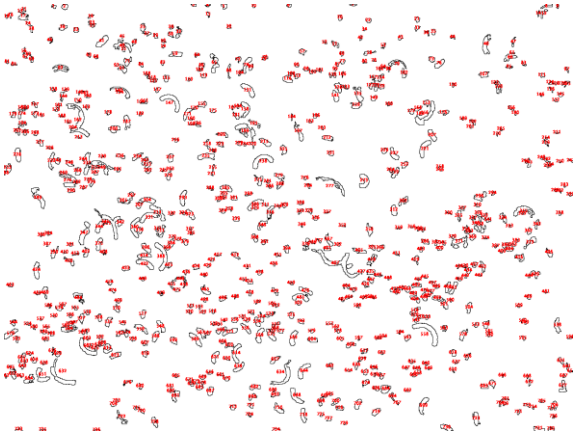

Figure 64. Non-milled Brenntag Spirulina powder 10× magnification with ImageJ drawing function applied

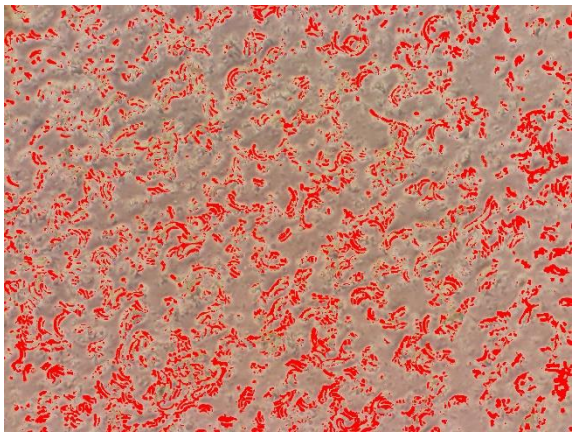

Figure 65. Milled Brenntag Spirulina powder 10× magnification with contrast and saturation adjustment

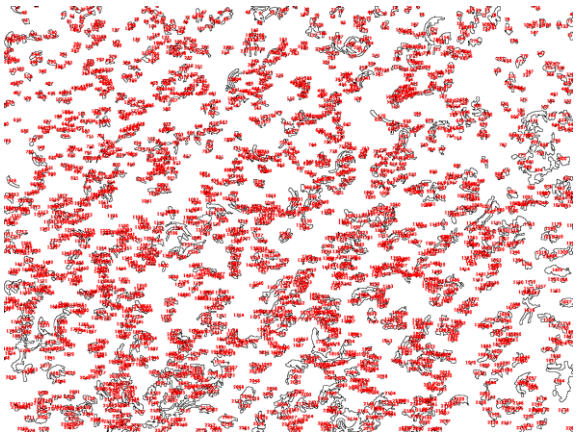

Figure 66. Milled Brenntag Spirulina powder 10× magnification with ImageJ drawing function applied

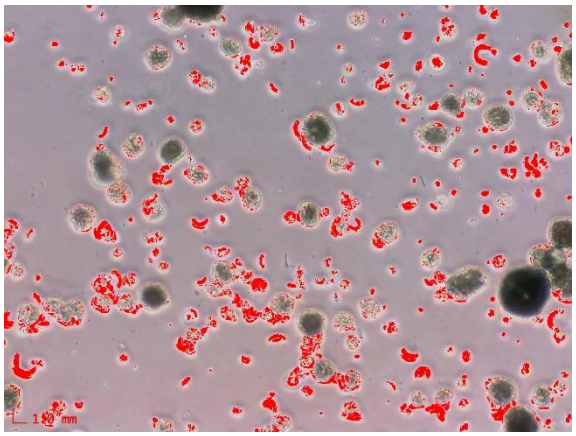

Figure 67. Non-milled Indian Spirulina powder 10× magnification with contrast and saturation adjustment

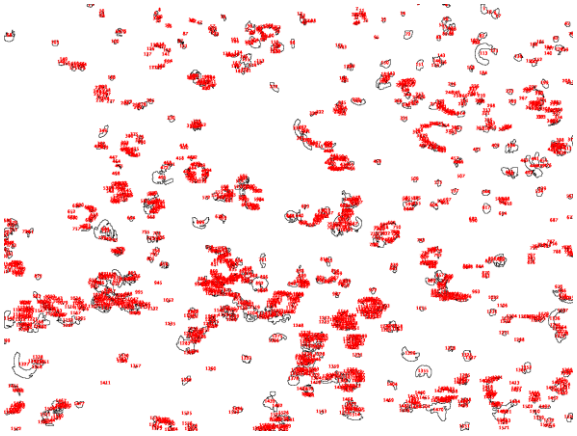

Figure 68. Non-milled Indian Spirulina powder 10× magnification with ImageJ drawing function applied

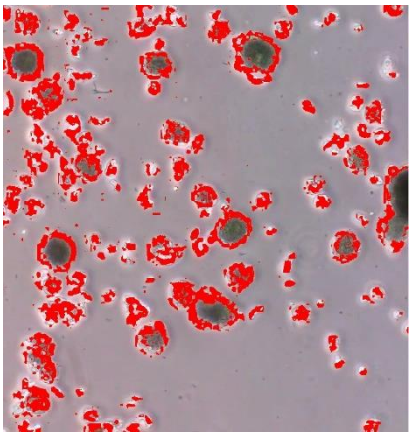

Figure 69. Milled Indian Spirulina powder 10× magnification with contrast and saturation adjustment

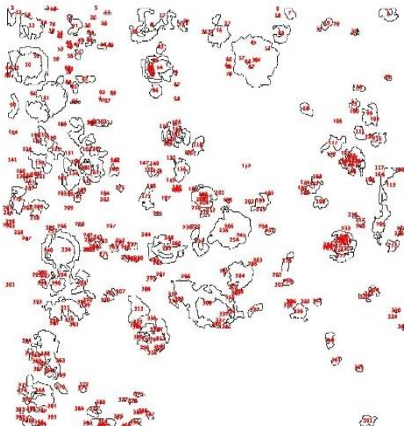

Figure 70. Milled Indian Spirulina powder 10× magnification with ImageJ drawing function applied

B.2 Leaching tests

B.2.1 First order leaching kinetic coefficients

The linearized first order kinetic equation form (Equation 7) is:

$$\log(C_e - C) = \log(C_e) - \frac{k_1}{2.303}t$$

Therefore k_1 can be calculated by looking at the slope of the graph:

$$k_1 = slope\ of\ graph \times (-2.303) \qquad \text{Equation 34}$$

Using Carbocraft non-milled as an example; Figure 22 shows the first order linearized form of the data as:

$$log(C_e - C)\ graph = -0.0887t + 1.0018$$

Therefore:

$$slope\ of\ the\ graph = -0.0887$$

Putting the slope into Equation 7 yields:

$$k_1 = -0.0887 \times (-2.303)$$

$$k_1 = 0.204\ h^{-1}$$

The same method was used to calculate all other first order kinetic coefficients.

B.2.2 Second order leaching kinetics

The linearized second order kinetic equation form for leaching (Equation 10) is:

$$\frac{t}{C} = \frac{1}{k_2 C_e^2} + \frac{t}{C_e}$$

Therefore k_2 and C_e can be calculated from a plot of t/C vs t using the slope and y-intercept of said graph:

$$slope\ of\ the\ graph\ = \frac{1}{C_e}$$

And:

$$y - intercept = \frac{1}{k_2 C_e^2}$$

Using Carbocraft non-milled as an example; Figure 25shows the second order linearization form of the data as:

$$\frac{t}{C} = 0.093t + 0.101$$

It is important to note that here the weighted linear regression of the data in the second order linear form has been used as it allows for more a more accurate representation of the data; it helps weight the distribution based on the error of the data points recorded in the experimental.

Therefore:

$$Slope\ of\ the\ graph\ = 0.093$$

Putting this slope into Equation 10:

$$0.093\ = \frac{1}{C_e}$$

Therefore:

$$C_e = 10.8\ mg.mL^{-1}$$

Using this C_e value and the y-intercept value of 0.101:

$$y - intercept = \frac{1}{k_2 C_e^2}$$

Becomes:

$$0.101 = \frac{1}{k_2 10.8^2}$$

Therefore:

$$k_2 = \frac{1}{0.101 \times 10.8^2}$$

$$k_2 = 0.084\ mL.mg^{-1}.h^{-1}$$

The initial extraction rate (IER), is another constant that contributes towards describing second order kinetics. It is an indication of the rate of initial solubilization that occurs when a solute first comes into contact with the solvent. From Equation 8 the initial extraction rate is given when t tends to 0, Equation 10 then becomes Equation 11:

$$IER = k_2 C_e^2$$ Equation 11

Using the constants calculated previously:

$IER = (0.084)(10.8)^2$

$IER = 9.9\ mg.mL^{-1}.h^{-1}$

B.3 Cell debris removal

B.3.1 Terminal settling velocity

Terminal settling velocities were calculated based on Stokes' Law (Green & Perry, 2008):

$$v_s = \frac{1}{18\mu} g(\rho_s - \rho_L) d^2$$ Equation 35

Where:

Symbol	Description	Value used for calc.
v_s	Terminal settling velocity (m.s^{-1})	-
μ	Viscosity of the fluid (Pa.s)	0.001
g	Force of gravity (m.s^{-2})	9.81
ρ_s	Density of the solid particles (kg.m^{-3})	1181
ρ_L	Density of the fluid (kg.m^{-3})	1000
d	Diameter of the particles (m)	Dependent on sample

The information above as well as the diameters from section 4.1 *Spirulina* powder size distributions were used to calculate the terminal settling velocities for each of the samples' particles (Brenntag, Carbocraft and Indian), milled and non-milled.

Carbocraft non-milled terminal settling velocity for the d_{80} diameter is shown as a sample calculation:

$$v_s = \frac{1}{18(0.001)}(9.81)(1181 - 1000)(\frac{0.51}{100})^2$$

$v_s = 0.0254\ m.s^{-1}$